SOME RESULTS IN MODEL-BASED ADAPTIVE AND SLIDING OBSERVER AIDED CONTROLLER STRUCTURE FOR ROBOT MANIPULATORS

A THESIS

submitted in fulfilment of the
requirements for the award of the degree
of
DOCTOR OF PHILOSOPHY
in
ELECTRONICS AND COMPUTER ENGINEERING

By

SUNIL KUMAR SINHA

DEPARTMENT OF ELECTRONICS AND COMPUTER ENGINEERING
UNIVERSITY OF ROORKEE
ROORKEE – 247 667 (INDIA)

JULY, 1996

Gratis

CANDIDATE'S DECLARATION

I hereby certify that the work which is being presented in the thesis entitled **"SOME RESULTS IN MODEL-BASED ADAPTIVE AND SLIDING OBSERVER AIDED CONTROLLER STRUCTURE FOR ROBOT MANIPULATORS"** in fulfilment of the requirement for the award of the Degree of Doctor of Philosophy and submitted in the Department of Electronics and Computer Engineering of the University is an authentic record of my own work carried out, during a period from March 1994 to July 1996, under the supervision of Prof. R.Mitra.

The matter presented in this thesis has not been submitted by me for the award of any other degree of this or any other University.

Sunil Kumar Sinha

This is to certify that the above statement made by the candidate is correct to the best of my knowledge.

Date : 23.7.96

DR. R. Mitra
Professor,
Deptt. of Electronics
& Computer Engg.
University of Roorkee
Roorkee 247 667

The Ph.D. Viva-Voce examination of Mr. Sunil Kumar Sinha, Research Scholar has been held on 8.9.97

Signature of Supervisor Signature of H.O.D. Signature of External Examiner

ABSTRACT

Robots have played a dominant role in the trends towards automation over the past years. The rapid development of its applications require controller that satisfies demands regarding tracking, speed and accuracy. Although, robot manipulators have been used in industry for a number of years, their full capabilities reach far beyond their present-day applications. At present, industrial applications of robot manipulators are mainly restricted to simple tasks. In order to improve the performance and capabilities, the application of advanced control concepts to robot manipulators is a necessity.

Two basic facts about the robot manipulator dynamics make the control problem a challenging one. Primarily, the dynamics are described by nonlinear, coupled second order differential equations. Secondly, the parameters of the model are partially unknown due to parametric variations disturbances and errors in modeling. Much of the recent research in robotic manipulator control has been directed towards the development of adaptive controller due to their effectiveness in high speed, high precision tasks and robustness to parametric uncertainty.

The development of controller structure in the present research work is inspired by the adaptive control strategy as reported in [7],[17],[23],[64],[73],[84]. Broadly, three new adaptive controller structures are proposed for robot manipulators. The sliding observer aided controller structure for adaptive case is heavily influenced by the work of Canudas et. al. [10]. Two new sliding observer aided adaptive controller structures are proposed by modifications in the existing sliding observer [10]. Further, two variations of nonlinear sliding observer based controller structures, motivated by [8]-[85], are also proposed for robot manipulators.

The aim of these proposed schemes are to improve tracking performance of robot manipulators and to satisfy the stability criterion in the Lyapunov sense. Performance of these new controllers have been verified through simulation. The work done in this thesis is briefly summarized below:

1. The controller structure for adaptive case, presented by Whitcomb et. al. [84], is based on position and velocity vectors. Their control law is modified by incorporation of acceleration term in feedback loop. This is based on two assumptions. The first is that the joint acceleration is measurable [17]-[23] and relatively noise free, and the second is that the inverse of sum of acceleration gain and estimated inertia matrix remains bounded. Simulation results show significant improvement in tracking error and velocity error for two different types of desired trajectories having different initial estimated parameters. The closed-loop system is shown to be globally asymptotically stable in the Lyapunov sense and has better convergence.

2. To overcome the noisy velocity measurement problem, a globally convergent adaptive controller structure for robot manipulators is presented by Berghuis et. al. [7]. Their controller structure has been modified by inclusion of nonlinear compensator [64] and virtual reference trajectories (sliding surface) [73]. In our work, three new structures of adaptive controller, associated with distinct form of sliding surfaces, are proposed and studied with respect to their tracking improvements (case -1,2 and 3). In case-1, all three virtual reference trajectories are considered where as case -2 uses the desired velocity reference trajectory instead of velocity virtual reference trajectory with other form of sliding surface. The proposed controller structure for case-3 consists of nonlinear compensator

and existing controller [7]. The asymptotic stability of the control algorithms are proved via the Lyapunov direct method. These proposed schemes improve tracking performance significantly, enhance robustness with respect to the noisy velocity measurement, especially in under- excited operations and also compensate the additional error (bounded by sliding surface and tracking error, [64]).

3. In another approach a bounded form (norm based) of adaptive controller structure is proposed. This is based on the inverse dynamics model of robot manipulator with a premise that if each parameter is known within some bounds the parameter adaptation can be prevented from going out of bounds and thus makes the system more robust. The stability of closed-loop system is investigated via the Lyapunov direct method. Simulation results, when compared with [7], clearly indicate drastic improvements in tracking performance.

4. It is known that velocity measurements are usually associated with rather high level of noise [10]. Only joint position measurements are assumed to be available, which is in contrast to full state measurements (positions and velocities). In this situation, estimated joint velocity vector obtained from a sliding observer is fed back to adaptive controller structure [10]. The proposed sliding observer structure is an extension of this by including the desired acceleration vector and a new uncertainty term (associated with desired trajectory based robot model properties) to estimate the velocity vector for adaptively controlled robot manipulator. The combined scheme is analysed with the Filippov's solution concept and tracking error dynamics via the Lyapunov stability criterion. The proposed

scheme shows the significant reduction in tracking error, velocity error and observation error (velocity).

5. The sliding observer scheme is further modified by including the tracking error and the observation error (position) in estimating velocity vector, to take into account the dynamic interaction between observer and controller dynamics. This means that the observer shall not only depend on the observation errors and controller not only on the tracking difference. This combined scheme is considered as a global control system with their gains tuned in order to ensure asymptotic tracking of the desired reference. The adaptation law and design vector, account for uncertainties on parameter vector associated with desired trajectory based model properties of robot, are derived using the Lyapunov direct method. Simulation results clearly indicate the improvements in comparison to [10].

6. In nonlinear systems the controller and the observer, in general, cannot be independently designed since the separation principle does not apply as in case of linear systems. In controller-observer scheme for robot manipulators presented by Canudas et. al. [8], the nonlinear sliding observer structure uses only observation error (position) in estimating velocity vector in order to fed back to controller structure. In view of nonlinear nature of robot manipulator and dynamic interaction between controller and observer, the square of tracking error and signum function of velocity observation error [85] are included as extended terms in the existing nonlinear sliding observer structure [8]. The first term reduces the observation error (velocity) due to application of the Filippov's solution concept and second term acts as a forcing (switching) element to

get good estimate of velocity. The closed-loop analysis is performed which is based on reduced order manifold dynamics and tracking error dynamics using the Lyapunov stability to ensure asymptotic stability. It is observed, through simulation, that drastic reduction in velocity error and observation error (velocity) results, in comparison to [8].

7. Again, the sliding observer is further modified by incorporating the sign-sign term in previously proposed observer structure. The observer scheme is termed as Sign-Sign Algorithm (SSA). The existing controller structure [8] is extended by incorporation of disturbance torque (as function of the desired position trajectory) in order to achieve the improved tracking performance of combined controller-observer scheme. The proposed scheme is illustrated by a simple example. The stability of closed-loop analysis is performed in the Lyapunov sense.

New model-based adaptive and sliding observer aided controller structures developed in this thesis are new solutions to many constraints, complexities and ambiguities involved in the control of robotic manipulators.

ACKNOWLEDGEMENTS

With a deep sense of indebtedness, it is my privilege to express sincere gratitude and reverence to Prof. R.Mitra for his meticulous guidance and constant encouragement. I thank him for giving his precious time freely at all the stages of this investigation. I am fortunate to have an opportunity to work under his supervision.

It gives me immense pleasure to express my deep regards to Prof. R.P. Agarwal, Head of the Department of Electronics and Computer Engineering for providing me the excellent and informal working conditions in the department to carry out this work.

A special thanks to Mr. P.R. Mangsuli for mailing important research papers from I.I.Sc., Bangalore.

I would also like to thank to my uncle, Prof. G.Nath, Ex-professor, I.I.Sc. Bangalore for his continuous support and encouragement.

Especially, I want to thank Mr. G.K. Saxena not for his cosmical but also the spiritual inspiration.

I gratefully acknowledge the financial support received from A.I.C.T.E. and Prof. S.C. Handa (Co-ordinator, Q.I.P. Centre) for extending the facilities provided during my stay at university of Roorkee.

Next, the author acknowledges with thanks his fellow research scholars in the UOR, who helped the author with their discussion to have clearer conceptions in his studies.

I am highly obliged to my parents, near and dears for their blessings and best wishes.

I am in dearth of words to express my abounding feelings to my spouse for her powerful supports and affection at various stages.

I wish to acknowledge Mr. T. Kapil (Times Computers) for carrying out word processing of the manuscript so efficiently.

Lastly, the author is grateful to the authorities of Kamla Nehru Institute of Technology, Sultanpur, for sponsoring him under Quality Improvement Programme Fellowship and granting necessary leave in this regard.

SUNIL KUMAR SINHA

CONTENTS

LIST OF FIGURES

LIST OF TABLES

LIST OF SYMBOLS

The following list summarizes most of the special symbols that appear in the thesis. In each case the symbol is defined in the text the first time it appears.

Symbol	Description
n	number of axes
τ	applied kth joint torque vector
m_{kj}	coefficients of inertia matrix M(q)
c_{ijk}	coefficients of Coriolis and centrifugal torque of matrix $C(q,\dot{q})$
$\dot{q}_i, \dot{q}_j$	ith,jth velocity vector
q_j	jth joint acceleration vector
$\phi_k(q)$	kth component of gravitational forces/torques
$g(q)$	joint gravitational forces/torques vector
$F(\dot{q})$	joint friction vector
$M(q)$	manipulator inertia matrix
$C(q,\dot{q})$	velocity coupling vector
w,mp	payload mass
J	actuator's inertia
$Y(q,\dot{q},\dot{q})$	regressor matrix
θ^*	known parameters vector
n_{jk}, n_{kj}	component of matrix $N(q,\dot{q})$
$\hat{M}(q)$	manipulator inertia matrix estimate
$\hat{C}(q,\dot{q})$	velocity coupling vector estimate
$\hat{g}(q)$	gravitational torque vector estimate
$\ddot{r}, \dot{r}, r$	desired trajectories in joint coordinated space for acceleration, velocity and position

K_1	proportional gain matrix
K_2	derivative gain matrix
$W(....)$	regressor matrix
$\hat{\theta}$	estimated parameter vector
e_1, e	tracking error
$e_2, \dot{e}$	velocity error
$\epsilon(e_1), \epsilon, \lambda$	normalized function
$\equiv$	is identically equal to
S	sliding surface
$\rightarrow$	approaches
K_3	acceleration gain constant
λ_o, ϵ_o	a positive constant
kg	constant diagonal matrix
$\lambda_m(.)$	minimum eigen value
$\lambda_M(.)$	maximum eigen value
I	identity matrix
Qn	matrix assoicated with minimum and maximum eigen value
ρ_1	norm of desired velocity trajectory
V	Lyapunov function
P_n	matrix associated with K_1 and M
$\dot{V}$	derivative of Lyapunov function
$\tilde{\theta}$	parameter error vector
lim	limit
$\|.\|$	Euclidean norm
Δ	square root of the ratio of minimum and maximum eigen vlaue

t	time
$\sigma_{n1}, \sigma_{n2}, \sigma_{n3}$	positive constants
S_1, S_2, S_3	sliding surfaces
$q_r, \dot{q}_r, \ddot{q}_r$	virtual reference trjaectories
K_i^T	transpose of K_i
M_m	lower bound of $M(q)$
M_M	upper bound of $M(q)$
C_M	upper bound of $C(q,\dot{q})$
L_∞	L_∞ norm
L_2	L_2 norm
$\theta^*(q)$	parameter function of position vector
$sgn(\tilde{x}_1)$	signum function
$M(x_1)^{-1}$	inverse of inertia matrix as a function of x_1
x_1, x_2	joint position and velocity vector
$\hat{x}_1, \hat{x}_2$	estimated joint position and velocity vector
$\beta(x_1, \dot{r})$	matrix associated with robot model properties
$\pi_o(.)$	robot model propertiesbased function
$\pi_1(.)$	robot model propertiesbased function
$M(e_1)$	matrix as a function of e_1
τ_d	disturbance torque
diag (α,β,γ)	diagonal matrix with diagonal element α,β,γ

Chapter - 1

INTRODUCTION

With advances in technology modernisation has taking place in the industrial sector. In contrast to manual labour often robots are used to perform prescribed jobs in harsh, dangerous, or unhealthy environments. The revolutionary changes have appeared in industry because of the installation of robot for performing different applications in areas such as in nuclear industries, deep under sea exploration and maintenance operation. Robot system has also been used increasingly in industrial automation without the involvement of human operator.

Improved control techniques are needed to fullfil the demand on manipulators performance such as speed and accuracy. The use of conventional linear control techniques limits the basic dynamics performance of robot manipulator due to reasons. First, the dynamic characteristics of robot manipulators are highly nonlinear and coupled. Second, the degradation of dynamic performance characteristics of robot manipulator governed by intertial properties. In view of high system performance over a wide range of tasks, many control techniques appear in literature. These are categorized in two classes, nonadaptive and adaptive control. In contrast to nonadaptive, the adaptive control plays an important role because of its robustness to parametric variations and disturbances. Under these two techniques a number of methods for dynamical control of robot manipulators have appeared in literature. These include resolved rate control, inverse problem, computed torque, variable structure control and observer based control.

Recently, considerable interest may be seen in the design of model-based

(computed torque) adaptive controller for robot manipulators because of its attractive features which compensate the inertial, coupling and gravity effects. In other direction, some work has been concerned with the problem of controlling robot manipulators by introducing observer scheme in order to estimate joint velocities. In practice, velocity measurements are obtained by sensors such as tachometers. Associated problems include discontinuities in the magnetic circuits of the tachometer stator at low velocities, ripple torques and other high frequency phenomenon, which reduce the quality of the measured velocity.

In the present work, broadly three new model-based adaptive controller structure are proposed for robot manipulators. First, the acceleration terms is included in previously developed controller structure [84] to form a new adaptation law. Secondly, a nonlinear compensator is used in existing controller structure [7] with three different forms of sliding surfaces for three types of controller structures. Thirdly, a bounded form of controller structure is proposed to improve tracking performance.

It is well known fact that the joint velocity measurements is corrupted with noise. This situation may deteriorate the dynamic performance of the manipulator because the value of the controller gain matrices are limited by the noise present in the velocity measurements. To avoid this problem, the observer based controller structures are considered for trajectory tracking of robot manipulators.

The sliding observer aided controller structure for adaptive case is influenced by the work of Canudas et. al. [10]. Two new sliding observer aided adaptive controller structures are proposed by modification in the existing sliding observer [10]. Former associated with new form of parameter uncertainty vector and latter one of tracking errors and velocity observation errors to take account the dynamic interaction between controller and observer. Further, two

types of nonlinear sliding observer based controller structures, motivated by [8],[85], are also proposed for robot manipulators. At the first, the proposed nonlinear sliding observer scheme is based on e^2-term, velocity observation error. Second, they are based on sign-sign function of observation error and tracking error. The controller structure of [8] is extended by including disturbance torque vector for latter one.

Performance of these new controllers have been verified through simulation. The simulation results are compared with previously developed control schemes. An imporatnt features of proposed controller structures is the improvement in tracking performance. The stability of proposed schemes is investigated in the sense of Lyapunov alongwith the region of attraction.

In brief, the problems and control strategies applied to the design of controller for robot manipulators are discussed covering adaptive control and sliding observer based adaptive and nonlinear control. A brief summary of the scope of the thesis is also included.

1.1 SYSTEM DESCRIPTION

A robot manipulator is known to have a complex dynamics. Good performance can be expected only if precise control strategies are employed. These sophisticated control require the use of realistic dynamic model of the robot manipulator. Two basic approaches are [3]:

(a) Newton-Euler formulation

(b) Lagrange - Euler formulation

The Newton-Euler formulation is derived by the direct interpretation of Newton's second law of motion, which describe dynamic systems in terms of force and momentum. The equation incorporates all the forces and moments acting on the individual manipulators links, including the coupling forces, moments between the

links and constraint forces acting between adjacent links. The equations obtained from the Newton-Euler formulation include the constraint forces acting between adjacent links. Thus, additional arithmetic operations are required to eliminate these unwanted terms and obtain explicit relations between the joint torques and the resultant motion in terms of joint displacements.

In the Lagrange-Euler formulation, or the Lagrangian formulation, the dynamic behavior is described in terms of work and energy using generalized coordinates. All the constraint forces and workless forces are automatically eliminated in this method and this leads to a compact and closed-form of expression in terms of joint torques and joint displacements.

The resulting closed-form of dynamic equation of an n-degree of freedom robot manipulator can be given in the form [59].

$$\tau_k = \sum_{j=1}^{n} m_{kj}\,\ddot{q}_j + \sum_{i=1}^{n}\sum_{j=1}^{n} c_{ijk}(q)\,\dot{q}_i\,\dot{q}_j + \phi_k(q), \qquad k = 1,2,\ldots. n \qquad (1.1)$$

where m_{kj} are the coefficients of inertia matrix, $\phi_k(q)$ are the gravitational forces and torques and τ_k is the actuating torques. $\ddot{q}_j$, $\dot{q}_j$ and q are the accelerations, velocities and positions, respectively. The coefficients c_{ijk} of the Coriolis and centrifugal terms are defined as

$$c_{ijk} = \frac{1}{2}\left\{\frac{\partial m_{kj}}{\partial q_i} + \frac{\partial m_{ki}}{\partial q_j} - \frac{\partial m_{ij}}{\partial q_k}\right\}$$

and are known as Christoffel symbols (of the first kind). It is common to express (1.1) in matrix form as

$$M(q)\ddot{q} + C(q,\dot{q})\dot{q} + g(q) = \tau \qquad (1.2)$$

where the k,jth element of the matrix $C(q,\dot{q})$ is given as

$$c_{kj} = \sum_{i=1}^{n} c_{ijk}\,(q)\dot{q}_i$$

$$= \sum_{i=1}^{n} \frac{1}{2} \left\{ \frac{\partial m_{kj}}{\partial q_i} + \frac{\partial m_{ki}}{\partial q_j} - \frac{\partial m_{ij}}{\partial q_k} \right\} \dot{q}_i \qquad (1.3)$$

M(q) is the nxn position-dependent manipulator inertia matrix; $C(q,\dot{q})\dot{q}$ is the n-vector of Coriolis and centrifugal torques, g(q) is the n-vector of gravitational torques.

Different dynamic models of robot manipulator have appeared in the literature. These may be categorized in the following forms:

Neglecting friction and other disturbances [8]-[10],[56],[63],[64],[71]-[77],[84] as

$$M(q)\ddot{q} + C(q,\dot{q})\dot{q} + g(q) = \tau \qquad (1.4a)$$

Using viscous and coulomb friction, [6], [12], [16], [17], [27], [28], [30], [47], [63], [64], [68], [69], [80], [81], as

$$M(q)\ddot{q} + C(q,\dot{q})\dot{q} + g(q) + F(\dot{q}) = \tau \qquad (1.4b)$$

where vector $F(\dot{q})$ represents the combination of viscous and coulomb friction, and another form [48],[60],[85] as

$$[M(q)+J]\ddot{q} + C(q,\dot{q})\dot{q} + g(q) = \tau \qquad (1.5)$$

where J represent actuator's inertia. The actuators, armature motors in many cases [48], [60], [85], are supposed to be able to generate the control torque using their dynamics.

Addition of payload in system dynamics gives significant effects on Inertia torque and Coriolis plus centrifugal torque. Under this assumption, in generalized way, the dynamics of robot manipulator can be expressed [7],[19],[68], as

$$M(q,w)\ddot{q} + C(q,\dot{q},w)\dot{q} + g(q) = \tau \qquad (1.6)$$

where w denotes the pay load. The system dynamics as expressed in (1.4a) is considered for the proposed schemes.

1.1.1 Fundamental Properties

The equations of motion are complex, nonlinear, coupled for all but the simplest robots. They have several fundamental properties which can be exploited to facilitate control system design [59].

Property 1: The inertia matrix M(q) is symmetric positive definite, and both M(q) and $M(q)^{-1}$ are uniformly bounded as a function of $q \in R^n$. It means that associated energy is always positive and skew symmetric matrix can be added to it without changing the value of the energy.

Property 2: There is an independent control input for each degree of freedom. The reason for doing this is to obtain decoupled subsystem.

Property 3: All of the constant parameters such as link masses, moment of inertias, etc., appear as coefficients of known functions of generalized coordinates. By defining each coefficient as a separate parameter, a linear relationship results so that one can write the dynamic equation(1.2) as

$$M(q)\ddot{q} + C(q,\dot{q})\dot{q} + g(q) = Y(q,\dot{q},\ddot{q})\theta^* = \tau \qquad (1.7)$$

Where $Y(q,\dot{q},\ddot{q})$ is an nxr matrix of known functions, named as regressor, and θ^* is an r-dimensional vector of parameters.

Property 4 : Defining the matrix $N(q,\dot{q}) = \dot{M}(q) - 2C(q,\dot{q})$, one observes that $N(q,\dot{q})$ is skew symmetric, i.e., the components n_{jk} of N satisfy the condition $n_{jk} = -n_{kj}$. However, $\dot{M} - 2C$ is itself skew symmetric only in the case that C is defined according to (1.2). It indicates that the so-called fictitious forces, defined by $C(q,\dot{q})\dot{q}$, do no work on the system.

1.2 PROBLEMS AND STRATEGIES FOR CONTROLLING ROBOT MANIPULATORS

The basic difficulty in controlling a robot manipulator arises from the fact that the dynamic equation describing the robot motion are inherently nonlinear and highly coupled. Physically, the coupling terms represent gravitational torques, which depend upon the positions of the joints, reaction torques, due to accelerations of other joints, Coriolis and centrifugal torques. These interaction torques depend upon the size and weight of the links of the manipulators as well as the change of manipulator configuration. The role of friction forces is unpredictable. The dynamics of the actuator further adds to the difficulties and complexities in model inaccuracies. These effects make the control of robot manipulator a complicated task and challenging.

In general, the main aspect associated with the control problems of robot manipulators is to achieve a desired system response with prescribed error limit. The control of robot manipulator is accomplished in two different stage. In the first stages, the controller structure is constructed. In the second stage,the control torque is applied to actuator so that the response of the robot manipulators of joint motion closely track the desired trajectory.

In the area of robot control research a large number of sophisticated control approaches have been developed during the last two decades. These provide almost perfect results on simulation or under laboratory conditions. The major strategies include nonadaptive and adaptive control, and are further subdivided

as nonlinear control, robust control, sliding mode control,computed torque control and observer based control. These are discussed below in brief.

Trajectory tracking based on linear multivariable theory using linearized model and decoupling is fascinating because of the comparably low computation effort [67]. However, because of the highly nonlinear system behavior the scheme refers to a limited application area where slow motion required. Linear feedback law based tracking control scheme has been proposed in [61] under the assumption that the gain approaches infinity the scheme becomes globally asymptotically stable. A high gain controller, which is unaffected by noisy velocity measurement problem, is proposed in [83]. A feedback law based on local, decoupled, and exact linearization has been proposed in [39]. Recently, the feedback linearization [66], [68], [70], of a robotic manipulator based control using variable structure compensator for robust tracking has been proposed [87], [88].

Nonlinear feedback control using approximate inverse dynamics model with additional feedback compensation has been proposed in [25]. The scheme is sensitive to parametric variations. The strategy, by incorporation of uncertainty and input constraints alongwith torque optimization in case of actuator saturation has appeared in [76].

A nonlinear switching-type control law under the assumptions that acceleration measurements are available and the bound of uncertainty vector depends upon derivative of state has appeared in [12]. The modified version of [74] is presented in [37] in order to estimate the upper bound on uncertainty instead of known uncertainty bound. A nonlinear robust feedback controller is derived with cubic expression of uncertainty by including actuator dynamics [48].

An attractive way to avoid the problems both of model uncertainty (nonlinear decoupling concepts) and of parameter variation (linear control concept) is to apply adaptive control. In the model reference adaptive

control(MRAC) concept, the model and system are guided by the same signal [1], [4], [20], [45], [46], [52], [56], [69] to reduce the modeling error and maintain the persistency of excitation for model and system both. In this direction, the pioneering work of Dubowsky et.al. [20] is modified for discontinuous control [4] and continuous control [52], [56] using unit vector adaptation law. For improving transient response and convergence speed the work [45] is extended in [46] by introduction of optimal auxiliary input.

The complete self-tuning type adaptive control using least square (see also [9]) for each joint have been applied to robot manipulators [38]. It is also referred as mixed concept i.e. feedforward component computes nominal torque from Newton-Euler equation and feedback component computes perturbation torque based on self-tuning control [43].

Adaptive control applied to robot manipulator [4], [69] are based on variable structure system. The computed torque method (inverse dynamics) based adaptive control shows global convergence [5], [7], [16], [17], [23], [24], [63], [64],[73],[75],[80],[84]. The passivity-based approach is studied in [58][63],[64]. Inverse dynamics controller used together with the addition of a term that allows preservation of the passivity properties of rigid robot in the closed loop is reported in [35]. An important drawback of passivity-based control is that they are not robust to velocity measurement noise. In order to reduce this problem a scheme is proposed in [7], [64]. The work [16], [17], [23], [24] are based on the assumption that joint acceleration measurements are available. The idea using joint acceleration measurements [16], [17], [23], [24], [49], [62], are avoided using identifier[30], sliding mode [73] and fixed estimate [75].

The inverse dynamics based adaptive law to estimate gravity term [80] and parameter uncertainty [37] is one of the strategies for globally convergent

control. Recently, keeping in view the fact that velocity measurements are corrupted by noise, the observer scheme is employed with controller either by using sliding observer for nonlinear case [8],[57], robust approach [9], or adaptive case [10] for motion control of robot manipulator. In these schemes, it is assumed that only joint position measurements are available.

1.3 DEFINITIONS AND PRELIMINARIES

Definition 1.3.1: vector norm

For a vector $x \in R^n$, the norm of x said to be the Euclidean or l_2 norm, is given by :

$$\|x\| = \left(\sum_{j=1}^{n} \|x_j\|^2 \right)^{1/2}$$

Definition 1.3.2: Matrix Norm

For a matrix $A \in R$, $\|A\|$ will be the corresponding induced norm

$$\|A\| = [\max_i \lambda_i (A^T A)]^{1/2}$$

where $\max_i \lambda_i(.)$ denotes the largest eigen value.

Definition 1.3.3: L_p functional norm

For a Lebesque measurable function f(t) :

$R^T \longrightarrow R^n$, the L_p norm for $p \in [1,\infty]$ is defined to be :

$$\|f(.)\|_p = \left[\int_0^{\infty} |f(\tau)|^p d\tau \right]^{1/p}$$

For $p = \infty$ the norm is defined to be,

$$\|f(.)\|_{\infty} = \underset{\tau \geq 0}{\text{Sup}} \, |f(\tau)| \text{ almost everywhere.}$$

Definition 1.3.4: Given two n x 1 vectors x and y, it implies

$$C(q,x)y = C(q,y)x$$

$$C(q,x+\alpha y) = C(q,x) + \alpha C(q,y)$$

for all $x,y,q \in R^n$, $\alpha \in R$.

Definition 1.3.5: Adaptive Control

It is defined as a feedback control system intelligent enough to adjust its characteristics in a changing environment so as to operate in an optimum manner according to some specified criterion.

Definition 1.3.6: A computed torque controller is a control algorithm which uses a model of the manipulator's dynamic behavior to ensure that a prescribed degree of damping is maintained for all configurations. It allows to cancel the nonlinearities associated with system dynamics.

Definition 1.3.7: Sliding mode

It is an important concept of variable structure system and defined as a special regime in the vicinity of the switching surface, $S = 0$, where the tangent or velocity vector of the state trajectory always points towards the switching surface. If sliding mode exists on $S = 0$, then S is termed as sliding surface.

Definition 1.3.8: Robot

According to RIA, a robot is define as a reprogrammable multifunctional manipulator designed to move materials, parts, tools, or specialized devices, through variable programmed motion for the performance of a variety of tasks.

Definition 1.3.9: Asymptotic Stability

An equilibrium point $\hat{x}$ of the system *H* is asymptotically stable if and only if for each $\epsilon > 0$ there exists a $\delta > 0$ such that if $\|x(o) - \hat{x}\| < \delta$,then $\|x(t) - \hat{x}\| < \epsilon$ for $t \geq 0$ and:

$x(t) \rightarrow \hat{x}$ as $t \rightarrow \infty$

Thus if an equilibrium point $\hat{x}$ is asymptotically stable then any solution which starts out sufficiently close to $\hat{x}$ stays close in the sense that $\|x(t) - \hat{x}\|$ remains small and, in addition, the solution asymptotically approaches $\hat{x}$ in the limit as $t \rightarrow \infty$.

1.4 SCOPE OF THE THESIS

In chapter 2, the control strategies for robotic manipulator under nonadaptive control and adaptive control category are reviewed. Several issues and recent trends are examined critically. The work related to controller -observer strategies are also systemically reviewed.

In chapter 3, three different type of controller structures are proposed. First, the acceleration error based controller structure is proposed with a new form of adaptation law for relatively noiseless environment for trajectory tracking of robot manipulator. Second, nonlinear compensator based three different forms of controller structure for three different types of sliding surfaces are proposed for the motion control of robot manipulator. Third, A norm based controller structure is proposed for trajectory tracking of robot manipulators. The stability investigation is also performed in the Lyapunov sense for all the proposed control scheme and the region of attraction is studied for their convergence. The proposed schemes give better tracking performance in comparison to [84], [7], respectively.

In Chapter-4., the sliding observer aided control concept is described in detail based on the existing work [8],[10]. The sliding observer aided adaptive control concept is restructured by modifying the configuration of sliding observer and uncertainty terms in order to ensure better asymptotic tracking of the desired reference. The existing nonlinear sliding observer aided control scheme of Canudas et. al. [8] is extended in view of dynamic interaction between controller and observer for comparative trajectory tracking performance. Similarly, this scheme is further extended by including the error based sign-sign term and disturbance torque in control law. The error analysis and stability investigation in the Lyapunov sense are also presented. Significant reduction in error responses are observed in comparison to [8],[10], respectively.

In chapter-5, some derivation of dynamic equation (regressor) and simplification are carried out for a robot manipulator. The simulation results of proposed algorithms are carried out to compare the tracking performance with the existing cases.

Chapter - 6 deals with the conclusion on the results obtained in the different proposed schemes. Some suggestions for future research in this area are also included.

Chapter - 2

LITERATURE SURVEY

During the past decade, many schemes for controlling the motion of robot manipulators have been appeared in literature. Mainly, they are divided into two categories, namely (i) nonadaptive control (ii) adaptive controller .The latter approach has been the subject of greater attention in recent years. Several techniques have been developed under these two categories. They include nonlinear decoupling, robust control, passivity approach, sliding mode (Variable structure), computed torque and observer based approach.

2.1 NONADAPTIVE CONTROL

The general characteristics of nonadaptive control approach is that they are fixed controllers. The schemes require an exact knowledge and explicit use of the complex robot dynamics and its parameters. Uncertainties in the parameters will certainly cause dynamic performance degradation. In such situations, compensation for nonlinearity, and joint decoupling techniques must be introduced to cope with high accuracy requirements [81].

Traditionally, the problem of joint motion control has been treated by the PID algorithms. The PID control, based on linearization and local stability, is limited to small angle movements [2]. Moreover, to ensure the stability, the gain matrices must satisfy complicated inequalities, which depend on the initial conditions.

The idea of resolved-rate control of the robot manipulator in terms of the position and orientation of the hand is introduced in [47]. The minimum time

solution along a specified path using linear programming is investigated. The proof of error convergence is based on linear approximation over small time interval. The control algorithm is inadequate because the changes of load in task cycle are neglected. The complex nature of control law in order to ensure the convergence of large error with nonlinear feedback design based of PID control is investigated in [25]. Its sensitivity to parameter variation appears as a drawback. In view of unmodelled friction effects and large inertia properties, a new robot control scheme using PID controller is proposed in [51]. This scheme require high gain feedback.

A robust tracking scheme for robot manipulators in the presence of model uncertainty and input constraints is developed by Spong et. al. [76]. A simple alternative solution to the robot manipulator control problem based on linear multivariable theory to provide robust steady-state tracking of a class of trajectories is proposed by Seraji [67]. This scheme consists of multivariable PD^2 + PD based controller alongwith multivariable PID feedback controller using feedforward and feedback controller concepts. The comparative performance of nonlinear feedforward control, feedback control and reduced order feedforward control scheme are established in real-time. The computed torque based control laws are introduced for joint coordinated control of robot manipulators in [83]. The modification of the Lyapunov function and use of lemma to handle third order term in the Lyapunov function derivative are also incorporated.

Without demonstrating the stability, nonadaptive robust control scheme with nonlinear and linear parts to compensate modeling errors and unknown disturbance is proposed by Kuo et. al. [40]. The nonlinear part decouples robot dynamics to obtain a set of equations in terms of each joints input-output and the linear part applies robust servomechanism theory to suppress the effect of modeling error and unknown disturbances. The model-based servo schemes are designed in [12]

to compensate for system uncertainties which utilizes a nonlinear switching type control law and bound of the model uncertainty. Qu et. al. [61] presented a control scheme for robust tracking control of robots by incorporating a linear feedback law to overcome the problem associated with [12]. The design parameter in the control law is a constant gain which depends only on the coefficients of a quadratic bound on the nonlinear terms in the dynamic equation. The simulation results is however not reported. In contrast to linear feedback, a nonlinear robust feedback controller is suggested in [48] including actuator dynamics and cubic form of uncertainties to guarantee global ultimate boundedness of the actual system output.

Spong [74] derived a robust control law for robot manipulator using a novel modification of the so-called Leitmann approach [15]. The parameter uncertainty bounds are needed to derive the control law and to prove uniform ultimate boundedness. As a result, precise bounds on the uncertainty have been difficult to compute. On the contrary, an additional control input is updated as a function of the estimate of the uncertainties upper bound in [74]. A variable structure compensator is introduced to cope with parameter uncertainties reported in [87], [88]. The boundary layer compensator is used, further, to reduce the chattering effect at the cost of control accuracy.

2.2 ADAPTIVE AND OBSERVER BASED CONTROL

An effective way to deal with parameter uncertainties of a robot manipulators is to apply adaptive control scheme in which the controllers are designed to compensate for the uncertainties automatically. It can be broadly classified into two categories on the basis of model [27]: (i) Model - reference Adaptive control and (ii) Self-tuning adaptive control. The adaptive control may be also classified on the basis of their control objective and the signal that

drives the parameter adaptation law. The control objective determines the controller structure whose parameters are to be adapted on-line. The adaptation law may be driven by a signal that measures either the prediction error or tracking error.

The pioneering work in the area of MRAC using steepest descent method for a class of manipulator is proposed in [20]. The control algorithm which minimizes a quadratic function of the error defined as the difference between the desired state vector and the robotic process state vector. The authors neglected couplings between joints of the manipulator and did not assure the convergence of their control law.

Balestrino et.al. [4] proposed a control algorithm based on discontinuous control signal of adaptive model following control system for robotic manipulators via hyperstability theory. The chattering due to sliding motion causes unmodelled resonance. As an alternative approach, using continuous signal for fast motion, MRAC algorithm is developed by Nicosia et.al. [56]. The controller however does not yield zero tracking error and required unbounded feedback gains for the convergence of the tracking error to zero. Using MRAC technique with uncertain parameter and integrable adaptive law, a control algorithm is proposed in [70]. Here, the Lyapunov function is used only as a intermediate step and did not appear in the final form of either the controller or the adaptive law. Nonlinear adaptive control schemes are proposed in [52] using continuous control inputs where control gains are adjusted adaptively. Based on the work of Corless et.al. [15] for system uncertainty, Singh [69] describes a switching-signal-synthesis adaptive scheme for model following (MFAC). The controller includes a dynamic compensator in feedback path unlike linear compensator [4], [70], [77]. Using optimal auxiliary input Lim et.al. [46] designed MRAC base control strategy to reduce transient oscillation and thus

improved convergence in comparison to their earlier contrast to previous work [45]. The control algorithms are valid for slow varying movement of robot manipulator.

Improved MRAC theory is used to develop adaptation algorithm by Seraji [68] using auxiliary signal. The scheme, employed as feedforward controller, which behaves as the inverse of the manipulator and auxiliary feedback controller.

Kovio et.al. [38] proposed a self-tuning type of control law using an autoregressive based model for the manipulator dynamics to compensate the nonlinearities. The parameters of the model and the controller gain are determined on-line by a recursive least-square identification algorithm and a weighted- one-step-ahead optimal control algorithm. The convergence property exists if the motion is along a straight line and circular arc. The control law assume that the interaction forces among the joints are negligible and during the adaptation process the elements of the linearized system remain constant. As part of the scheme [43],[44], an optimal adaptive self-tuning controller of the linearized system is used to compute perturbation torque and input torques computed from the Newton-Euler equation of motions. Convergence of control law is not explicitly shown. In view of linearization of nonlinear model around the desired trajectory an adaptive control scheme based on local parameter optimization is proposed by Takegaki et.al.[78] under the assumption of slowly time-varying variational system dynamics of the manipulators.

Choi et.al. [13] extended the work of Lee et.al. [43] by the inclusion of payload and parameter uncertainties. Resolved motion rate and acceleration control are one of the ideas which are introduced Luh et.al. [47] and Lee et.al. [44], respectively, in order to control the robot manipulator using Newton-Euler formulation of equation of motion.

Almost all previous work is based on standard MRAC or self-tuning regulator theory for linear time-invariant plants. The stability proofs are only valid to the extent that coefficients of the linearized manipulator system vary sufficiently slowly. On the contrary, the computed torque formulation yields a that suppresses uncertainties and disturbances and tracks the desired trajectories uniformly in all configuration of manipulators.

The results of Craig et.al.[17] are based on adaptive inverse dynamics which is a special case of the idea of feedback linearization of nonlinear systems. A globally convergent scheme of robot manipulator is based on the assumptions of bounded estimated parameters, availability of joint accelerations measurements and boundedness of inverse of estimated inertia matrix. The adaptation law is the form of linear-in-parameterization technique [16]. By dropping the assumption, that joint acceleration measurements are available [62], Hsu et.al. [30] proposed a adaptive control using explicit identifier, basically, a first order filter and discrete time upgradation of the parameter values. Without using the additional filters, the adaptive pure computed torque (PD part is omitted) algorithm is proposed by Gu et. al. [28]. It is suggested that PD control is not necessary to ensure stability and no large feedback gains are required.The alternative formulation of adaptive inverse dynamics control which overcomes the assumption on boundedness of the inverse of the estimated inertia matrix is proposed in [75] using fixed parameter estimate instead of varying estimate.

In contrast to [17], Slotine et.al. [73] proposed a nominal type of controller structure with sliding surface and applying skew-symmetry properties established global asymptotic stability. The Lyapunov stability for an adaptive controller that ensure only convergence to zero for the velocity tracking error. The idea of this controller design philosophy is to reshape the robot system's

natural energy such that the control objective is achieved and designated as passivity approach [59].

The work of Sadegh et.al. [64] is conceptually different from the adaptive inverse dynamics in that the control objective is not feedback linearization but only preservation of the passivity properties of the robot in the closed loop. The form of Coriolis and centripetal acceleration compensation controller is bilinear function of the joint and model reference velocities instead of a quadratic function of the joint velocities [63],[64]. In [63], the problem of noise correlation between estimation error and adaptation signal appeared, which is removed in their extended work [64]. A reduction of sensitivity to velocity measurement noise appeared. The principle of passivity-based direct adaptive control for industrial manipulator is experimentally verified and implementation issues are discussed in [42]. An important drawback of these schemes is that they are not robust to velocity measurement noise. Specially, in underexcited operation, when performing a regulation task, the well-known phenomenon of parameter drift in the adaptation law is occur due to presence of quadratic terms in the measured velocity. To avoid noisy velocity measurement problem, a globally convergent adaptive control scheme for robot motion control is proposed in [7]. The adaptation law enhanced robustness with respect to noisy velocity measurements and controller does not require the inclusion of high gain loops that may excite the unmodelled dynamics and amplify the noise level.

Kelly et.al. [35] proposed an inverse dynamics controller with the additional term which allows preservation of the passivity of the closed loop system. The control law consists of a computed torque and feedforward compensation part. The scheme is an intermediate approach between computed torque and passivity approach.

Bayard et.al. [5] introduced asymptotically stable adaptive control laws for robotic manipulator. The energy-like Lyapunov function, which retains the nonlinear character and structure of dynamics instead of quadratic forms, is incorporated. The scheme avoids the velocity measurement problem by inclusion of reference trajectory based control law but requires high controller gain in order to overcome the uncertainty in the initial parameters errors and compensate for the dependency on the magnitude of the desired trajectory velocity. The computed torque based robust scheme for adaptive case in order to estimate the bound of model uncertainty is proposed by Chen [12]. The adaptive scheme relies on the functional properties of the model uncertainty.

Tomei [80] presented PD control algorithm that is adaptive with respect to gravity parameter of the robot manipulator. In contrast to [2], where PID control algorithm ensure only local asymptotic stability, a globally convergence scheme is proposed with upper and lower bound of the inertia matrix. One integrator is needed against the n-integrators required by PID controller in [2]. The generalized model-based adaptive control approach to the trajectory tracking of robot manipulator is proposed in [60]. It includes both the full-order actuator dynamics and second order manipulator dynamics. The scheme is associated with local bound stability.

A globally asymptotically stable model-based adaptive controller is proposed in [84] with a new Lyapunov function. Using filtered torque in adaptation law to ensure convergence of tracking error a globally convergent adaptive scheme is developed in [49] for controlling robot manipulators.

Feng et.al. [24] considered the Lyapunov-like concept to design an adaptive control law, with assumption that acceleration measurements [17] of joints are required, in task space. It is further investigated to achieve robustness to bounded disturbances. An adaptive control algorithm based on prediction error and

sliding mode based parameter estimate is proposed in [23] on same methodology as appear in [24].

As the technology advances, the controller simplicity becomes less important than tracking accuracy. It is no longer prohibitive to consider a more accurate model and look for better tracking performance with a slightly more complicated control scheme. It is well known fact that the joint velocity and joint acceleration measurements are corrupted with noise. The majority of adaptive controllers is based on full state measurements (positions and velocities) [59]. In contrast to joint position measurements the velocity measurements are often contaminated with high level of noise. This situation may detoriate the dynamic performance of the manipulator because the value of the controller gain matrices are limited by the noise present in the velocity measurements. Exploiting the model properties of the robot dynamics, a nonlinear observer is proposed in [57] for rigid joint robots to reconstruct the joint velocities. The associated error dynamics is shown to be locally asymptotically stable. The proposed observer is inserted in the feedback to controller structure. Two cases point to point control and the trajectory control are discussed. The observer furnishes the state estimate directly in the physical coordinates, so that no transformation is needed. The convergence of the proposed observer is local and of control law is global. The size of the region of attraction depends only on the observer gain constant.

Canudas et.al. [9] proposed a sliding observer scheme to estimate the joint velocities for controller to control the motion of robot manipulator. The control law involves Leitmann procedure [15] to take account for uncertainties due to model error. It is shown to be locally exponentially stable under model parameter uncertainties and bounded torque disturbances.

Canudas et.al. [10] extended the work of [9] for adaptive control of robot manipulator. The sliding observer equation have discontinuities on its right side so that the Filippov's solution concept is applied. It indicates that the dynamics on the switching surface is an average of the dynamics on each side of discontinuity surface. The uncertainty vector is assumed in terms of boundedness of coefficients matrix of system dynamics. The introduction of an adaptation loop reduces the chattering at control law level because of its dependency on estimated state and parameter vectors and hence contains no terms proportional to discontinuities. The observer scheme depends on only position observation error.

Canudas et.al. [8] presented two alternative approaches for trajectory tracking control using nonlinear estimated state feedback. The first scheme is based on smooth function whereas the second uses switching gain. The stability of smooth scheme is local whereas the nonsmooth scheme gives an arbitrarily large attraction region and globally asymptotically exponentially stable. In contrast to observer scheme, an extended Kalman filter is used to estimate joint velocity and inertial parameter along with computed torque for position measurements in order to control the motion of robotic manipulator adaptively as proposed in [27]. Statistical data is required for Kalman filter. A passivity-based approach to controller-observer scheme is reported in [6]. This combined scheme is based on the assumptions: (i) The desired energy function must match the closed -system (ii) Velocity of the robot system is to be bounded. An adaptive nonlinear observer is designed to observe the acceleration instead of measuring it by feedback in [85]. A third order robot model is used with this controller-observer scheme to deal with uncertainties in both robot and motor dynamics.

Current control schemes for robot manipulator are categorized systematically. The chattering phenomenon occurs, if variable structure control (sliding mode) schemes are applied to robotic manipulators caused by the

excitement of high frequency dynamics. The adaptive control schemes are superior in view of tracking performance over nonadaptive control under parameter uncertainties compensation. The adaptive control based schemes are reviewed for robot manipulators that are proposed till date by other researchers. Almost, all the results reported in the literature are based on simulations studies.

The observer based control schemes are also reviewed critically. The observers are employed to estimate the joint velocities because the actual velocities are corrupted with noise. New ideas and improvements would automatically follow. Broadly, three new adaptive controller structures are proposed for robot manipulators as presented in subsequent chapter-3.

Chapter - 3

ADAPTIVE CONTROL STRATEGY

3.1 INTRODUCTION

The contributions of the present work are the improvements in the controller structure of the existing schemes of Whitcomb et. al. [84] and Berghuis et. al. [7]. The controller structure of [84] consists of fixed proportional, derivative feedback control and inverse dynamics (computed torque) based adaptive law. The estimated parameter vector (adaptation law) is a function of position, velocity errors and clever included normalization term. The Lyapunov function is included to ensure globally asymptotically stability in tracking error and controller parameter error. Including acceleration term in controller structure [84], a new form of adaptation law results. This proposed scheme gives significant improvements in tracking performance.

A scheme for trajectory tracking of robot manipulator to enhance robustness with respect to noisy velocity measurements is proposed in [7]. The basic requirement is that the adaptation law should not sensitive to velocity measurement noise and does not require high gain. Also it should not excite unmodelled torsional modes which aggravates the noise sensitivity. In order to reduce tracking error and velocity error, a nonlinear compensator based controller structures are proposed with different form of sliding surfaces.

3.1.1 Controller Structure

The controller structure in [84] is basically an adaptive model-based control algorithm which utilizes feedforward reference trajectory information rather than actual state information. The control law and adaptation law are recalled as

$$\tau = \hat{M}(q)\,\ddot{r} + \hat{C}(q,\dot{q})\dot{r} + \hat{g}(q) + K_1 e_1 + K_2 e_2$$
$$= W(q,\dot{q},\dot{r},\ddot{r})\;\hat{\theta} + K_1 e_1 + K_2 e_2 \qquad (3.1)$$

where $r,\dot{r},\ddot{r}$ are desired trajectory informations. W(.) represents linear-in-parameterization (array of known nonlinear function) as Craig et. al. [17]; $e_1 = r-q$ and $e_2 = \dot{r}-\dot{q}$ are known as tracking error and velocity error respectively. $\hat{\theta}$ is a vector of estimated parameter obtained via the adaptation law given as

$$\dot{\hat{\theta}} = kg\; W^T(q,\dot{q},\dot{r},\ddot{r})\;(e_2 + \epsilon\, e_1);\; \epsilon(e_1) = \frac{\epsilon_o}{1+\|e_1\|} \equiv \epsilon \qquad (3.2)$$

where adaptive gain matrix kg be any symmetric positive definite matrix.

The adaptive control for robot manipulator as presented in [7] is :

$$\tau = \hat{M}(q)\,\ddot{r} + \hat{C}(q,\dot{q}-\lambda e)\dot{r} + \hat{g}(q) - K_1 e - K_2 \dot{e}$$
$$= W(q,\dot{q}-\lambda e,\dot{r},\ddot{r})\;\hat{\theta} - K_1 e - K_2 \dot{e} \qquad (3.3)$$

and

$$\dot{\hat{\theta}} = kg\; W^T(q,\dot{q}-\lambda e,\dot{r},\ddot{r})S \qquad (3.4)$$

where $\lambda = \frac{\lambda_o}{1+\|e\|}$, $S = \dot{e} + \lambda e$ known as sliding surface, $e = q - r$.

In this scheme, it is assumed that the actual velocity measurements are associated with noise. To diminish the noise problem, it may be advantageous to replace $\dot{q}$ by $\dot{q} - \lambda e$ in controller structure. The adaptation law depends upon the sliding surface 'S' which can be viewed as a stable first order differential equation in e with S as an input. The system dynamics of robot manipulator incorporates variable pay load and is estimated via the adaptation law (3.4).

3.2 PROPOSED CONTROLLER STRUCTURES

In this section, three new controller structures are considered for trajectory tracking of robot manipulators. At the first stage, the acceleration term is included in existing controller structure (3.1) for relatively noise free situation which permits acceleration measurements [16], [17],[23], [24], [49], [62]. Under this, controller gets more information about the system dynamics and reduction of the controller- system mismatch is possible. Secondly, a nonlinear compensator is used in existing controller structure (3.3) with three different forms of sliding surfaces for three slightly different controller structures. The state error trajectories are forced to enter into sliding modes with low value of controller gain. The nonlinear feedback compensation term takes part in compensating the additional error caused by the replacement of actual system trajectory to desired reference trajectory in model-based linear-in-parameterization (regressor) term. Thirdly, a bounded form of controller structure is proposed with the following aims : (i) In order to make the system more robust, the parameter adaptation can be prevented from going out of bounds if each parameter is known within some bounds [28]. (ii) The convergence of control law depends on the choice of feedback gain proportional to maximum tracking error. If the tracking error exceeds this limit, convergence is no longer guaranteed [53], [66].

The objective of the proposed controller structures are to satisfy the fundamental requirements to improve the trajectory tracking performance of robot manipulators. The problem addressed in the proposed scheme is the construction of control law 'τ' that causes the robot position and velocity to track r and $\dot{r}$ asymptotically, that is, $q \rightarrow r$, $\dot{q} \rightarrow \dot{r}$, respectively.

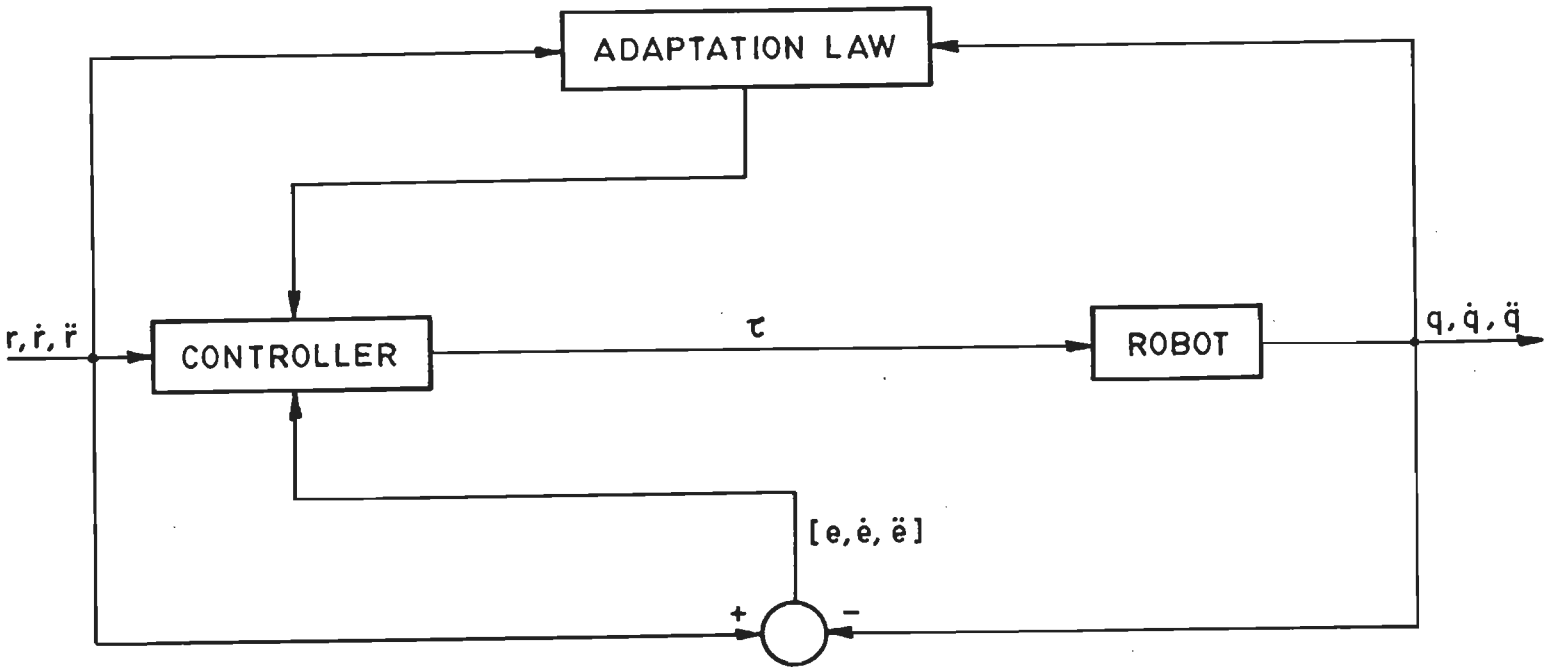

Fig. 3-1 Structure of the Robot Control System Using Acceleration Term

3.2.1 Proposed Adaptive Controller Structure Using Acceleration term

In this section, an adaptive controller structure is presented by combining the idea of [24], [84], and assumptions of [17] for relatively noise free environment (Fig. 3.1).

Defining $e_1 = r - q$, $e_2 = \dot{r} - \dot{q}$, where q and $\dot{q}$ are actual position and velocity vector respectively, the adaptive controller is considered as

$$\begin{aligned}\tau &= \hat{M}(q)\,\ddot{r} + \hat{C}(q,\dot{q})\dot{r} + \hat{g}(q) + K_1 e_1 + K_2 e_2 + K_3(\ddot{r} - \ddot{q}) \\ &= W(q,\dot{q},\dot{r},\ddot{r})\;\hat{\theta} + K_1 e_1 + K_2 e_2 + K_3(\ddot{r} - \ddot{q})\end{aligned} \tag{3.5}$$

where $\hat{M},\hat{C}$ and $\hat{g}$ are estimated value of M,C, and g, respectively, which are evaluated by adaptation law (3.6), and $K_i = K_i^T > 0$, $i = 1,2$. The desired trajectory $r,\dot{r},\ddot{r}$ are known in advance. $\hat{\theta}$ are adjusted according to the following adaptation law, which is derived in Appendix-I using Lyapunov direct method as

$$\dot{\hat{\theta}} = kg\; W^T(q,\dot{q},\dot{r},\ddot{r})\; P(q)^T(e_2 + \epsilon\,(e_1)e_1) \tag{3.6}$$

where $kg = kg^T > 0$, $P(q) = \hat{M}(q)\,[K_3 I + \hat{M}(q)]^{-1}$ and

$\epsilon(e_1) = \dfrac{\epsilon_o}{1 + \|e_1\|} \equiv \epsilon$, I = identity matrix with ϵ_o a positive constant, and $\|.\|$ is the Euclidean norm.

3.2.1.1 Error System Formulation

Applying control law 'τ' (3.5) to robot system (3.7), the error system results which is used in Lyapunov stability to obtain the adaptation law. In the absence of friction and other disturbances, consider a standard n-degrees of freedom rigid robot model of the form (1.2):

$$M(q)\,\ddot{q} + \dot{C}(q,\dot{q})\dot{q} + g(q) = W(q,\dot{q},\ddot{q})\,\theta^{*} = \tau,\ q \in R^{n} \qquad (3.7)$$

From (3.5) and (3.7), it follows (in error state-space form) by choosing state $e = e_1$ and $\dot{e} = e_2$:

$$\dot{e}_1 = e_2$$
$$\dot{e}_2 = -\,M'^{-1}\,[C(q,\dot{q})\,e_2 + K_1 e_1 + K_2 e_2 + W(q,\dot{q},\dot{r},\ddot{r})\,\tilde{\theta}\,] \qquad (3.8)$$

where, $M' = [\hat{M}(q) + K_3 I]$, $\tilde{\theta} = \hat{\theta} - \theta^{*}$ denotes the parameter error vector whose adjustment over time must be established in such a way that $e_1 \rightarrow 0$ as if θ^{*} were known.

Assuming small ϵ_o

$$\epsilon_o \leq [\,\lambda_m(K_1)\,\lambda_m(M)]^{1/2} / \lambda_M(M) \qquad (3.9)$$

where,

$$\lambda_m(K_1) \leq \|K_1\| \leq \lambda_M(K_1)$$
$$\lambda_m(K_2) \leq \|K_2\| \leq \lambda_M(K_2)$$

$\lambda_m(.)$ and $\lambda_M(.)$ denote the minimum and maximum eigen value, respectively. $\lambda_m(M)$, $\lambda_M(M)$ and C_M are described as $0 < \lambda_m(M) \leq \|M(q)\| \leq \lambda_M(M)$; $\|C(q,x)\| \leq C_M \|x\|$, for all x. K_3 is chosen as a constant diagonal matrix (may be time varying, [24]), such that

$$\lambda_m(K_3) \leq \|K_3\| \leq \lambda_M(K_3) \qquad (3.10)$$

The upper and lower bounds of these parameters are used to prove the asymptotic stability of the proposed scheme in the sense of the Lyapunov.

3.2.1.2 Stability of the Control Scheme

In order to show the closed-loop system is globally convergent and stable in the sense that tracking error will converge to zero asymptotically with all other signals remaining bounded, consider the Lyapunov function candidate, which is given in [84], as

$$V = \frac{1}{2} e_1^T K_1 e_1 + \frac{1}{2} e_2^T M(q)\, e_2 + \epsilon\, e_1^T M(q)\, e_2 + \frac{1}{2} \tilde{\theta}^T kg^{-1}\, \tilde{\theta}$$

$$= \frac{1}{2} e^T \begin{bmatrix} K_1 & \epsilon M \\ \epsilon M & M \end{bmatrix} e + \frac{1}{2} \tilde{\theta}^T kg^{-1}\, \tilde{\theta}$$

$$= \frac{1}{2} e^T P_n\, e + \frac{1}{2} \tilde{\theta}^T kg^{-1}\, \tilde{\theta} \qquad (3.11)$$

Taking the time derivative of (3.11) along the trajectories (3.8), we find (see Appendix - I, (a1.11))

$$\dot{V} \leq - \epsilon\, \lambda_m (Q_n)\, \|e\|^2 \qquad (3.12)$$

where, $e^T = [\, e_1^T \;\; e_2^T \,]$ and

$$Q_n \triangleq \begin{bmatrix} \lambda_m(P).\lambda_m(K_1) & -\frac{1}{2}[\lambda_M(P) + 2]C_M\rho_1 + \frac{1}{2}\lambda_M(P)\lambda_M(K_2) \\ & + \frac{1}{2}[(\lambda_M(P)-1)\,\epsilon_o^{-1}\,\lambda_M(K_1)] \\ -\frac{1}{2}[\lambda_M(P) + 2]C_M\rho_1 + \frac{1}{2}\lambda_M(P).\lambda_M(K_2) & \frac{1}{2\epsilon_o}\lambda_m(P).\lambda_m(K_2) \\ + \frac{1}{2}[(\lambda_M(P)-1)\,\epsilon_o^{-1}\,\lambda_M(K_1)] & \end{bmatrix} \qquad (3.13)$$

and $\underset{t\in R}{\text{Sup}} \left\| \frac{d^i r}{dt^i} \right\| = \rho_i < \infty \ , \ i = 0,1,2.$

$\dot{V}$ is nonpositive. This shows that $e \in L_2^{2n} \cap L_\infty^{2n}$ and $\tilde{\theta} \in L_\infty^r$ [59]. In other words, if both side of (3.12) is integrated, it is seen that $\sqrt{\in}\|e\|$ is square integrable function [53]. Thus e is also a square integratable function, but square integratable function whose derivative is bounded must tend to zero, hence, $\lim_{t\to\infty} \|e\| \to 0$. This shows tracking error converge to zero asymptotically.

In the Lyapunov synthesis, the Lyapunov function is regarded as the defining distance from the origin in the error state-space, and its derivative gives a quantitative estimate of the speed that the state error is approaching the closed region including the origin with respect to the parameter variation. The convergence speed is calculated by $-\dot{V}/V$, hence the settling time [45].

From equation (3.12) and (3.11), one can find (see Appendix-I for details)

$$\frac{-\dot{V}(e)}{V(e)} \geq 2 \left[\in \lambda_m((Q_n)P_n^{-1}) - \frac{\beta_2 \Delta^3 \|e_{2o}\|^3 - \beta_1 \Delta^2 \|e_{2o}\|^2}{r_f^2 \lambda_m(P_n)} \right]$$

$$\geq 2 \, [S1\text{-}T1(e_{2o}, r_f)] \qquad (3.14)$$

Equation (3.14) implies that

$$V(e) \leq Ve(o) e^{-2(S1-T1)(t-t_o)} \qquad (3.15)$$

$$\text{i.e.} \quad \|e\| \leq \Delta \|e_o\| \, e^{-2(S1-T1)(t-t_o)} \qquad (3.16)$$

It states that the exponential convergence rate of trajectory e(t) towards a ball $S(r_f)$ is at least (S1-T1). It follows that the maximum time needed to settle in a ball $S(r_f)$; $r_f > r_m$, is given (S1-T1 > 0) by

$$T(\epsilon, e_o, e_{2o}, r_f) = \frac{1}{S1\text{-}T1(e_{2o}, r_f)} \quad \ln \left| \frac{\Delta \, \|e_o\|}{r_f} \right| \tag{3.17}$$

The rate of convergence depends upon the proper choice of matrix Q_n. The region of attraction is given by (Appendix-I)

$$\|x\| < \sqrt{\frac{L_m}{L_M}} \left\{ \left[\frac{2\lambda_m(P)(\lambda_m(K_1)\ \lambda_m(K_2))^{1/2} - \lambda_M(P)\ \lambda_M(K_2) - [\lambda_m(P)-1]\ \epsilon_o^{-1}\ \lambda_M(K_1)}{(\lambda_M(P)\ +2)\ C_M} \right] - k_c \right\} \tag{3.18}$$

The size of the region of attraction can be enlarged by increasing the gain constant K_2 and keeping K_3 small. Large region of attraction may be found out in comparison to [84].

3.2.1.3 Discussions

(i) The matrix K_3 is incorporated to ensure that the inversion of $[\hat{M}(q) + K_3 I]$ remains bounded. With this choice, the stability of closed-loop systems has been established. The matrix K_3 is equal to a constant diagonal matrix. By doing so the matrix $[\hat{M}(q) + K_3 I]$ will always be invertible for all times. Therefore, the boundedness of joint accelerations could be expected. It is evident from (3.6) that the present estimate of parameters depend upon the previous estimate of inertia matrix so that convergence of parameter errors to zero (close to zero) is possible provided that proper initial parameters are chosen.

(ii) The conditions for stability (Appendix -I) show that the constant ϵ_o significantly affects the adaptation speed and it depends on the desired velocity trajectory ρ_1. In other words, ϵ_o upper bounds the convergence rate.

(iii) Usually robot motion is associated with three variables i.e. position, velocity and acceleration. It is supposed here that the measurement of joint accelerations are available. Although, It is true that the acceleration measurements may be corrupted with noise, for relatively noise free situation one can still assume the availability of joint accelerations.

(iv) The region of attraction of Whitcomb et.. al.[84] is derived as

$$\|x\| < \sqrt{\frac{L_m}{L_M}} \left\{ \frac{2}{3} \left[\frac{(2\lambda_m(K_1)\ \lambda_m(K_2))^{1/2} - \lambda_M(K_2)}{\lambda_M(M')} \right] - k_c \right\}$$

3.2.2 Proposed Adaptive Controller Structure Using Nonlinear Compensator and Sliding Surface

Adaptive controller structures are constructed here by combining the idea of [7], [64],[73],[84] with different forms of sliding surfaces for trajectory tracking of robot manipulators(Fig. 3.2).

(i) Case -1

Let the control law be given as

$$\tau = \hat{M}(q)\ (\ddot{r} - \lambda_o \dot{e}) + \hat{C}(q,\dot{q}-\lambda\ e)\ (\dot{r} - \lambda_o e) + \hat{g}(q) - \lambda_o K_2 e - K_2 \dot{e} - \sigma_{n1} \|e\|^2 S_1$$

$$= W(q,\dot{q}-\lambda e,\ \dot{r}-\lambda_o e,\ \ddot{r}-\lambda_o \dot{e})\ \hat{\theta} - \lambda_o K_2 e - K_2 \dot{e} - \sigma_{n1} \|e\|^2 S_1 \qquad (3.19)$$

where $e = q - r$; $S_1 = \dot{e} + \lambda_o e$; $K_2 = K_2^T > 0$; $\lambda \equiv \frac{\lambda_{o1}}{1+\|e\|}$; $\hat{M}$, $\hat{C}$, $\hat{g}$ are estimated value of M,C and g, respectively.

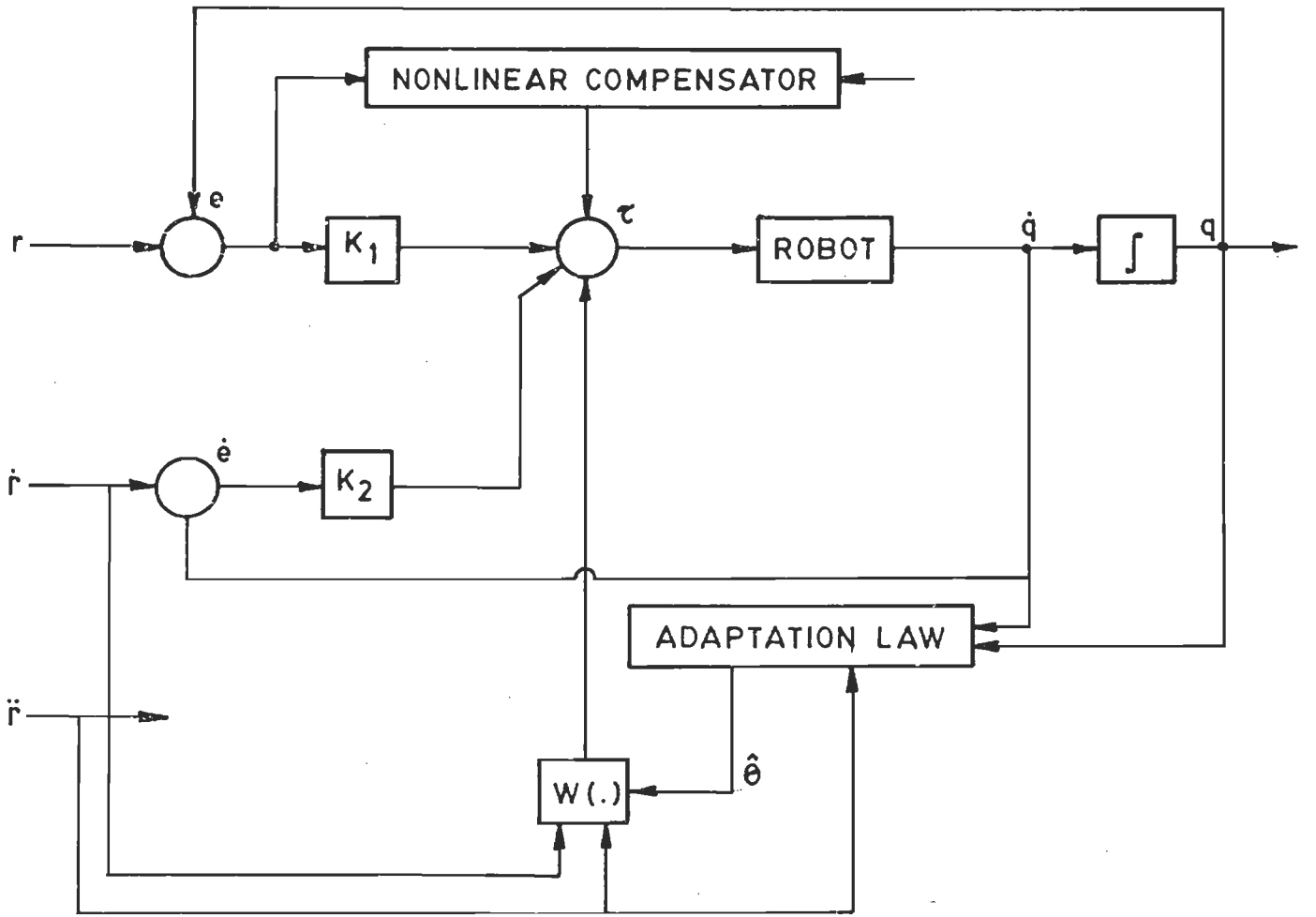

Fig. 3.2 Block diagram of Robot Control Using Nonlinear Compensator

The control law incorporates the sliding surface S_1, by replacing the desired trajectory by virtual reference trajectory, represented as [73]

$$q_r = r - \lambda_o \int_o^t e\, dt \tag{3.20a}$$

$$\dot{q}_r = \dot{r} - \lambda_o e \tag{3.20b}$$

$$\ddot{q}_r = \ddot{r} - \lambda_o \dot{e} \tag{3.20c}$$

$$S_1 = \dot{q} - \dot{q}_r = \dot{q} - \dot{r} + \lambda_o e = \dot{e} + \lambda_o e \tag{3.20d}$$

The adaptation law (3.2) are derived via the Lyapunov stability criterion given in Appendix - II (a2.9) as

$$\dot{\hat{\theta}} = -kg\, W^T(q, \dot{q} - \lambda e, \dot{r} - \lambda_o e, \ddot{r} - \lambda_o \dot{e})\, (\dot{e} + \lambda_o e) \tag{3.21}$$

The idea of [13] is used to construct the sliding surface S_1. The constant λ_o is able to bound the position error in order to lie on the sliding surface S_1. The $\hat{\theta}$ incorporates the estimated value of M, C and g. The nonlinear compensator feedback term is caused by the additional error in linear-in-parameterization formulation. The idea of [64], applying MVT (mean value theorem), is incorporated in order to show that the additional error is bounded by S_1 and e(see Appendix - 2). It is assumed that $\sigma_{n1} > 0$ and $\lambda_{o1} \neq \lambda_o$.

(iii) Case- 2

In this structure an adaptive controller, slightly different form in comparison to case - 1 by approximation of $(\dot{r} - \lambda_o \dot{e})$ to $\dot{r}$ i.e. $\dot{q}_r$ is approximated by $\dot{r}$, is considered. The control law is given as

$$\tau = \hat{M}(q)\,(\ddot{r} - \lambda_o \dot{e}) + \hat{C}(q,\dot{q}-\lambda e)\,\dot{r} + \hat{g}(q) - K_1 e - K_2 \dot{e} - \sigma_{n2}\|e\|^2 S_2 \quad (3.22)$$

$$= W(q,\dot{q}-\lambda e,\dot{r},\ddot{r}-\lambda_o \dot{e})\,\hat{\theta} - K_1 e - K_2 \dot{e} - \sigma_{n2}\|e\|^2 S_2 \quad (3.23)$$

where $e = q-r$; $S_2 = \lambda_o \dot{e} + \lambda e$; $K_1 = K_1^T > 0$; $K_2 = K_2^T > 0$; $\lambda \equiv \frac{\lambda_{o1}}{1+\|e\|} = \frac{\lambda_o}{1+\|e\|}$;

In this case, it is assumed that $\lambda_{o1} = \lambda_o$.

The adaptation law is derived in Appendix-II as

$$\dot{\hat{\theta}} = -\lambda_o kg\, W^T(q,\dot{q}-\lambda e,\dot{r},\ddot{r}-\lambda_o \dot{e})\,(\lambda_o \dot{e} + \lambda e) \quad (3.24)$$

The constant λ_o affects significantly the speed of parameter estimation. kg is any positive definite diagonal matrix.

(iii) Case - 3

In this case, the form of control law is the addition of nonlinear feedback term to algorithm of [7]. The virtual reference trajectories [73] are completely approximated by desired reference trajectory. The control law is given as

$$\tau = \hat{M}(q)\,\ddot{r} + \hat{C}(q,\dot{q}-\lambda e)\,\dot{r} + \hat{g}(q) - K_1 e - K_2 \dot{e} - \sigma_{n3}\|e\|^2 S_3 \quad (3.25)$$

$$= W(q,\dot{q}-\lambda e,\dot{r},\ddot{r})\,\hat{\theta} - K_1 e - K_2 \dot{e} - \sigma_{n3}\|e\|^2 S_3 \quad (3.26)$$

where $e = q-r$; $S_3 = \dot{e} + \lambda e$; $K_1 = K_1^T > 0$; $K_2 = K_2^T > 0$; $\lambda \equiv \frac{\lambda_{o1}}{1+\|e\|}$;

The nonlinear compensator is used in control law due to additional error $W(q,\dot{q},\dot{q},\dot{q}) - W(q,\dot{q}-\lambda e,\dot{r},\ddot{r})$ which is bounded by S_3 and e (Appendix - II).

The adaptation law derived in Appendix - II, in order to estimate M,C, and g, is obtained as

$$\dot{\hat{\theta}} = -kg\, W^T(q,\dot{q}-\lambda e,\dot{r},\ddot{r})\,(\dot{e} + \lambda e) \quad (3.27)$$

where kg is any symmetric positive definite diagonal matrix.

3.2.2.1 Error System Formulation

The dynamic equation of rigid robot model is expressed by (3.7). The function W(.) represent the linear-in-parameterization as Craig et. al. [17]. In order to derive an adaptation law using the Lyapunov direct method, the error system is required. It gives the information that how error trajectories are converge to zero asymptotically

(i) For Case - 1

From eq. (3.7) and (3.19), the error equation results obtained as

$$M(q)\ddot{e} + \lambda_o M(q)\dot{e} + C(q,\dot{q})\dot{e} + \lambda C(q,e)\dot{r} + \lambda_o C(q,\dot{q}-\lambda e)e + \lambda_o K_2 e + K_2\dot{e} + \sigma_{n1}\|e\|^2 S_1$$

$$= W(q,\dot{q}-\lambda e,\ \dot{r}-\lambda_o e,\ \ddot{r}-\lambda_o \dot{e})\ \tilde{\theta} \qquad (3.28)$$

where,

$$\tilde{\theta} = \hat{\theta} - \theta^* \qquad (3.29)$$

The vector S_1 gives the information about boundedness and convergence of q and $\dot{q}$. It can be seen as a stable first order differential equation in 'e' with S_1 as an input. Thus for bounded initial conditions, boundedness of S_1 implies boundedness of e and $\dot{e}$. If $S_1 \rightarrow 0$ as $t \longrightarrow \infty$, so do $e \rightarrow 0$ and $\dot{e} \longrightarrow 0$ [64].

(ii) For Case - 2

Substituting (3.23) into (3.7), we get the error equation

$$M(q)\ \ddot{e} + \lambda_o M(q)\dot{e} + C(q,\dot{q})\dot{e} + \lambda C(q,e)\dot{r} + K_1 e + K_2\dot{e} + \sigma_{n2}\|e\|^2 S_2$$

$$= W(q,\dot{q}-\lambda e,\ \dot{r},\ \ddot{r}-\lambda_o \dot{e})\ \tilde{\theta} \qquad (3.30)$$

Since the S_2 is define as a function of the constant λ_o, which bounds the position error and velocity error to lie on the sliding surface S_2. Following the same type of arguments as in section 3.2.2., for sliding surface, it observed that if $S_2 \longrightarrow 0$ as $t \longrightarrow \infty$, so do $e \longrightarrow 0$ and $\dot{e} \longrightarrow 0$

(iii) For Case - 3

The error equation may be obtained, by substituting (3.25) into (3.7), as

$$M(q)\,\ddot{e} + C(q,\dot{q})\dot{e} + \lambda C(q,e)\dot{r} + K_1 e + K_2 \dot{e} + \sigma_{n3}\|e\|^2 S_3 = W(q,\dot{q}-\lambda e, \dot{r}, \ddot{r})\,\tilde{\theta} \qquad (3.31)$$

Where $\tilde{\theta}$ is defined in section 3.2.2. σ_{n3} is a positive constant. Prominently, the error equation drives the stability analysis in the sense of Lyapunov.

3.2.2.2 Stability of Control Schemes

The following physical properties are consider as

$$0 \le M_m \le \|M(q)\| \le M_M$$

$$\|C(q,\dot{q})\| = C_M (\|e\| + \rho_1)$$

$$\lambda_{o1} < \min \left[\frac{\lambda_m(K_2)}{3M_M + 2C_M} , \frac{4\lambda_m(K_2)}{\lambda_m(K_2) + \lambda_M(K_2)} \right]$$

$$\lambda_m(K_1) \le \|K_1\| < \lambda_M(K_1)$$

$$\lambda_m(K_2) \le \|K_2\| < \lambda_M(K_2) \qquad (3.32)$$

where, $\lambda_m(.)$ and $\lambda_M(.)$ denote the minimum and maximum eigen values. In other words, the upper and lower bounds on these parameters are required for stability analysis. The stability proof of the scheme is considered by choosing the Lyapunov function candidate and taking the derivative along the respective error trajectories.

(i) For Case -1

Recalling the Lyapunov function candidate (Appendix-II, (a2.1))

$$V = \frac{1}{2} S_1^T M(q) S_1 + \frac{1}{2} e^T K_2 e + \frac{1}{2} \tilde{\theta}^T kg^{-1} \tilde{\theta} \qquad (3.33)$$

Taking the derivative of the Lyapunov function along the error trajectories (3.28), we find (see Appendix-II)

$$\dot{V} \leq -\lambda_o \begin{bmatrix} \|S_1\| \\ \|e\| \end{bmatrix}^T \lambda_m(Q_1) \begin{bmatrix} \|S_1\| \\ \|e\| \end{bmatrix} \qquad (3.34)$$

$\dot{V}$ is a nonpositive function bounded as from (3.33) that S_1, $e \in L_\infty^n, \dot{e}, S_1 \in L_\infty^n$. Now, because $\lambda \in L_\infty$ we conclude from (3.34) that S_1, $e \in L_2^n$. From square integrability and uniform continuity of e we conclude that it converges to zero [7].

The region of attraction (Appendix-II) is given by with $x^T = [e^T, \dot{e}^T]$

$$\|x\| < \sqrt{\frac{L_m}{L_M}} \left[\frac{-\lambda_o C_M - (\lambda_o^2 C_M^2 - 4\sigma_{n1} p)^{1/2}}{2\sigma_{n1}} \right] \qquad (3.34a)$$

where, $$p = \frac{1}{4} \frac{\left[\lambda_o C_M + \frac{\lambda_M(K_2)}{\lambda_o} \right]^2}{\lambda_m(K_2)} - \left[\frac{\lambda_o C_M + \lambda_m(K_2)}{\lambda_o} \right]$$

Decreasing σ_{n1} one can enlarge the region of attraction. The right side of (3.34a) is positive by hypothesis (a2.7). Large region of attraction can be find out in contrast to [7] by proper choice of initial conditions and parameter.

(ii) For Case -2

The Lyapunov function candidate is considered as

$$V = \frac{1}{2} S_2^T M(q) S_2 + \frac{1}{2} e^T K_1 e + \frac{1}{2} \tilde{\theta}^T k g^{-1} \tilde{\theta} \qquad (3.35)$$

The time derivative of (3.35) along the error trajectories (3.30), we find (see Appendix - II)

$$\dot{V} \leq - \begin{bmatrix} \|S_2\| \\ \|\lambda e\| \end{bmatrix}^T \lambda_m(Q_2) \begin{bmatrix} \|S_2\| \\ \|\lambda e\| \end{bmatrix} \tag{3.36}$$

$\dot{V}$ is nonpositive. Global convergence follows from the same type of arguments used in case-1.

Similarly, one can get the region of attraction (Appendix -II)

$$\|x\| < \sqrt{\frac{L_m}{L_M}} \left\{ \left[\frac{-2(((\lambda_m(K_2)((\lambda_o-1)/\lambda_o)\ C_M + \lambda_o C_M)^{1/2})\ \frac{\lambda_o-1}{\lambda_o} - \frac{1}{2}\lambda_M(K_2))}{(\lambda_o-1)\ C_M} \right] \frac{1}{2}(\lambda_o-1)\lambda_o C_M - k_c \right\} \tag{3.36a}$$

where $\|\dot{q}\| \leq k_c$. The region of attraction can be enlarged by increasing K_2 and keeping low value of λ_o. The right hand side of (3.36a) is positive by virtue of hypothesis (a2.21)

(iii) For Case-3

The Lyapunov function candidate is given as

$$V = \frac{1}{2} S_3^T M(q)\ S_3 + \frac{1}{2} e^T K_1\ e + \frac{1}{2}\ \tilde{\theta}^T\ kg^{-1}\ \tilde{\theta} \tag{3.37}$$

In Appendix-II, the derivative of the Lyapunov function (3.37) along the error trajectories (3.31), it is found as

$$\dot{V} \leq - \begin{bmatrix} \|S_3\| \\ \|\lambda e\| \end{bmatrix}^T \lambda_m(Q_3) \begin{bmatrix} \|S_3\| \\ \|\lambda e\| \end{bmatrix} \tag{3.38}$$

$\dot{V}$ is nonpositive. Global convergence follows from the same type of arguments used in case-1.

The region of attraction is determined as (Appendix - II)

$$\|x\| < \sqrt{\frac{L_m}{L_M}} \left[\frac{\frac{1}{2}\left[\lambda_M(K_2) + (\rho_1 + \lambda_o) C_M\right]}{(\lambda_o^{-1} \lambda_m(K_1))^{1/2}} - \frac{[\lambda_m(K_2) - \lambda_o C_M - 2\lambda_o M_M]^{1/2}}{\sqrt{\sigma_{n3}}} \right] \quad (3.38a)$$

The upper bound on K_2 if increased keeping σ_{n3} lower value, the region of attraction can be enlarged. By virtue of hypothesis (a 2.32), the right hand side of (3.38a) is positive.

3.2.2.3 Discussions

(i) The design parameter λ_o and λ_{o1} have different value in case -1 (see also [28]). λ_o takes part to bound the position error to lie on the sliding surface and λ_{o1} is the measure of robustness to noise sensitivity properties.

(ii) In case-2, the constant λ_o appears in adaptation law, which slow down the speed of estimation causes the reduction of difference between rate of change of inertia matrix and rate of change of parameter adaptation,if $\lambda_o < 1$.

(iii) In case-1 and case-2, the term $\lambda_o M(q) \dot{e}$, reduces the discontinuities due to acceleration and caused by formation of virtual reference trajectory as clear from (3.18) and (3.22) respectively.

(iv) The condition by which position error lie on sliding surface is derived as:

$$S_1 = 0 \Rightarrow \lambda_o \leq \|\dot{e}\|/\|e\|$$

$$S_2 = 0 \Rightarrow \|\dot{e}\| \leq \frac{\|e\|}{1+\|e\|}$$

$$S_3 = 0 \Rightarrow \lambda_o < \frac{\|\dot{e}\| (1+\|e\|)}{\|e\|}$$

(v) The λ factor is needed in controller to be able to bound the cubic term, $S_i C(q,\dot{e})\, e$, $i = 1,2,3$ by quadratic terms. If $\dot{V}$ is evaluated, an additional term $e^T \dot{M}(q)e$ is obtained. Using the skew symmetric properties this amounts to an extra term in $e^T C(q,\dot{q})e$. This term cannot be compensated by the control and can only be bounded in terms of e and $\dot{e}$ with a bound on $\dot{r}$ [7].

(vi) The region of attraction for [7] is derived with $x^T = [e^T, \dot{e}^T]$;

$$\|x\| < \sqrt{\frac{L_m}{L_M}} \left\{ 2 \left[\frac{(\lambda_m(K_2) - \lambda_o C_M - 2\lambda_o M_M)\ \lambda_o^{-1}\lambda_m(K_1))^{1/2} - \frac{1}{2}\lambda_M(K_1)}{C_M} \right] - \frac{1}{2}\lambda_o C_M \right\}$$

The large region of attraction can be found for case-1 and case-2 while comparing [7] but case-3 have lower value.

3.2.3 Proposed Adaptive Controller Structure in Bounded Form

A bounded form of adaptive controller structure is presented in this section. The control scheme in bounded form consists of PD controller as feedforward to ensure trajectory tracking, reference trajectory information based linear-in-parameter (regressor) term multiplied by unknown parameter vector and nonlinear feedback compensator. The bounded form of controller structure, coefficients M_M and C_M bound the actual system dynamics, is considered for stable control. The unknown parameters belong to some interval θ_{min} and θ_{max} and take the supremum of M_M, C_M over these intervals [7].

Consider the control law inspired by [7] , [64], given in bounded form as

$$\begin{aligned} \tau &= \|\hat{M}(q)\|\, \ddot{r} + \|\hat{C}(q,\dot{q}-\lambda e)\|\, \dot{r} + \hat{g}(q) - K_1\|e\| - K_2\|\dot{e}\| - \sigma_n\|e\|^2 S \\ &= W(\|\dot{q}-\lambda e\|, \dot{r}, \ddot{r})\|\hat{\theta}\| - K_1\|e\| - K_2\|\dot{e}\| - \sigma_n\|e\|^2 S \end{aligned} \qquad (3.39)$$

where $e = q - r$; $S = \dot{e} + \lambda e$; $K_1 = K_1^T > 0$; $K_2 = K_2^T > 0$; $\lambda \equiv \frac{\lambda_o}{1 + \|e\|}$; The desired trajectories are known in advance. The auxiliary nonlinear feedback term is to compensate for the additional error introduced by the modification of the adaptive controller i.e. $[W(q,\dot{q},\dot{q},\dot{q}^{\cdot}) - W(\|\dot{q}-\lambda e\|,\dot{r},\dot{r}^{\cdot})]\theta$ [64]. The bounded control input is applied to system dynamics of robot manipulator, as a result, 'q' becomes bounded.

The bounded parameter $\|\hat{\theta}\|$, adjusted according to adaptation law, is derived in Appendix - III, as

$$\dot{\tilde{\theta}} = -kg\ W^T(\|\dot{q}-\lambda e\|,\ \dot{r},\ \dot{r}^{\cdot})\ (\dot{e} + \lambda e) \tag{3.40}$$

$$\|\hat{\theta}\| = \tilde{\theta} + \theta^*(q)$$

where $kg = kg^T > 0$, $\|.\|$ is defined as Euclidean norm. kg is any positive definite constant matrix. λ factor takes part to lie the error trajectory on the sliding surface and as well as to robustify the scheme in presence of noisy velocity.

3.2.3.1 Error System Formulation

The dynamic equation of rigid robot model is expressed by (3.7). Substituting (3.39) into (3.7), the error equation obtained as

$$M(q)\ \dot{e}^{\cdot} + C(q,\dot{q})\dot{e} + K_1\ \|e\| + K_2\ \|\dot{e}\| + \sigma_n \|e\|^2 S = W(\|\dot{q}-\lambda e\|,\dot{r},\ \dot{r}^{\cdot})\ \tilde{\theta} \tag{3.41}$$

Where, $\tilde{\theta} = \|\hat{\theta}\| - \theta^*(q)$ denotes the parameters vector whose adjustment over time must be established in such a way that $\|e\| \longrightarrow 0$ as $t \rightarrow \infty$.

3.2.3.2 Stability of Control Scheme

The Lyapunov direct method is used to proof the stability of the bounded form of adaptive control scheme. The physical properties are follows as described by (3.32).

Now, consider the Lyapunov function candidate

$$V = \frac{1}{2} S^T M(q) S + \frac{1}{2} e^T K_1 e + \frac{1}{2} \tilde{\theta}^T kg^{-1} \tilde{\theta} \qquad (3.42)$$

Taking the time derivative of the Lyapunov function along (3.41), we get (see Appendix-III)

$$\dot{V} \leq - \begin{bmatrix} \|S\| \\ \|\lambda e\| \end{bmatrix}^T \lambda_m(Q) \begin{bmatrix} \|S\| \\ \|\lambda e\| \end{bmatrix} - \sigma_n \|e\|^2 \|S\|^2 \qquad (3.43)$$

$\dot{V}$ is nonpositive function bounded as from (3.42) that S, $e \in L_\infty^n$, $\dot{e}$, $S \in L_\infty^n$. Now, because $\lambda \in L_\infty$ it is concluded from (3.43) that S, $e \in L_2^n$. If $\|\hat{\theta}\| - \theta^*$ and S are bounded $t = 0$, they remain bounded for all $t \geq 0$. To complete the proof, it is necessary to show $S \rightarrow 0$, $e \rightarrow 0$ as $t \rightarrow \infty$. This can be accomplished by applying Barbalat's lemma to continuous, nonnegative function:

$$V_1 = V - \int_0^t (\dot{V}(\zeta) + (S'^T(\zeta) \lambda_m(Q) S'(\zeta) + \sigma_n \|e\|^2 \|S\|^2) \, d\zeta$$

with

$$\dot{V}_1 = - S'^T \lambda_m(Q) S' - \sigma_n \|e\|^2 \|S\|^2$$

since the boundedness of S′ implies that all signals are bounded, hence $\dot{S}$ is bounded, that in turn proves V_1 to be uniformly continuous function of time. Since V_1 is bounded below by 0, and $\dot{V}_1 \leq 0$ for all t, use of Barbalat's lemma proves that $\lim_{t \rightarrow \infty} \dot{V}_1 = 0$, which implies $\lim_{t \rightarrow \infty} S' = 0$. The region of attraction is expressed by (3.38a).

3.2.3.3 Discussions

(i) The estimation is the upper bound of the parameter rather than parameter itself. Therefore, the requirement of persistency of excitation is avoided

and the problems inherent to integral adaptation law, such as the "Parameter drift instability" do not appear.

(ii) In contrast to Craig et. al. [17], θ^* is assumed as a function of joint position ($\theta^*(q)$) so that the coefficients M_M and C_M bound the actual system dynamics.

(iii) If each parameter is known within some bounds, the parameter adaptation can be prevented from going out of bounds and thus makes the system more robust [28].

(iv) The convergence of the control law depends on the choice of feedback gain proportional to maximum tracking error. If the tracking error exceeds this limit, convergence is no longer guaranteed [53],[66].

(v) In order to implement the adaptive controller, one needs to calculate the element of $W(q,\dot{q},\dot{q},\dot{q}^{\cdot})$ in real time. This procedure may be excessively time consuming since it involves computations of highly nonlinear functions of joint position and velocities. The real time implementation of such a scheme, is rather difficult. To overcome this difficulty q and $\dot{q}$ replaced by r and $\dot{r}$ respectively to form $W(\|\dot{q}-\lambda e\|,\dot{r},\dot{r}^{\cdot})$. Due to this replacement, the error may introduced. In order to compensate this form of error, an auxiliary nonlinear feedback term is included in control law [64].

Chapter - 4

SLIDING OBSERVER AIDED CONTROL STRATEGY

4.1 INTRODUCTION

In this section, the sliding observer based control strategy for robot manipulator is considered under the assumption that only joint positions, and not full state measurements (positions and velocities) are available [59]. The purpose of including a sliding observer to estimate joint velocities is to improve the tracking performance. The various approaches in literature are based on sliding observer aided adaptive control [10] and nonlinear form of sliding observer [8] for trajectory tracking of robot manipulator. The sliding observer structure of [10] is a function of observation error (position) and parameter uncertainties vector (function of bounded estimated velocity). It is also suggested that the reduction of chattering is possible by introduction of an adaptation loop at control law level. An asymptotically stable closed loop system results from this scheme. On the other hand, the nonlinear sliding observer based controller structure are found promising in view of the nonlinear nature of robot manipulator in [8]. The physical robot properties are explicitly exploited to show exponential convergence of the observation error vector. The scheme yield exponentially stable closed-loop systems (tracking error and observation error system). The Filippov's solution concept is applied so that the dynamic behavior in sliding patch is represented as an average dynamics in order to simplify the solution. Both schemes are described in subsequent subsections.

4.1.1 Controller-Observer Structure

The control law reported in [10] is given as

$$\tau = \tau_o + W(x_1, \dot{z}, \hat{\theta})\, \tilde{x}_2$$
$$= \hat{M}(x_1)\ddot{z} + \hat{C}(x_1, x_2)\dot{z} + \hat{g}(x_1) - K_D S + W(x_1, \dot{z}, \tilde{\theta})\tilde{x}_2 \qquad (4.1)$$

where,

$$\dot{z} = \dot{r} - \Lambda e \qquad (4.2)$$

$$\ddot{z} = \ddot{r} - \Lambda \dot{e} \qquad (4.3)$$

$$S = x_2 - \dot{z} = \dot{e} + \Lambda e \qquad (4.4)$$

with K_D is a positive definite constant matrix. $\tilde{x}_2 = \hat{x}_2 - x_2$ is the velocity observation error vector and x_1 the joint position vector.

The observer is given in [10] by the following differential equation with right-hand side discontinuities as

$$\dot{\hat{x}}_1 = \hat{x}_2 - \Gamma_1 \tilde{x}_1 - \Lambda_1 \operatorname{sgn}(\tilde{x}_1) \qquad (4.5a)$$

$$\dot{\hat{x}}_2 = -\Lambda_2 \operatorname{sgn}(\tilde{x}_1) - W(x_1, \dot{z}, \hat{\theta})(S' - \Lambda_1 \operatorname{sgn}(\tilde{x}_1)) + v \qquad (4.5b)$$

where $\hat{\theta}$ is the estimate of the unknown parameter vector θ. v is introduced in order to robustify the observation error dynamics vis-a-vis the uncertainties on θ.

Applying the Filippov's solution concept and the Lyapunov direct method, the following form of adaptation law and uncertainties vector are derived in [10], given as :

$$\dot{\hat{\theta}} = -\Gamma^{-1} Y(x_1, \hat{x}_2 - \Lambda_1 \operatorname{sgn}(\tilde{x}_1), \dot{z}, \dot{z}' + \Lambda\Lambda_1 \operatorname{sgn}(\tilde{x}_1))\, (S' - \Lambda_1 \operatorname{sgn}(\tilde{x}_1)) \qquad (4.6)$$

and

$$v = v(\hat{x}_2, \tau, \tilde{x}_1)$$

$$= \begin{cases} -\phi(\hat{x}_2, \tau)\Lambda_1 \operatorname{sgn}(\tilde{x}_1)/\lambda_1 & \text{if } \|\Lambda_1 \operatorname{sgn}(\tilde{x}_1)\| \neq 0 \\ 0 & \text{if } \|\Lambda_1 \operatorname{sgn}(\tilde{x}_1)\| = 0 \end{cases} \qquad (4.7)$$

where (in sliding patch),

$$S' = \hat{x}_2 - \dot{z}$$

$$S = S' - \Lambda_1 \mathrm{sgn}(\tilde{x}_1) \tag{4.8}$$

$$x_2 = \hat{x}_2 - \Lambda_1 \mathrm{sgn}(\tilde{x}_1) \tag{4.9}$$

$$\dot{z}' = \dot{z}' + \Lambda\Lambda_1^{-1} \mathrm{sgn}(\tilde{x}_1) \tag{4.10}$$

and Γ, Λ and Λ_1 are positive constant diagonal matrix.

The design consists of an adaptation law and uncertainty vector 'v' which contain discontinuities in terms of $\mathrm{sgn}(\tilde{x}_1)$, such that system dynamics asymptotically tends to zero while the error states remain bounded. The expression 'v' incorporates the term $\phi(\hat{x}_2,\tau)$ which is derived in [10] as follows:

The expression η is

$$\eta = - M(x_1)^{-1} C(x_1,x_2)x_2 - M(x_1)^{-1} g(x_1) + M(x_1)^{-1} \tau$$

then, according to the robot model properties

$$\|\eta\| \le \sigma_o \|\hat{x}_2\|^2 + \sigma_o\lambda_1 + \lambda_1^2 + \sigma_1 + \sigma_2 \|\tau\| = \phi(\hat{x}_2,\tau)$$

The scalar and positive function ϕ thus defines a measurable upper bound $\|\eta\|$.

Canudas et al. [8] presented a nonlinear sliding observer to estimate the velocities and calculate the control law for trajectory tracking of robot manipulator. The control law incorporates the desired trajectory based robot model properties and the sliding observer takes the form of robot dynamics based on estimated velocity.

The control law is given in [8] as

$$\tau = M(x_1)[\ddot{r} - K_v(\hat{x}_2 - \dot{r}) - K_p (x_1 - r) + C(x_1,\dot{r})\dot{r} + g(x_1) + \pi_o(x_1,\dot{r}) \tag{4.11}$$

where K_v and K_p are positive constant diagonal matrix. x_1 is the joint position

and $\hat{x}_2$ is the estimated velocity vector. The term $\pi_o(x_1,\dot{r})$ is based on physical model properties of robot.

The structure of the sliding observer in [8] given by the following differential equations:

$$\dot{\hat{x}}_1 = \hat{x}_2 - \Gamma_1 \tilde{x}_1 - \Lambda_1(\hat{x})\, sgn(\tilde{x}_1) \qquad (4.12a)$$

$$\dot{\hat{x}}_2 = \Gamma_2 \tilde{x}_1 - \Lambda_2(\hat{x})\, sgn(\tilde{x}_1) + \beta(x_1,\hat{x}_2) + u \qquad (4.12b)$$

where Γ_1 and Γ_2 are positive definite constant diagonal matrices. $\Lambda_1 = diag[\gamma_1^i]$ $\forall$ i = 1,2,...n, and

$$\Lambda_2(x_1, \hat{x}_2) = M(x_1)^{-1} [Q \Lambda_1 + \pi_1(x_1, \hat{x}_2)\Lambda_1] \qquad (4.13a)$$

where Q is a diagonal positive definite matrix. π_1 is defined in Appendix - VI. The dynamic behavior inside the resulting reduced order manifold is given in [8] as

$$\dot{\tilde{x}}_2 = -M(x_1)^{-1}[C(x_1,x_2) + Q]\, \tilde{x}_2 \qquad (4.13b)$$

The closed-loop analysis is performed on the basis of the reduced order manifold dynamics and the tracking error dynamics in the sense of Lyapunov. This leads to an augmented system globally asymptotically exponentially stable system. The local attraction areas are characterized in terms of controller and observer gains, initial state values and robot model parameter.

4.2 PROPOSED OBSERVER STRUCTURE

In this section, Two new sliding observer aided of adaptive controller structures are proposed by modifications in the existing sliding observer[10].

Further, two types of nonlinear sliding observer based controller structures, motivated by [10],[85], are also proposed for robot manipulators.

Firstly, the observer form of [10] is modified by incorporating the desired acceleration trajectory and uncertainties vector based on desired reference trajectory (Fig.4.1). Secondly, the observer structure is further modified by inclusion of tracking error and observation error to estimate the velocity vector in view of dynamic interaction between controller and observer. Both modified schemes are based on adaptive control to reduce chattering at control law level and also to improve the tracking performance of robot manipulators in comparison to existing work [10].

In view of nonlinear nature and coupled structure of robot system the observer design is very complex. Canudas et. al. [8] presented nonlinear form of observer by avoiding actual velocity measurements and using full system dynamic model to estimate the velocity vector for trajectory tracking of robot manipulators. In order to improve the tracking performance, the observer structure [8] is modified by inclusion of velocity observation error and e^2- term (square of tracking error) in connection to dynamic interaction between controller and observer (Fig.4.2). Because of the technology advancements controller-observer simplicity weighs less important than tracking accuracy. It is no longer prohibitive to consider a more accurate model and look for better tracking performance with a slightly more complicated controller-observer structure. It may be seen that when the controller and observer are independently designed it is not guarantee that both together yields a stable local closed-loop system behavior. Thus, they are regarded as a global control structure with their gains tuned in order to ensure asymptotic tracking of the desired trajectory.

Similarly, the nonlinear sliding observer is further modified by sign-sign function associated with observation error and tracking error. The observer

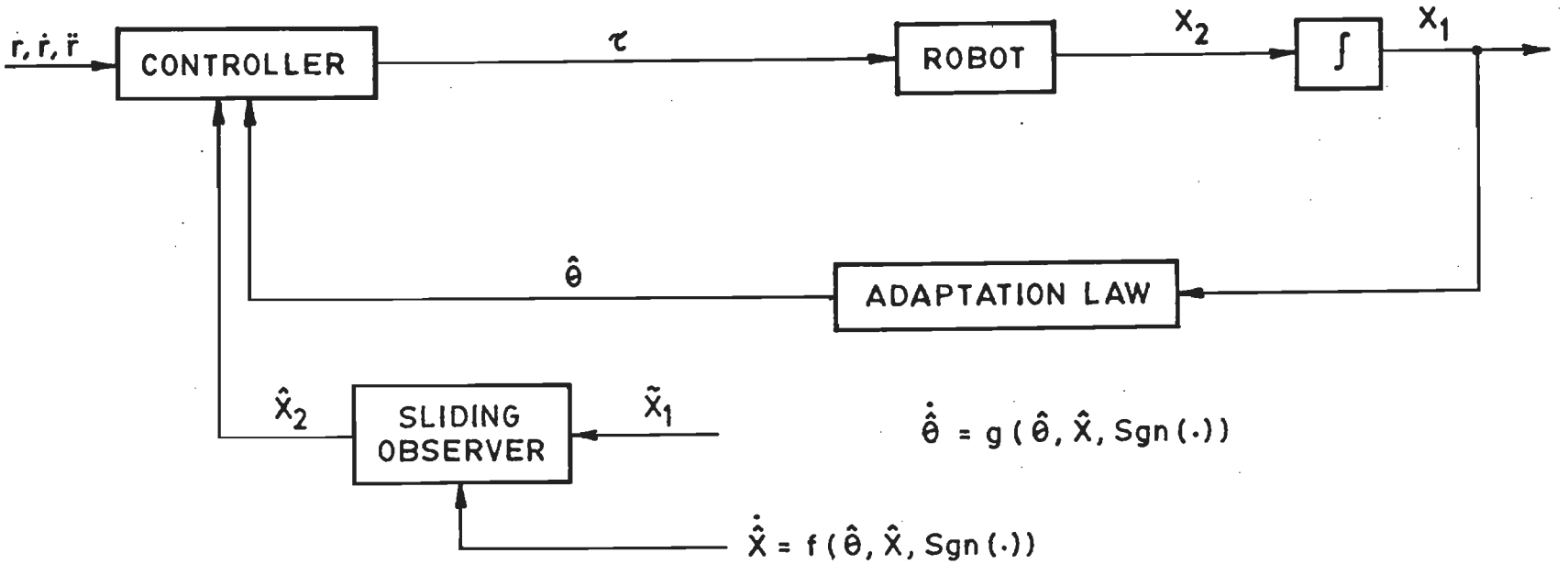

Fig. 4.1 Structure of Sliding Observer Aided Adaptive Control for Robot

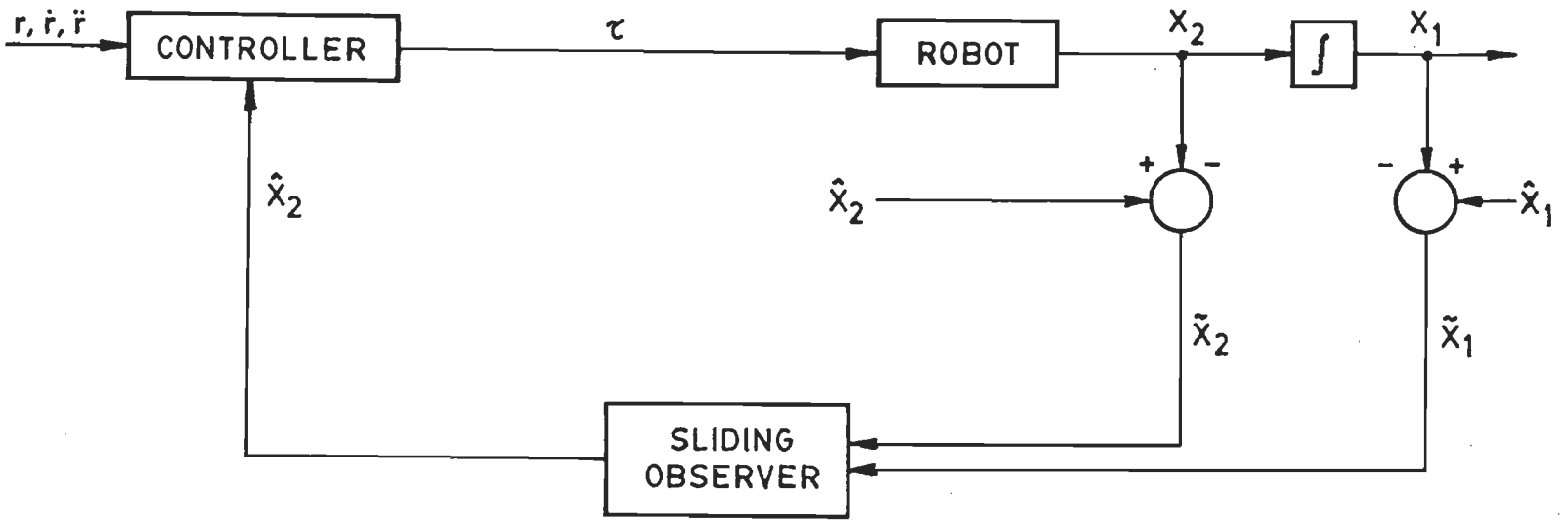

Fig. 4.2 Structure of Nonlinear Sliding Observer Aided Controller for Robot

structure is considered as Sign-Sign Algorithm(SSA). The "Sgn(.)" is usual signum function to be interpreted as element by element operator when applied to a vector. The sign operator on the velocity observation error which makes each velocity estimate to the boundary on which velocity observation error lies and is insensitive to the distance to the boundary. The sign-sign term forces the velocity observation error, according to the sign function of tracking error, to lie on the average of two-half spaces defined by reduced order manifold dynamics. This indicate that the dynamics in the manifold created by two discontinuous surfaces can be computed as the average of the dynamics of each side of the discontinuity surface and hence formally determined by the invariance of the manifold. It is possible to get good velocity estimate (or zero velocity observation error) by sign-sign term as forcing element to ensure good tracking performance.

4.2.1 Adaptive Control Using Sliding Observer with New Uncertainty Vector

In this combined scheme, the observer structure of [10] is modified by inclusion of desired acceleration trajectory information and dependence of design vector on desired reference information based robot model properties to get asymptotic stability of closed-loop system. The adaptation law, observer state and the control law are developed simultaneously. These are designed using reduced order manifold dynamics (Filippov's solution concept) [10].

Define $\tilde{x}_1 = \hat{x}_1 - x_1$ and $\tilde{x}_2 = \hat{x}_2 - x_2$ as the estimation or observation error. $\hat{x}_1$ is used only to get observation error in the sliding observer structure. $\hat{x}_1$ and $\hat{x}_2$ are the estimates of x_1 (actual position) and x_2 (actual velocity) respectively. To estimate the states x_1 and x_2, the proposed structure of sliding observer is given by following differential equation;

$$\dot{\hat{x}}_1 = \hat{x}_2 - \Gamma_1 \tilde{x}_1 - \Lambda_1 \, sgn(\tilde{x}_1) \tag{4.14a}$$

$$\dot{\hat{x}}_2 = \ddot{r} - \Gamma_2 \tilde{x}_1 - \Lambda_2 sgn(\tilde{x}_1) - W(x_1, \dot{q}_r, \hat{\theta})(S' - \Lambda_1 \, sgn(\tilde{x}_1)) + v \tag{4.14b}$$

where $\Gamma_1, \Gamma_2, \Lambda_1, \Lambda_2$ are the design matrices. The term v incorporates the uncertainties on parameter vector θ. W(.) is defined by (4.21).

The structure of control law be given as [recalling [10]].

$$\tau_1 = \hat{M}(x_1)\ddot{q}_r + \hat{C}(x_1, x_2)\dot{q}_r + \hat{g}(x_1) - K_2 S \tag{4.15}$$

where $\hat{M}(x_1)$ and $\hat{C}(x_1, x_2)$ are the estimates of $M(x_1)$ and $C(x_1, x_2)$ respectively. K_2 is a positive constant diagonal matrix. The control law incorporates the sliding surface 'S', replacing the desired trajectory by virtual reference trajectory, represented as

$$q_r = r - \Lambda \int_0^t e \, dt \tag{4.16a}$$

$$\dot{q}_r = \dot{r} - \Lambda e \tag{4.16b}$$

$$\ddot{q}_r = \ddot{r} - \Lambda \dot{e} \tag{4.16c}$$

where $e = x_1 - r$ is the tracking error vector and Λ is a positive constant diagonal matrix. One can define

$$S = \dot{q} - \dot{q}_r = \dot{e} + \Lambda e \tag{4.16d}$$

It is assumed that only joint positions are available. The vector x_2 is estimated via sliding observer structure as described by (4.14). Now, with the following definitions:

$$\ddot{q}_r' = \ddot{r} - \Lambda (\hat{x}_2 - \dot{r}) = \ddot{q}_r - \Lambda \tilde{x}_2 \tag{4.17}$$

$$S' = \hat{x}_2 - \dot{q}_r = S + \tilde{x}_2 \tag{4.18}$$

where S′ represent the error between estimated velocity vector and velocity virtual reference trajectory. Substituting (4.16) - (4.18) into (4.15) and using the properties of C(.), we get

$$\tau = \tau_1 - \hat{M}(x_1)\Lambda\,\tilde{x}_2 + \hat{C}(x_1,\dot{q}_r)\tilde{x}_2 - K_2\,\tilde{x}_2 \tag{4.19}$$

$$= \tau_1 + W(x_1,\dot{q}_r,\hat{\theta})\,\tilde{x}_2 \tag{4.20}$$

where $\hat{\theta}$ is the estimate of the unknown parameter vector and W(.) is given as

$$W = W(x_1,\dot{q}_r,\hat{\theta}) = -\hat{M}(x_1)\Lambda + \hat{C}(x_1,\dot{q}_r) - K_2 \tag{4.21a}$$

where $\hat{\theta}$, using reduced order manifold dynamics (see Appendix-IV), is adjusted as

$$\dot{\hat{\theta}} = -\Gamma^{-1}\,Y(x_1,\hat{x}_2-\Lambda_1 sgn(\tilde{x}_1),\,\dot{q}_r,\,\dot{q}_r' + \Lambda\Lambda_1\,sgn(\tilde{x}_1))\,(S'-\Lambda_1 sgn\,(\tilde{x}_1)) \tag{4.21b}$$

and

$$v = v(r,\tau,\,\tilde{x}_2,\,\dot{r}')$$

$$= \begin{cases} -[\phi(\dot{r},\tau) + \|\dot{r}'\|]\;\Lambda_1 sgn(\tilde{x}_1)/\lambda_1 & \text{if } \|\Lambda_1 sgn(\tilde{x}_1)\| \neq 0 \\ 0 & \text{if } \|\Lambda_1 sgn(\tilde{x}_1)\| = 0 \end{cases} \tag{4.21c}$$

where $\phi(\dot{r},\tau)$ is defined in subsection 4.2.1.2. It represent the ideal case to compensate the uncertainties on parameter vector. The new expression 'v' depends on the bounded terms $\dot{r}$ and $\dot{r}'$. Therefore, the bounded form of parameter uncertainties results.

4.2.1.1 Error System Formulation

The system dynamics of n-degrees of freedom rigid robot system is described by (3.7). In state-space representation, choosing $x_1 = q$, $x_2 = \dot{q}$, system model (3.7) can be expressed [10] as :

$$\dot{x}_1 = x_2 \tag{4.22a}$$

$$\dot{x}_2 = H(x_1,x_2) + \bar{M}(x_1)^{-1}\tau \tag{4.22b}$$

where,

$$H(x_1,x_2) = - \bar{M}(x_1)^{-1} [\bar{C}(x_1,x_2)x_2 + \bar{g}(x_1)] \tag{4.22c}$$

Substituting the control law in robot dynamics (3.7), we obtain

$$\bar{M}(x_1)\dot{S} + \bar{C}(x_1,x_2)\, S = \bar{M}(x_1)\, \ddot{q}_r + \bar{C}(x_1,x_2)\dot{q}_r + \bar{g}(x_1) - K_2 S + W(x_1,\dot{q}_r,\hat{\theta})\, \tilde{x}_2 \tag{4.23}$$

The dynamic behavior of sliding surface S is represented as

$$\dot{S} = \bar{M}^{-1}(x_1)[-(\bar{C}(x_1,x_2)+K_2)S + Y(x_1,x_2,\dot{q}_r,\ddot{q}_r)\tilde{\theta} + W(x_1,\, \dot{q}_r,\, \hat{\theta})\tilde{x}_2] \tag{4.24}$$

where,

$$Y = Y(x_1,x_2,\dot{q}_r,\ddot{q}_r) = \bar{M}(x_1)\ddot{q}_r + \bar{C}(x_1,x_2)\dot{q}_r + \bar{g}(x_1) \tag{4.25}$$

The observation error dynamic equation can be obtain, from (4.14) and (4.22), as

$$\dot{\tilde{x}}_1 = \tilde{x}_2 - \Gamma_1\, \tilde{x}_1 - \Lambda_1\, \mathrm{sgn}\,(\tilde{x}_1) \tag{4.26a}$$

$$\dot{\tilde{x}}_2 = \ddot{r} - \Gamma_2\, \tilde{x}_1 - \Lambda_2\, \mathrm{sgn}\,(\tilde{x}_2) - W(x_1,\, \dot{q}_r,\, \hat{\theta})(S' - \Lambda_1\, \mathrm{sgn}\,(\tilde{x}_1) + v + \eta) \tag{4.26b}$$

where, $\eta = -H(x_1,\hat{x}_2) - \bar{M}^{-1}(x_1)\tau$

These equations (4.26) together with (4.24) describe the complete closed-loop system error dynamics.

4.2.1.2 New Uncertainty Vector

In contrast to [10], the structure of η is modified by replacing the x_1 to desired joint position trajectory r and $\hat{x}_2$ to $\dot{r}$ respectively to robustify the observer error dynamics. It means that the expression 'v' (4.21c) becomes bounded due to boundedness of r and $\ddot{r}$.

Now, the term η turns into new form as

$$\eta = - M(r)^{-1} C(r,\dot{r}) \dot{r} - M(r)^{-1} [g(r) - \tau] \qquad (4.27)$$

Applying the boundedness properties on (4.27), there exists positive constants σ_o, σ_1 and σ_2, we get

$$\|\eta\| \leq \sigma_{01} \|\dot{r}\|^2 + \sigma_{11} + \sigma_{12} \|\tau\| = \phi(\dot{r},\tau) \qquad (4.28)$$

The scalar and positive function ϕ defines the upper bound on $\|\eta\|$ such that

$$\sigma_o > \|M(r)\| > 0 \; ; \; \sigma'_o > \|M(r)^{-1}\| > 0; \; \|C(r,\dot{r})\dot{r}\| \leq \sigma_2 \|\dot{r}\|^2 \; ;$$

$$\sigma_{o1} < \sigma'_o \sigma_2; \; \sigma_{11} < \sigma'_o \sigma_1; \; \sigma_{12} < \sigma'_o \; ;$$

The uncertainties vector $\|\eta\|$ is adjusted via equation (4.21c) (see also Appendix -IV).

4.2.1.3 Stability of the Controller- Observer Scheme

The stability proof via the Lyapunov direct method is investigated in two fold. First, the stability in sliding patch is investigated by choosing the Lyapunov function as given in [10] and the closed-loop stability is analysed with different form of the Lyapunov function.

Recalling from Appendix - IV (a4.4), the Lyapunov function candidate

$$V = \frac{1}{2} S^T M S + \frac{1}{2} \tilde{x}_2^T \tilde{x}_2 + \frac{1}{2} \tilde{\theta}^T \Gamma \tilde{\theta} \qquad (4.29)$$

It is found that (a4.11, Appendix -IV)

$$\dot{V} \leq - \lambda_m(K_2) \|S\|^2 - \lambda_m(\Lambda_2 \Lambda_1^{-1}) \|\tilde{x}_2\|^2 \qquad (4.30)$$

From Appendix - IV, $\|e_s(0)\|^2 \leq \lambda_1$ i.e $e_s(t)$ lie in the sliding patch.

If λ_1 verifies the inequality (a4.15) of Appendix- IV, $\hat{x}_1(0) = x_1(0)$ i.e. initial condition, v and $\hat{\theta}$ are satisfied (4.21), then $\lim_{t \to \infty} \|S\|^2 = 0$, $\lim_{t \to \infty} \|\tilde{x}_2\|^2 = 0$, $\|\tilde{\theta}\|^2 < \infty$ for all t. It implies that $S \to 0$ as $t \to \infty$, so do e and $\dot{e}$ i.e.

$$\lim_{t \to \infty} e = 0$$

$$\lim_{t \to \infty} \dot{e} = 0 \qquad (4.31)$$

In other words, $\dot{S} \in L_\infty^{2n}$, S is uniformly continuous and using the implication $S \in L_2^{2n} \Rightarrow S \to 0$ as $t \to \infty$ so do $e \to 0$, $\dot{e} \to 0$ as $t \to \infty$

The closed-loop stability is investigated by choosing slightly different from of the Lyapunov function (Appendix - IV).

$$V = \frac{1}{2} S^T M S + \frac{1}{2} e_1^T K_2 e_1 + \frac{1}{2} \tilde{x}_2^T \tilde{x}_2 + \frac{1}{2} \tilde{\theta}^T \Gamma \tilde{\theta} \qquad (4.32)$$

and

$$\dot{V} \leq - \lambda_m(Q) \|Z\|^2 \qquad (4.33)$$

where $\lambda_m(Q)$ is defined in Appendix-IV.

Since $V \leq V(0)$ $\forall$ $t \geq 0$, then

$$\dot{V} \leq - \Lambda \lambda_m(Q) \|Z\|^2 \qquad (4.34)$$

$$\leq - \beta \|Z\|^2 \qquad (4.35)$$

The inequality (4.34) ensures the boundedness of Z. Z is uniformly continuous, moreover,

$$\beta \int_0^\infty \|Z\|^2 \, dt \leq - \int_0^\infty \dot{V} \, dt = V(0) - V(\infty) < \infty \qquad (4.36)$$

and therefore,

$$\lim_{t \to \infty} \|Z\| = 0 \qquad (4.37)$$

that implies $e_1 \rightarrow 0$, $e_2 \rightarrow 0$, $\tilde{x}_2 \rightarrow 0$ as $t \rightarrow \infty$.

$\lambda_m(Q)$ is symmetric positive definite matrix (a4.21) if the following condition is satisfied:

$$\lambda_m(K_2) > \lambda_M(K_2) \left(1 + \frac{1}{2\Lambda}\right) \qquad (4.37a)$$

From Appendix - IV, it is found that the region of attraction is the entire state-space, that is, defined by L_m and L_M.

4.2.1.4 Discussions

(i) The vector $\|\eta\|$ is bounded because of its functional dependence on desired trajectory. Hence, the design vector v is bounded. It is used to robustify the observation error dynamics vis-a-vis uncertainties on parameter vector.

(ii) The estimated velocity is provided by a sliding observer, into which the desired acceleration is fed forward, in order to keep the estimated velocity within the input bound.

(iii) The uncertainties term appears on boundedness of the inertia matrix, gravity components and boundedness of the Coriolis and centripetal forces. The design constants, associated with these boundedness of coefficients matrix, reduce the uncertainties on parameter vector and enhance the

tracking performance so that tracking error and velocity observation error tend asymptotically to zero.

(iv) The region within which the switching surface is invariant is noted as "sliding patch". The Chattering motion on the switching surface is unsuitable phenomenon and creates high frequency components, in result, discontinuities occur in control law. This unsuitable phenomenon can be reduced by replacing the switching function by saturation one or applying boundary layer theory [87],[88], but tracking performance detoriates. Alternatively, an adaptation loop may reduce the chattering in control law because of its dependency on the estimated values.

4.2.2 Tracking Error Based Sliding Observer Aided Adaptive Control

The sliding observer of [10] is further extended by inclusion of tracking error in previously modified (section 4.2.1) form to provide a proper tuning between controller and observer. In this case, the sliding observer is modified in evaluating the velocity estimation as follows:

$$\dot{\hat{x}}_1 = \hat{x}_2 - \Gamma_1 \tilde{x}_1 - \Lambda_1 \, sgn(\tilde{x}_1) \qquad (4.38a)$$

$$\dot{\hat{x}}_2 = \ddot{r} - \Gamma_2 \tilde{x}_1 - \Gamma_e(x_1 - r) - \Lambda_2 sgn(\tilde{x}_1) - W(x_1, \dot{q}_r, \hat{\theta})(S' - \Lambda_1 sgn(\tilde{x}_1)) + v \qquad (4.38b)$$

where $\Gamma_1, \Gamma_2, \Lambda_1, \Lambda_2$ and Γ_e are the design matrices. The term v is made to account the uncertainties on parameter vector θ. $\hat{x}_1$ and $\hat{x}_2$ are the estimates of x_1 and x_2, respectively.

The structure of control law be given by equation (4.20) recalled as

$$\tau = \tau_1 + W(x_1, \dot{q}_r, \hat{\theta}) \, \tilde{x}_2 \qquad (4.39)$$

where,

$$\tau_1 = \hat{M}(x_1)\ddot{q}_r + \hat{C}(x_1, x_2)\dot{q}_r + \hat{g}(x_1) - K_2 S$$

and W(.) is define in equation (4.21), q_r, $\dot{q}_r$, $\ddot{q}_r$ are defined in equation(4.16).

where $\hat{M}(x_1)$ and $\hat{C}(x_1,x_2)$ are the estimates of $M(x_1)$ and $C(x_1,x_2)$ respectively. K_2 is a positive constant diagonal matrix.

The adaptation law is derived in Appendix-V obtain as

$$\dot{\hat{\theta}} = - \Gamma^{-1} Y(x_1,\hat{x}_2-\Lambda_1 sgn(\tilde{x}_1), \dot{q}_r, \ddot{q}_r + \Lambda\Lambda_1 sgn(\tilde{x}_1)) (S'-\Lambda_1 sgn(\tilde{x}_1) \quad (4.40)$$

and the term v is obtained as

$$v = v(r,\tau, \tilde{x}_2, \dot{r}) = \begin{cases} -[\phi(\dot{r},\tau) + \|\ddot{r}\|] \Lambda_1 sgn(\tilde{x}_1)/\lambda_1 & \text{if } \|\Lambda_1 sgn(\tilde{x}_1)\| \neq 0 \\ 0 & \text{if } \|\Lambda_1 sgn(\tilde{x}_1)\| = 0 \end{cases} \quad (4.41)$$

where $\phi(\dot{r},\tau)$ is defined by (4.28). In (4.41), the term v depends on the desired trajectory information, hence it is bounded due to boundedness of $\dot{r}$ and $\ddot{r}$. Thus, the robustness of observation error dynamics increases. The term W compensates the term WS′ of control law.

4.2.2.1 Error System Formulation

The system dynamics of n-degrees of freedom rigid robot system is described by (3.7). In state-space representation, choosing $x_1 = q$, $x_2 = \dot{q}$, system model (3.7) can be expressed [10] as,

$$\dot{x}_1 = x_2$$
$$\dot{x}_2 = - M(x_1)^{-1} [C(x_1,x_2)x_2 + g(x_1) - \tau] \quad (4.42)$$

The dynamic behavior in sliding surface S can be represented as

$$\dot{S} = M^{-1}(x_1)[-(C(x_1,x_2)+K_2)S + Y(x_1,x_2,\dot{q}_r,\ddot{q}_r)\tilde{\theta} + W(x_1, \dot{q}_r, \hat{\theta})\tilde{x}_2] \quad (4.43a)$$

where,

$$Y = Y(x_1, x_2, \dot{q}_r, \ddot{q}_r) = \tilde{M}(x_1)\ddot{q}_r + \tilde{C}(x_1, x_2)\dot{q}_r + \tilde{g}(x_1) \qquad (4.43b)$$

The observation error dynamic equation can be expressed, from (4.38), (4.42), as

$$\dot{\tilde{x}}_1 = \tilde{x}_2 - \Gamma_1 \tilde{x}_1 - \Lambda_1 \text{ sgn } (\tilde{x}_1) \qquad (4.45a)$$

$$\dot{\tilde{x}}_2 = \ddot{r} - \Gamma_2 \tilde{x}_1 - \Gamma_e e_1 - \Lambda_2 \text{ sgn } (\tilde{x}_2)$$

$$- W(x_1, \dot{q}_r, \hat{\theta})(S' - \Lambda_1 \text{ sgn } (\tilde{x}_1) + v + \eta \qquad (4.45b)$$

where, $\eta = - M(x_1)^{-1} [C(x_1, x_2)x_2 + g(x_1) - \tau]$

The term v is to cope with uncertainties on parameter vector. In observation error dynamics (4.45), the desired acceleration vector reduces the discontinuities in velocity estimation, in results, the velocity observation error is bounded.

4.2.2.2 Stability of Controller-Observer Structure

The stability proof in the Lyapunov sense is investigated in Appendix - V in sliding patch and based on augmented error system. Former indicates that the errors lie on sliding surface and later gives the convergence of augmented error to zero or close to zero with satisfaction of adaptation law and vector v.

From Appendix - V, (a5.13), it follows

$$\dot{V} \leq - \lambda_m(K_2) \|S\|^2 - \lambda_m(\Lambda_2 \Lambda_1^{-1}) \|\tilde{x}_2\|^2 - \lambda_M(\Gamma_e) \|e\| \|\tilde{x}_2\| \qquad (4.46)$$

Using the same type of arguments in Appendix-IV, (a4.13) - (a4.15), it follows that

$$\|e_{s1}(0)\|^2 \leq \lambda_1 \tag{4.47}$$

so that $e_{s1}(t)$ lie in the sliding patch where $e_{s1}^T = [S^T, \tilde{x}_2^T, \tilde{\theta}^T, e^T]$.

Consider the augmented error 'Z' as described in Appendix - V. Using the Lyapunov function (a5.13), it is found

$$\dot{V} \leq - \Lambda \lambda_m(Q_s) \|Z\|^2 \tag{4.48}$$

$\lambda_m(Q_s)$ is symmetric positive definite (a5.15) matrix if following condition is satisfied:

$$\lambda_M(K_2) < \frac{\left(\frac{1}{4} \frac{[\lambda_M(\Gamma_e)]^2 \lambda_m(K_2)}{\lambda_m(\Lambda_2 \Lambda_1^{-1})} - [\lambda_m(K_2)]^2 \right)^{1/2}}{\left(1 + \frac{1}{2\Lambda}\right)} \tag{4.49}$$

Following the same type of arguments (4.35)-(4.37), it can be shown that $\|Z\| \longrightarrow 0$ as $t \longrightarrow \infty$ i.e. $e_1 \longrightarrow 0$, $e_2 \longrightarrow 0$, $\tilde{x}_2 \longrightarrow 0$ as $t \longrightarrow \infty$. It is shown to be asymptotically stable system. From Appendix - V, it is found that the entire state-space defined by L_m and L_M considered as the region of attraction.

4.2.2.3 Discussions

(i) In order to get good velocity estimates, the tracking error term is included to previous work to fulfill the dynamic interaction so that tracking error, observation error converge to zero and as well as velocity error converge to zero, for a proper initial condition.

(ii) Since the design vector v is bounded function of desired trajectory information, which shows robustness of the scheme.

(iii) It is not possible to design reduced order sliding observer in proposed scheme because the output error is only dependent on the position x_1 and its estimates.

(iv) Due to switching terms in the observer and adaptation law, the chattering motion occurs on the switching surface. In order to get average dynamics on each side of discontinuity surface the Filippov's solution concept (reduced order manifold dynamics) is applied on observer structure. The reduction of chattering may possible by introduction of an adaptation loop.

4.2.3 Extended Nonlinear Sliding Observer Aided Controller Structure

In this section, the observer structure of [8] is extended by introduction of signum function of velocity observation error and square of tracking error. The new nonlinear sliding observer is inspired by [8],[85]. In order to show the improvement in various error response the controller structure of [8] is considered with proposed sliding observer. The robot system is highly nonlinear in nature. In this context, the nonlinear sliding observer structure [8] is taken into consideration for accurate trajectory tracking of robot manipulator by its structural change. The purpose of observer to estimate the velocity vector in order to avoid noisy nature of actual velocity measurements for controlling the motion of robot.

The new form of sliding observer to estimate position x_1 and velocity x_2 is given by following differential equation:

$$\dot{\hat{x}}_1 = \hat{x}_2 - \Gamma_{e1}\, e_1^2 - \Lambda_1(\hat{x}_1)\, \mathrm{sgn}(\tilde{x}_1) - \Gamma_1\, \tilde{x}_1 \qquad (4.50a)$$

$$\dot{\hat{x}}_2 = \ddot{r} - \Gamma_{e2}\, e_1^2 - \Lambda_2(\hat{x}_1,\hat{x}_2)\, \mathrm{sgn}(\tilde{x}_1) + \beta(x_1,\dot{r}) + u_1 - u_2 - \Gamma_2\, \tilde{x}_1 \qquad (4.50b)$$

where, Γ_1 and Γ_2 are positive definite constant diagonal matrices, Γ_1 = diag $\{\gamma_1^i\}$, Γ_2 = diag $\{\gamma_2^i\}$,Γ_{e1} = diag $\{\gamma_{e1}^i\}$, Γ_{e2} = diag $\{\gamma_{e2}^i\}$ and the matrices $\Lambda_1(.)$ and $\Lambda_2(.)$ are given as:

$$\Lambda_1 = \text{diag } \{\gamma_1^i\}, \forall\ i = 1,2,..n \tag{4.51}$$

$$\Lambda_2(x_1,\hat{x}_2) = M(x_1)^{-1}[Q\ \Lambda_1 + \pi_1(x_1,\hat{x}_2)\Lambda_1] \tag{4.52}$$

where Q is a diagonal positive definite matrix, and

$$u_2 = M(x_1)^{-1}(1+\sigma^2)\ \tilde{x}_2 + L_1\ \text{sgn}(\tilde{x}_2)\ \xi \tag{4.53}$$

where L_1 and σ^2 are design matrices to cope uncertainty between controller and observer. $\beta(x_1,\hat{x}_2)$ of [8] is replaced by $\beta(x_1,\dot{r})$ in proposed observer structure (4.50). The definition of ξ is given (based on robot model properties) as

$$\xi = \xi_o + \xi_1 \| \tau \| + \xi_2 \| \hat{x}_2 \|^2 \tag{4.54}$$

The desired trajectory r,$\dot{r}$ and $\ddot{r}$ are bounded function of time. The $\hat{x}_1$ and $\hat{x}_2$ are the estimates of x_1 and x_2, respectively, and $\tilde{x}_1 = \hat{x}_1 - x_1$, $\tilde{x}_2 = \hat{x}_2 - x_2$ are the observation error vectors. $e_1 = x_1 - r$ and $e_2 = x_2 - \dot{r}$ denote the tracking error and velocity error respectively.

The control law of [8] is considered here, associated with estimated velocity instead of actual one, as

$$\tau = M(x_1)\ [\ddot{r} - K_2(\hat{x}_2 - \dot{r}) - K_1 e_1] + C(x_1,\dot{r})\dot{r} + g(x_1) + \pi_o(x_1,\dot{r})(\hat{x}_2 - \dot{r}) \tag{4.55}$$

where $\pi_o(x_1,\dot{r})$ is defined by following the physical model properties [8] (see Appendix - VI), which are inherent to robot dynamics. The gain matrices are $K_i = K_i^T > 0$, i = 1,2.

4.2.3.1 Error System Formulation

The state-space representation of (3.7), by choosing the state vector $x_1 = q$ and $x_2 = \dot{q}$, is given as :

$$\dot{x}_1 = x_2 \tag{4.56a}$$

$$\dot{x}_2 = \beta\,(x_1, x_2) + u_1 \tag{4.56b}$$

where,

$$\beta(x_1, x_2) = -\,M(x_1)^{-1}\, C(x_1, x_2)x_2 \tag{4.57a}$$

$$u_1 = M(x_1)^{-1}\,[\,\tau - g(x_1)] \tag{4.57b}$$

The observation error equation can be obtained from (4.50) and (4.56) - (4.57), as

$$\dot{\tilde{x}}_1 = -\,\Gamma_1\,\tilde{x}_1 - \Gamma_{e1}\,e_1^2 - \Lambda_1(\hat{x}_1)\,\mathrm{sgn}(\tilde{x}_1) + \tilde{x}_2 \tag{4.58a}$$

$$\dot{\tilde{x}}_2 = \ddot{r} - \Gamma_2\tilde{x}_1 - \Lambda_2(\hat{x}_1, \hat{x}_2)\,\mathrm{sgn}(\tilde{x}_1) - \Gamma_{e2}e_1^2 + \beta(x_1, \dot{r}) - \beta(x_1, x_2) - M(x_1)^{-1}(1+\sigma^2)\tilde{x}_2 - L_1\mathrm{sgn}(\tilde{x}_2)\xi \tag{4.58b}$$

The Filippov's solution concept (reduced order manifold dynamics) indicates that the dynamics on the switching surface is an average of the dynamics on each side of the discontinuity surface.

For simplicity's sake, consider Λ_1 to be a diagonal matrix i.e. $\Lambda_1 = \lambda_1 I$. The hypersurface $\tilde{x}_1 = 0$ is invariant as long as $|\tilde{x}_2^i| < (\lambda_1 - \gamma_{e1}^i\, e_1^2)$, if $|e_1^2| < \lambda_{e1}^2$. The region within which the surface is invariant is called as sliding patch. If $\tilde{x}_1 = 0 \Rightarrow \dot{\tilde{x}}_1 = 0$, then $\mathrm{sgn}(\tilde{x}_1) = \Lambda_1^{-1}(\tilde{x}_2 - \Gamma_{e1}\, e_1^2)$.

The dynamic behavior in the sliding patch is, according to the Filippov's solution concept, given as

$$\dot{\tilde{x}}_2 = \ddot{r} - M(x_1)^{-1}\,[Q + C(x_1,\hat{x}_2)]\,[\tilde{x}_2 - \Gamma_{e1}\, e_1^2] - \Gamma_{e2}\, e_1^2 + \beta(x_1,\dot{r}) - \beta(x_1,x_2) - M(x_1)^{-1}(1+\sigma^2)\tilde{x}_2 - L_1 \mathrm{sgn}(\tilde{x}_2)\xi \qquad (4.59)$$

The tracking error dynamics in error state-space, from (4.50) and (4.56), can be obtained as

$$\dot{e}_1 = e_2 \qquad (4.60a)$$

$$\dot{e}_2 = - M(x_1)^{-1}\,[C(x_1,x_2)e_2 + M(x_1)K_2(\hat{x}_2 - \dot{r}) + M(x_1)\,K_1(x_1 - r) + C(x_1,e_2)\dot{r} - \pi_o(x_1,\dot{r})\,(\hat{x}_2 - \dot{r})] \qquad (4.60b)$$

The augmented error vector ($\tilde{x}_1 = 0$ remain attractive) is defined as

$$e_o = \begin{pmatrix} e_1 \\ e_2 \\ \tilde{x}_2 \end{pmatrix} \qquad (4.61)$$

An augmented error vector is used for closed-loop analysis by introducing the Lyapunov function as given in subsequent subsection.

4.2.3.2 Stability of Closed-loop System

In order to show the closed-loop system (4.59) and (4.60) is exponential stable in the sense that variable in the loop remains bounded and tracking error e_1, velocity error e_2 and observation error $\tilde{x}_2$ converge to zero asymptotically as t approaches ∞, consider the Lyapunov function candidate (Appendix-VI) with $e^T = [e_1\ e_2]^T$:

$$V(e,\tilde{x}_2) = \frac{1}{2}\, e_1^T K_1 e_1 + \frac{1}{2}\, e_2^T\, M(x_1) e_2 + \frac{1}{2}\, \tilde{x}_2^T\, M(x_1)\tilde{x}_2 + e_1^T\, M(x_1) e_2 \qquad (4.62)$$

Taking the time derivative of (4.62), along (4.59) and (4.60), it is found in Appendix - VI that

$$\dot{V}(e, \tilde{x}_2) \leq - \lambda_{inf}\{ M(e_1)\} \|e_o\|^2 \qquad (4.63)$$

where $M(e_1)$ is a matrix and function of tracking error e_1

For exponential stability , it is necessary that

$\zeta_1 > 0$

$$\lambda_m(K_1) > \frac{\left\{c_o + \frac{1}{2} c_1 - \frac{1}{2} (\lambda_M(M)-1)\ \lambda_M(K_1) \right\}^2}{\lambda_m(M)\left\{2\ \lambda_m(M)\ (\lambda_m(K_2)-1)-c_o \right\}} \qquad (4.64)$$

hence,

$$\lambda_{inf}\{M(e_1)\} > 0 \qquad (4.65)$$

Applying these inequality (4.63) is nonpositive. It follows that $V(e,\tilde{x}_2)$ is bounded, hence $\sqrt{\|e_o\|}$ is an L^2 function [53]. But and L^2 function whose derivative is bounded must tend to zero [53]; hence, $\|e_o\| \longrightarrow 0$ means $e_1 \longrightarrow 0$, $e_2 \longrightarrow 0$ and $\tilde{x}_2 \longrightarrow 0$ as t approaches ∞, as desired.

From Appendix - VI, the region of attraction is given as :

$$\|x\| < \frac{1}{c_3} \left\{ \left\{ \left\{ (\frac{1}{2} [\lambda_M(M)-1](\lambda_M(K_1) - c_o - \frac{1}{2} c_1)) + [(\lambda_m(M)\lambda_m(K_1)) \right.\right.\right.$$

$$.(2\lambda_m(M)[\lambda_m(K_2)-1] - c_o)]^{1/2} (c_2 + q_o + (1+\sigma^2))^{1/2} - (\lambda_m(M)\lambda_m(K_1))^{1/2}$$

$$\left.\left.\left. .(\frac{1}{2} \lambda_M(M)\lambda_M(K_2) - \frac{5}{2} c_o - \frac{1}{2} c_1) \right\} / (2\lambda_m(M)[\lambda_m(K_2)-1]-c_o)^{1/2} \right\} - \frac{1}{2} \lambda_M(M)\lambda_M(K_2) - c_o \right\} \qquad (4.65a)$$

where $x^T = [e,\dot{e}]^T$. In contrast to [8], large region of attraction appeared for proposed scheme.

4.2.3.3 Discussions

(i) The "sgn($\tilde{x}_2$)" is usual signum function to be interpreted as element by element operator when applied to a vector ξ. The sign operator on the $\tilde{x}_2$ which makes each velocity estimate sensitive to the boundary on which $\tilde{x}_2$ lies, and insensitive to distance to the boundary.

(ii) From (a6.12), a region is defined in terms of e_1 as

$$\|e_1\| < \frac{\frac{1}{2}\lambda_M(M)\,\lambda_M(K_2) - c_o}{\frac{1}{2}\lambda_M(M)\lambda_M(\Gamma_{e2}) - \frac{1}{2}\lambda_M(\Gamma_{e2}) - \frac{1}{2}q_o\,\lambda_M(\Gamma_{e2}) - (c_1+c_o)\,\lambda_M(\Gamma_{e1})}$$

In order to get $\|e_1\|$ as small value, Γ_{e1}, Γ_{e2} and q_o have chosen large value.

4.2.4 Sign-Sign function Based Nonlinear Sliding Observer Aided Controller Structure

A novel form of nonlinear sliding observer based on sign-sign function, which is associated with observation error and tracking error, to estimate the velocity vector is proposed. The overall control scheme consists of proposed sliding observer along with controller structure of [8] in addition to disturbance torque. The observer scheme takes the advantage of full robot dynamics to make the observer system nonlinear. The switching gain associated with sign-sign function is to force observation error to lie on the sliding surface. As for linear systems, the separation principle cannot apply in nonlinear systems. In this regard the controller and the observer cannot be independently designed. In order to show dynamic interactions between controller and observer along with closed-loop stability to get asymptotic tracking of

desired references $(r,\dot{r})$, a nonlinear sliding observer is reconstructed to improve the various error response. In this context, the structure of sliding observer to estimate the position x_1 and velocity x_2 is given by following differential equation :

$$\dot{\hat{x}}_1 = \hat{x}_2 - \Gamma_{e1}\, e_1^2 - \Lambda_1(\hat{x}_1)\, \mathrm{sgn}(\tilde{x}_1) - \Gamma_1\, \tilde{x}_1 \qquad (4.66a)$$

$$\dot{\hat{x}}_2 = \ddot{r} - \Gamma_{e2}\, e_1^2 - \Lambda_2(\hat{x}_1,\hat{x}_2)\, \mathrm{sgn}(\tilde{x}_1) + \beta(x_1,\dot{r}) + u_1 - u_2 - \Gamma_2\, \tilde{x}_1 \qquad (4.66b)$$

where $\hat{x}_1$ is to find $\tilde{x}_1 = \hat{x}_1 - x_1$ in observer structure only. Γ_1, Γ_2, Γ_{e1} and Γ_{e2} are positive definite constant diagonal matrices, $e_1 = x_1 - r$. $\Lambda_1(.)$, $\Lambda_2(.)$ and u_2 are given as

$$\Lambda_1 = \lambda_1 I \qquad (4.67)$$

$$\Lambda_2(x_1,\hat{x}_2) = M(x_1)^{-1}[Q\, \Lambda_1 + \pi_1(x_1,\hat{x}_2)\Lambda_1] \qquad (4.68)$$

$$u_2 = M(x_1)^{-1}(1+\sigma^2)\, \tilde{x}_2 + L_1\, \mathrm{sgn}\,(\tilde{x}_2)\, \xi + L_2\, \mathrm{sgn}\,(\tilde{x}_2)\, \mathrm{sgn}\,(e_1) \qquad (4.69)$$

where Q,σ,L_1 and L_2 are diagonal positive definite design matrices, $\tilde{x}_2 = \hat{x}_2 - x_2$ and $\pi_1(x_1,\hat{x}_2)$ is defined in Appendix - VI by following the physical model properties of robot [8]. The vector ξ is defined in the form using boundedness properties of robot model given [8] as

$$\xi = \xi_o + \xi_1 \| \tau \| + \xi_2 \| \hat{x}_2 \|^2 \qquad (4.70)$$

where ξ_o, ξ_1 and ξ_2 are constant based on bound of coefficient of system dynamics.

Recalling (4.55), the control law associated with actual position and estimated velocity is expressed by including the disturbance vector :

$$\tau = M(x_1)\, [\ddot{r} - K_2\, (\hat{x}_2 - \dot{r}) - K_1 e_1] + C(x_1,\dot{r})\dot{r} + g(x_1) + \pi_o(x_1,\dot{r})(\hat{x}_2 - \dot{r}) - \tau_d \qquad (4.71)$$

where $\pi_o(x_1,\dot{r})$ is defined by following the physical model properties [8] (see Appendix-VI) and $K_i = K_i^T > 0$, $i = 1,2$. τ_d denotes the disturbance vector.

4.2.4.1 Error System Formulation

The following are state-space representation of (3.7) by choosing the state vector $x_1 = q$ and $x_2 = \dot{q}$:

$$\dot{x}_1 = x_2 \tag{4.72a}$$

$$\dot{x}_2 = \beta (x_1,x_2) + u_1 \tag{4.72b}$$

where,

$$\beta(x_1,x_2) = - M(x_1)^{-1} C(x_1,x_2)x_2 \tag{4.73a}$$

$$u_1 = M(x_1)^{-1} [\tau - g(x_1)] \tag{4.73b}$$

The observation error dynamics can be obtained from (4.66) and (4.72) - (4.73) as

$$\dot{\tilde{x}}_1 = - \Gamma_1\tilde{x}_1 - \Gamma_{e1} e_1^2 - \Lambda_1(x_1,\hat{x}_2) \, sgn(\tilde{x}_1) + \tilde{x}_2 \tag{4.74a}$$

$$\dot{\tilde{x}}_2 = \ddot{r} - \Gamma_2\tilde{x}_1 - \Lambda_2 (x_1,\hat{x}_2) \, sgn(\tilde{x}_1) - \Gamma_{e2} e_1^2 + \beta(x_1,\dot{r}) - \beta(x_1,x_2) - M(x_1)^{-1}(1+\sigma^2)\tilde{x}_2 - L_1 sgn(\tilde{x}_2)\xi - L_2 \, sgn(\tilde{x}_2) \, sgn(e_1) \tag{4.74b}$$

For applying the Filippov's solution concept, consider Λ_1 to be a diagonal matrix i.e. $\Lambda_1 = \lambda_1 I$. If $\tilde{x}_1 = 0 \Rightarrow \dot{\tilde{x}}_1 = 0$ then $sgn(\tilde{x}_1) = \Lambda_1^{-1}(\tilde{x}_2 - \Gamma_{e1}e_1^2)$. The dynamic behavior in the sliding patch is given as

$$\dot{\tilde{x}}_2 = \ddot{r} - M(x_1)^{-1} [Q+C(x_1,\hat{x}_2)] (\tilde{x}_2 - \Gamma_{e1} e_1^2) - \Gamma_{e2} e_1^2 + \beta(x_1,\dot{r}) - \beta(x_1,x_2) - M(x_1)^{-1}(1+\sigma^2)\tilde{x}_2 - L_1 sgn(\tilde{x}_2)\xi - L_2 \, sgn(\tilde{x}_2) \, sgn(e_1) \tag{4.75}$$

From (4.71) and (4.72), we get the error state-space form as

$$\dot{e}_1 = e_2 \tag{4.76a}$$

$$\dot{e}_2 = - M(x_1)^{-1} [C(x_1,x_2)e_2 + M(x_1)K_2(\hat{x}_2-\dot{r}) + M(x_1) \, K_1(x_1-r) + C(x_1,e_2)\dot{r} - \pi_o(x_1,\dot{r}) \, (\hat{x}_2 - \dot{r}) + \tau_d] \tag{4.76b}$$

Tracking error dynamics arises due to control law (4.71) being applied to robot system (4.72).

The augmented error vector ($\tilde{x}_1 = 0$) is defined as

$$e_o = \begin{bmatrix} e_1 \\ e_2 \\ \tilde{x}_2 \end{bmatrix} \tag{4.77}$$

4.2.4.2 Stability of Closed-loop System

To establish closed-loop system as exponentially asymptotically stable, consider the following Lyapunov function candidate with $e^T = [e_1, e_2]^T$

$$V(e, \tilde{x}_2) = \frac{1}{2} e_1^T K_1 e_1 + \frac{1}{2} e_2^T M(x_1) e_2 + \frac{1}{2} \tilde{x}_2^T M(x_1) \tilde{x}_2 + e_1^T M(x_1) e_2 \tag{4.78}$$

From Appendix - VII, it is found

$$\dot{V}(e, \tilde{x}_2) \leq - \lambda_{inf} \{ M(e_1) \} \|e_o\|^2 - \|\tau_d\| \|e_2\| \tag{4.79}$$

with condition for $\dot{V}(e, \tilde{x}_2) \leq 0$

$$\|L_1 \xi + L_2\| \geq \|\ddot{r}\| , \quad \|\tau_d\| > 0 \tag{4.80}$$

$$\zeta_1 > 0 \tag{4.81}$$

$$\lambda_m(K_1) > \frac{\left\{ c_o + \frac{1}{2} c_1 - \frac{1}{2} (\lambda_M(M)-1) \lambda_M(K_1) \right\}^2}{\lambda_m(M) \left\{ 2 \lambda_m(M) (\lambda_m(K_2)-1) - c_o \right\}} \tag{4.82}$$

From (a7.2), the region of attraction is determined as expressed by (4.65a). In contrast to [8], large region of attraction appeared for proposed scheme.

4.2.4.3 Discussions

(i) Including disturbance torque in controller equation (4.71), it may possible to find better tracking accuracy.

(ii) Sign-Sign function is associated with tracking error and velocity observation error and acts as a switching function (forcing element) to get good estimate of velocity.

Chapter - 5

SIMULATION RESULTS

5.1 ROBOT SYSTEM

The equations of motion of the robot systems are (3.7):

$$M(q)\ddot{q} + C(q,\dot{q})\dot{q} + g(q) = \tau \qquad (5.1)$$

The following forms of robot system are used for simulation purpose:

(i) Three - DOF robot system

(ii) Two-DOF robot system with mass

(iii) Two-DOF robot sysem without mass

(i) Three -DOF Robot System

The following coefficients of matrices are given for the three-DOF robot system (Fig. 5.1):

$$\begin{aligned}
M_{11} &= A_1 + A_2 \sin^2 q_2 + A_3 \sin^2(q_2 + q_3) + A_4 \sin q_2 \sin(q_2 + q_3) \\
M_{12} &= M_{13} = M_{31} = 0 \\
M_{22} &= A_5 + A_4 \cos q_3 \\
M_{23} &= M_{32} = A_6 + A_7 \cos q_3 \\
M_{33} &= A_8
\end{aligned} \qquad (5.2)$$

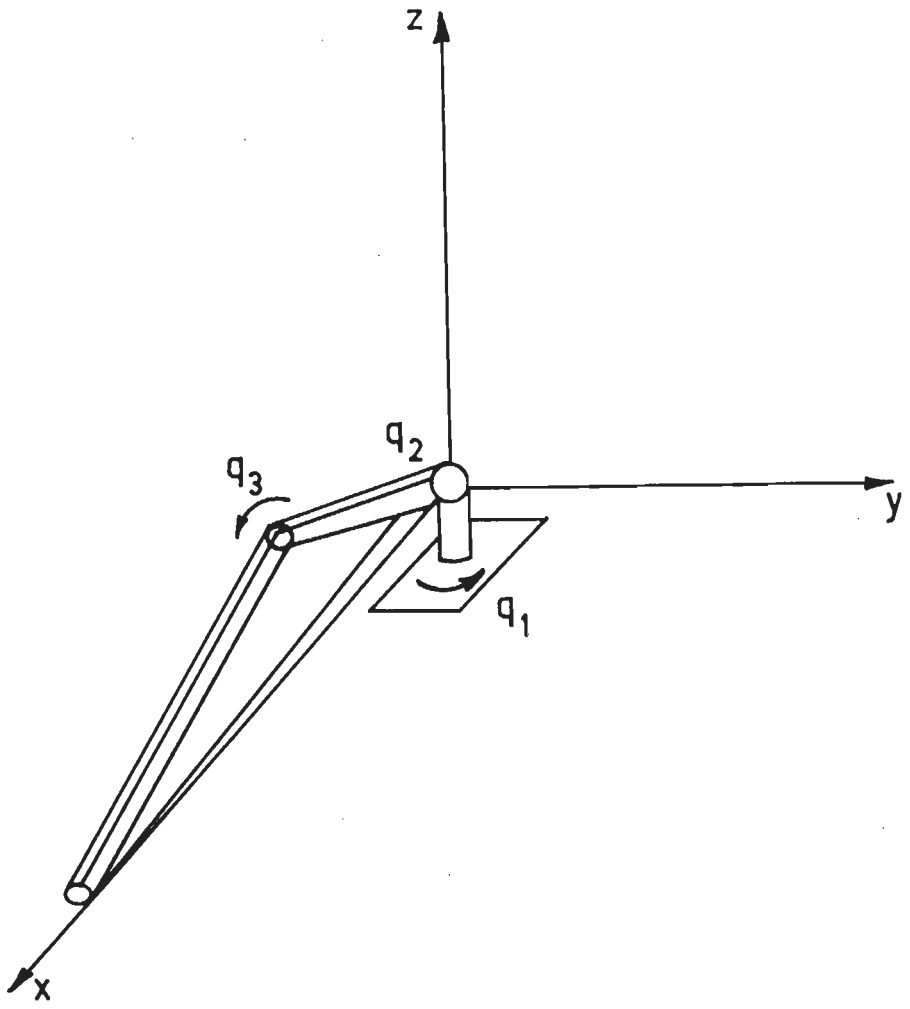

Fig. 5.1 Three Joint Revolute Robotic Manipulators

$$C_{11} = \frac{1}{2}\Big\{A_2 \sin(2q_2)\,\dot{q}_2 + A_3 \sin(2(q_2+q_3))\,(\dot{q}_2+\dot{q}_3) + A_4(\sin q_2 \cos(q_2+q_3)\dot{q}_3 + \sin(q_3+2q_2)\dot{q}_2)\Big\}$$

$$C_{12} = \frac{1}{2}\Big\{A_2 \sin(2q_2)\dot{q}_1 + A_3\sin(2(q_2+q_3))\dot{q}_1 + A_4\sin(q_3+2q_2)\dot{q}_1\Big\}$$

$$C_{13} = \frac{1}{2}\Big\{A_3\sin(2(q_2+q_3))\dot{q}_1 + A_4\sin q_2 \cos(q_2+q_3)\dot{q}_1\Big\}$$

$$C_{21} = -C_{12}$$

$$C_{22} = -\frac{1}{2}A_4\sin(q_3)\dot{q}_3$$

$$C_{23} = -\frac{1}{2}A_4\sin(q_3)\dot{q}_2 - A_7\sin(q_3)\dot{q}_3$$

$$C_{31} = -C_{13}$$

$$C_{32} = \frac{1}{2}A_4\sin(q_3)\dot{q}_2$$

$$C_{33} = 0.0 \qquad (5.3)$$

$$g(q_1) = 0.0$$

$$g(q_2) = -A_9\sin(q_2) - A_{10}\sin(q_2+q_3)$$

$$g(q_3) = -A_{10}\sin(q_2+q_3) \qquad (5.4)$$

Numerical values of these constant parameters are given in Table-I[4].

(ii) Two-DOF robot system with mass

The robot system used in simulation is expressed by (5.1) with

$$M(q) = \begin{bmatrix} 8.77+1.02\cos q_2 & 0.76+0.51\cos q_2 \\ 0.76+0.51\cos q_2 & 0.62 \end{bmatrix} + mp \begin{bmatrix} 2+2\cos q_2 & 1+\cos q_2 \\ 1+\cos q_2 & 1 \end{bmatrix}$$

$$C(q,\dot{q}) = \begin{bmatrix} -0.51\ \sin q_2\ \dot{q}_2 & -0.51\ \sin q_2(\dot{q}_1+\dot{q}_2) \\ 0.51\ \sin q_2\ \dot{q}_1 & 0 \end{bmatrix} + mp \begin{bmatrix} -\sin q_2\ \dot{q}_2 & -\sin q_2\ (\dot{q}_1+\dot{q}_2) \\ \sin q_2\ \dot{q}_1 & 0 \end{bmatrix}$$

$$g(q) = 0.0 \qquad (5.5)$$

It is moving in the horizontal plane (Fig.5.44, $g(q) = 0$ [7]).

(iii) Two-DOF robot system without mass

The physical parameters of robot sytem (5.1) are given [6] as

$$M(q) = \begin{bmatrix} 9.77+2.02\ \cos q_2 & 1.26+1.01\ \cos q_2 \\ 1.26+1.01\ \cos q_2 & 1.12 \end{bmatrix}$$

$$C(q,\dot{q}) = \begin{bmatrix} -1.01\ \sin q_2\ \dot{q}_2 & -1.01\ \sin q_2(\dot{q}_1+\dot{q}_2) \\ 1.01\ \sin q_2\ \dot{q}_1 & 0 \end{bmatrix}$$

$$g(g) = g \begin{bmatrix} 8.11\ \sin q_1 + 1.13\ \sin(q_1+q_2) \\ 1.13\ \sin(q_1+q_2) \end{bmatrix} \qquad (5.6)$$

It is moving in vertical plane (Fig.5.72).

5.1.1 Desired Trajectory (Test Signal)

The following forms of desired trajectories (test signal) are assumed for simulation purpose [4],[6],[7],[48]:

(1) Cosine form without crossing zero ([4], Fig.5.2-5.4);

(A) : $r_1 = (\pi/2) - (0.45\ \cos(2\pi t))$ rad

(B) : $r_2 = (\pi/1.6) - (0.5\ \cos(2\pi t))$ rad

(C) : $r_3 = (\pi/2) - (0.2\ \cos(2\pi t))$ rad (5.7)

(2) Exponential form ([48], Fig.5.23-5.25);

(D) : $r_1 = (\pi/2)\ (1-(1+3t)\ e^{-3t})$ rad

(E) : $r_2 = (\pi/3)\ (1-(1+3t)e^{-3t})$ rad

(F) : $r_3 = (\pi/2)\ (1-(1+3t)\ e^{-3t})$ rad (5.8)

(3) Mixed form ([7], Fig.5.45)

(G) : $r_1 = -1.3454742 + 0.1027998\ (\cos 1.3156\ \pi t)$ $0 \le t \le 0.4$

$$= -1.3538518 + \frac{1.633539}{2\pi}\left[\frac{2\pi}{1.1}(t-0.4) - \sin\left(\frac{2\pi}{1.1}(t-0.4)\right)\right] \quad 0.4 \le t \le 1.5$$

$= 0.2794272$ $t > 1.5$

(H) : $r_2 = 1.0192722 + \frac{0.7703882}{2}\left[1 - \sin\left(\frac{3\pi}{2} + \frac{\pi}{0.75}(t-0.75)\right)\right]$ $0 \le t \le 1.5$

$= 1.0192722$ $t > 1.5$

(5.9)

(4) Cosine form with crossing zero ([6], Fig.5.73-5.74)

(I) : $r_1 = 0.1 \cos\left(\frac{3\pi}{10}\right) t$ rad

(J) : $r_2 = 0.3 \cos\left(\frac{7\pi}{10}\right) t$ rad (5.10)

5.2 SIMULATION OF PROPOSED ADAPTIVE CONTROL STRUCTURE USING ACCELERATION TERM

In this section, simulation results are presented to illustrate the performance of the proposed structure(Section 3.2.1) and compared with the structure which uses no acceleration error loop [84]. For this, a simpler three degree of freedom robot arm is used (Fig. 5.1). The physical parameters of this

are given in Table-I [4]. The actuators were assumed with no dynamics and no power limitations. The equations of motion of the robot system is governed by (5.1) and its coefficients of matrices are from (5.2) - (5.4). Simulation results are based on cosine form (Fig.5.2-5.4,(5.7)) and exponential form (Fig.5.23-5.25,(5.8)) of desired trajectory (test signal) in joint coordinated space. The robot parameter $\theta^* = [A_1,.....A_{10}]$ is given in Table-I.

Table - I

Physical parameters for three-DOF robot system

A_1	23.380
A_2	9.2063
A_3	2.4515
A_4	5.4000
A_5	82.3990
A_6	2.6274
A_7	2.7000
A_8	25.779
A_9	189.170
A_{10}	52.928

The regressor matrix $W(q,\dot{q},\dot{r},\ddot{r})$ is given by (5.11).

The regressor matrix $W(.)$ is given by $W(q.\dot{q}.\dot{r}.\ddot{r}) =$

$$\begin{bmatrix}
\ddot{r}_1 & \sin^2 q_2 \ddot{r}_1 + \frac{1}{2}\sin(2q_2) & \sin^2(q_2+q_3)\ddot{r}_1 + \frac{1}{2}\sin(2(q_2+q_3) & \frac{1}{2}\sin q_2 \cos(q_2+q_3).(\dot{q}_3\dot{r}_1 + \dot{q}_1\dot{r}_3) & 0 & 0 & 0 & 0 & 0 & 0 \\
 & .(\dot{q}_2\dot{r}_1 + \dot{q}_1\dot{r}_2) & .(\dot{q}_2+\dot{q}_3)\dot{r}_1 + \dot{q}_1\dot{r}_2 + \dot{q}_1\dot{r}_3 & +\sin(q_2+q_3)\sin q_2 \ddot{r}_1 & & & & & & \\
 & & & + \frac{1}{2}\sin(q_2+q_3)(\dot{q}_2\dot{r}_1 + \dot{q}_1\dot{r}_2) & & & & & & \\
0 & -\frac{1}{2}\sin(2q_2)\dot{q}_1\dot{r}_1 & -\frac{1}{2}\sin(2(q_2+q_3))\dot{q}_1\dot{r}_1 & \cos q_3 \ddot{r}_2 - \frac{1}{2}\sin(q_3+2q_2)\dot{q}_1\dot{r}_1 & \ddot{r}_2 & \ddot{r}_3 & \cos q_3 \ddot{r}_3 - \sin q_3 \dot{q}_3 \dot{r}_2 & 0 & \sin q_2 & \sin(q_2+q_3) \\
 & & & -\frac{1}{2}\sin q_3 \dot{q}_3 \dot{r}_2 - \frac{1}{2}\sin q_3 \dot{q}_2 \dot{r}_3 & & & & & & \\
0 & 0 & -\frac{1}{2}\sin(2(q_2+q_3))\dot{q}_1\dot{r}_1 & -\frac{1}{2}\sin q_2 \cos(q_2+q_3)\dot{q}_1\dot{r}_1 - \sin q_3 \dot{q}_2 \dot{r}_2 & 0 & \ddot{r}_2 & \cos q_3 \ddot{r}_2 & \ddot{r}_3 & 0 & \sin(q_2+q_3)
\end{bmatrix} \tag{5.11}$$

The controller (section 3.2.1) setting for this simulation are given below :

$\epsilon_o = 0.001, K_1 = \text{diag}[-65,-50,-25], K_2 = \text{diag}[-9,-8,-5], K_3 = \text{diag}[-0.001,-0.06,-0.001];$

$\epsilon_o = 0.3,\ K_1 = \text{diag}[-65,-50,-25],\ K_2 = \text{diag}[-9,-8,-5],\ K_3 = \text{diag}[-0.2,-1.9,0.-0.2];$

Simulation is performed for two cases : (i) Initial estimated parameter $\hat{\theta} = 0$, e(0) = 0; (ii) Initial estimated parameter $\hat{\theta} = \frac{1}{2}\theta^*$, e(0) = 0; For these cases, the error graphs are shown in Fig.5.5-5.22 and Fig.5.26-5.43. Tracking error graphs are shown on the basis of percentage (error as percent of max. input) whereas velocity error graphs are in rad/s. These results are given in Table - II.

Table - II

Maximum errors for whitcomb's case and proposed case

Trajectory	Response	Initial estimated parameter	Whitcomb's case			Proposed case		
			Joint-1	Joint-2	Joint-3	Joint-1	Joint-2	Joint-3
Cosine test signal	Tracking error(%)	$\hat{\theta}=0$	0.5421	0.8536	0.2625	0.4238	0.2921	0.2252
		$\hat{\theta}=\frac{1}{2}\theta^*$	1.2010	0.8525	0.6754	0.4421	0.7649	0.4558
	Velocity error (rad/s)	$\hat{\theta}=0$	0.1758	0.1621	0.2739	0.1059	0.1389	0.1532
		$\hat{\theta}=\frac{1}{2}\theta^*$	0.4182	0.1852	0.2218	0.0853	0.1652	0.2025
Exponential test signal	Tracking error(%)	$\hat{\theta}=0$	1.9121	0.6989	0.8995	0.5012	0.1105	0.9115
		$\hat{\theta}=\frac{1}{2}\theta^*$	1.8992	0.3821	0.4231	1.7539	0.3415	0.3828
	Velocity error (rad/s)	$\hat{\theta}=0$	0.0652	0.0295	0.0713	0.0031	0.0009	0.0052
		$\hat{\theta}=\frac{1}{2}\theta^*$	0.0341	0.0272	0.0523	0.0336	0.0270	0.0476

It is clear that the maximum error for each joint is less for proposed case in comparison to [84].

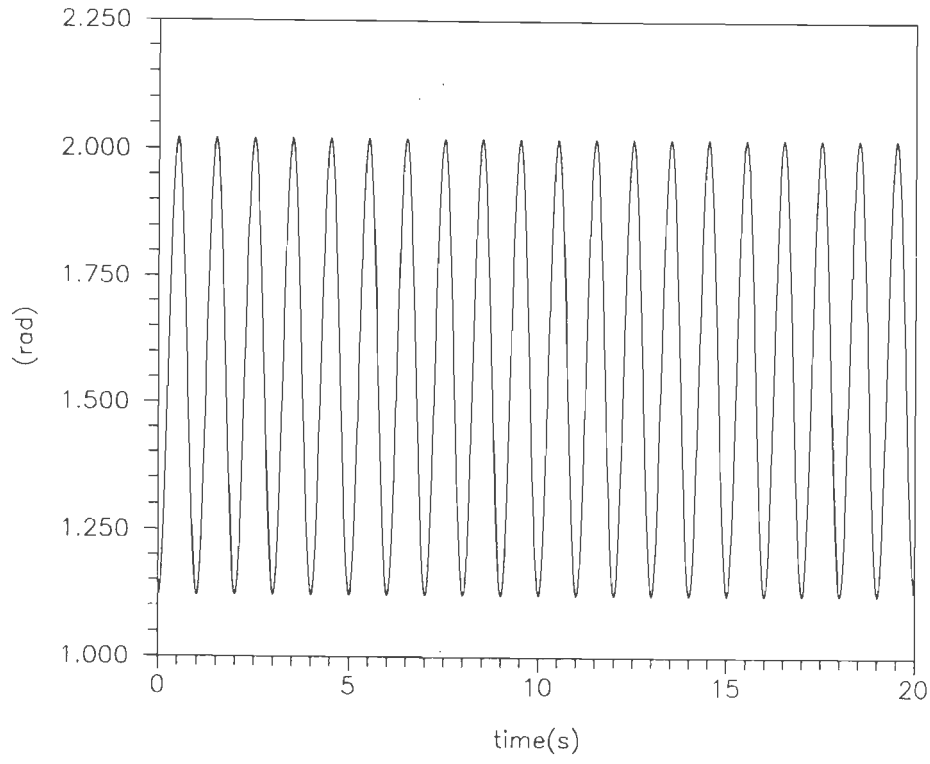

Fig.5.2 Desired trajectory for joint-1 (test signal 'A').

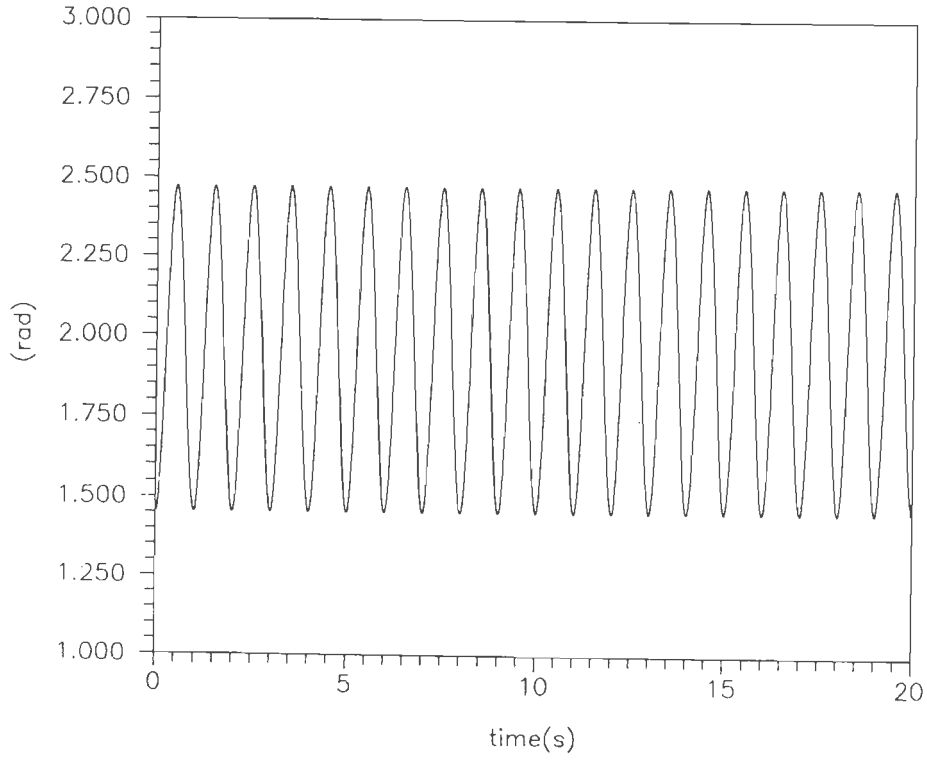

Fig.5.3 Desired trajectory for joint-2 (test signal 'B').

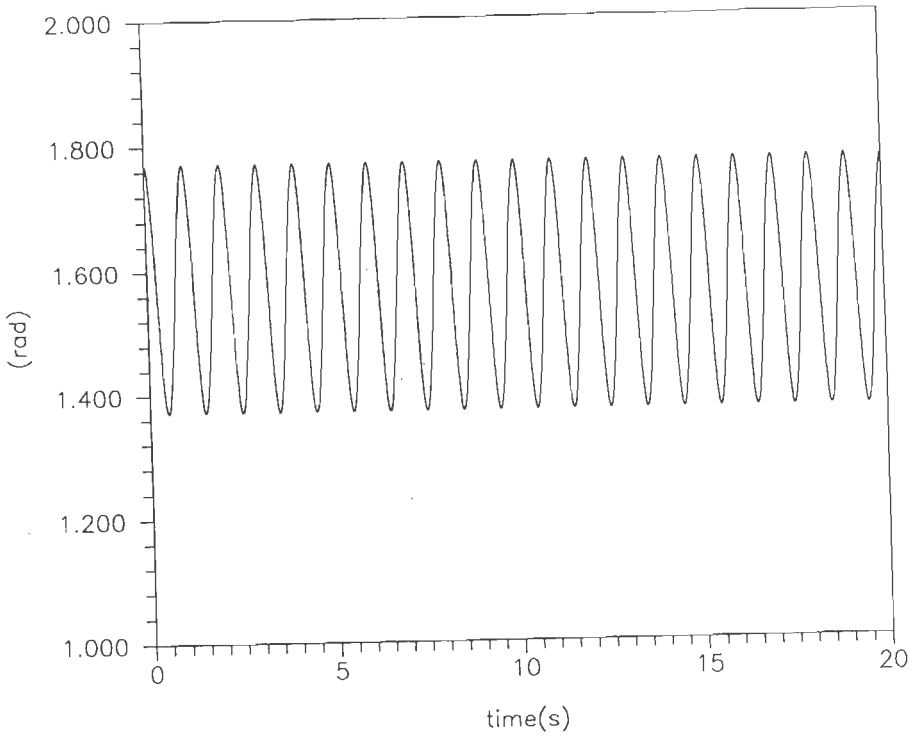

Fig.5.4 Desired trajectory for joint-3 (test signal 'C').

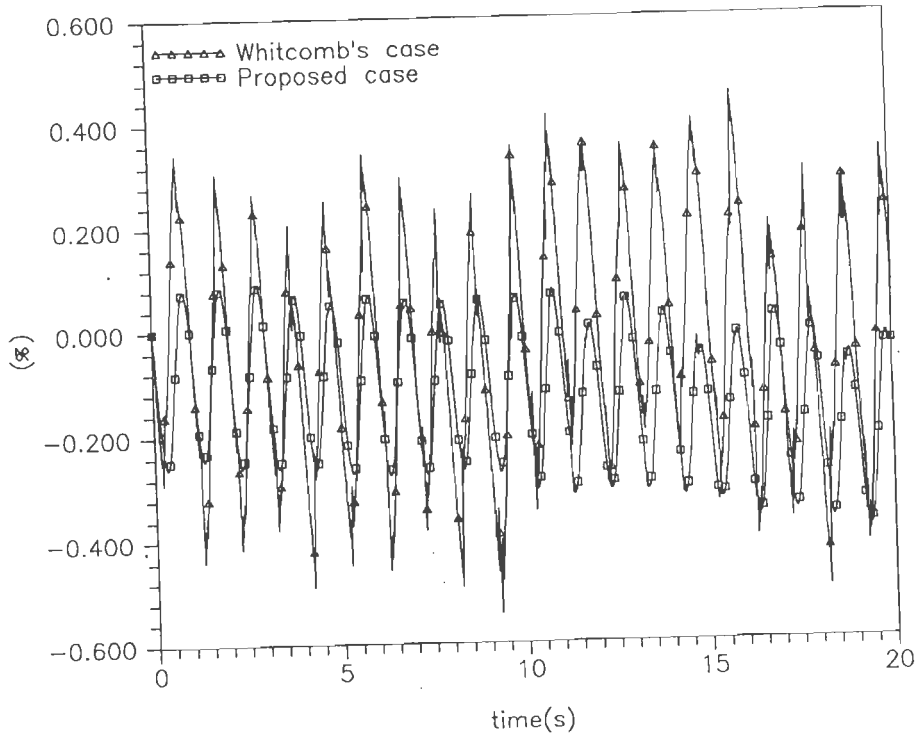

Fig.5.5 Tracking error as percent of max. input for test signal 'A', joint-1, $\hat{\theta}(0)=0$.

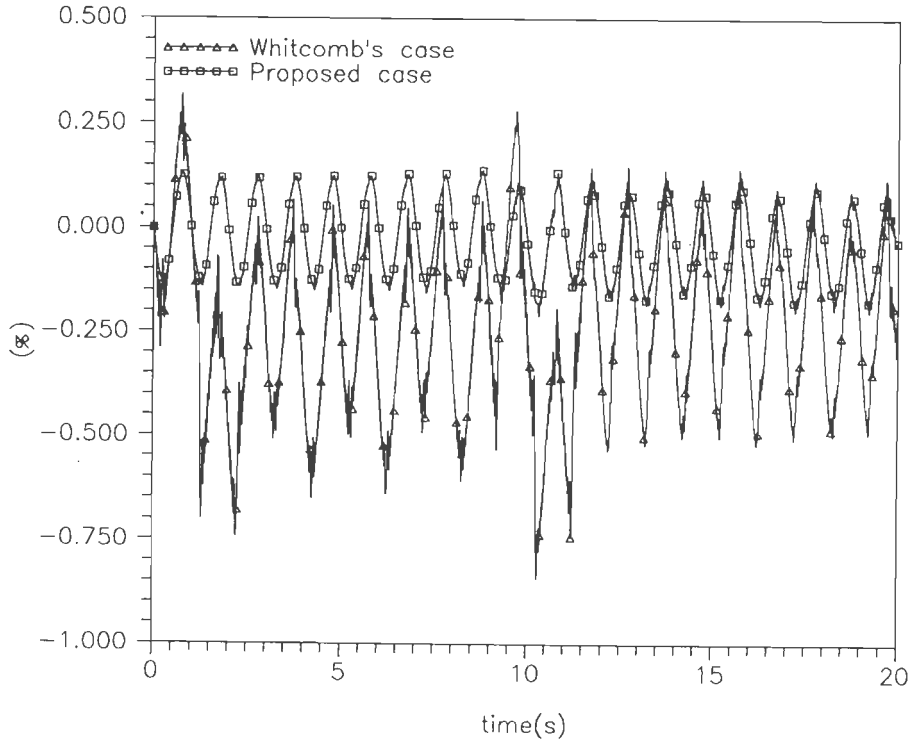

Fig.5.6 Tracking error as percent of max. input for test signal 'B',joint-2, $\hat{\theta}(0)=0$.

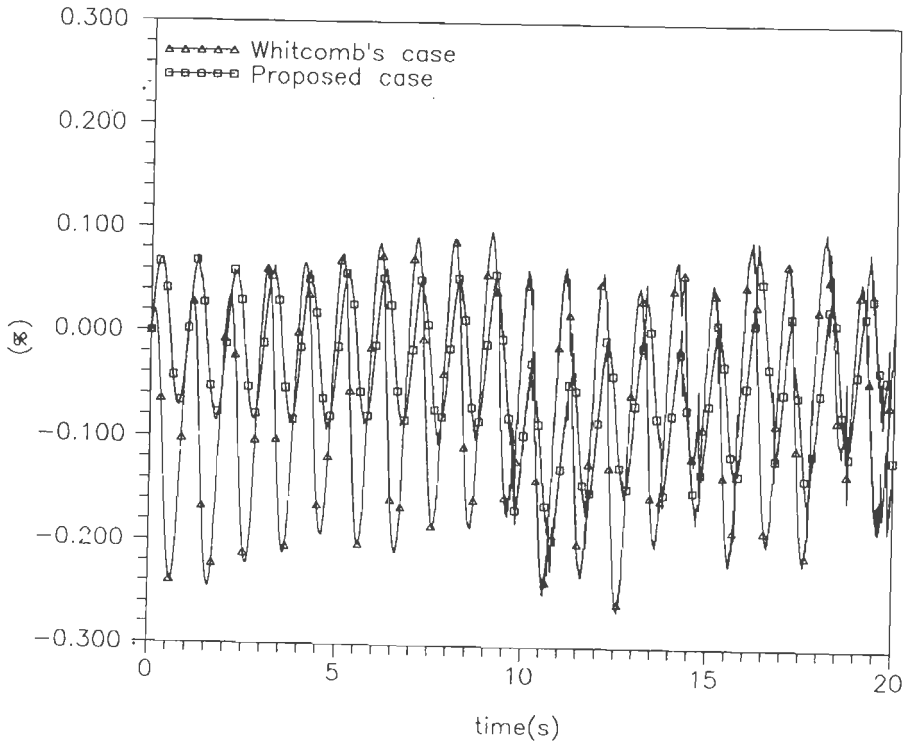

Fig.5.7 Tracking error as percent of max. input for test signal 'C',joint-3, $\hat{\theta}(0)=0$

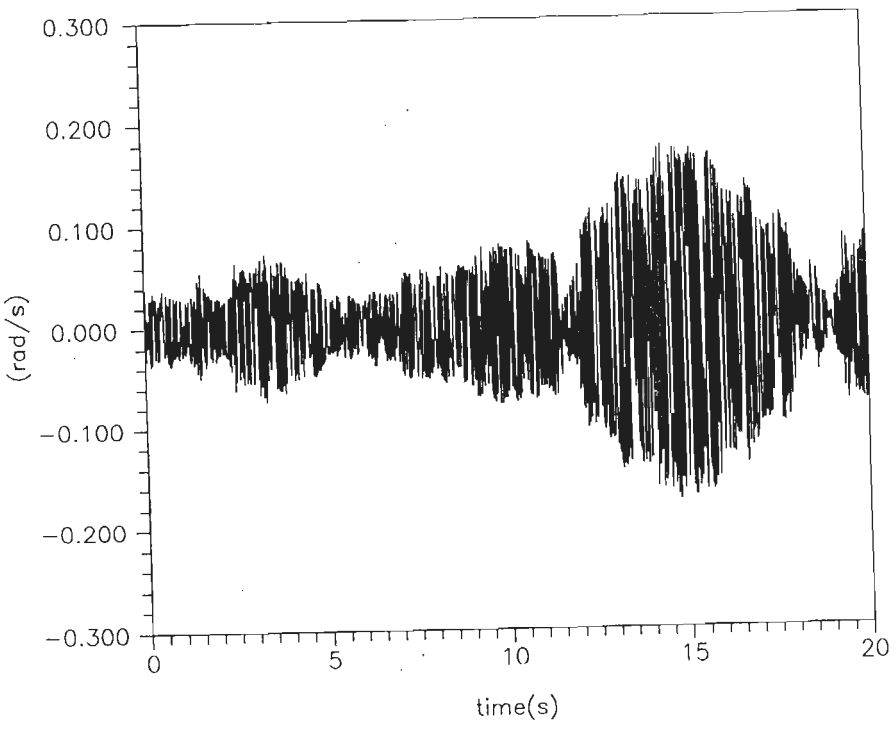

Fig.5.8 Velocity error for test signal 'A' (Whitcomb's case), joint-1, $\hat{\theta}(0)=0$.

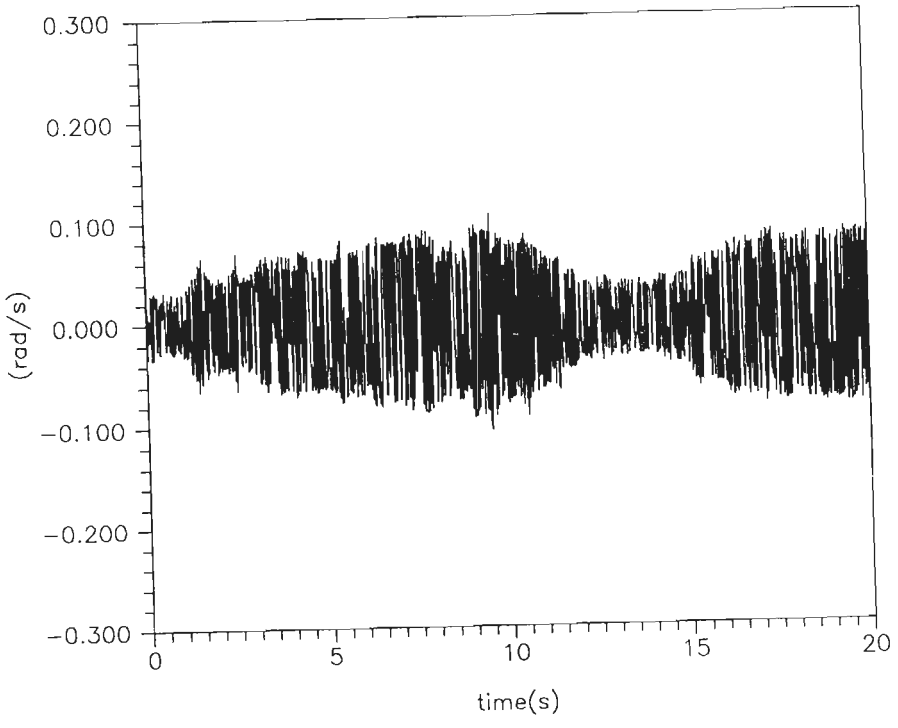

Fig. 5.9 Velocity error for test signal 'A'(Proposed case),joint-1, $\hat{\theta}(0)=0$.

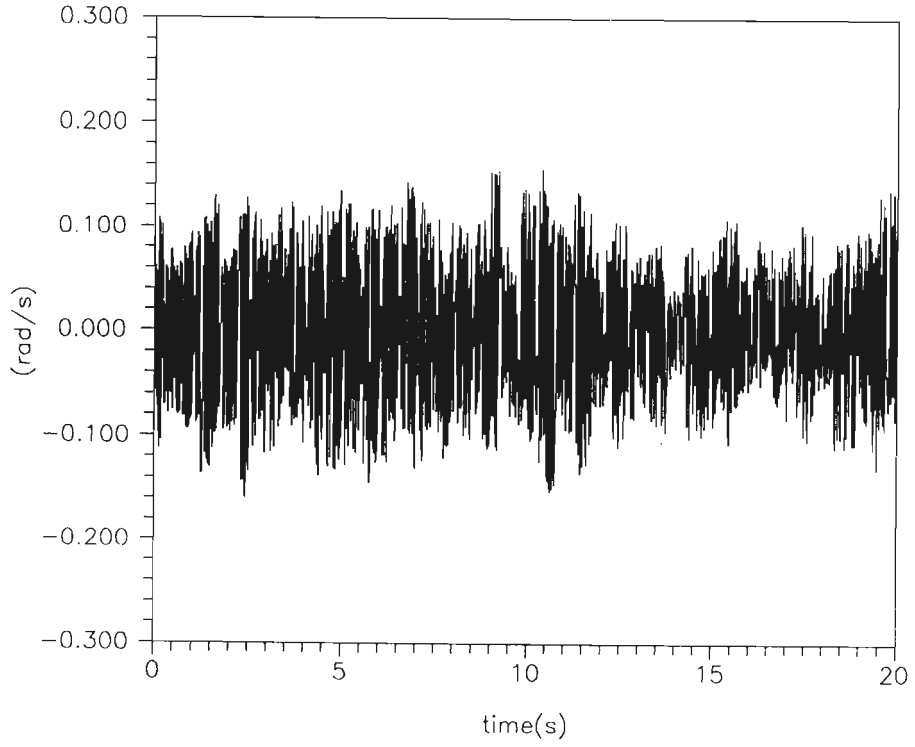

Fig.5.10 Velocity error for test signal'B' (Whitcomb's case),joint-2, $\hat{\theta}(0)=0$.

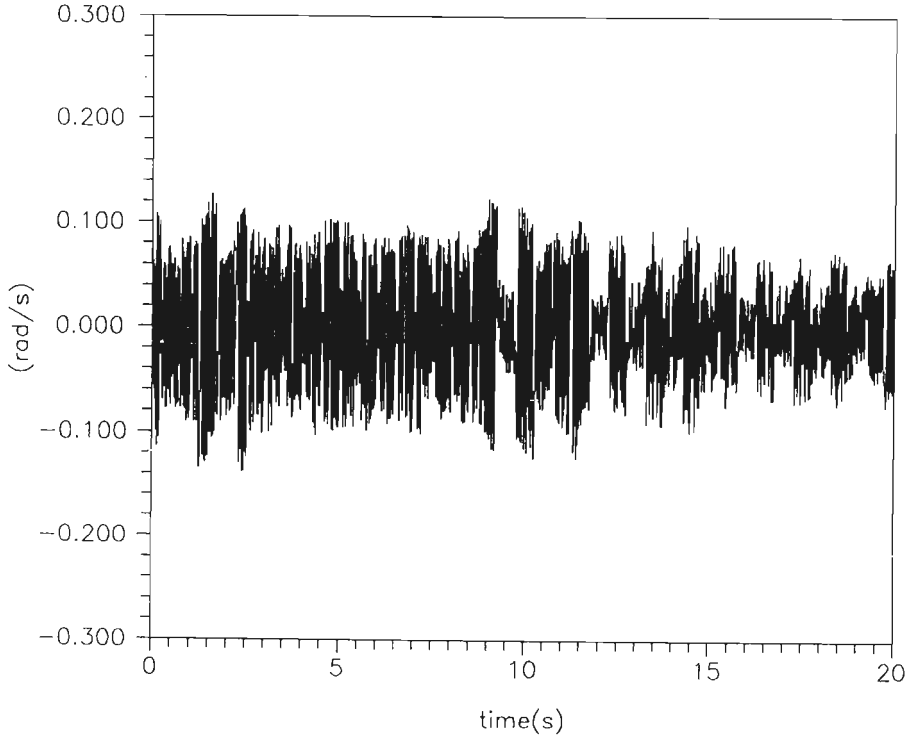

Fig.5.11 Velocity error for test signal 'B'(Proposed case), joint-2, $\hat{\theta}(0)=0$.

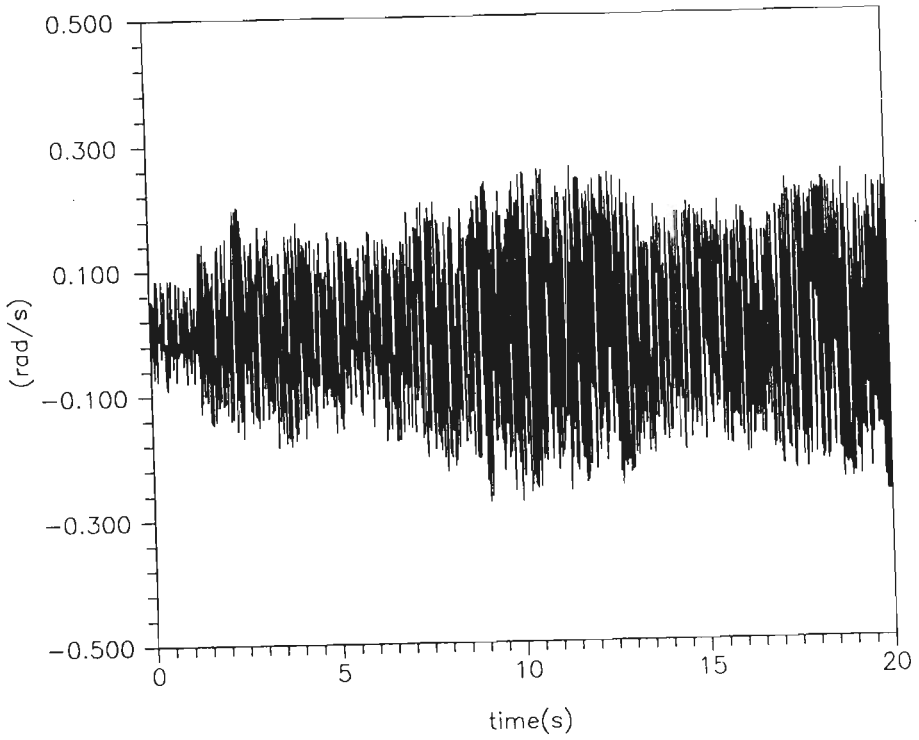

Fig.5.12 Velocity error for test signal 'C'(Whitcomb's case), joint-3 $\hat{\theta}(0)=0$.

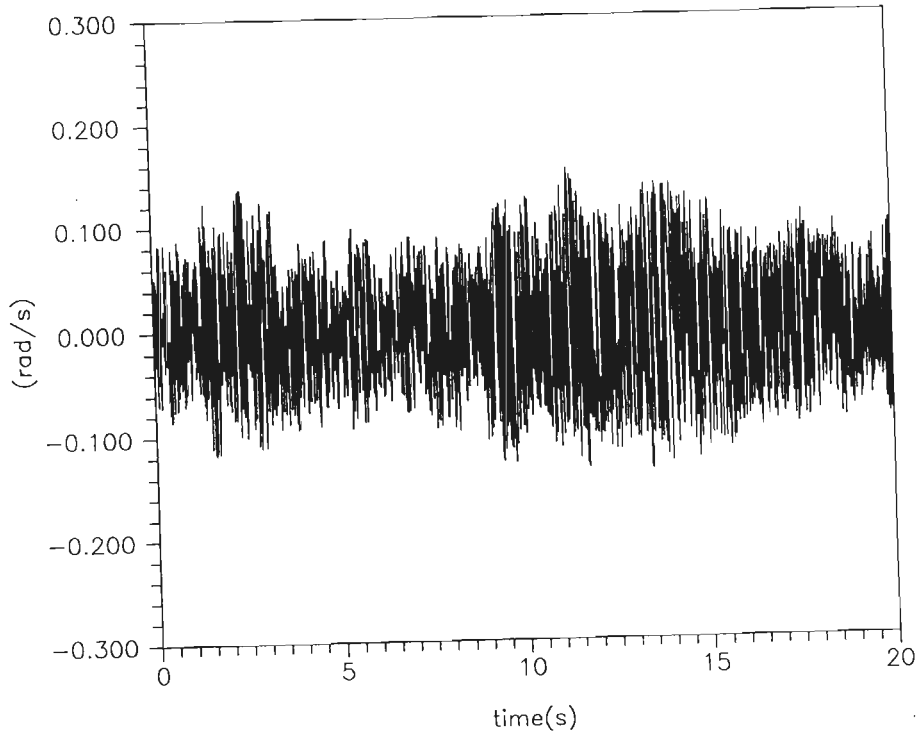

Fig.5.13 Velocity error for test signal 'C'(Proposed case), joint-3, $\hat{\theta}(0)=0$.

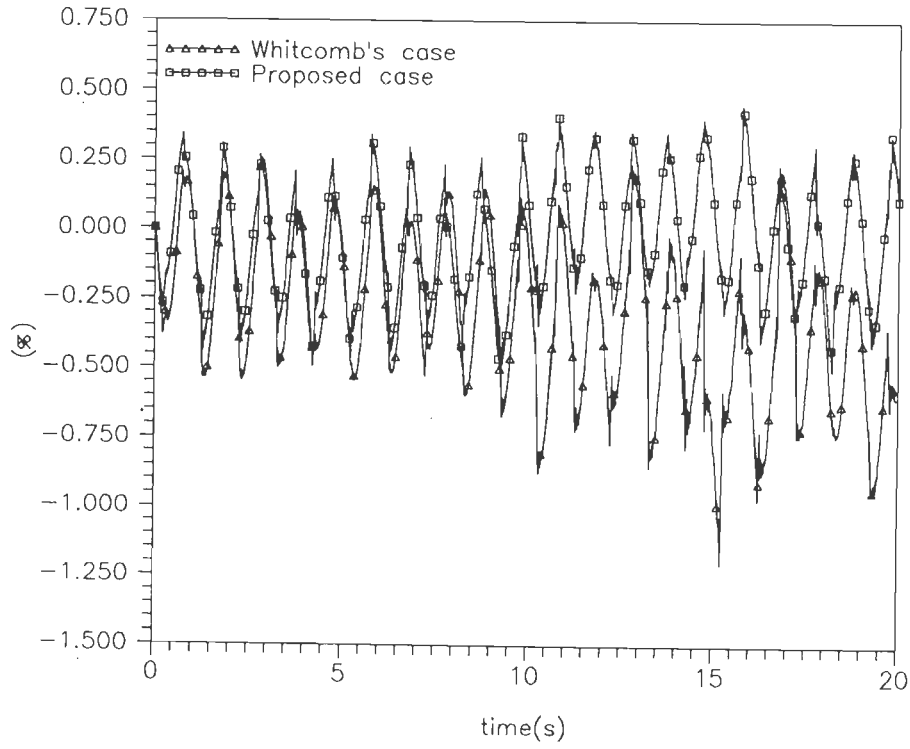

Fig.5.14 Tracking error as percent of max. input for test signal 'A',joint-1, $\hat{\theta}(0)=1/2\theta^{*}$.

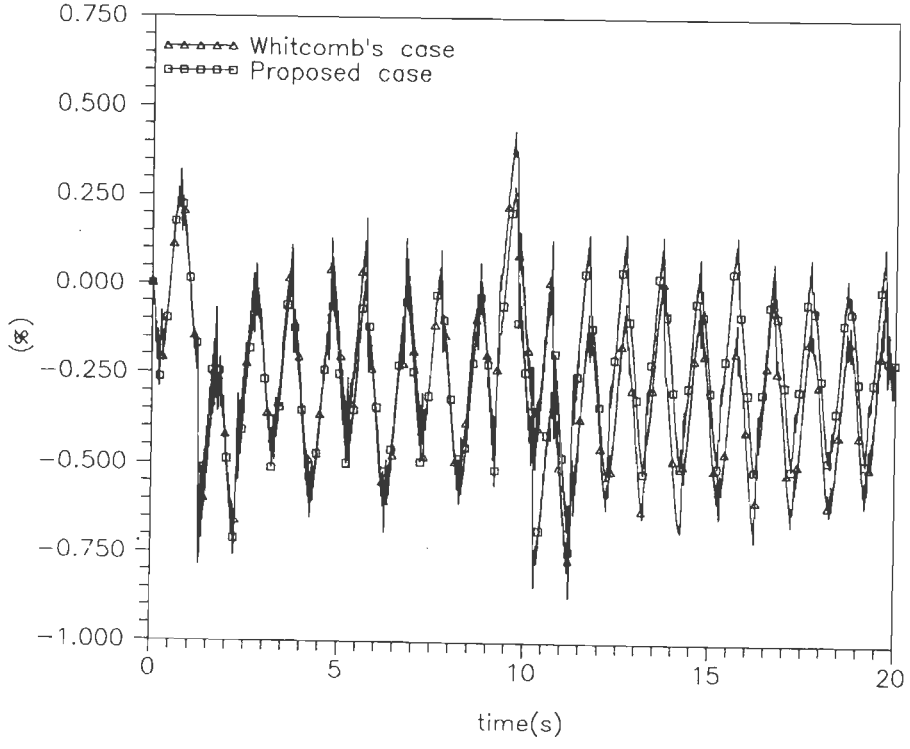

Fig.5.15 Tracking error as percent of max. input for test signal 'B',joint-2, $\hat{\theta}(0)=1/2\theta^{*}$.

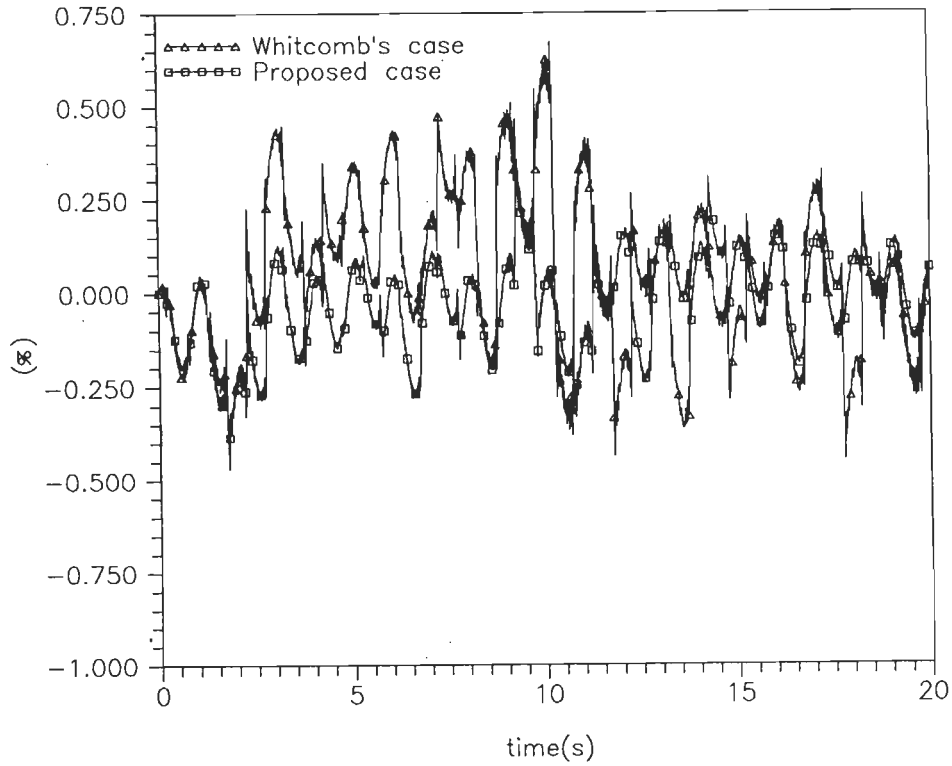

Fig.5.16. Tracking error as percent of max. input for test signal'C',joint-3, $\hat{\theta}(0) = 1/2\ \theta^*$.

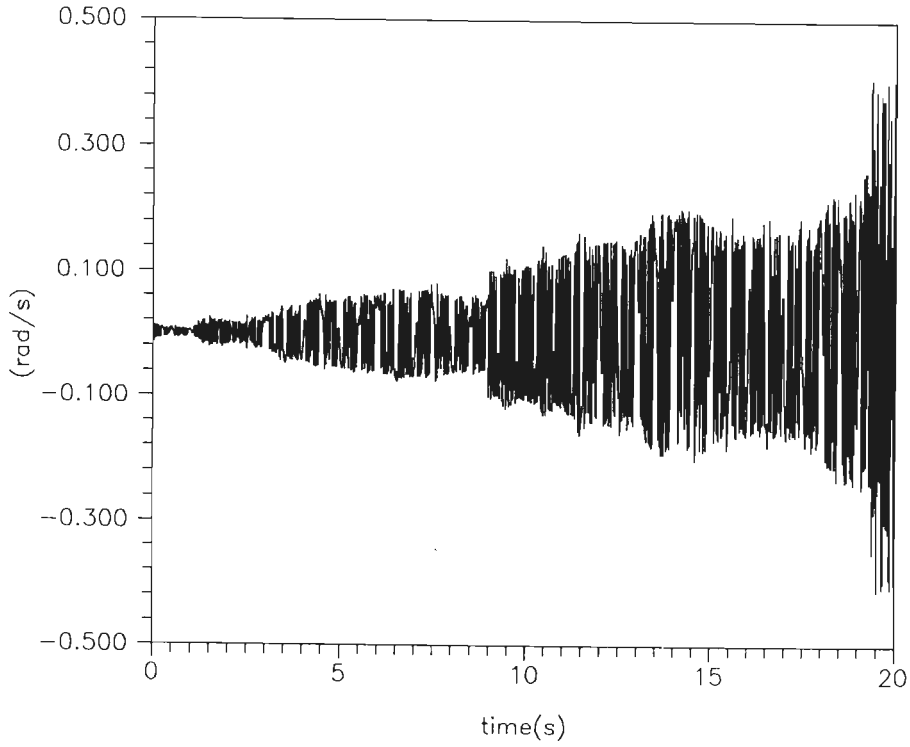

Fig.5.17. Velocity error for test signal'A' (Whitcomb's case),joint-1, $\hat{\theta}(0)=1/2\theta^{*}$.

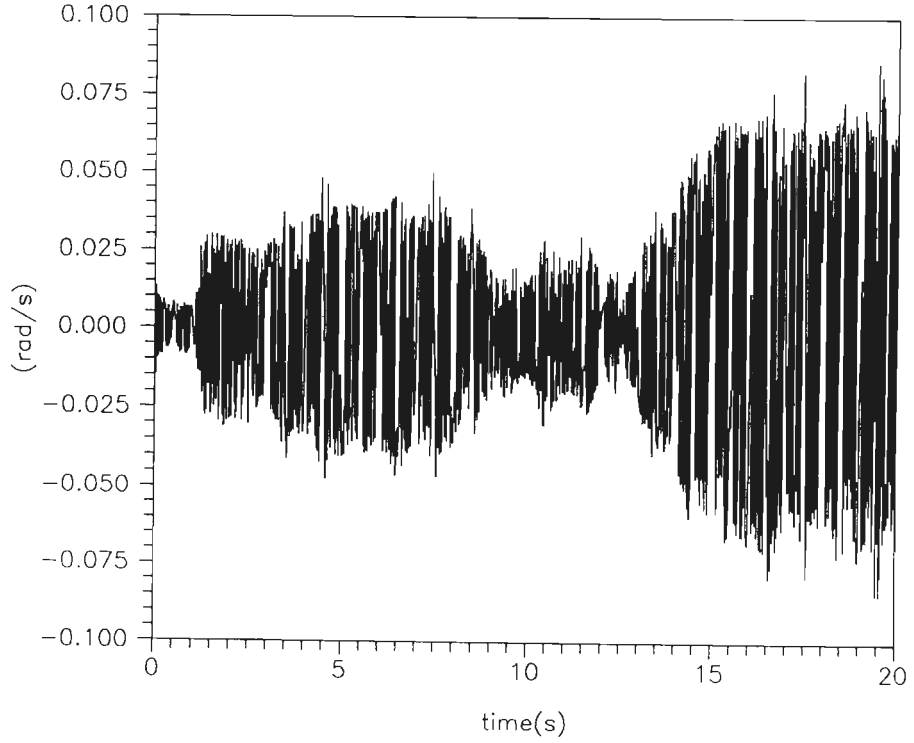

Fig.5.18. Velocity error for test signal 'A'(Proposed case),joint-1, $\hat{\theta}(0)=1/2\theta^{*}$.

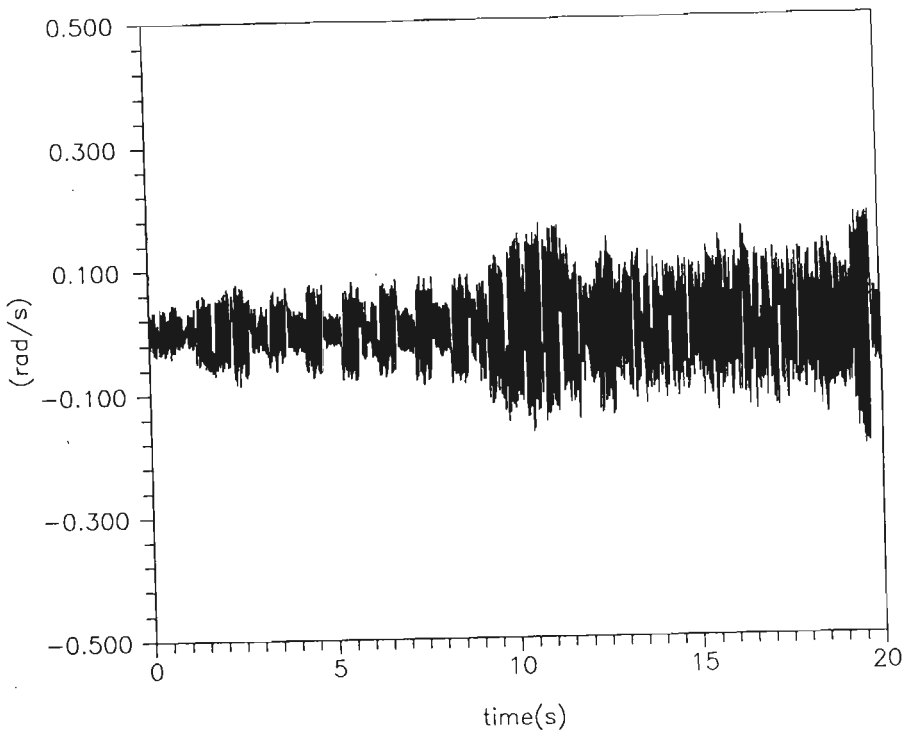

.Fig.5.19 Velocity error for test signal 'B'(Whitcomb's case),joint-2, $\hat{\theta}(0)=1/2\theta^{*}$.

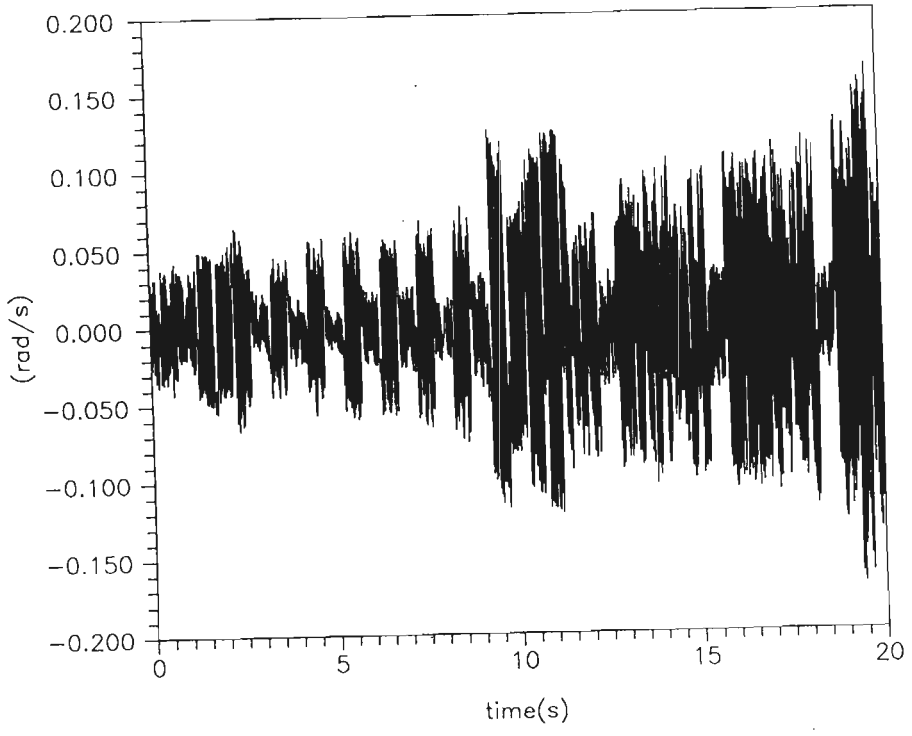

Fig.5.20 Velocity error for test signal 'B'(Proposed case),joint-2, $\hat{\theta}(0)=1/2\theta^{*}$.

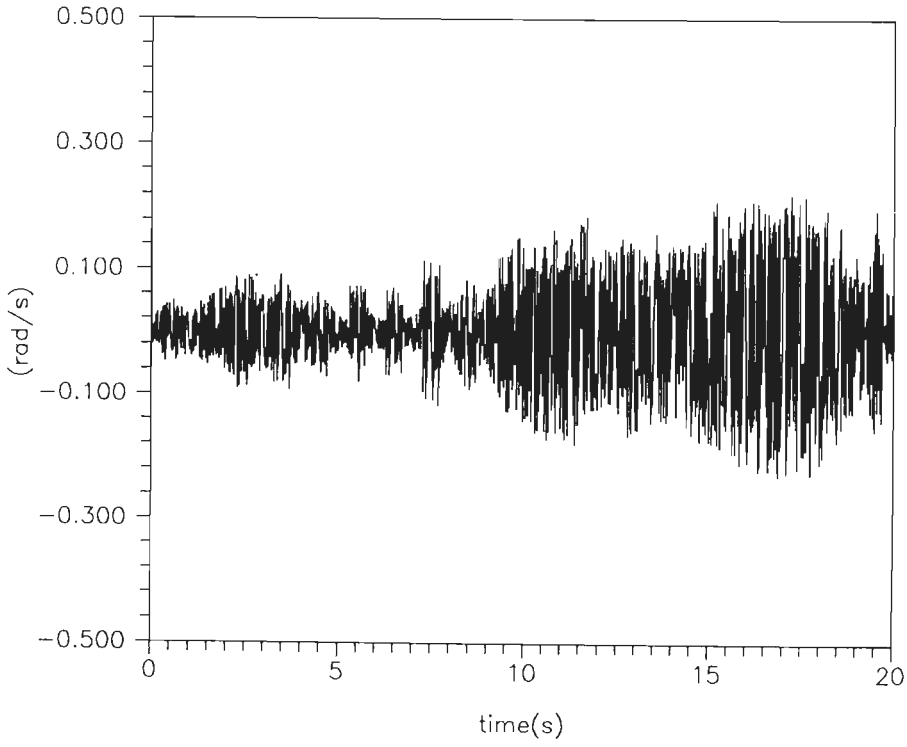

Fig.5.21 Velocity error for test signal 'C'(Whitcomb' scase), joint-3, $\hat{\theta}(0)=1/2\theta^{*}$.

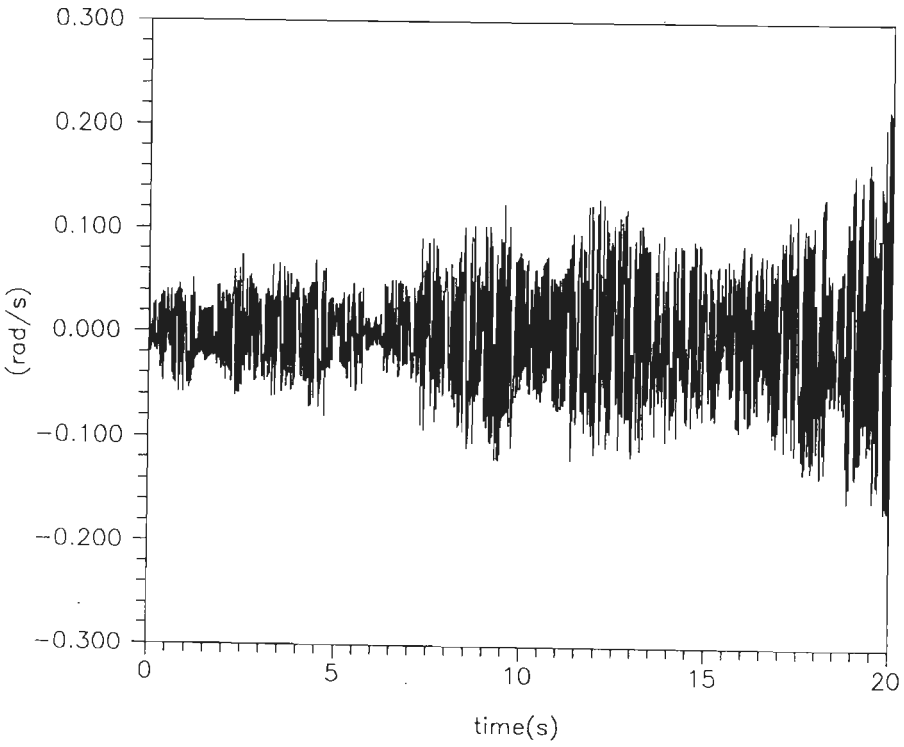

Fig.5.22 Velocity error for test signal 'C'(Proposed case), joint-3, $\hat{\theta}(0)=1/2\ \ \theta^{*}$.

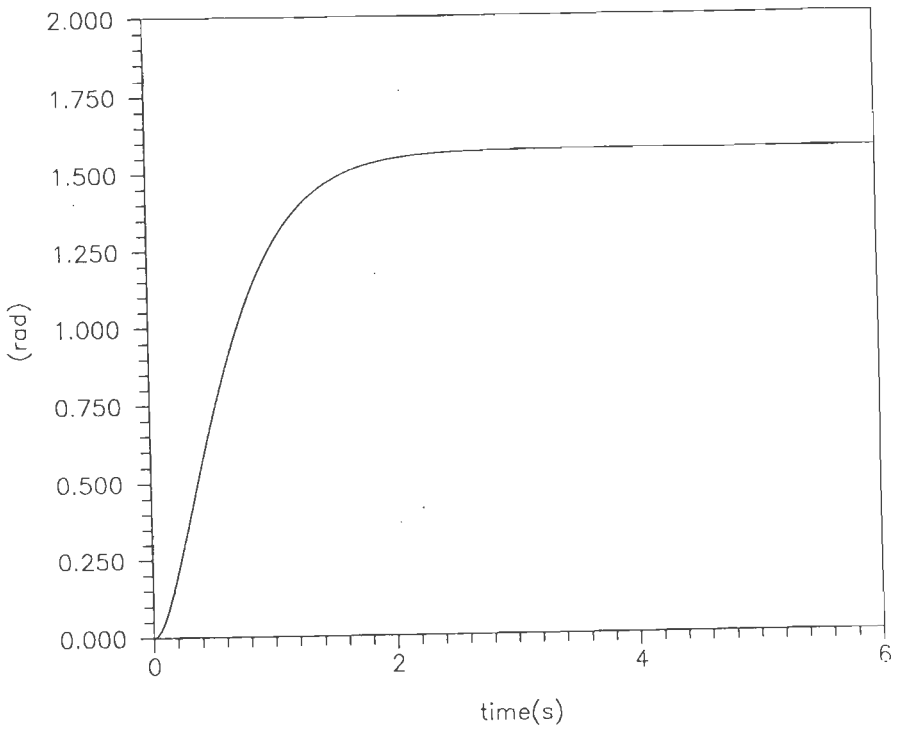

Fig.5.23 Exponential desired trajectory for joint-1(test signal 'D').

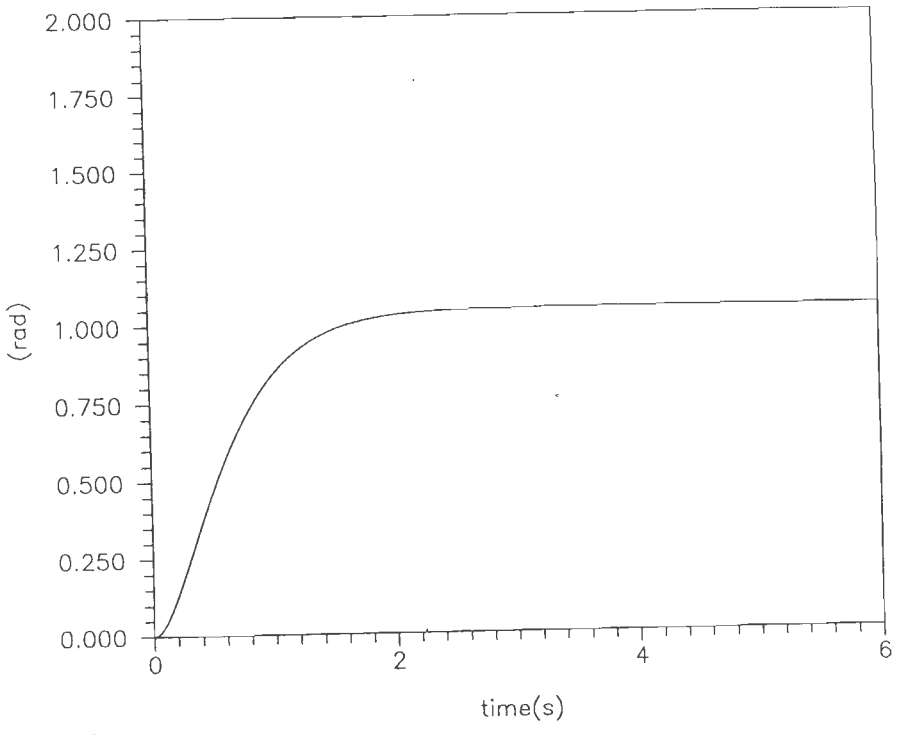

Fig.5.24 Exponential desired trajectory for joint-2(test signal 'E').

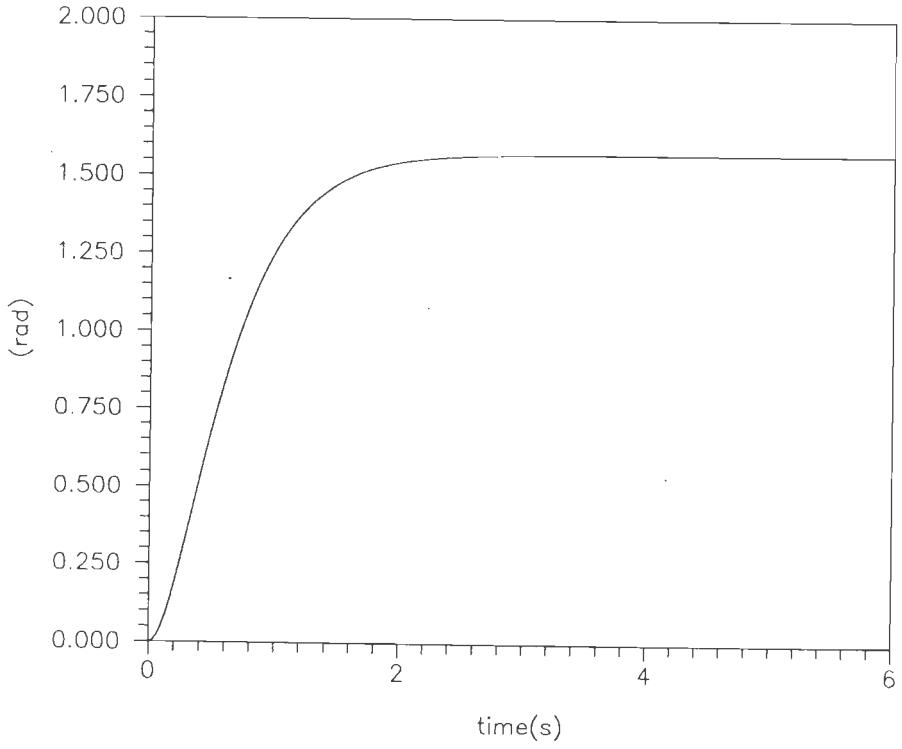

Fig.5.25 Exponential desired trajectory for joint-3(test signal 'F').

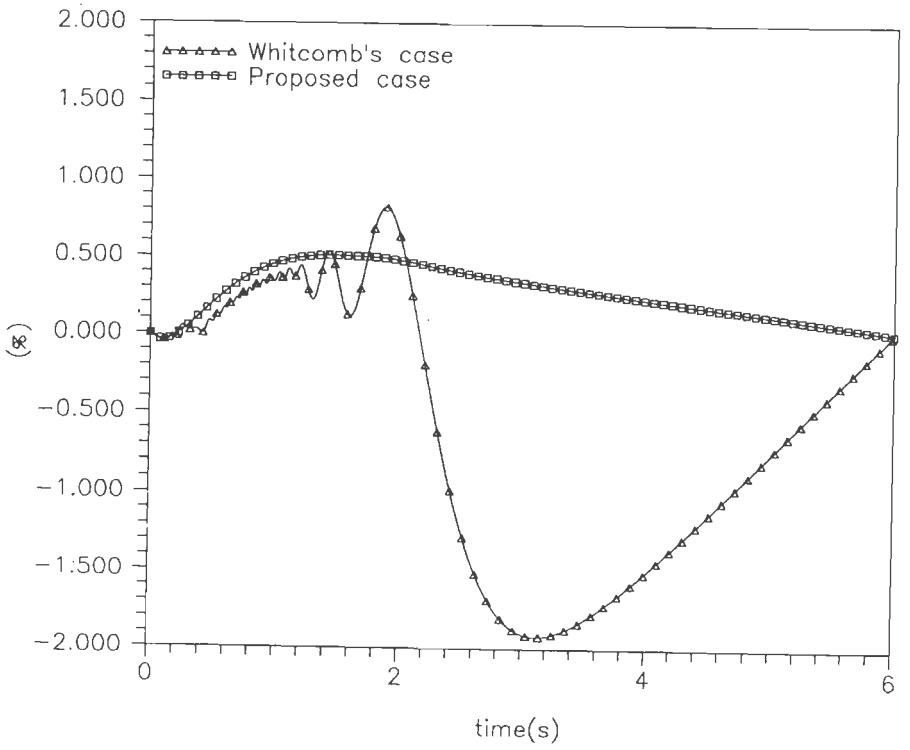

Fig.5.26 Tracking error as percent of max. input for test signal'D',joint-1, $\hat{\theta}(0)=0$.

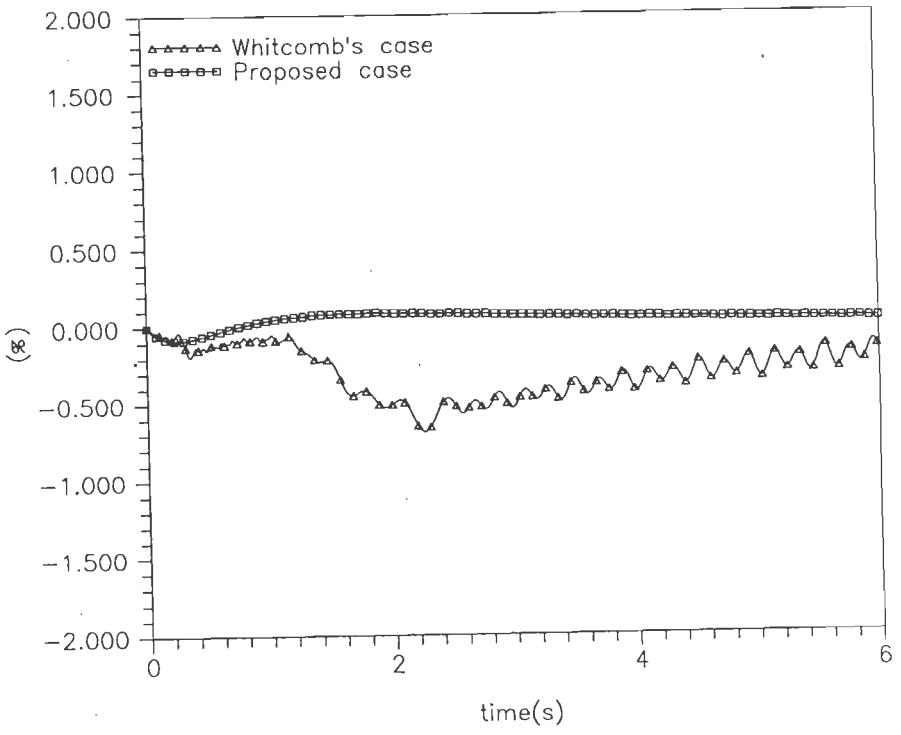

Fig.5.27 Tracking error as percent of max. input for test signal'E',joint-2, $\hat{\theta}(0)=0$.

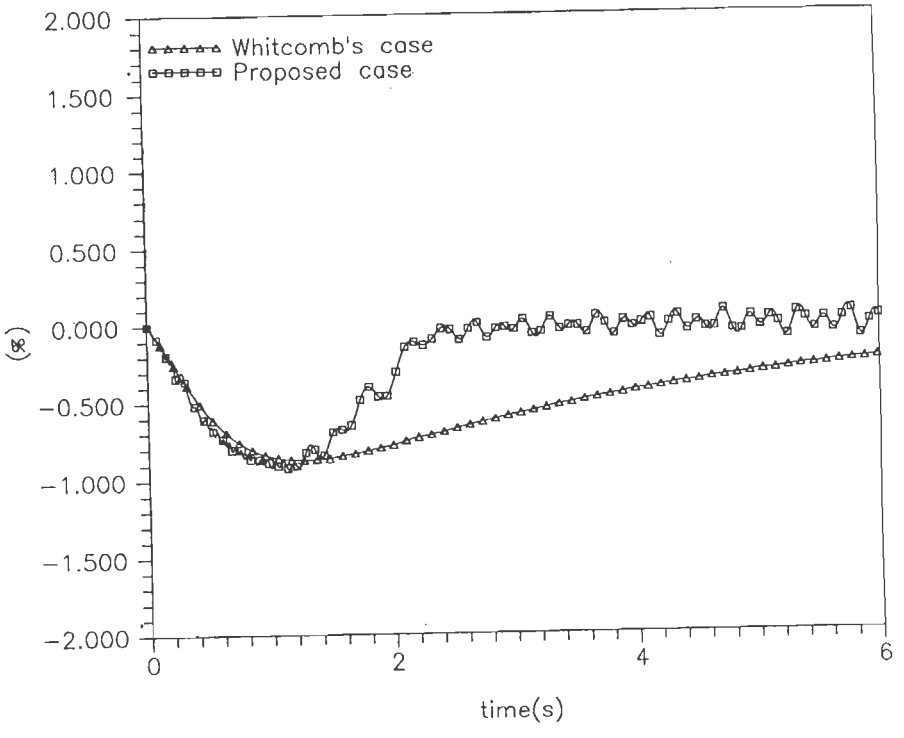

Fig.5.28 Tracking error as percent of max. input for test signal'F',joint-3, $\hat{\theta}(0)=0$

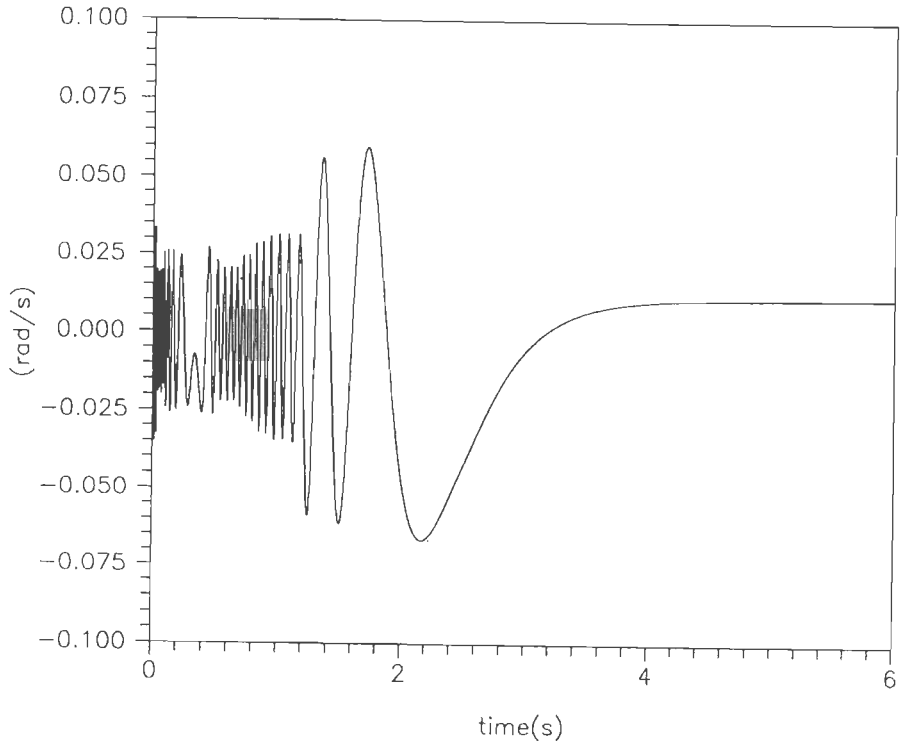

Fig.5.29 Velocity error for test signal 'D'(Whitcomb's case),joint-1, $\hat{\theta}(0)=0$.

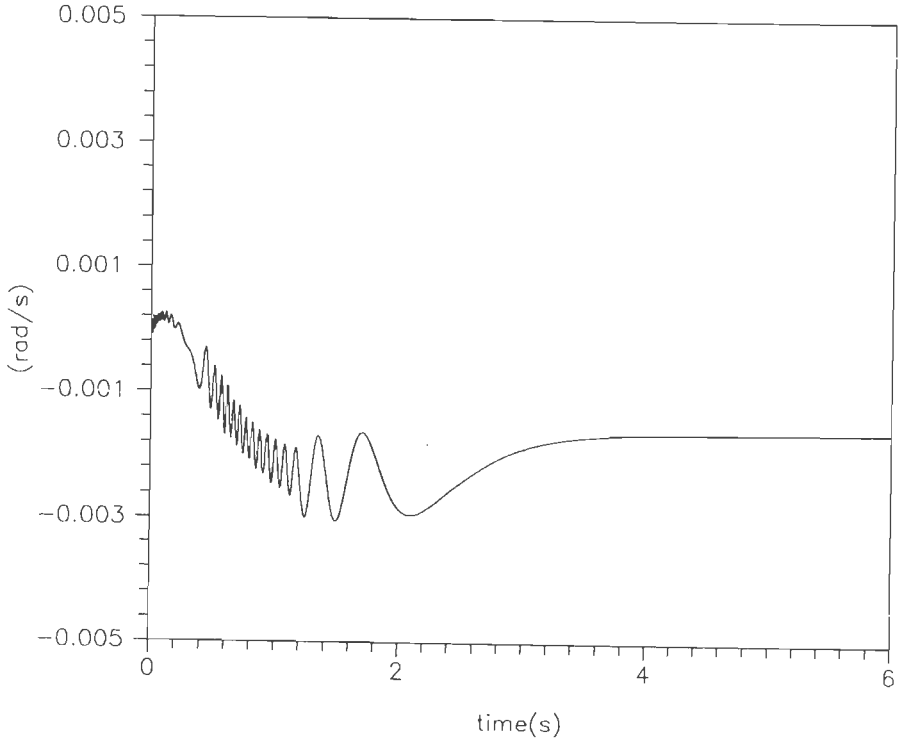

Fig.5.30 Velocity error for test signal 'D'(Proposed case), joint-1, $\hat{\theta}(0)=0$.

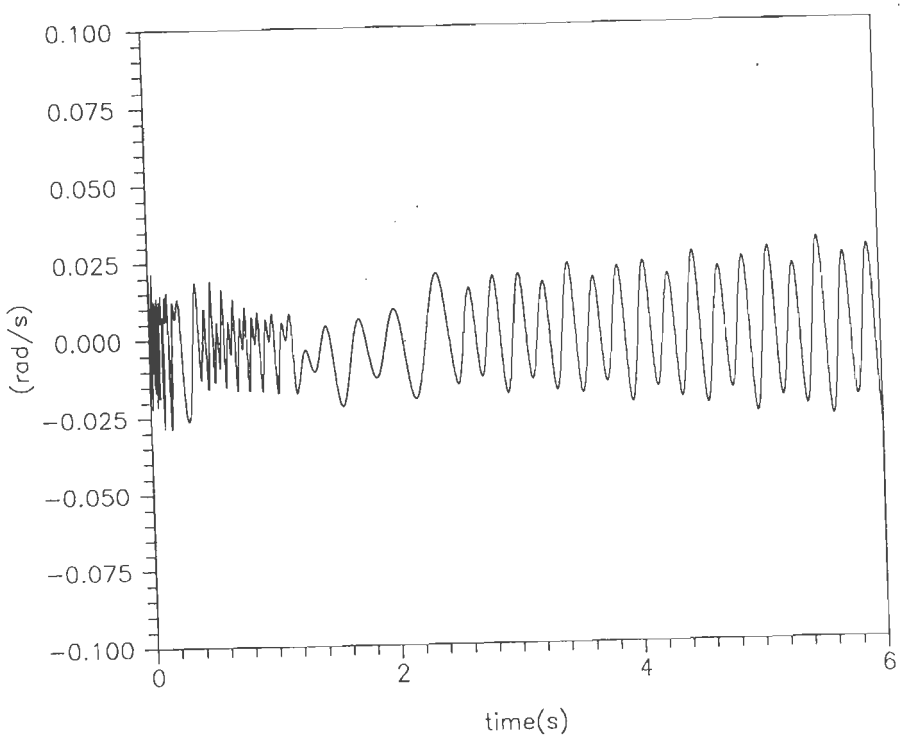

Fig.5.31 Velocity error for test signal 'E'(Whitcomb's case),joint-2, $\hat{\theta}(0)=0$.

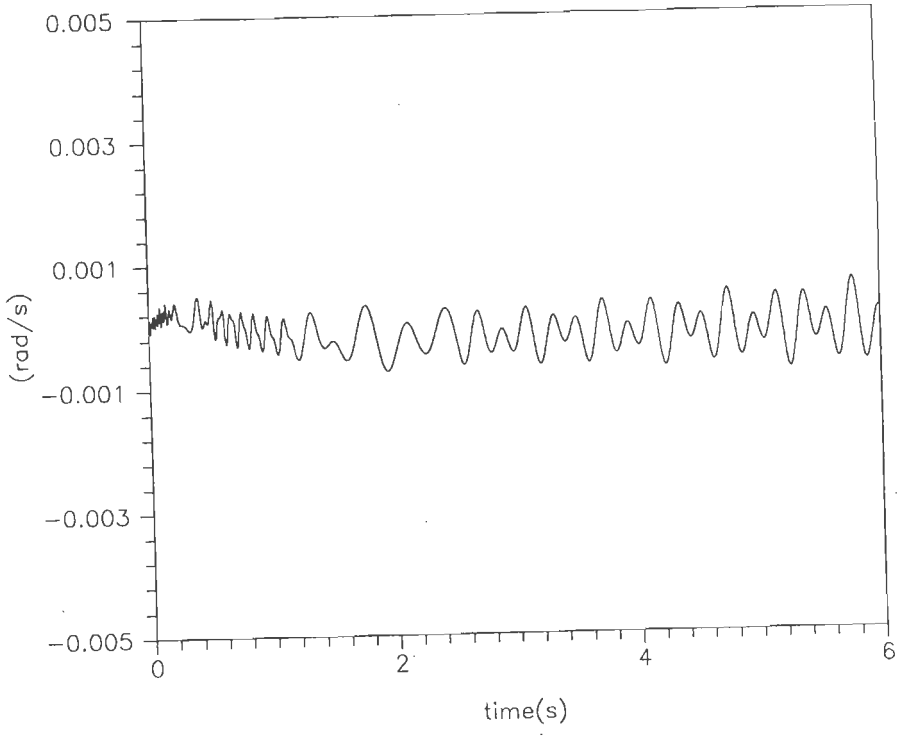

Fig.5.32 Velocity error for test signal 'E'(Proposed case), joint-2, $\hat{\theta}(0)=0$.

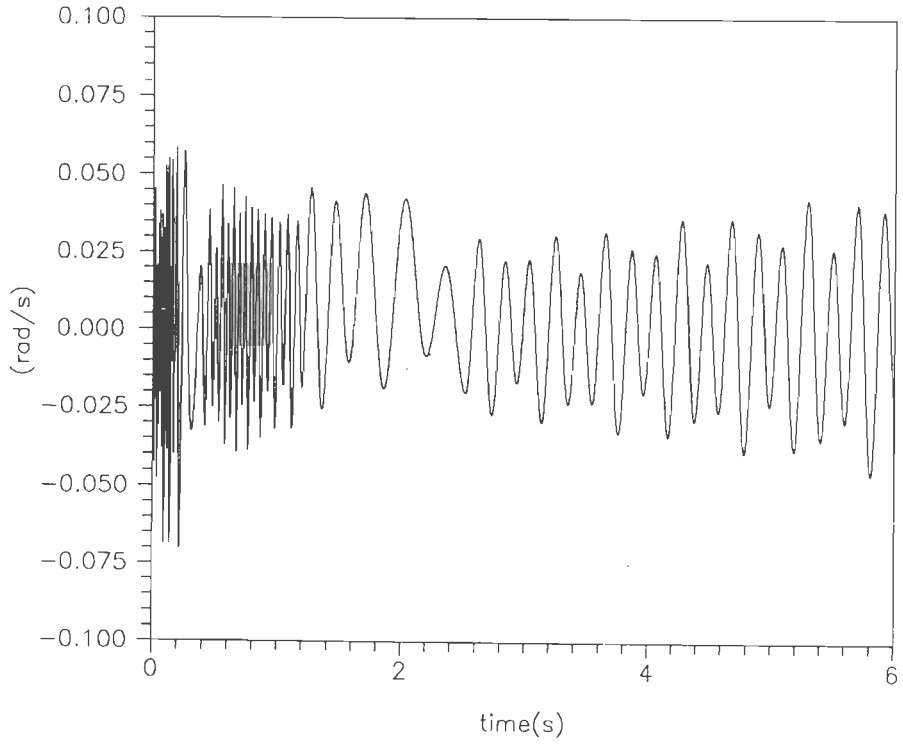

Fig.5.33 Velocity error for test signal 'F'(Whitcomb's case), joint-3, $\hat{\theta}$=(0).

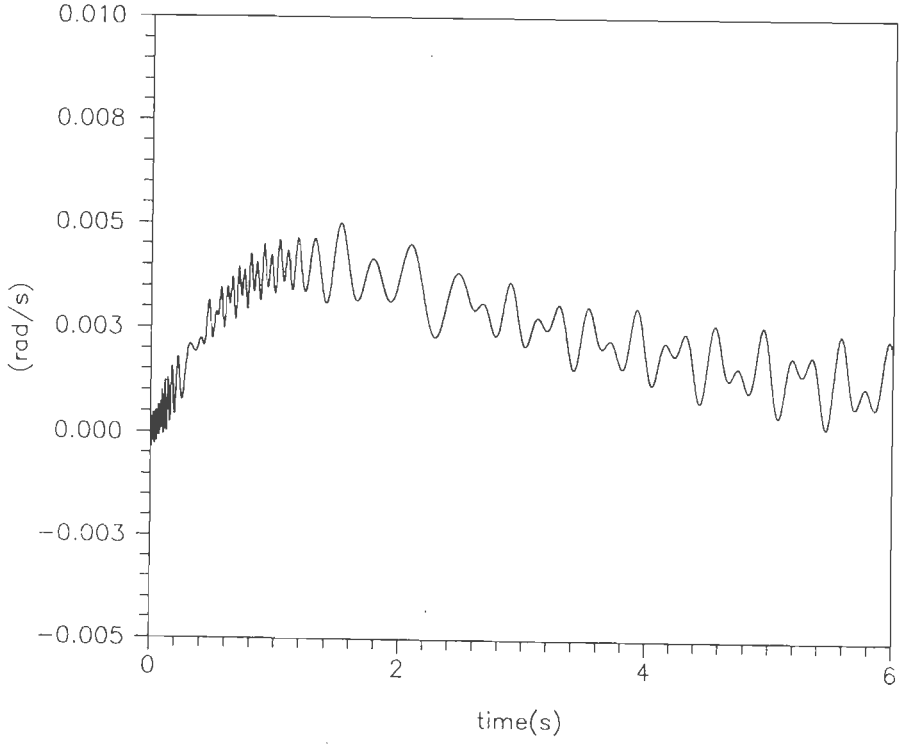

Fig.5.34 Velocity error for test signal 'F'(Proposed case),joint-3,$\hat{\theta}$=(0).

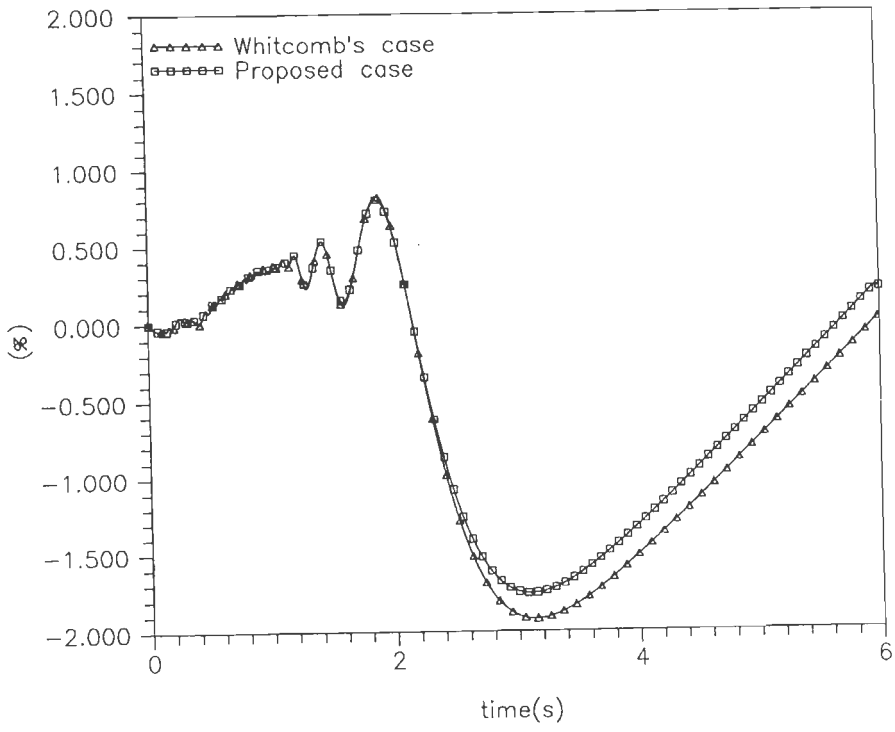

Fig.5.35 Tracking error as percent of max. input for test signal 'D',joint-1, $\hat{\theta}(0)=1/2\theta^{*}$.

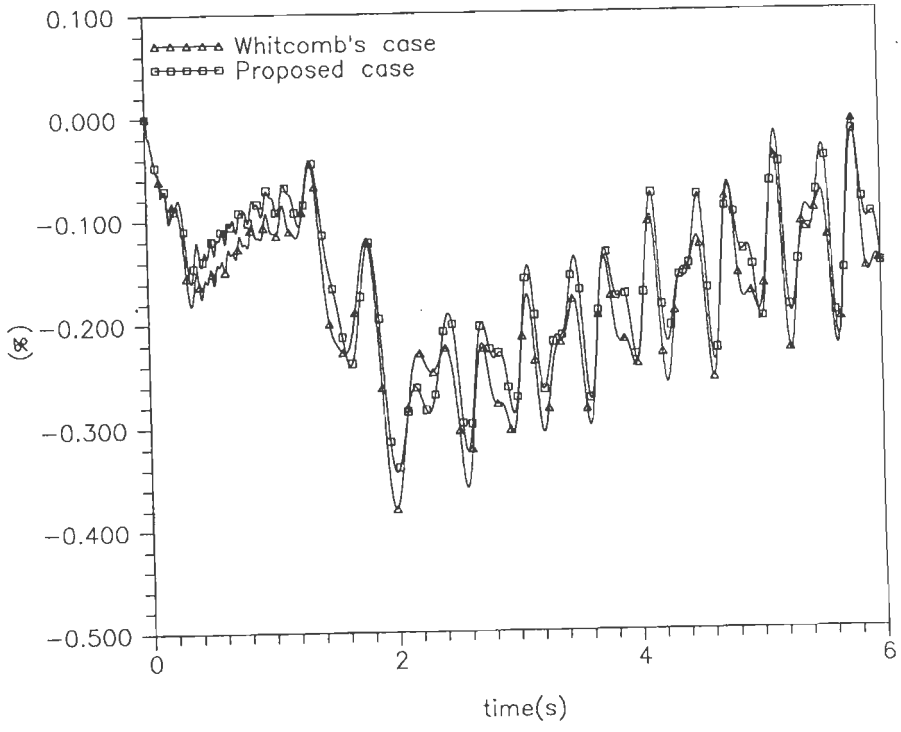

Fig.5.36 Tracking error as percent of max. input for test signal 'E',joint 2, $\hat{\theta}(0)=1/2\theta^{*}$.

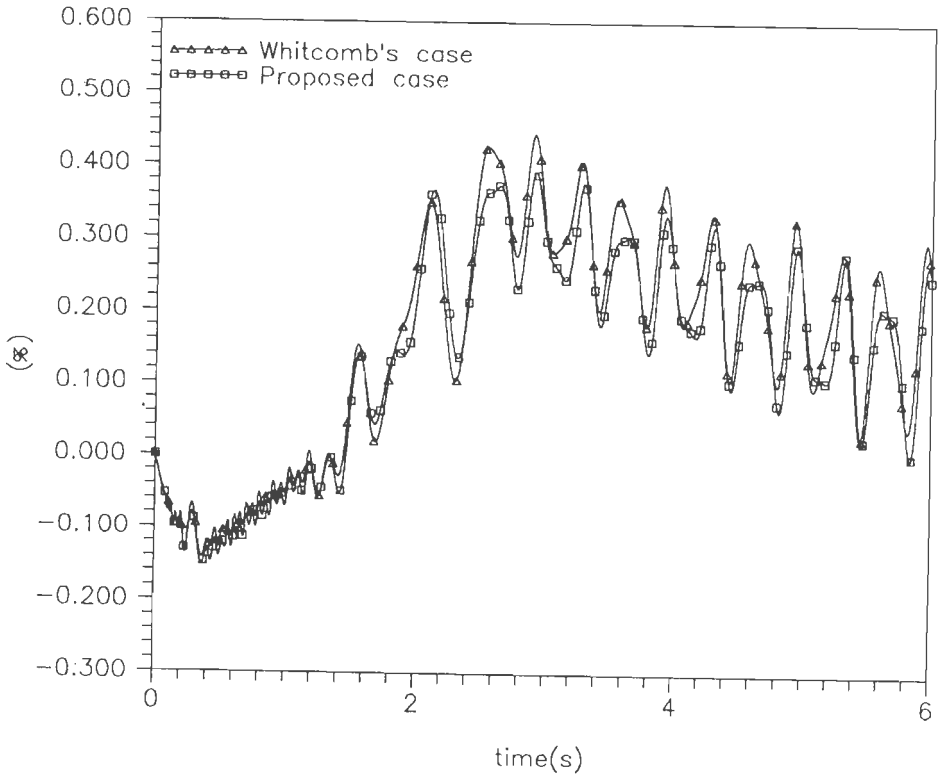

Fig.5.37 Tracking error as percent of max. input for test signal'F',joint-3, $\hat{\theta}(0)=1/2\theta^{*}$.

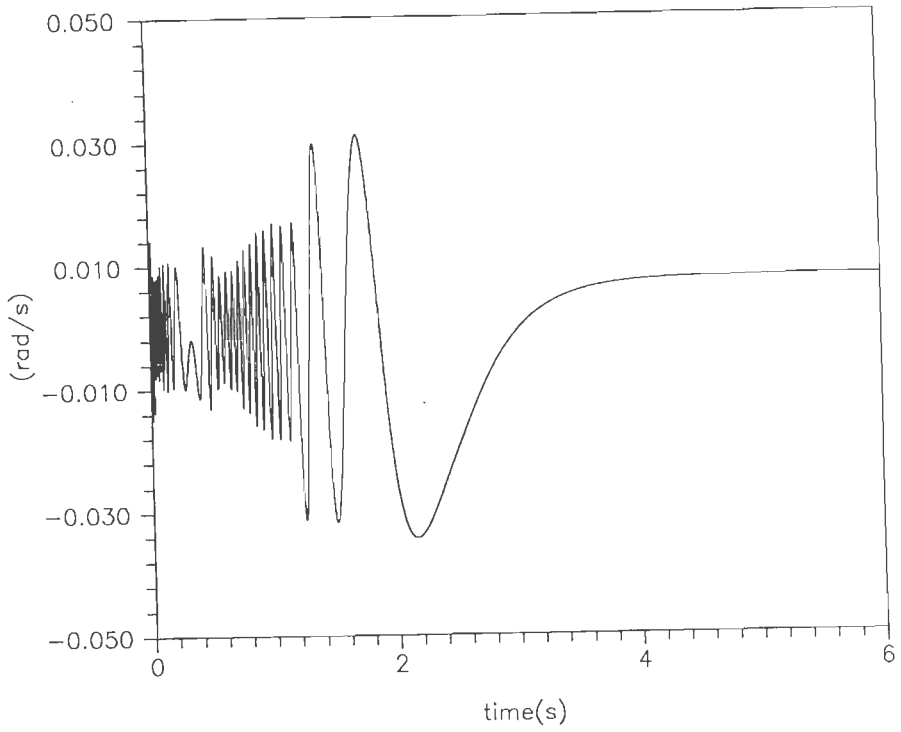

Fig.5.38 Velocity error for test signal 'D'(Whitcomb's case),joint-1, $\hat{\theta}(0)=1/2\theta^{*}$.

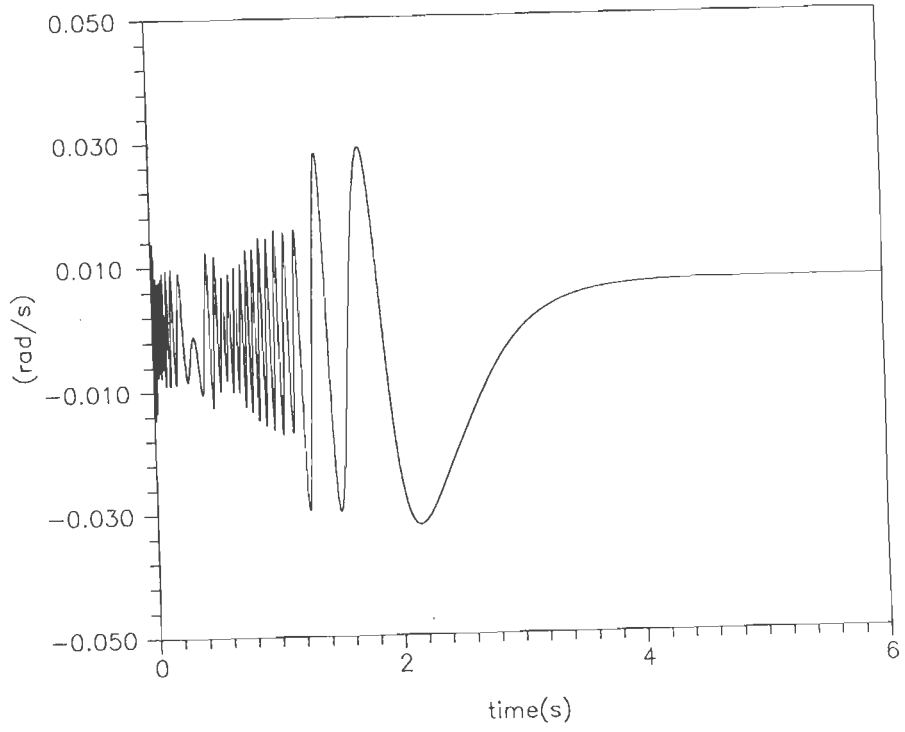

Fig.5.39 Velocity error for test signal 'D' (Proposed case),joint-1, $\hat{\theta}(0)=1/2\theta^{*}$.

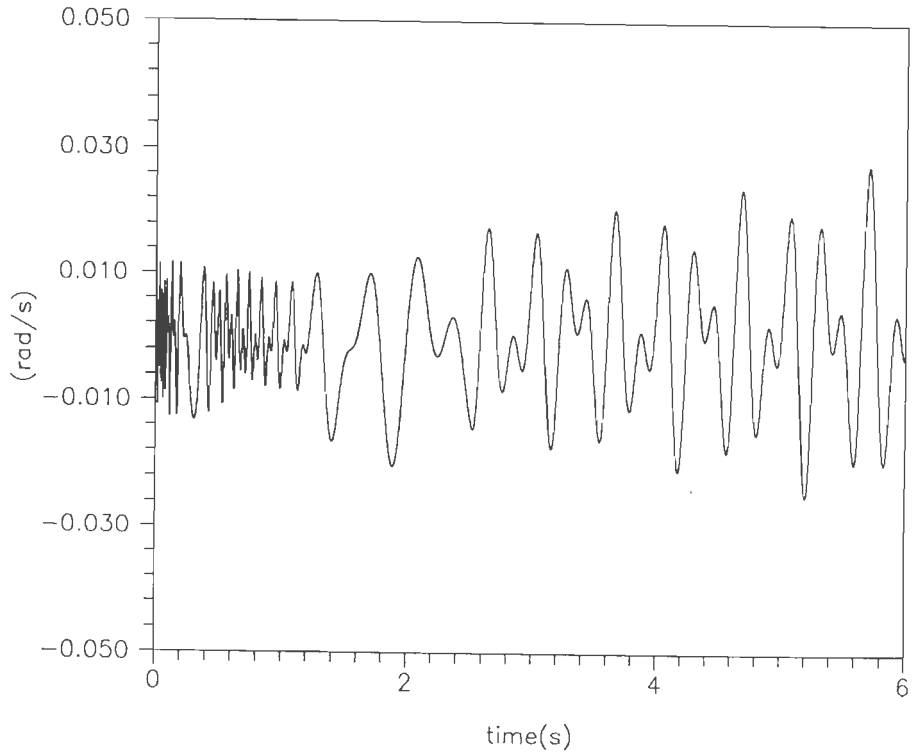

Fig.5.40 Velocity error for test signal 'E' (Whitcomb's case), joint-2, $\hat{\theta}(0)=1/2\theta^{*}$.

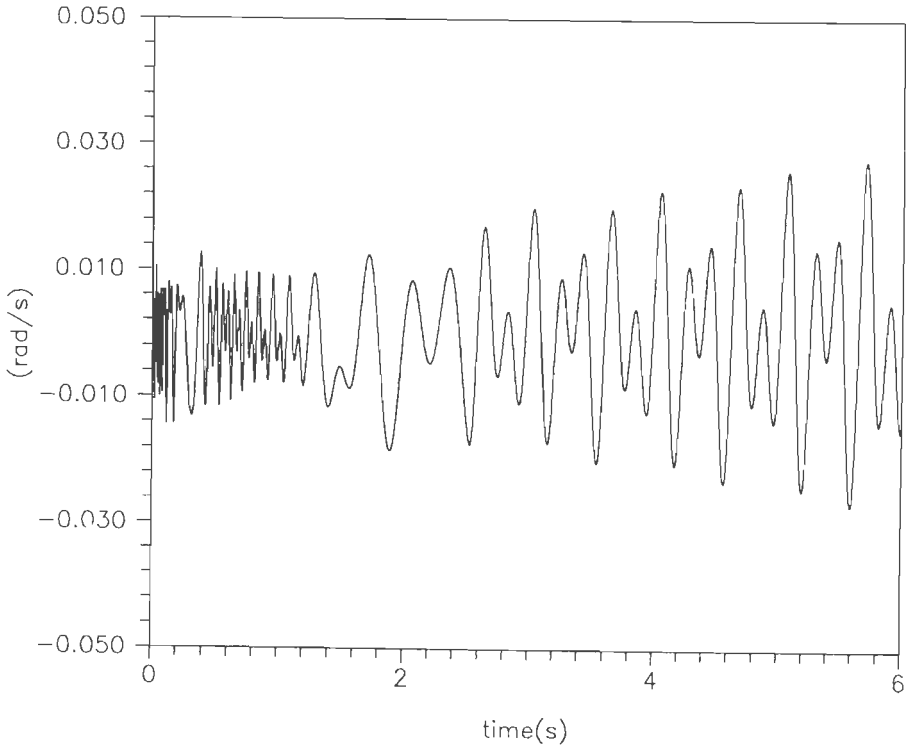

Fig.5.41 Velocity error for test signal 'E' (Proposed case), joint-2, $\hat{\theta}(0)=1/2\theta^{*}$.

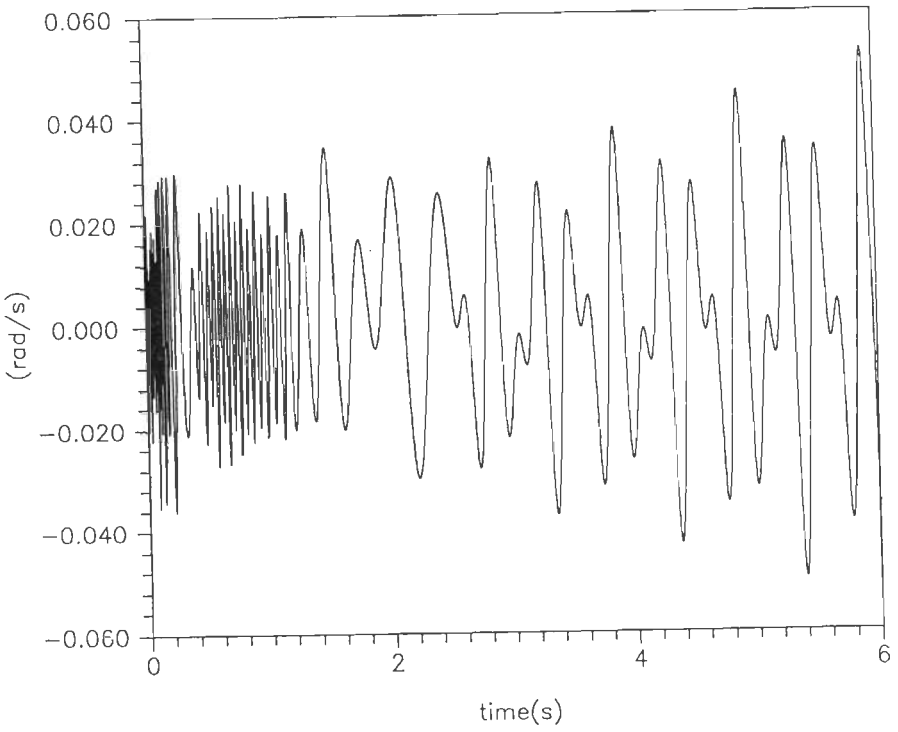

Fig.5.42 Velocity error for test signal 'F' (Whitcomb's case),joint-3, $\hat{\theta}(0)=1/2\theta^{*}$.

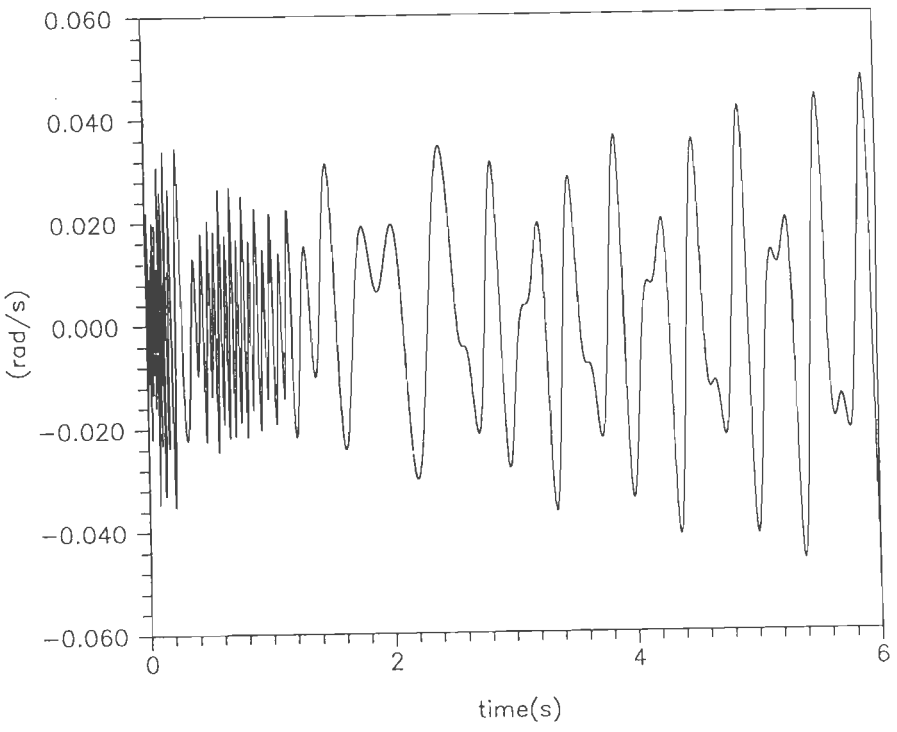

Fig.5.43 Velocity error for test signal 'F' (Proposed case),joint-3, $\hat{\theta}(0)=1/2\theta^{*}$.

5.3 SIMULATION OF PROPOSED ADAPTIVE CONTROL STRUCTURE USING NONLINEAR COMPENSATOR

The effectiveness of the proposed adaptive control structures (section 3.2.2) are illustrated as tracking performance of a two-DOF robot system (with mass) which is moving in the horizontal plane (Fig.5.44, $g(q)=0$). Its coefficients of matrices are described by (5.5). Adaptive control structures are simulated for desired trajectory (test signal 'G', 'H') as shown in Fig.5.45. Mathematically, it can be expressed as given by (5.9).

The regresser matrix for three cases are given as (see equation (5.12),(5.13) and (5.14), respectively :

(i) $W(q,\dot{q} - \lambda e, \dot{r} - \lambda_o e, \ddot{r} - \lambda_o \dot{e})$

(ii) $W(q,\dot{q} - \lambda e, \dot{r}, \ddot{r} - \lambda_o \dot{e})$

(iii) $W(q,\dot{q} - \lambda e, \dot{r}, \ddot{r})$

The following constant matrices are chosen as given below [7] : The controller settings for this simulation is obtained in order to satisfy the condition (3.32).

(i) case -1

$$\lambda_o = 0.5,\ \lambda_{o1} = 1.0,\ K_2 = 25I,\ kg = 15,\ \sigma_{n1} = 9000\ I$$

(ii) case -2

$$\lambda_o = 0.5,\ \lambda_{o1} = 0.5,\ K_1 = 75I,\ K_2 = 40I,\ kg = 15,\ \sigma_{n2} = 9000\ I$$

(iii) case -3

$$\lambda_o = 0.5,\ K_1 = 75I,\ K_2 = 40I,\ kg = 15,\ \sigma_{n3} = 9000\ I$$

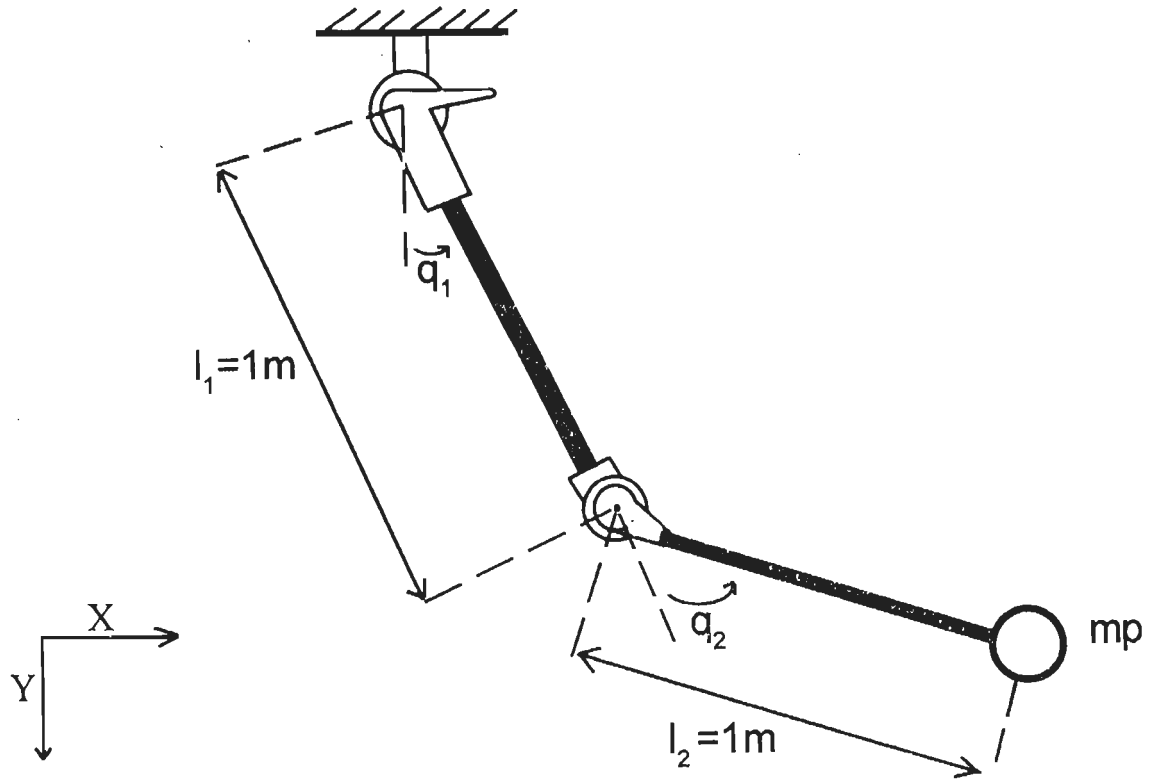

Fig. 5.44 Two-DOF Robot System with Mass

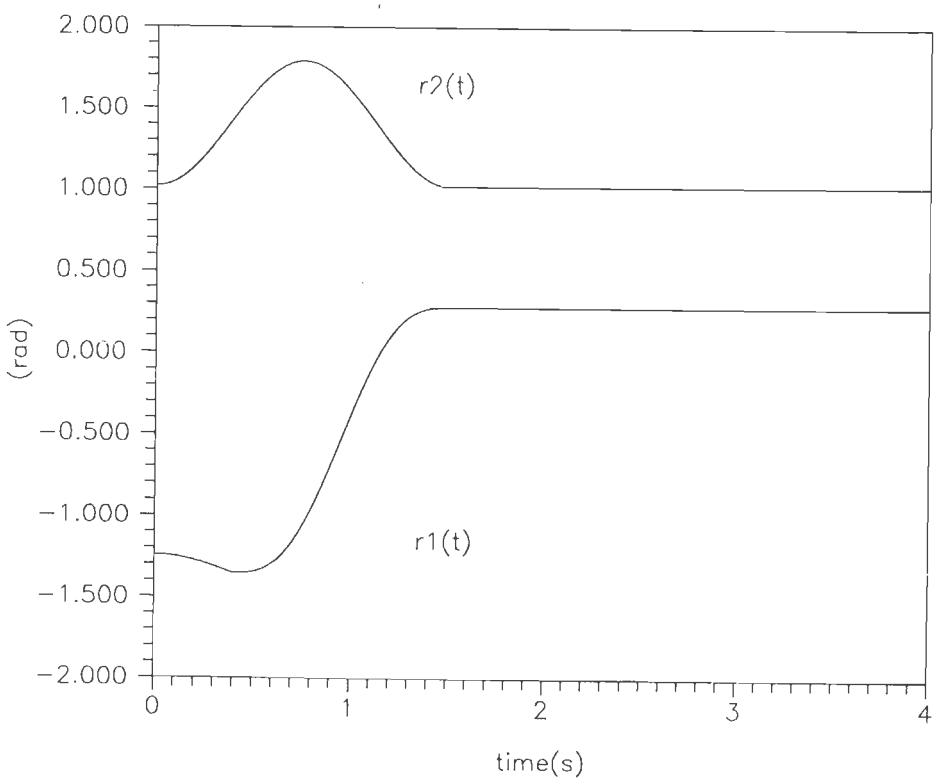

Fig.5.45 Desired trajectories for joint-1 and joint-2 (test signal 'G'and'H').

(i) $W(q.\dot{q} - \lambda e.\ \dot{r} - \lambda_o e.\ \ddot{r} - \lambda_o \dot{e}) =$

$$\begin{bmatrix}
\ddot{r}_1 - \lambda_o \dot{e}_1 & \ddot{r}_1 - \lambda_o \dot{e}_1 & \ddot{r}_2 - \lambda_o \dot{e}_2 & \cos q_2 (\ddot{r}_2 - \lambda_o \dot{e}_2) - \sin q_2 \dot{q}_2\ (\dot{r}_1 - \lambda_o e_1) + \lambda \sin q_2 (\dot{r}_2 - \lambda_o e_2) e_1 & 0 & 2(1+\cos q_2)(\ddot{r}_1 - \lambda_o \dot{e}_1) + (1+\cos q_2)(\ddot{r}_2 - \lambda_o \dot{e}_2) - \sin q_2 \dot{q}_2 \\
 & & & -\sin q_2 (\dot{q}_1 + \dot{q}_2)(\dot{r}_2 - \lambda_o e_2) + \sin q_2 \lambda ((\dot{r}_1 - \lambda_o e_1) + (\dot{r}_2 - \lambda_o e_2)) & & (\dot{r}_1 - \lambda_o e_1) - \sin q_2 (\dot{q}_1 + \dot{q}_2)(\dot{r}_2 - \lambda_o e_2) + \sin q_2 \lambda (\dot{r}_2 - \lambda_o e_2) \\
 & & & & & e_1 + \sin q_2 \lambda (\dot{r}_2 - \lambda_o e_2) e_1 + \sin q_2 \lambda ((\dot{r}_1 - \lambda_o e_1) + (\dot{r}_2 - \lambda_o e_2)) \\
0 & 0 & \ddot{r}_1 - \lambda_o \dot{e}_1 & \cos q_2 (\ddot{r}_1 - \lambda_o \dot{e}_1) + \sin q_2 \dot{q}_1 (\dot{r}_1 - \lambda_o e_1) - \sin q_2 \lambda (\dot{r}_1 - \lambda_o e_1) e_1 & \ddot{r}_2 - \lambda_o \dot{e}_2 & (1+\cos q_2)(\ddot{r}_1 - \lambda_o \dot{e}_1) + (\ddot{r}_2 - \lambda_o \dot{e}_2) + \sin q_2\ \dot{q}_1 (\dot{r}_1 - \lambda_o e_1) \\
 & & & & & -\sin q_2 \lambda (\dot{r}_1 - \lambda_o e_1) e_1
\end{bmatrix} \tag{5.12}$$

(ii) $W(q,\dot{q} - \lambda e, \dot{r}, \ddot{r} - \lambda_o \dot{e}) =$

$$\begin{bmatrix} \ddot{r}_1 - \lambda_o \dot{e}_1 & \ddot{r}_1 - \lambda_o \dot{e}_1 & \ddot{r}_2 - \lambda_o \dot{e}_2 & \cos q_2(\ddot{r}_2 - \lambda_o \dot{e}_2) - \sin q_2 \dot{q}_2 \dot{r}_1 + \lambda \sin q_2 \dot{r}_2 e_1 & 0 & 2(1+\cos q_2)(\ddot{r}_1 - \lambda_o \dot{e}_1) + (1+\cos q_2)(\ddot{r}_2 - \lambda_o \dot{e}_2) - \sin q_2 \dot{q}_2 \\ & & & -\sin q_2(\dot{q}_1 + \dot{q}_2)\ddot{r}_2 + \sin q_2 \lambda(\dot{r}_1 + \ddot{r}_2)e_2 & & \ddot{r}_1 - \sin q_2(\dot{q}_1 + \dot{q}_2)\dot{r}_2 + \sin q_2 \lambda \dot{r}_2 e_1 + \sin q_2 \lambda(\dot{r}_1 + \dot{r}_2)e_2 \\ 0 & 0 & \ddot{r}_1 - \lambda_o \dot{e}_1 & \cos q_2(\ddot{r}_1 - \lambda_o \dot{e}_1) + \sin q_2 \dot{q}_1 \dot{r}_1 - \sin q_2 \lambda \dot{r}_1 e_1 & \ddot{r}_2 - \lambda_o \dot{e}_2 & (1+\cos q_2)(\ddot{r}_1 - \lambda_o \dot{e}_1) + (\ddot{r}_2 - \lambda_o \dot{e}_2) + \sin q_2 \dot{q}_1 \dot{r}_1 - \sin q_2 \lambda \dot{r}_1 e_1 \end{bmatrix} \quad (5.13)$$

(iii) $W(q,\dot{q} - \lambda e, \dot{r}, \ddot{r}) =$

$$\begin{bmatrix} \ddot{r}_1 & \ddot{r}_1 & \ddot{r}_2 & \cos q_2 \ddot{r}_2 - \sin q_2 \dot{q}_2 \dot{r}_1 + \lambda \sin q_2 \dot{r}_2 e_1 & 0 & 2(1+\cos q_2)\ddot{r}_1 + (1+\cos q_2)\ddot{r}_2 - \sin q_2 \dot{q}_2 \dot{r}_1 - \sin q_2 (\dot{q}_1 + \dot{q}_2)\dot{r}_2 \\ & & & -\sin q_2 (\dot{q}_1 + \dot{q}_2)\dot{r}_2 + \sin q_2 \lambda (\dot{r}_1 + \dot{r}_2) e_2 & & + \sin q_2 \lambda \dot{r}_2 e_1 + \sin q_2 \lambda (\dot{r}_1 + \dot{r}_2) e_2 \\ 0 & 0 & \ddot{r}_1 & \cos q_2 \ddot{r}_1 + \sin q_2 \dot{q}_1 \dot{r}_1 - \sin q_2 \lambda \dot{r}_1 e_1 & \ddot{r}_2 & (1+\cos q_2)\ddot{r}_1 + \ddot{r}_2 + \sin q_2 \dot{q}_1 \dot{r}_1 - \sin q_2 \lambda \dot{r}_1 e_1 \end{bmatrix} \quad (5.14)$$

Trajectory tracking performance of the existing case [7] and proposed cases are shown in Fig. 5.46-5.61. Table -III indicates the maximum error for all the cases. The estimated pay load mass 'mp' for all cases are shown in Fig. 5.62-5.65.

Table -III

Maximum errors for Berghuis case and three proposed cases

Response	Berghuis case[7]		Proposed case-1		Proposed case-2		Proposed case-3	
	Joint-1	Joint-2	Joint-1	Joint-2	Joint-1	Joint-2	Joint-1	Joint-2
Tracking error (%)	0.7132	0.7484	0.6250	0.6521	0.3235	0.5473	0.6310	0.5488
Velocity error (rad/s)	0.4232	0.5251	0.3952	0.3946	0.4175	0.3879	0.3681	0.4190

The results from Fig. 5.46-5.61 are tabulated in Table - III. The tracking performance of the proposed cases are better in comparison to [7].

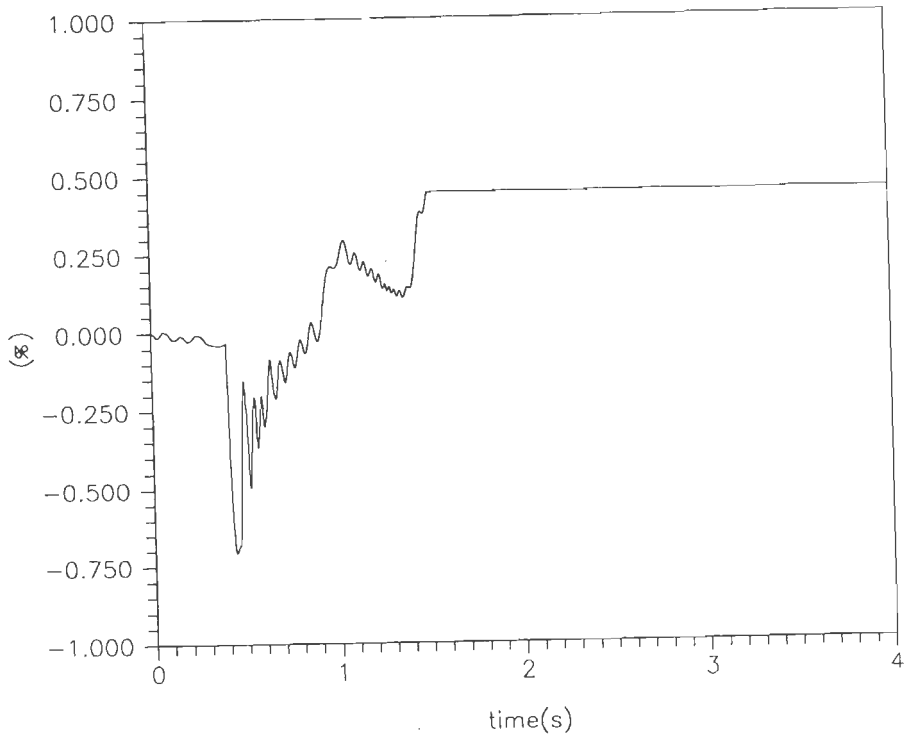

Fig.5.46 Tracking error as percent of max. input for test signal 'G'(Berghuis case), joint-1.

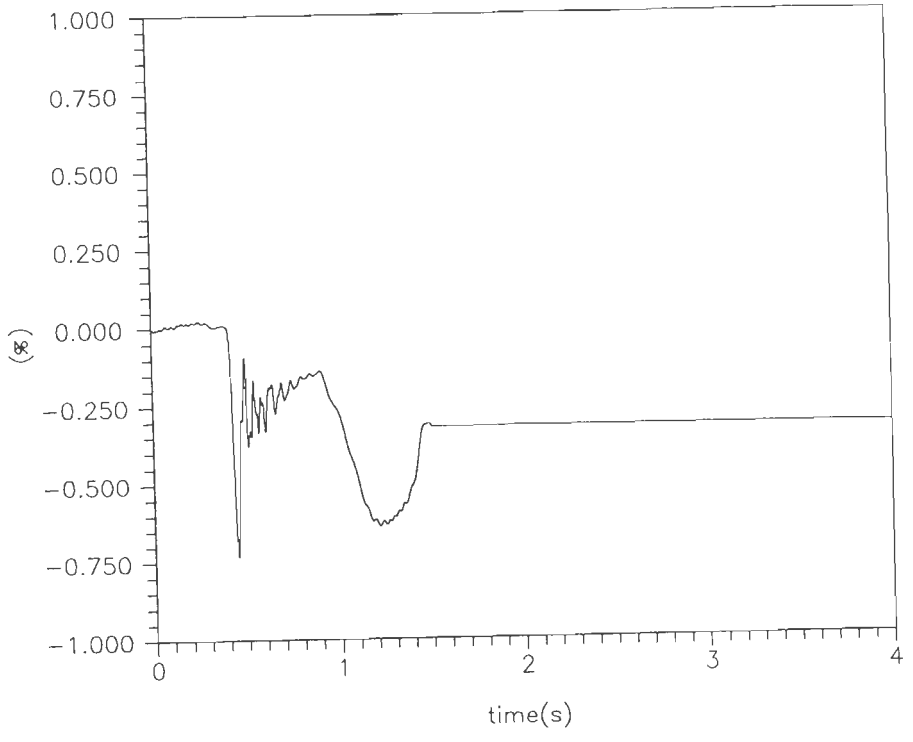

Fig.5.47 Tracking error as percent of max. input for test signal 'H'(Berghuis case), joint-2.

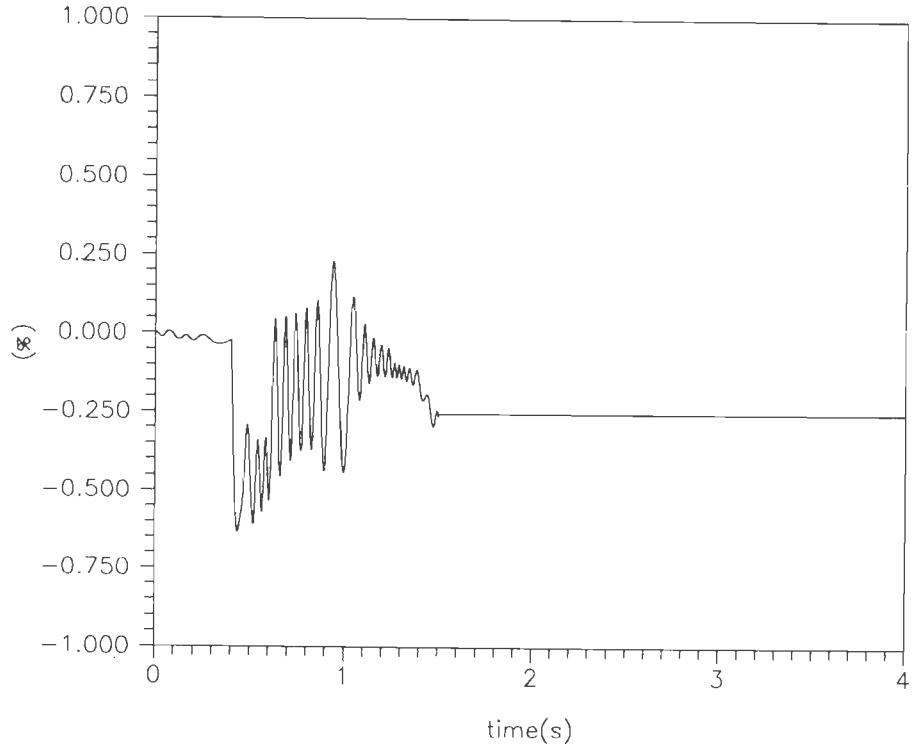

Fig.5.48 Tracking error as percent of max. input for test signal 'G'(Proposed case-1), joint-1.

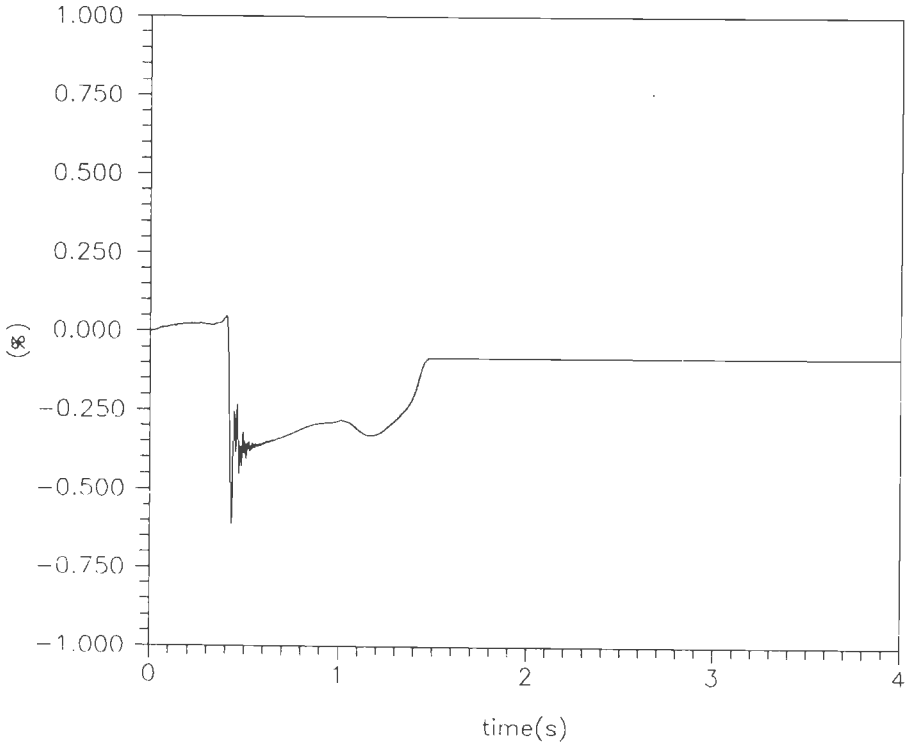

Fig.5.49 Tracking error as percent of max. input for test signal 'H'(Proposed case-1), joint-2.

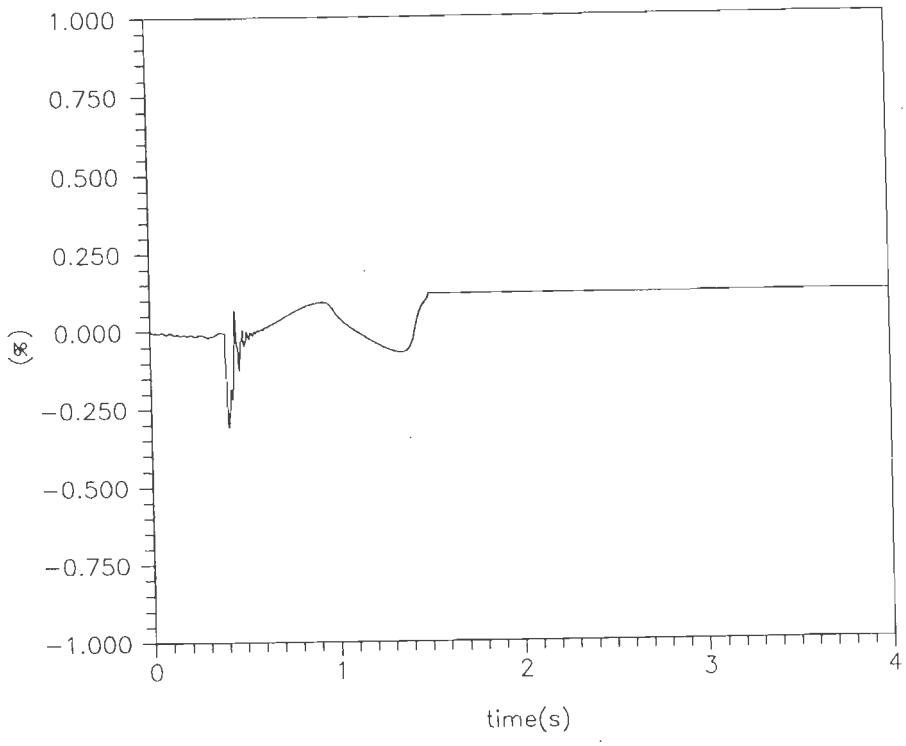

Fig.5.50 Tracking error as percent of max. input for test signal 'G'(Proposed case-2), joint-1.

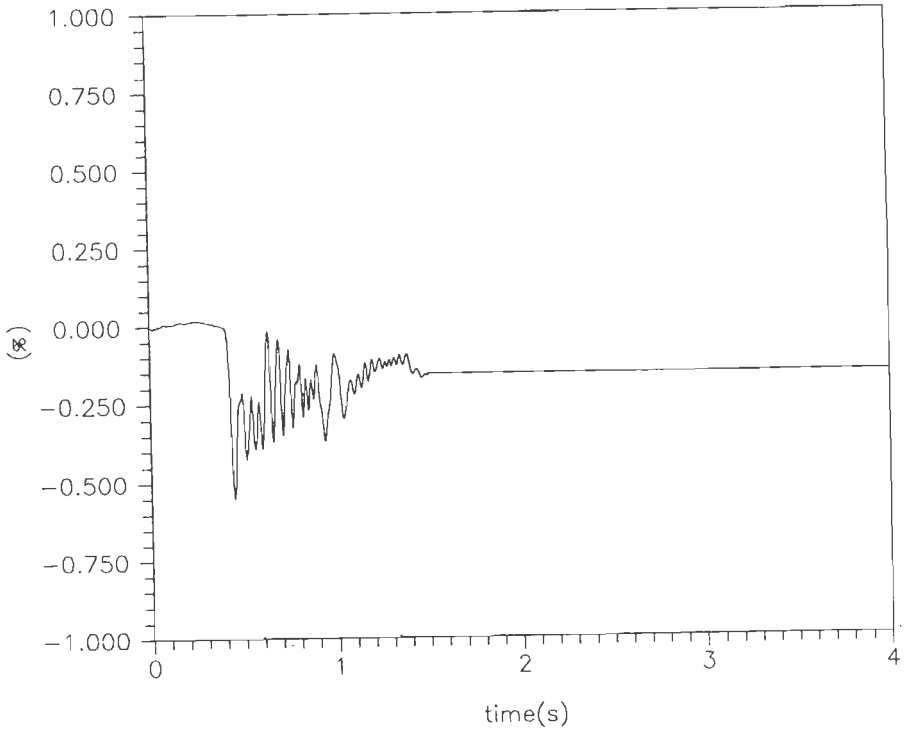

Fig.5.51 Tracking error as percent of max. input for test signal 'H'(Proposed case-2), joint-2.

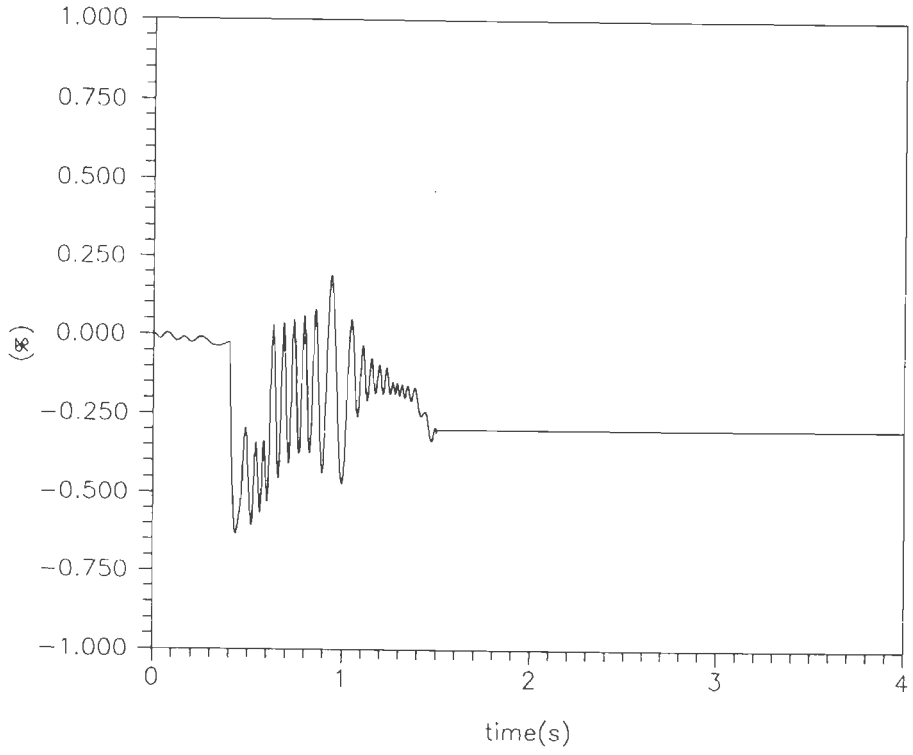

Fig.5.52 Tracking error as percent of max. input for test signal 'G'(Proposed case-3), joint-1.

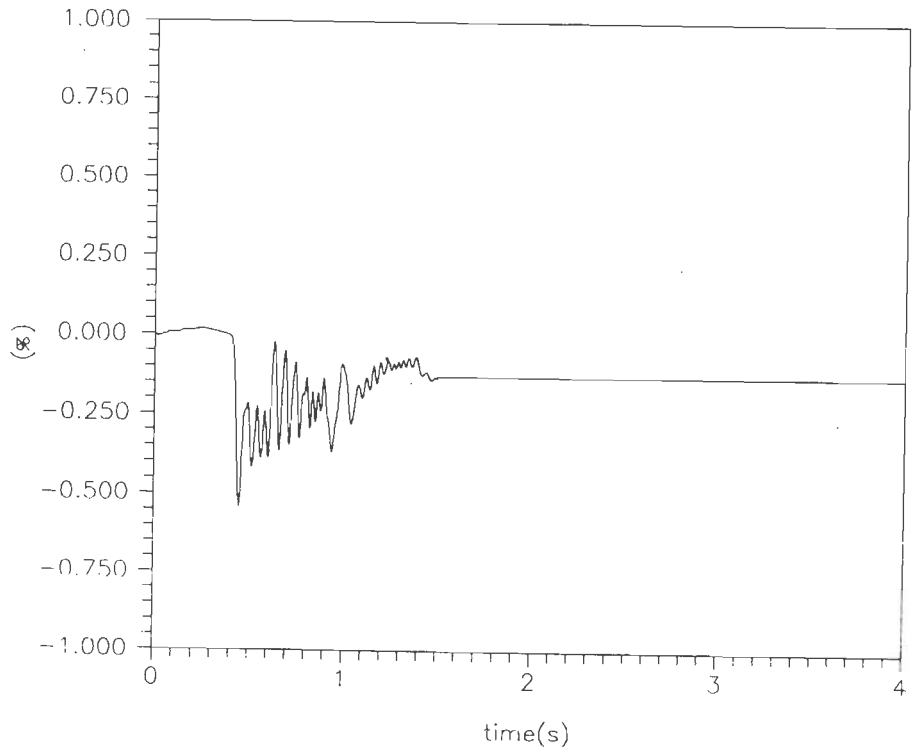

Fig.5.53 Tracking error as percent of max. input for test signal 'H'(Proposed case-3), joint-2.

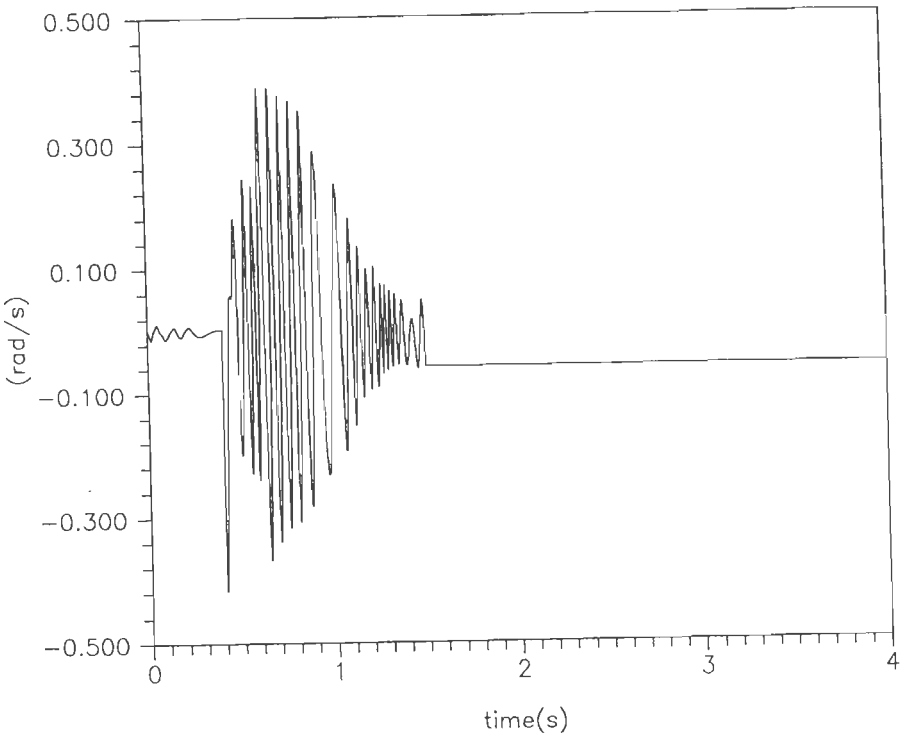

Fig.5.54 Velocity error for test signal 'G'(Berghuis case), joint-1.

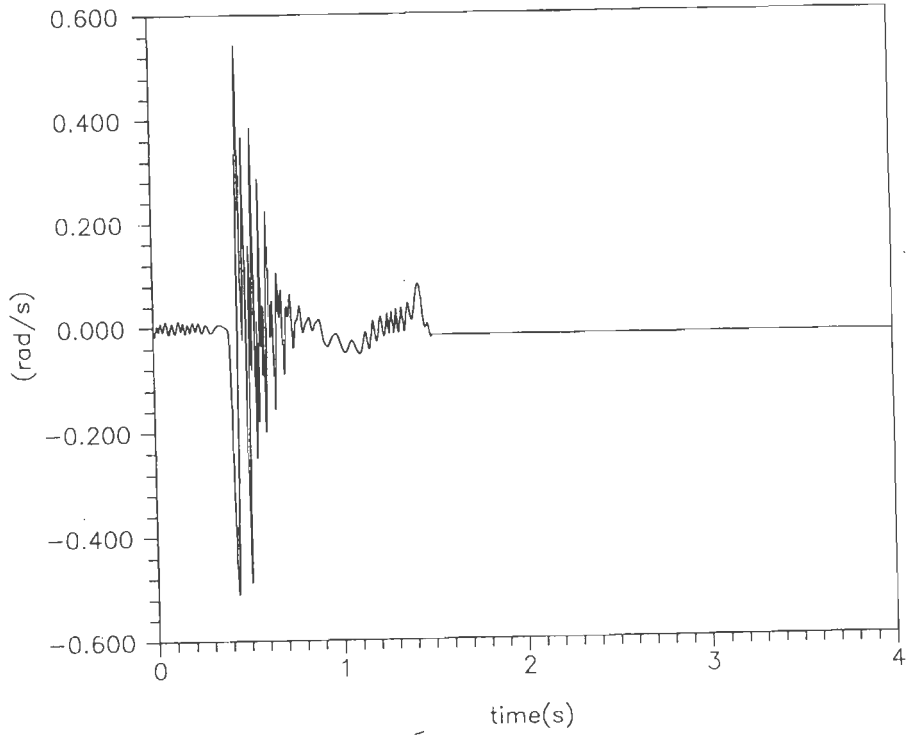

Fig.5.55 Velocity error for test signal 'H'(Berghuis case), joint-2.

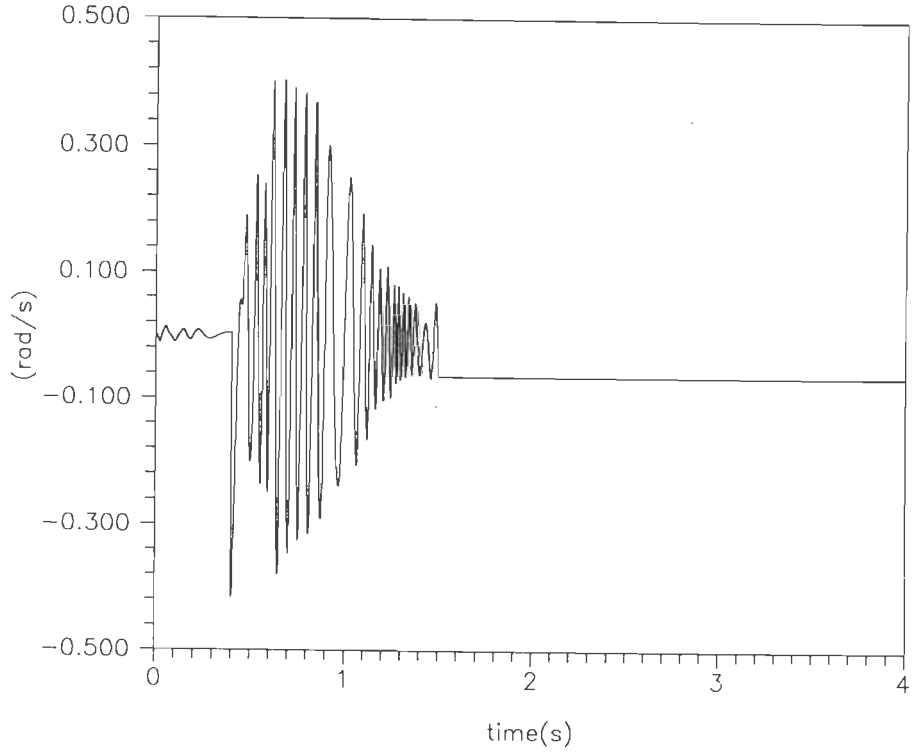

Fig.5.56 Velocity error for test signal 'G'(Proposed case-1), joint-1.

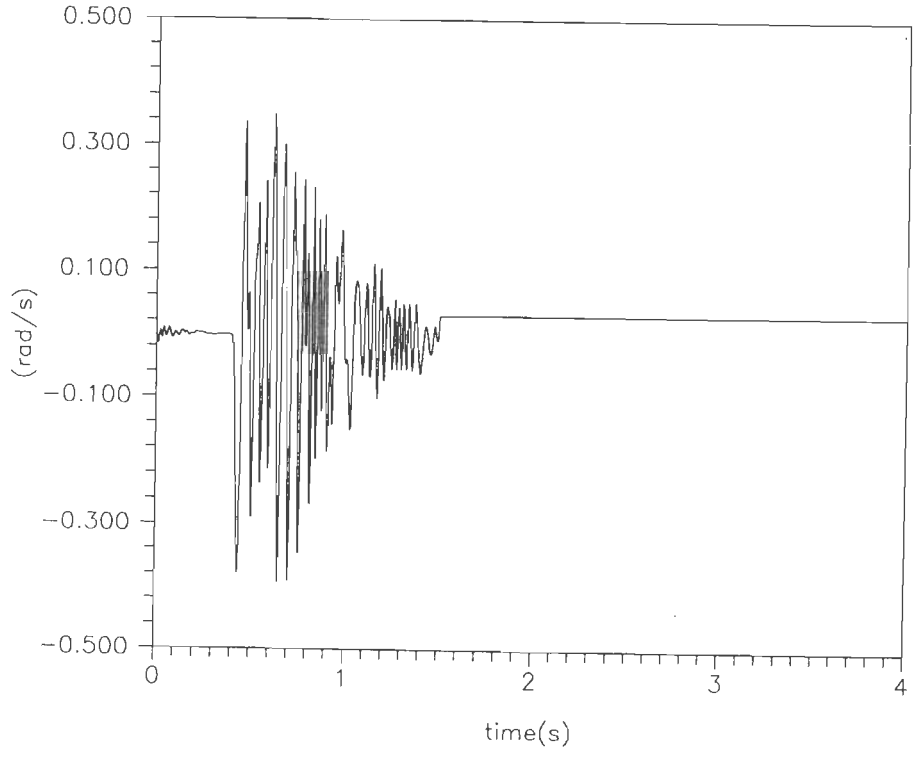

Fig.5.57 Velocity error for test signal 'H'(Proposed case-1), joint-2.

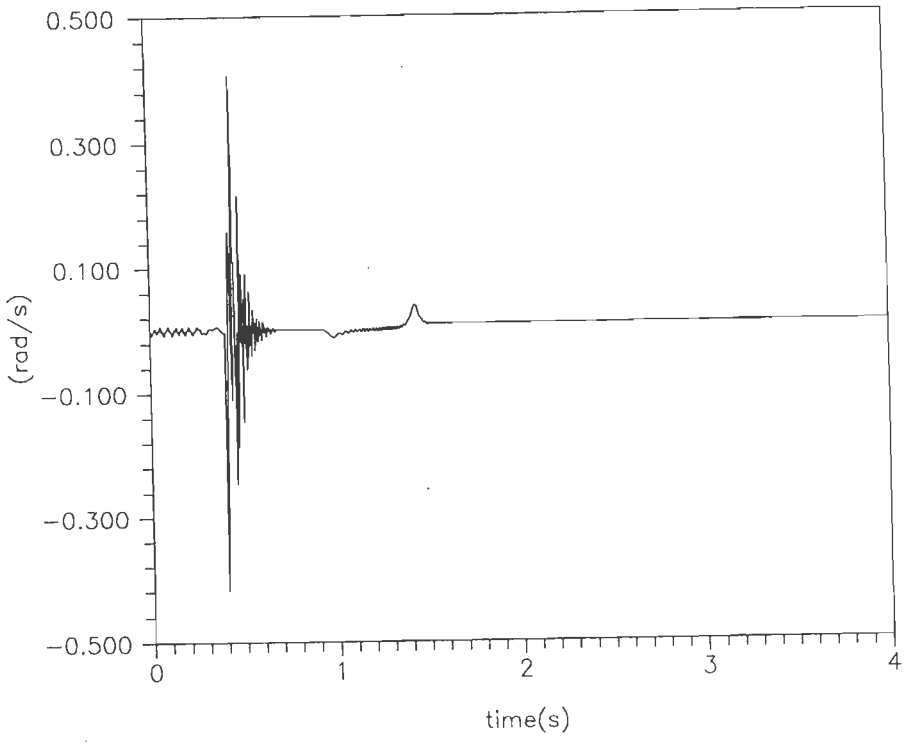

Fig.5.58 Velocity error for test signal 'G'(Proposed case-2), joint-1.

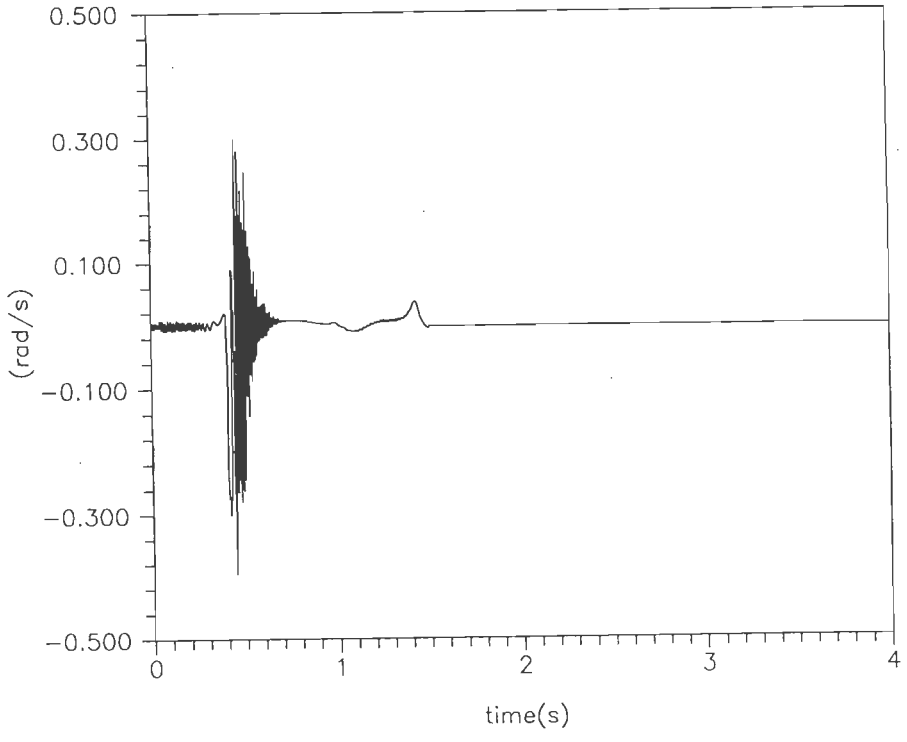

Fig.5.59 Velocity error for test signal 'H'(Proposed case-2), joint-2.

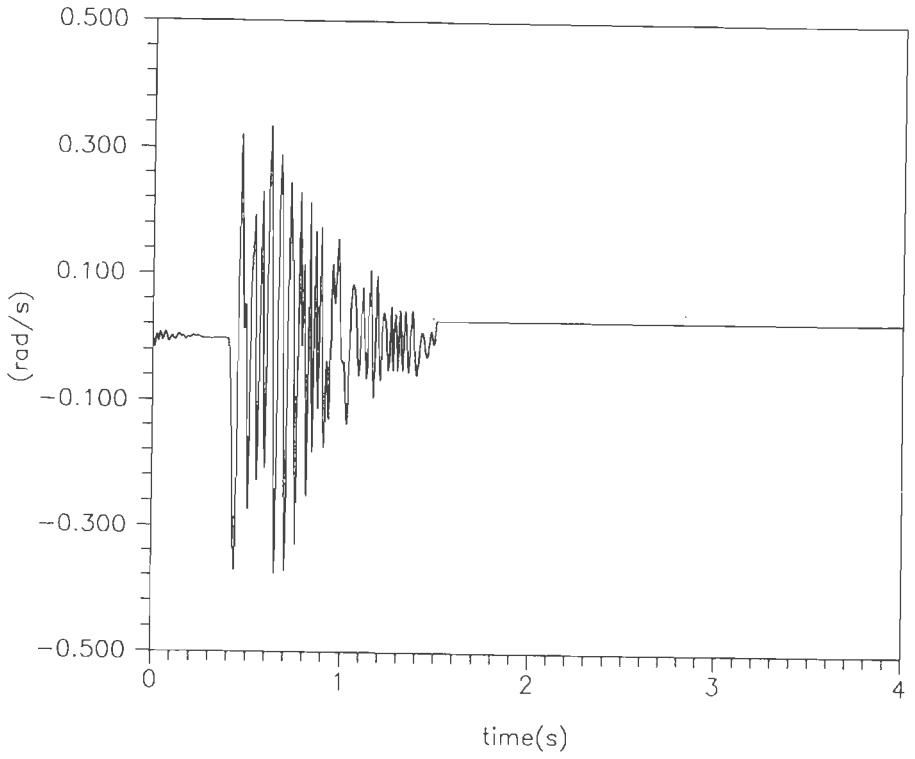

Fig.5.60 Velocity error for test signal 'G'(Proposed case-3), joint-1.

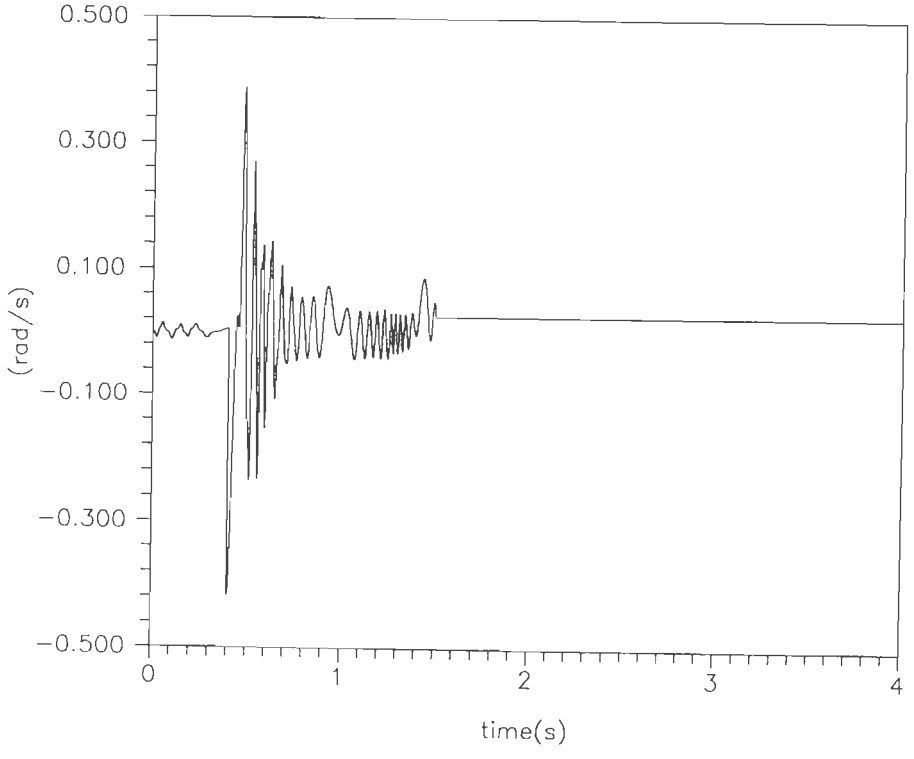

Fig.5.61 Velocity error for test signal 'H'(Proposed case-3), joint-2.

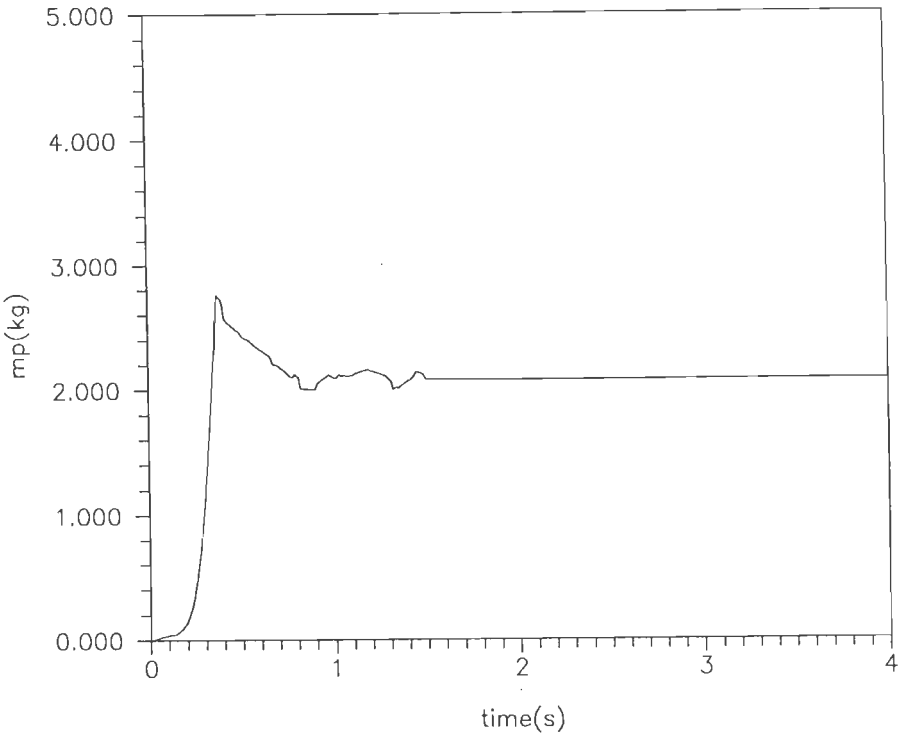

Fig.5.62 Estimated mass for Berghuis case.

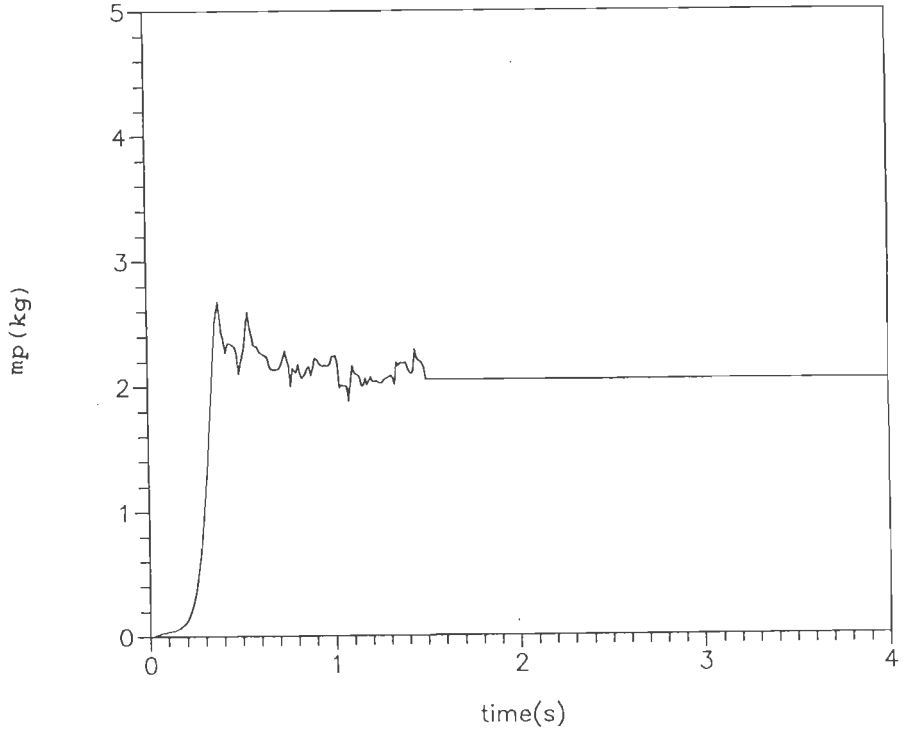

Fig.5.63 Estimated mass for Proposed case-1.

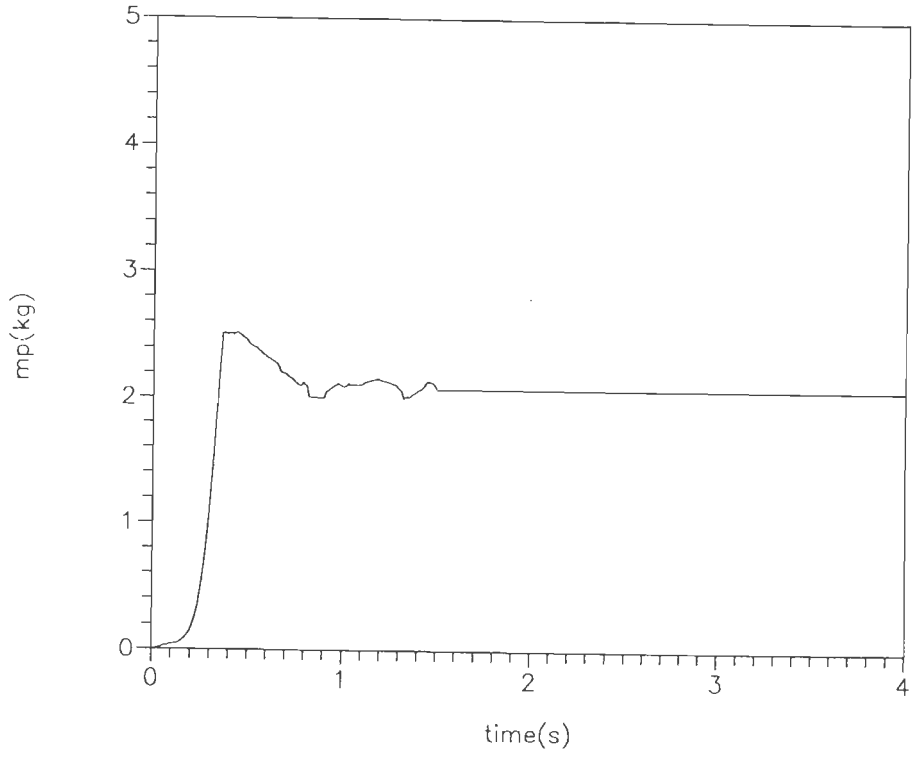

Fig.5.64 Estimated mass for Proposed case-2.

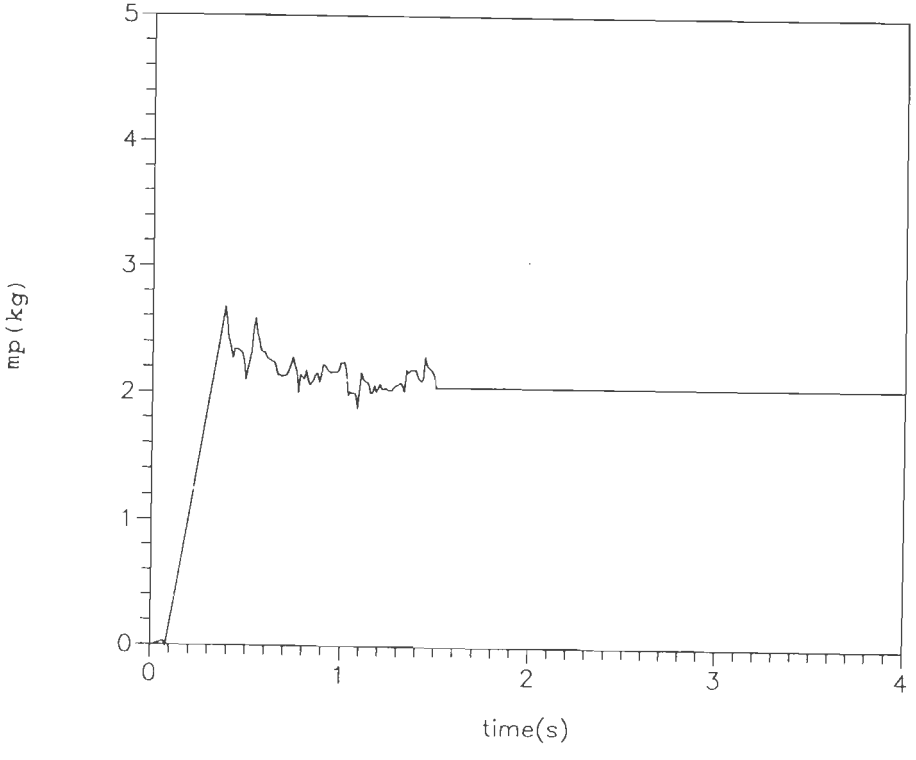

Fig.5.65 Estimated mass for Proposed case-3.

5.4 SIMULATION OF BOUNDED FORM OF ADAPTIVE CONTROLLER STRUCTURE

The simultation results of the proposed bounded form of Adaptive controller structure is illustrated with simple example of a two-DOF robot system (Fig. 5.44) moving in horizontal plane, i.e. $g(q) = 0$. The robot sytem used in simulation is expressed by (3.7). The physical parameters are given by (5.5). The unknown parameter belong to some interval θ_{min} and θ_{max} and take the supremum of M_M, C_M over these intervals [7]. In this regard, the regressor matrix have chosen in the following form :

$$W(\|\dot{q} - \lambda e\|, \dot{r}, \ddot{r}) =$$

$$\begin{bmatrix} \ddot{r}_1 & \ddot{r}_2 & 0 & \dot{r}_1 & \dot{r}_2 & 0 & 0 \\ 0 & \ddot{r}_1 & \ddot{r}_2 & 0 & 0 & \dot{r}_1 & \|\dot{q} - \lambda e\| \end{bmatrix} \qquad (5.15)$$

In this case eq. (5.1) is modified as

$$M(q)\,\ddot{q} + C(q,\dot{q})\dot{q} + g(q) = W(\dot{q}, \ddot{q})\,\theta^*(q)$$

where $\theta^*(q)^T = [\, M_{11} \;\; M_{12} \;\; M_{22} \;\; C_{11} \;\; C_{12} \;\; C_{21} \;\; C_{22} \,]^T$, M_{11}, M_{12}, M_{22} and $C_{11}, C_{12}, C_{21}, C_{22}$ are the element of matrix $M(q)$ and $C(q,\dot{q})$, rspectively. Desired trajectories (test signal 'G', 'H') are described by ((5.9),Fig.5.45). For simulation use, the following set of parameters are chosen as given in [7] :

$\lambda_o = 0.5$, $K_1 = 75I$, $K_2 = 40I$, $kg = 12$, $\sigma_n = 5000\ I$, $M_M = 20$, $C_M = 5$;

Trajectory tracking of robot manipulators of the proposed adaptive controller structure for joint -1 and joint -2 are shown in Fig. 5.66-5.69. The estimated value of M_M and C_M can depicted from Fig. 5.70 and Fig. 5.71 respectively.

Table - IV

Maximum errors for bounded form of controller structure

Response	Proposed case	
	Joint-1	Joint-2
Tracking error (%)	0.4225	0.2251
Velocity error (rad/s)	0.4228	0.1326

It is found that the tracking performance of proposed case are drastically reduced in comparison to Berghuis case [7].

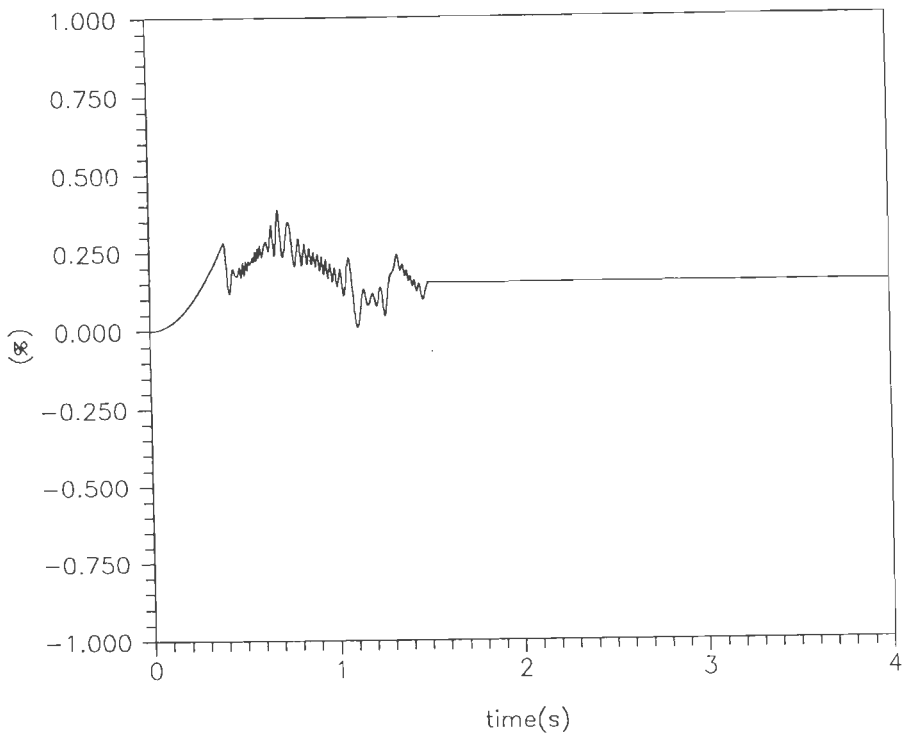

Fig.5.66 Tracking error as percent of max. input for test signal 'G'(Proposed bounded form), joint-1.

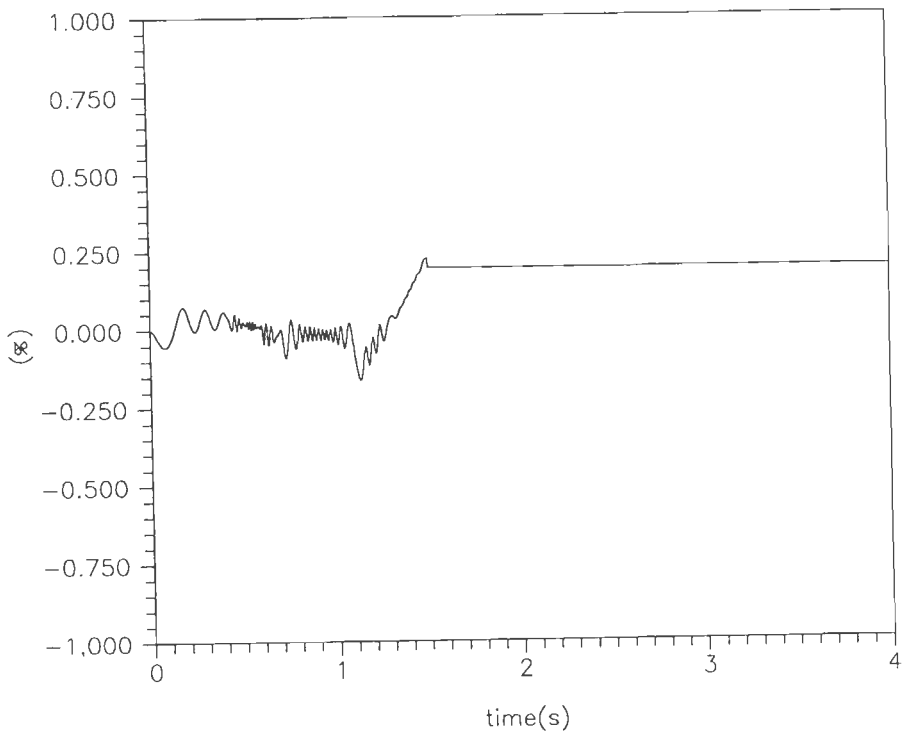

Fig.5.67 Tracking error as percent of max. input for test signal 'H'(Proposed bounded form), joint-2.

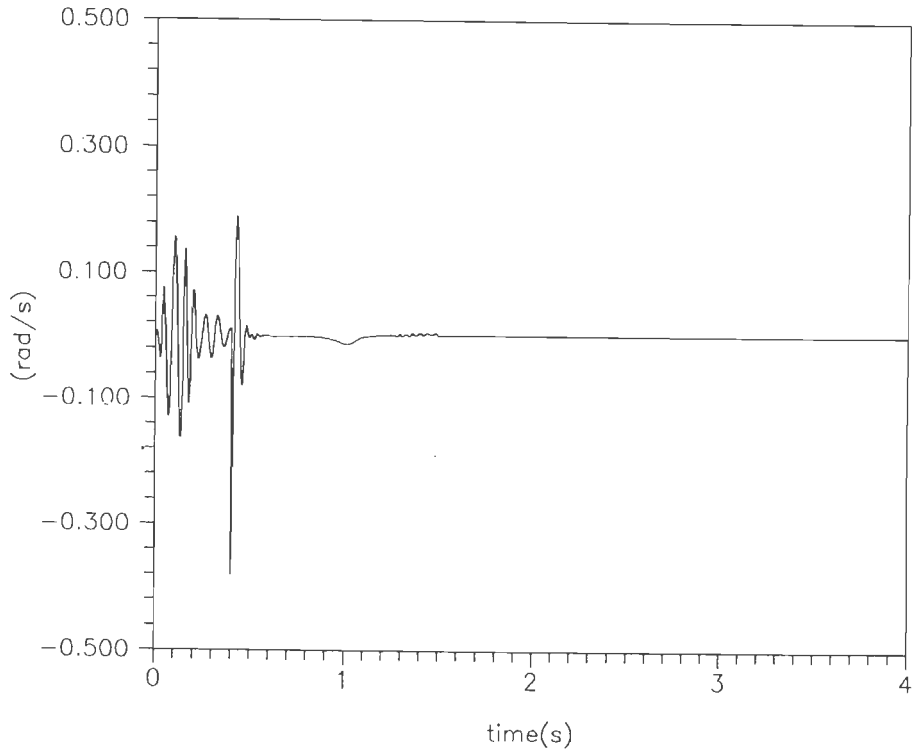

Fig.5.68 Velocity error for test signal 'G'(Proposed bounded form), joint-1.

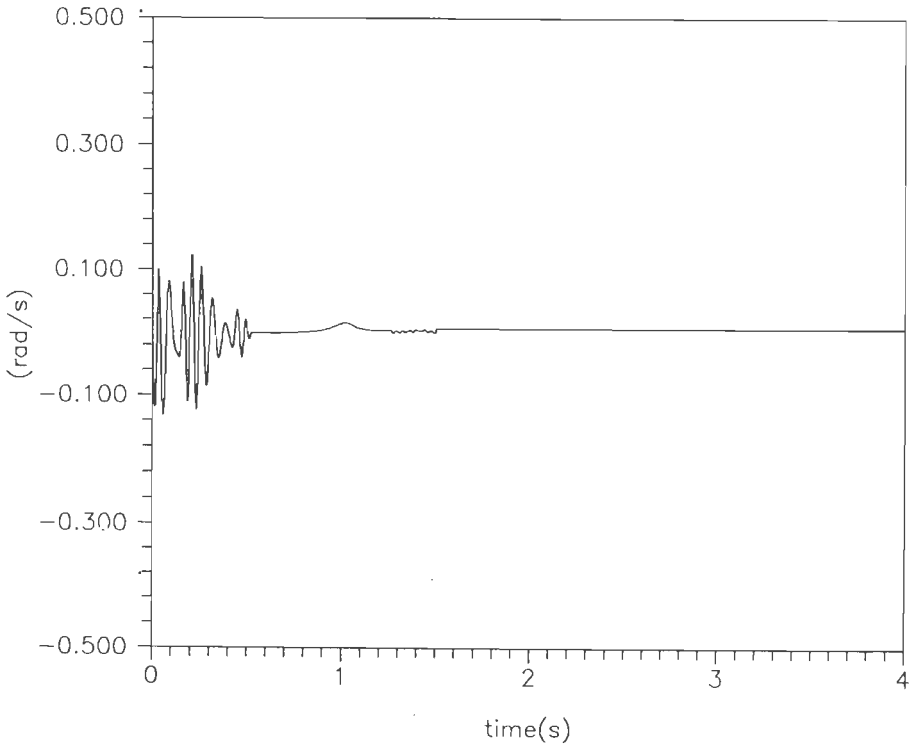

Fig.5.69 Velocity error for test signal 'H'(Proposed bounded form), joint- 2.

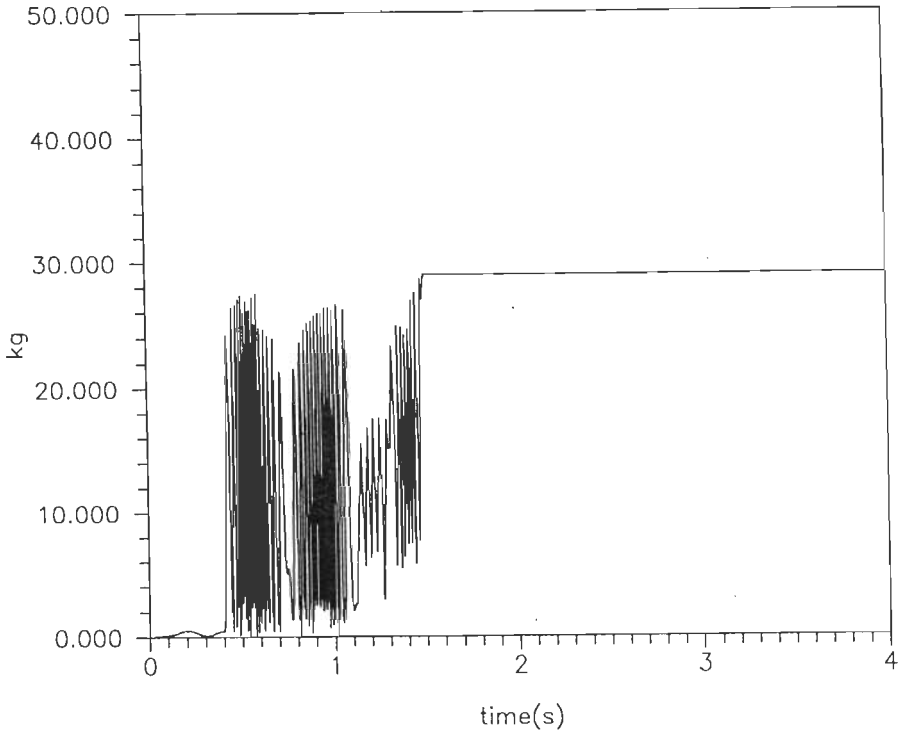

Fig.5.70 Estimated M_M for bounded form of controller.

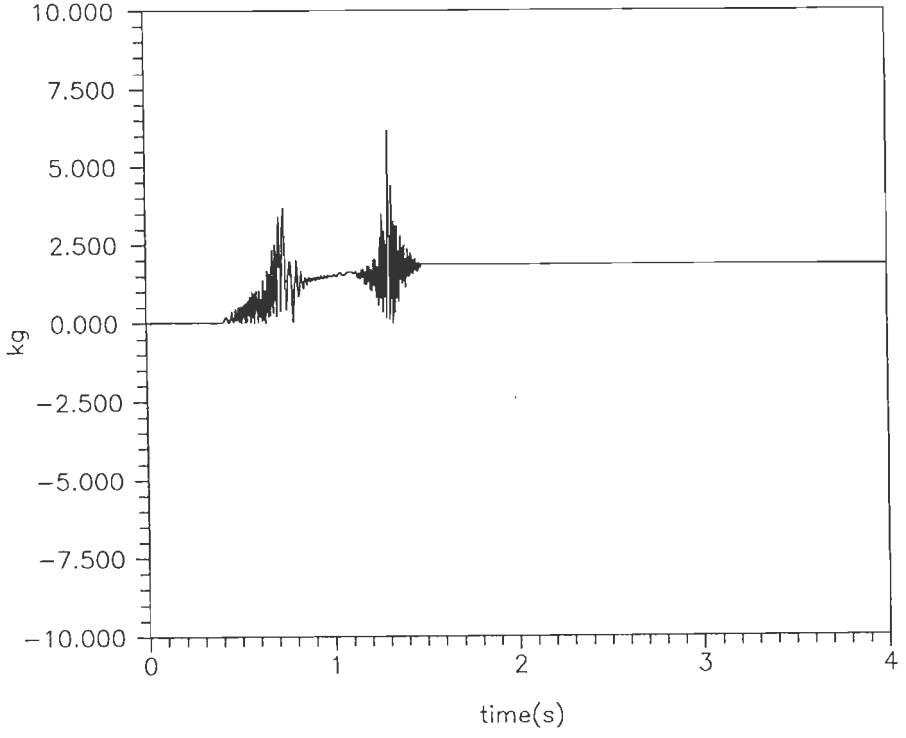

Fig.5.71 Estimated C_M for bounded form of controller.

5.5 SIMULATION OF SLIDING OBSERVER BASED ADAPTIVE CONTROL WITH NEW UNCERTAINTY VECTOR

A sliding observer aided adaptive control with uncertainty vector (section 4.2.1) is illustrated for two-DOF robot system (Fig. 5.72). The physical parameter of robot system (5.1) is described by (5.6).

The following design parameters have chosen for simulation purpose :

Λ_1 = diag [0.1,0.1] ; Λ_2 = diag [0.1,0.1]; Γ_1 = diag[0.001, 0.001];

Γ_2 = diag[10,10]; K_2 = diag [200, 200]; Γ^{-1} = $17I_9$, I_9 = 9x9 identity matrix;

$\sigma_{o1}=1$, σ_{11} = 8; σ_{12} = 8; Λ = diag [10,1]; λ_1 = 0.001.

The regressor matrix $Y(x_1,\hat{x}_2 - \Lambda_1 sgn(\tilde{x}_1), \dot{q}_r,\dot{q}_r' + \Lambda\Lambda_1 sgn(\tilde{x}_1))(S'-\Lambda_1 sgn(\tilde{x}_1))$ is expressed by (5.16).

Tracking errors for joint-1 and joint-2 are less than 5.6% in contrast to Canudas's case [10] as appeared in Fig.5.75-5.76. Since the design criterion $\tilde{x}_1 = 0$ is consider same for proposed case so the observation error or estimation error for position are same as Canudas case[10] indicated in Fig.5.77 and Fig.5.78. In Fig.5.80 and Fig.5.82, the improvements in velocity error appears in proposed case for joint-1 and joint-2, respectively. The observation error(velocity) is also improved as shown in Fig.5.84 and 5.86 in comparison to Fig.5.83 and Fig.5.85, respectively. Hence, the overallperformance of proposed one is drastically improved.

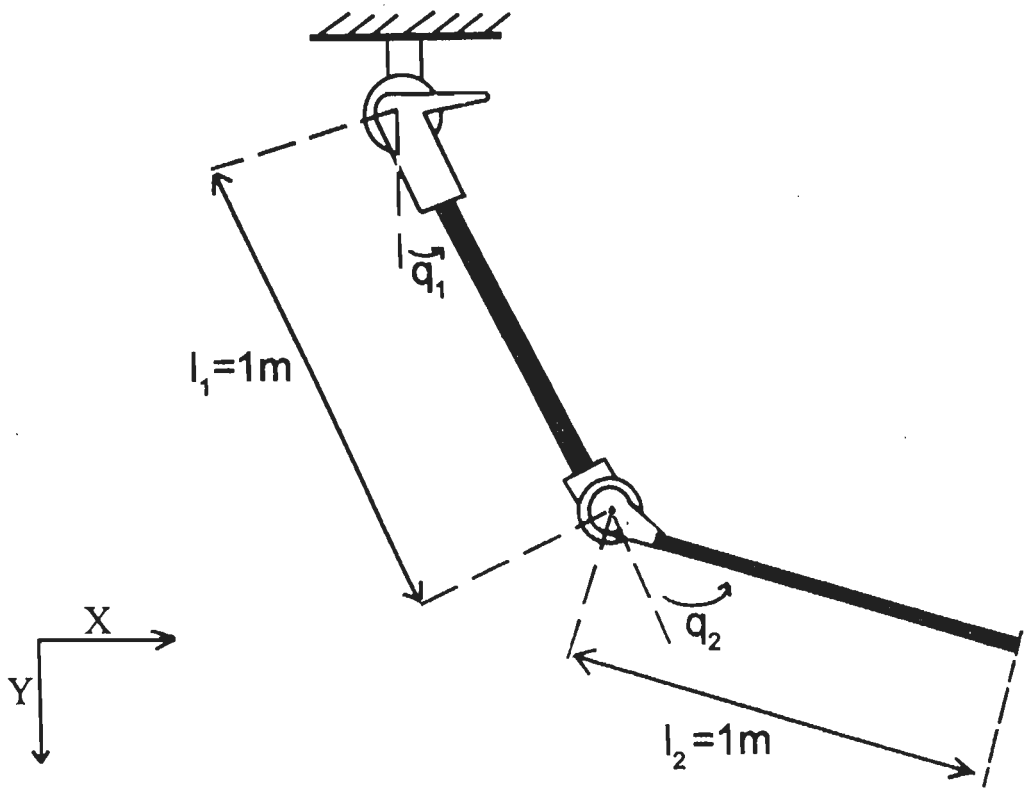

Fig. 5.72 Two-DOF Robot System

The regressor matrix $Y(x_1, \hat{x}_2 - \Lambda_1 sgn(\tilde{x}_1), \dot{q}_r, \ddot{q}_r' + \Lambda\Lambda_1 sgn(\tilde{x}_1))(S' - \Lambda_1 sgn(\tilde{x}_1)) =$

$$\begin{bmatrix} \ddot{q}_{r1} & \ddot{q}_{r1}\cos x_1(0) & \ddot{q}_{r2} & \ddot{q}_{r2}\cos x_1(0) & 0 & \sin x_1(0)x_2(1) - \sin x_1(0)(x_2(0)+x_2(1))\dot{q}_{r2} & \dot{q}_{r1} & g\sin x_1(0) & g\sin(x_1(0)+x_1(1)) \\ 0 & 0 & \ddot{q}_{r1} & \ddot{q}_{r1}\cos x_1(0) & \ddot{q}_{r2} & \sin x_1(0)x_2(0) & \dot{q}_{r1} & 0 & g\sin(x_1(0)+x_1(1)) \end{bmatrix} \quad (5.16)$$

where,

$$\dot{q}_r = \ddot{q}_r' + \Lambda\Lambda_1 sgn(\tilde{x}_1)$$

$$x_2 = \hat{x}_2 - \Lambda_1 sgn(\tilde{x}_1)$$

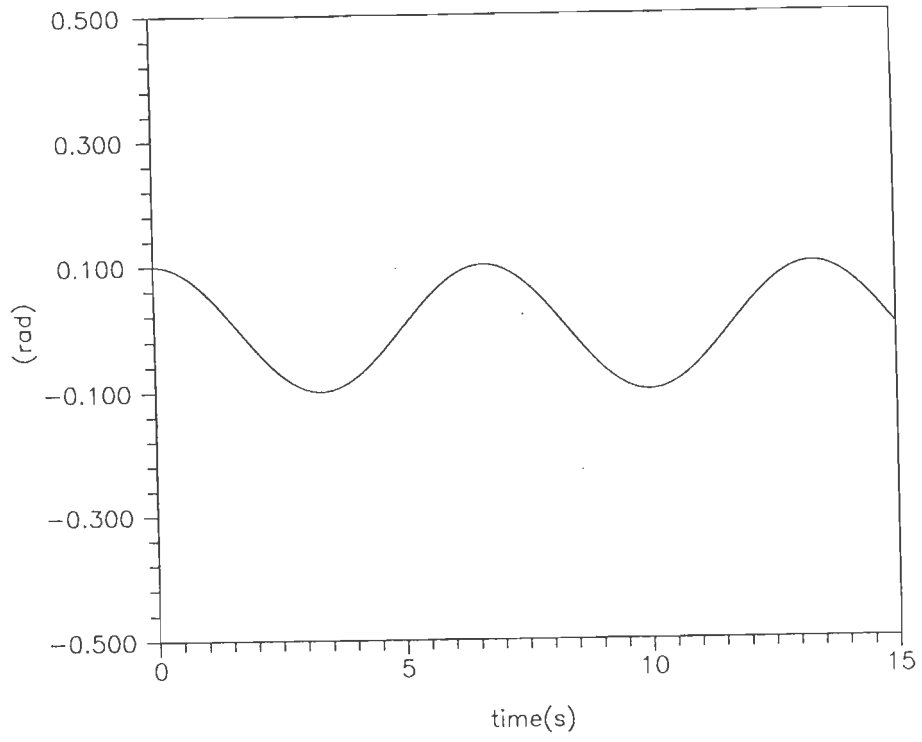

Fig.5.73 Desired trajectory for joint-1 (test signal 'I').

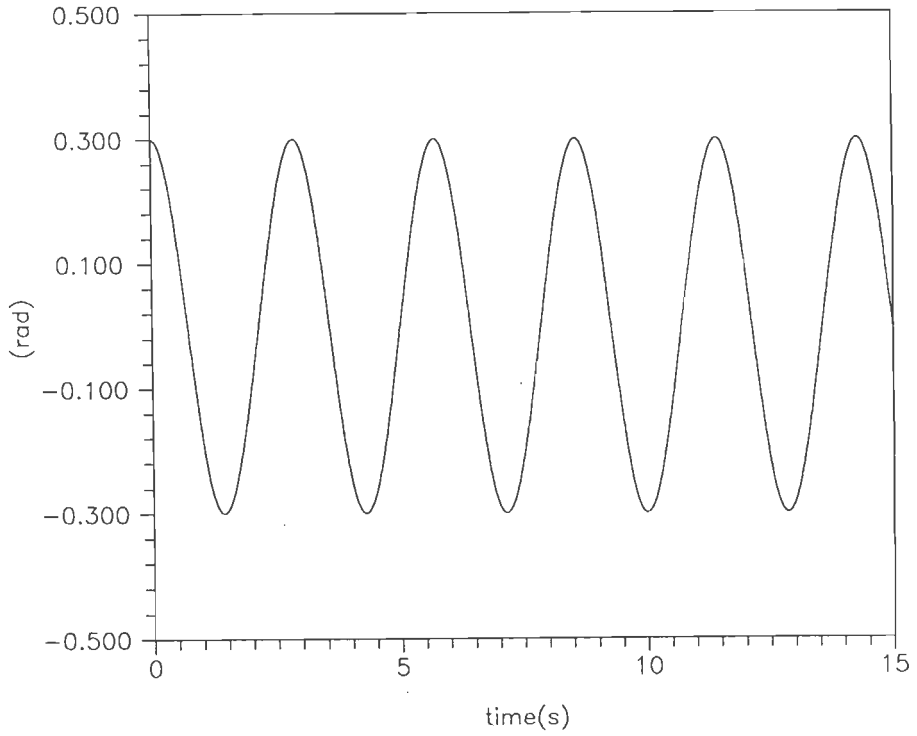

Fig.5.74 Desired trajectory for joint-2 (test signal 'J').

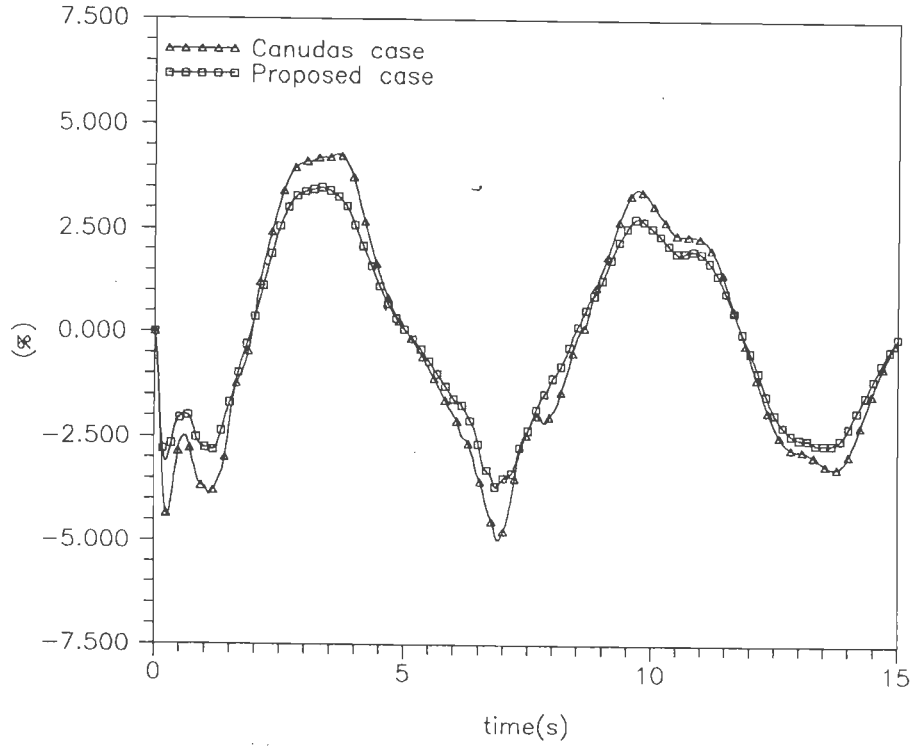

Fig.5.75 Tracking error as percent of max. input for test signal 'I',joint- 1.

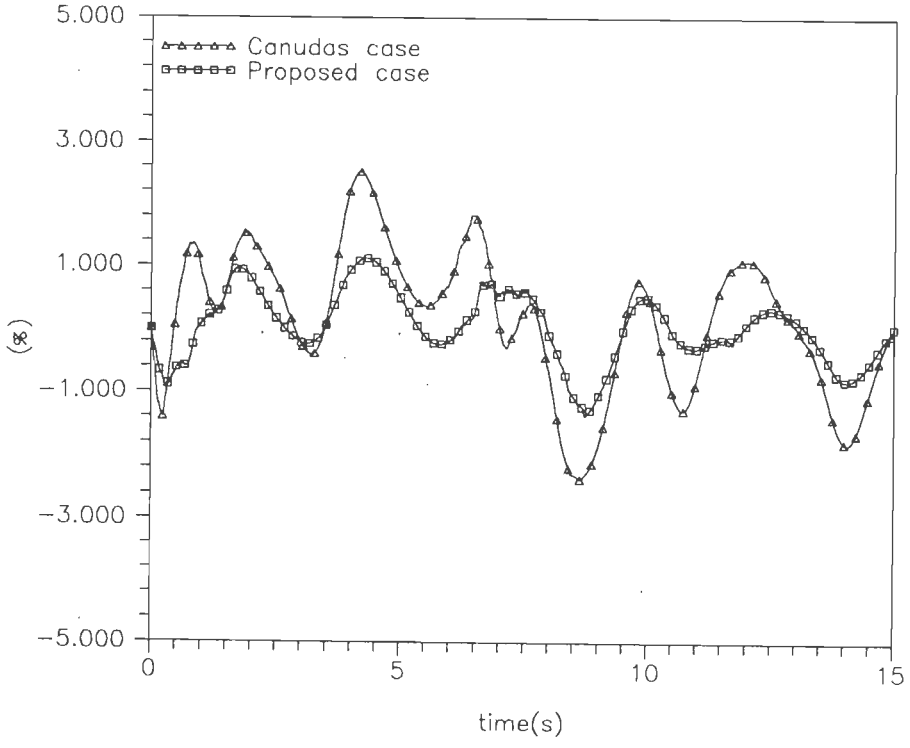

Fig.5.76 Tracking error as percent of max. input for test signal 'J',joint- 2.

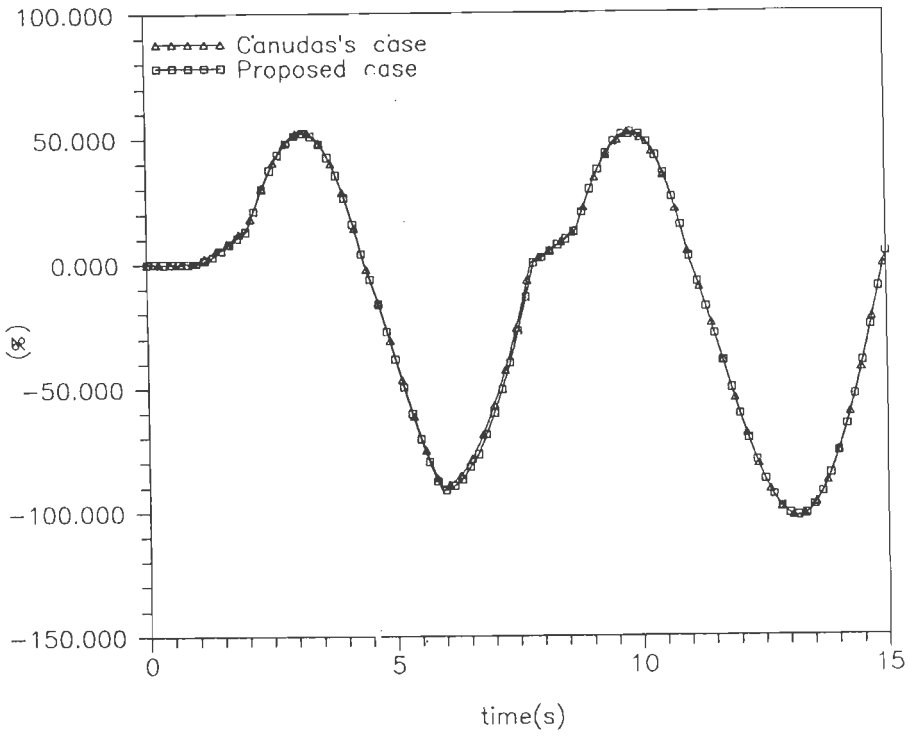

Fig.5.77 Observation error (position) as percent of max. input for test signal 'I',joint-1.

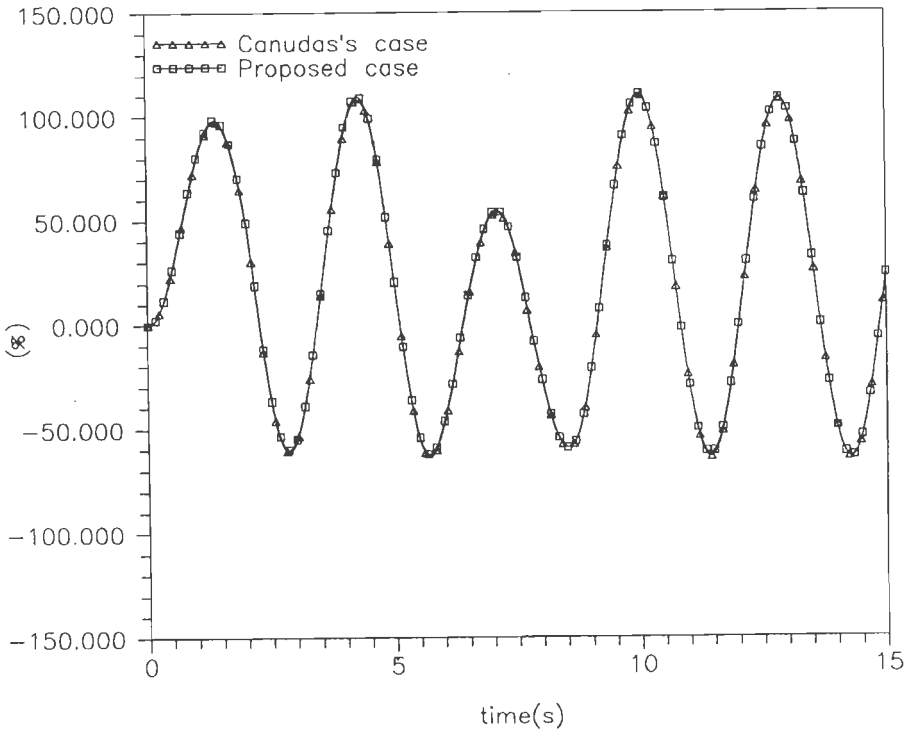

Fig.5.78 Observation error (position) as percent of max. input for test signal 'J',joint-2.

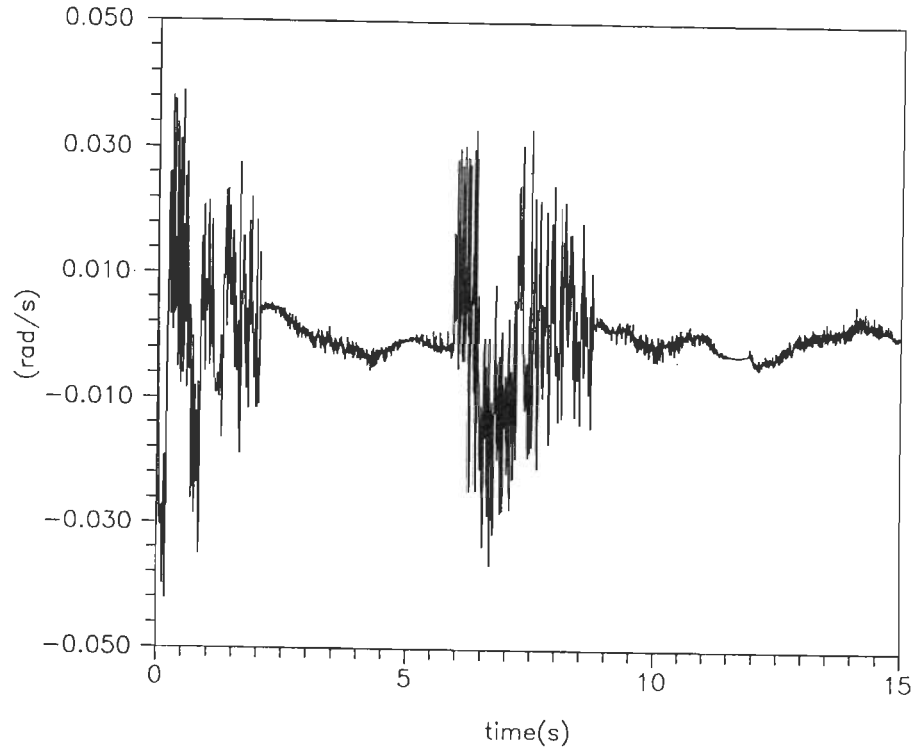

Fig.5.79 Velocity error for test signal 'l'(Canudas case[10]), joint-1.

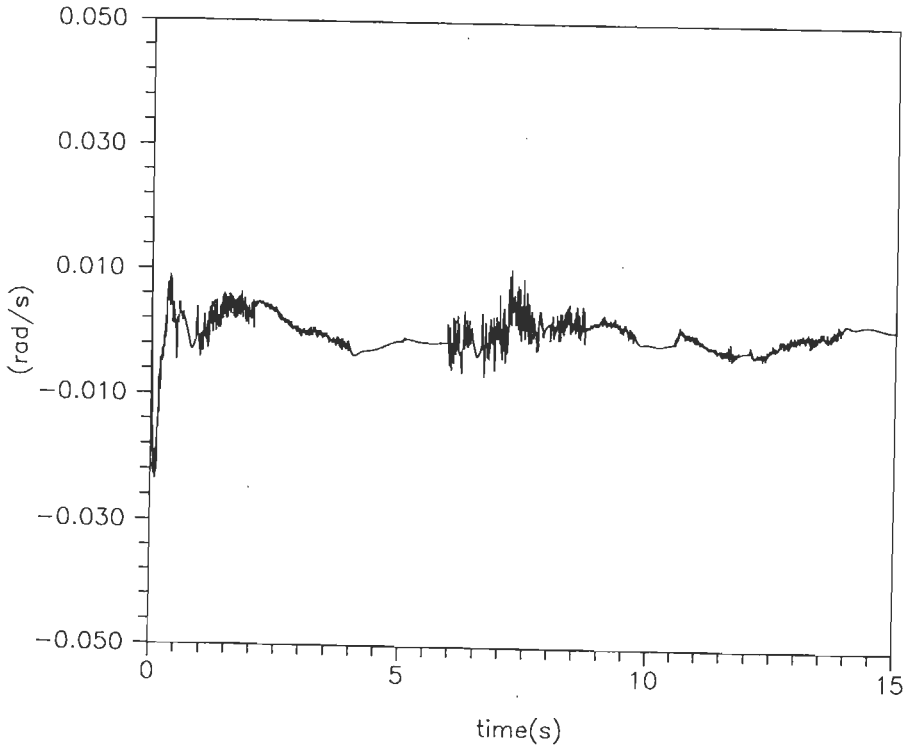

Fig.5.80 Velocity error for test signal 'l'(Proposed case, section 4.2.1), joint-1.

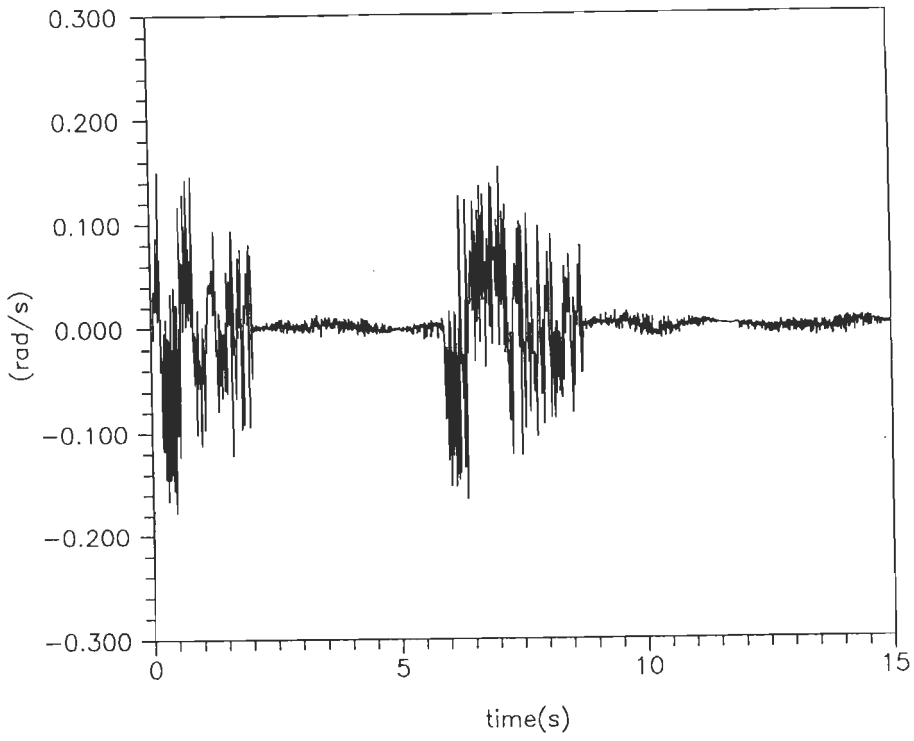

Fig.5.81 Velocity error for test signal 'J'(Canudas case[10]), joint-2.

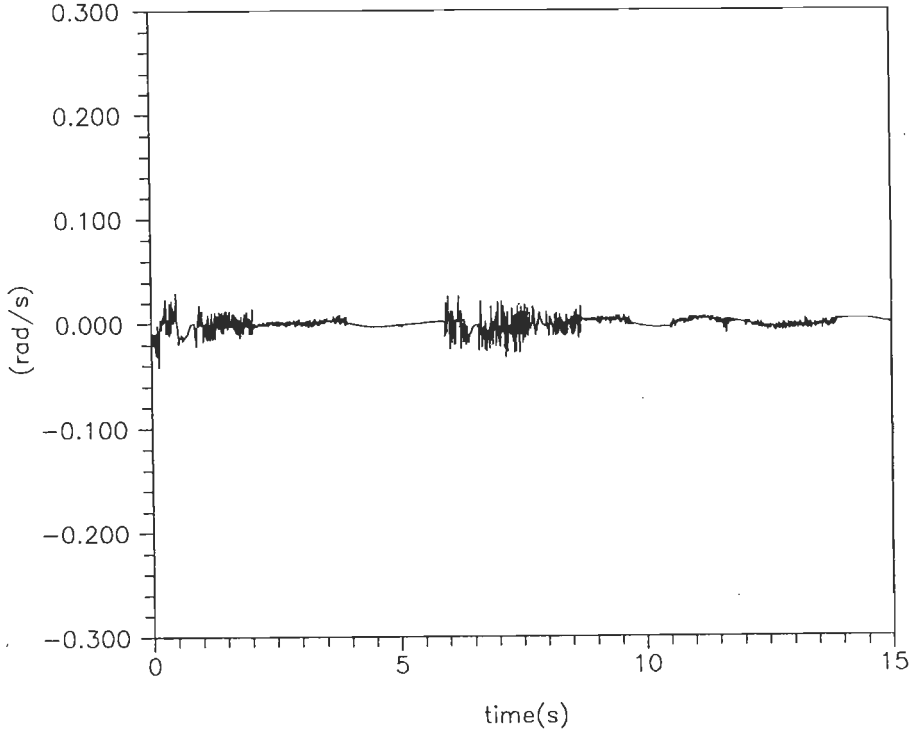

Fig.5.82 Velocity error for test signal 'J'(Proposed case, section 4.2.1), joint-2.

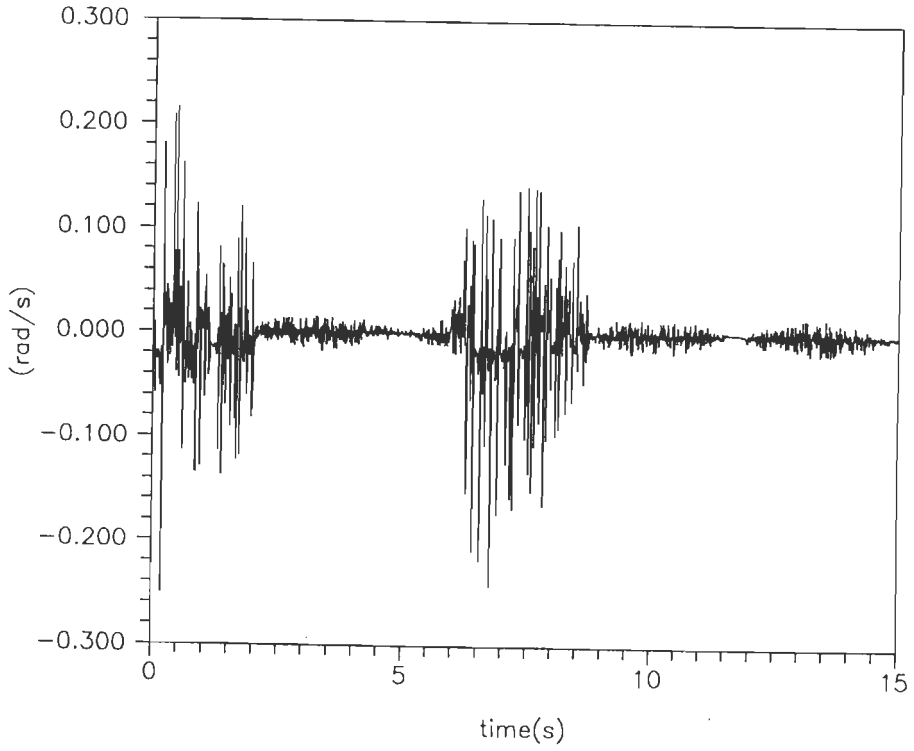

Fig.5.83 Velocity observation error for test signal 'l'(Canudas case[10]), joint-1.

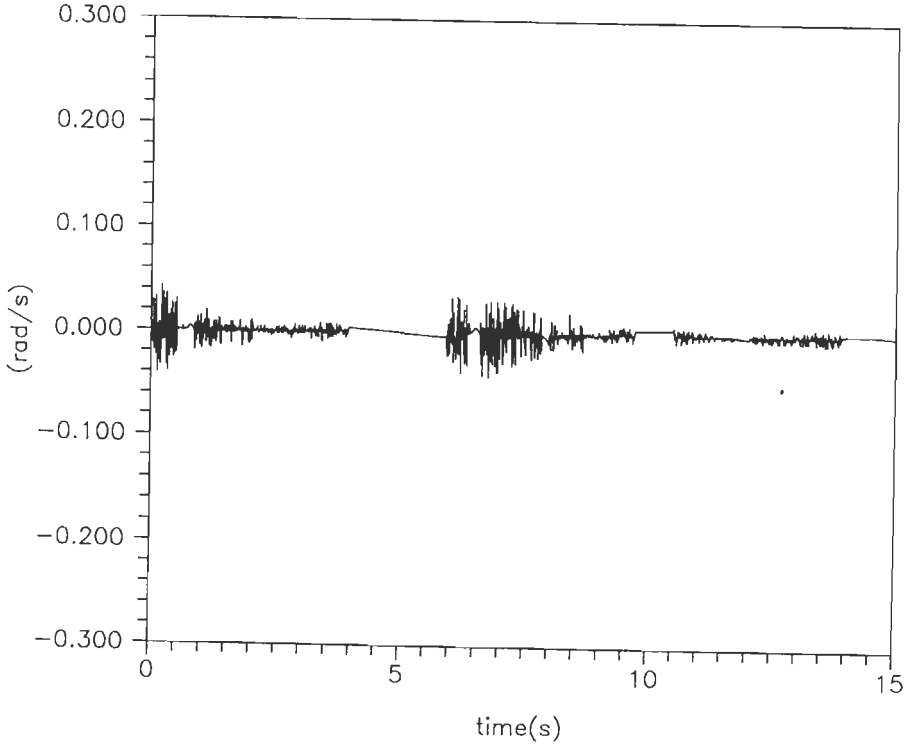

Fig.5.84 Velocity observation error for test signal 'l'(Proposed case, section 4.2.1), joint-1.

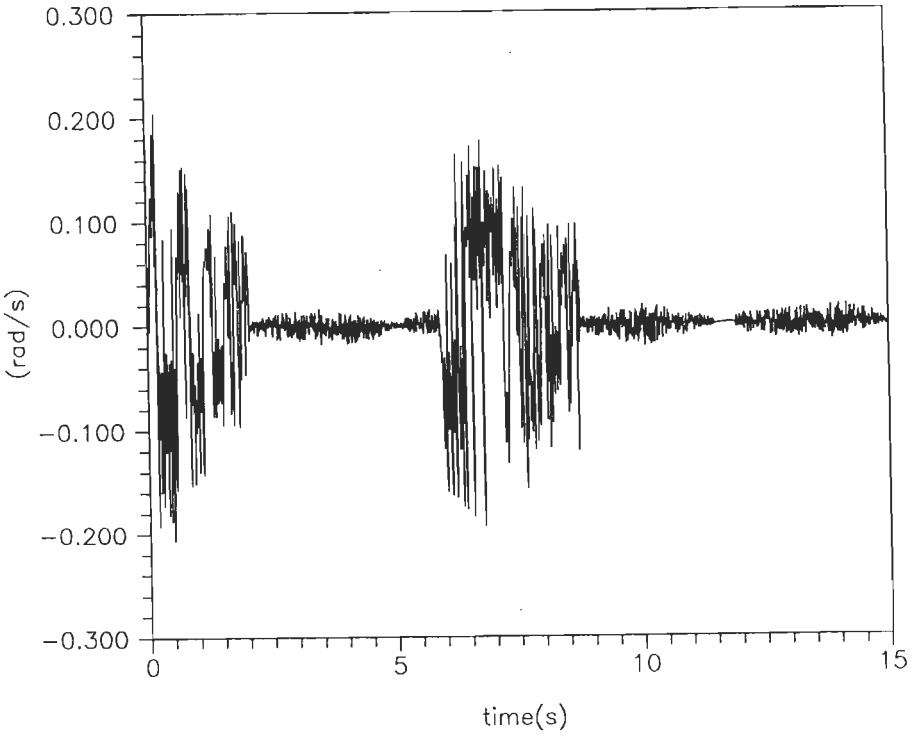

Fig.5.85 Velocity observation error for test signal 'J'(Canudas case[10]), joint-2.

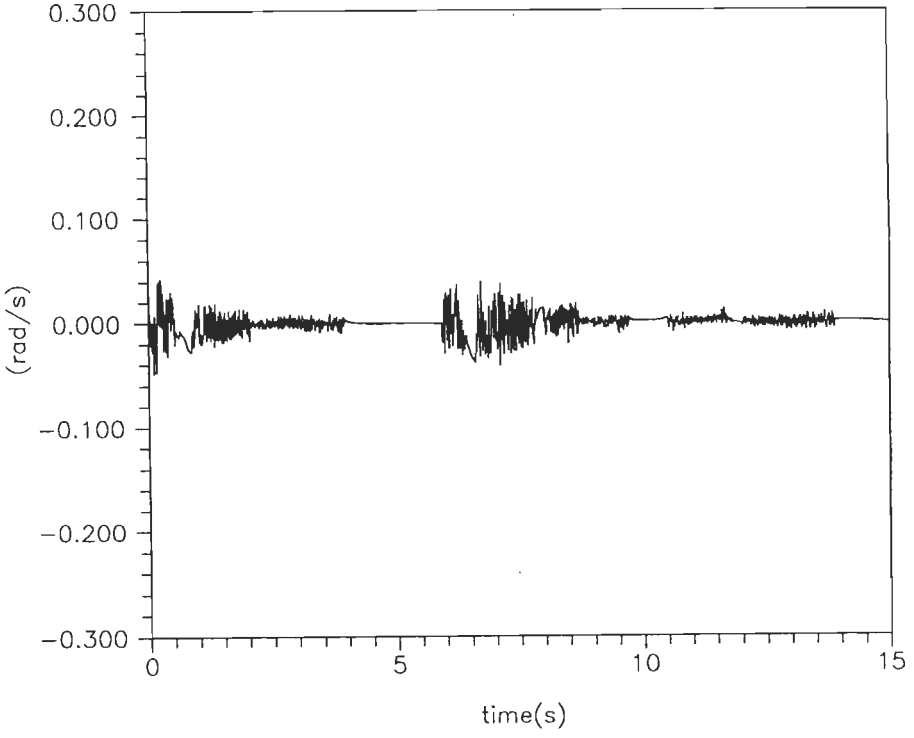

Fig.5.86 Velocity observation error for test signal 'J'(Proposed case, section 4.2.1), joint-2.

The maximum value of different error response are given in Table-V.

Table -V

Maximum errors for Canudas case [10] and proposed case

Response	Canudas's Case[10]		Proposed Case	
	Joint -1	Joint -2	Joint -1	Joint -2
Tracking errors (%)	5.600	3.00	4.200	1.43
Observation error (Position) (%)	93.1	108.5	93.1	108.5
Velocity errors (rad/s)	0.0432	0.1825	0.0302	0.0296
Velocity observation errors (rad/s)	0.2565	0.2118	0.1056	0.1554

Drastic reduction, especially, in tracking error and velocity error appeared in comparison to [10].

5.6 SIMULATION OF TRACKING ERROR BASED SLIDING OBSERVER AIDED ADAPTIVE CONTROLLER

To investigate the performance of proposed combined controller observer structure (section 4.2.2) a simple two-DOF robot system is considered for simulation purpose. The physical parameter of the robot system (5.1) is given in (5.6). The desired trajectories (test signal 'I' and 'J') are shown in Fig.5.73 and Fig.5.74 for joint -1 and joint -2 respectively (see also (5.10)).

The design parameter are taken as

Λ_1 = diag [0.1,0.1] ; Λ_2 = diag [0.1,0.1]; Γ_1 = diag[0.001, 0.001];

$\Gamma_e = \Gamma_2$ = diag[10,10]; K_2 = diag [280, 280]; $\Gamma^{-1} = 17 I_8$, I_8 = 8x8 identity matrix;

$\sigma_{o1} = 1$, σ_{11} = 8; σ_{12} = 8; Λ = diag [10,1]; λ_1 = 0.001.

The regressor matrix Y(.) is given by (5.16). Various error trejectories are shown in Fig.5.87-5.94. Table - VI shows the maximum errors of different response such as tracking error, observation error (position), velocity errors and velocity observation errors.

Table - VI

Maximum errors for proposed case

(tracking error based sliding observer)

Response	Proposed Case	
	Joint-1	Joint -2
Tracking errors (%)	3.5	1.26
Observation errors (Position) (%)	110.00	145.2
Velocity errors (rad/s)	0.0177	0.0412
Velocity observation errors (rad/s)	0.0294	0.0425

Observation error (position) and velocity error are slightly increased of joint-2 in comparison to previous proposed case but still one can take the improved performance in comparison to [10].

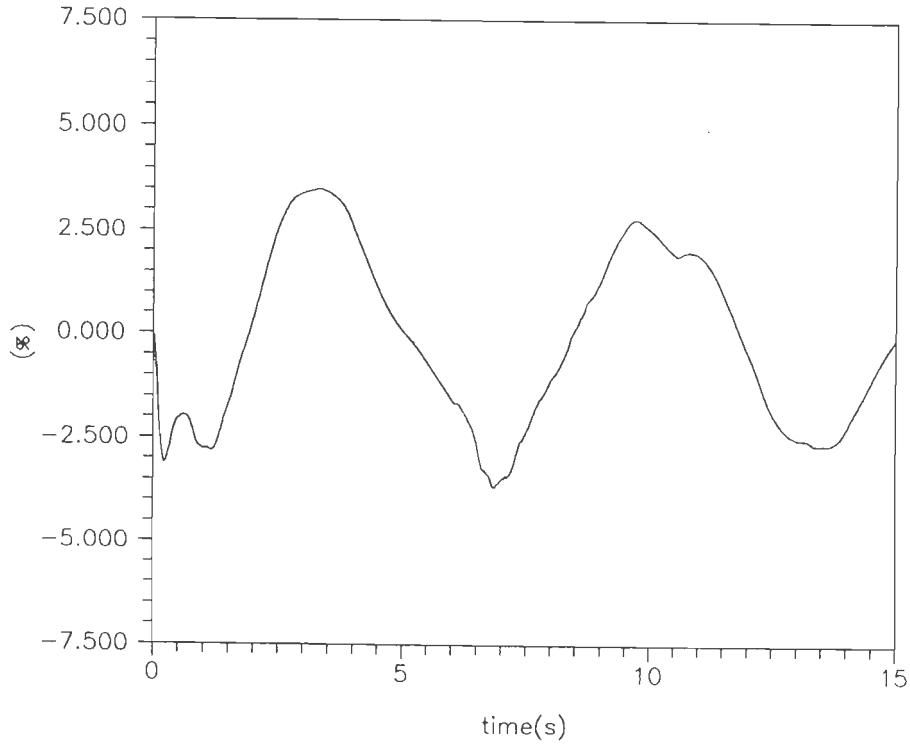

Fig.5.87 Tracking error as percent of max. input for test signal 'I' (Proposed case, section 4.2.2), joint-1.

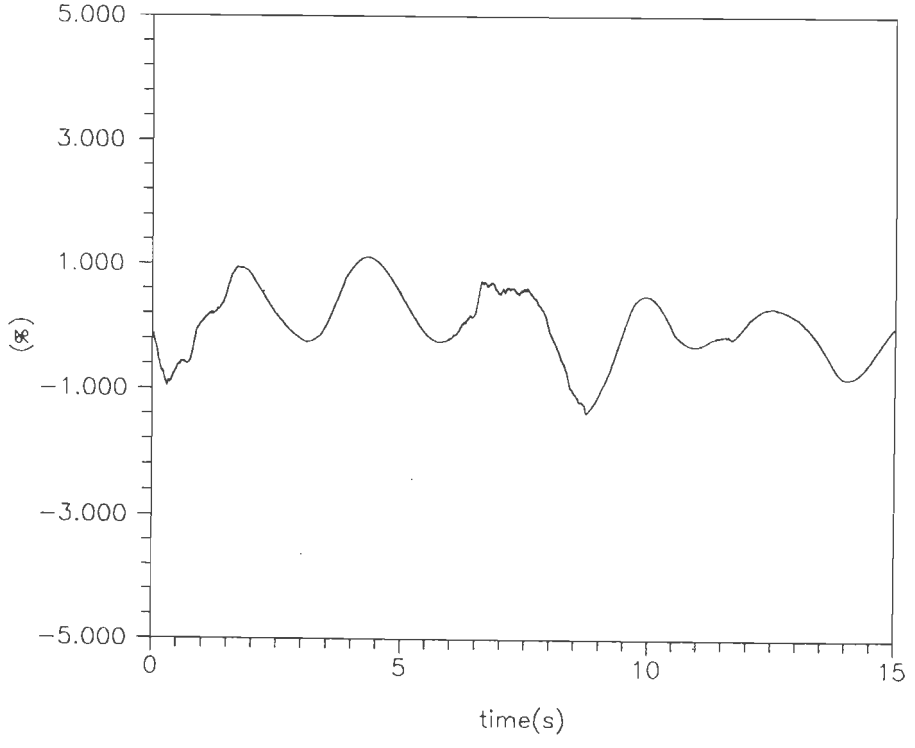

Fig.5.88 Tracking error as percent of max. input for test signal 'J' (Proposed case, section 4.2.2), joint-2.

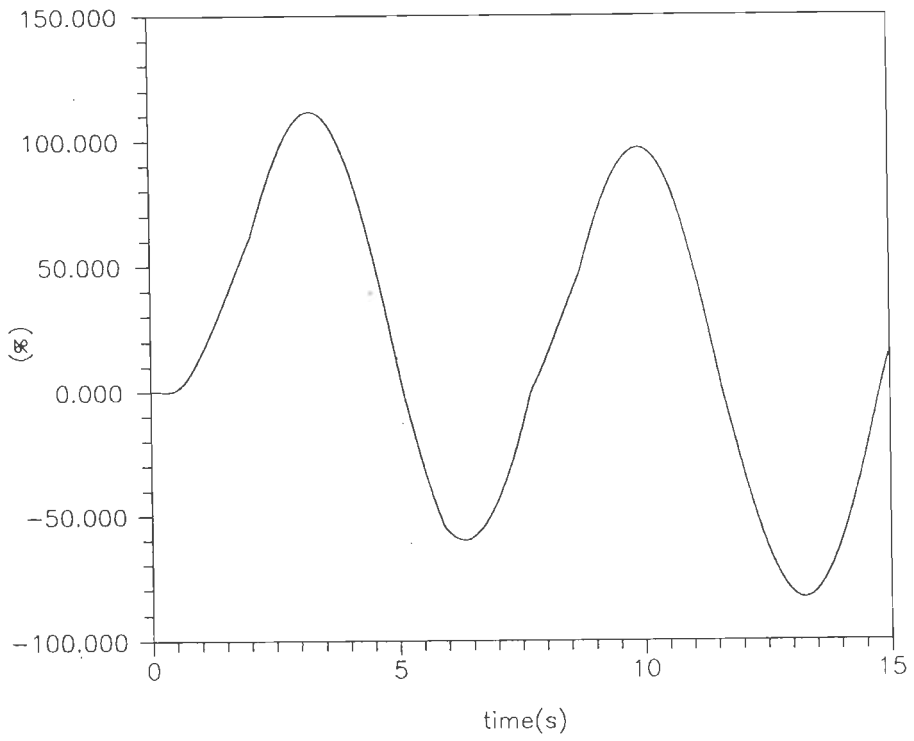

Fig.5.89 Observation error (position) as percent of max. input for test signal 'I'(Proposed case, section 4.2.2),joint-1.

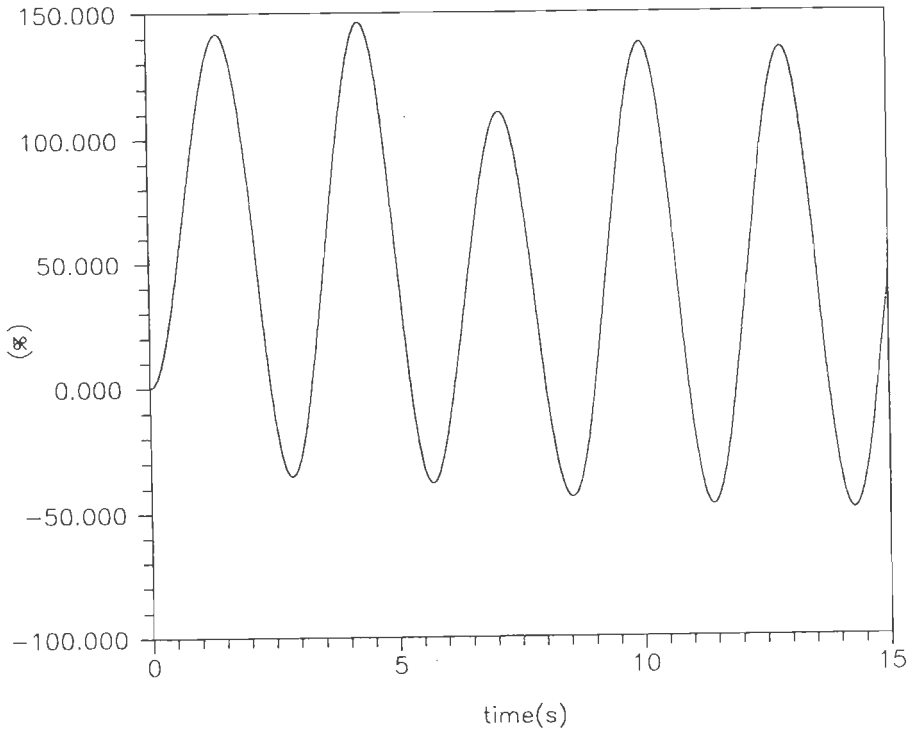

Fig.5.90 Observation error (position) as percent of max. input for test signal 'J'(Proposed case, section 4.2.2),joint-2.

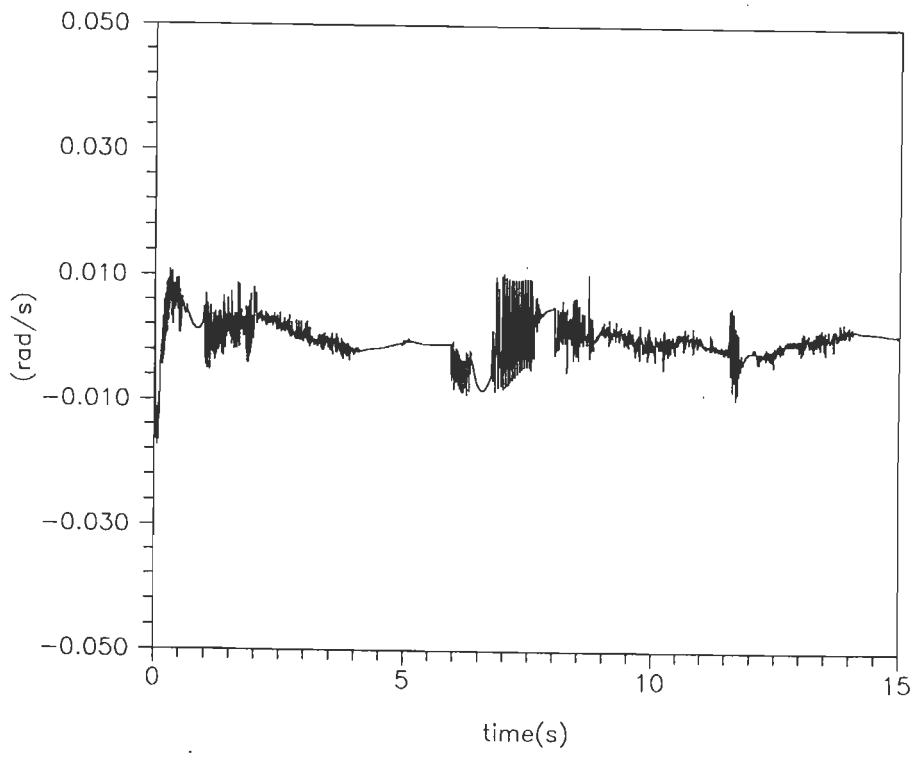

Fig.5.91 Velocity error for test signal 'I' (Proposed case, section 4.2.2), joint-1.

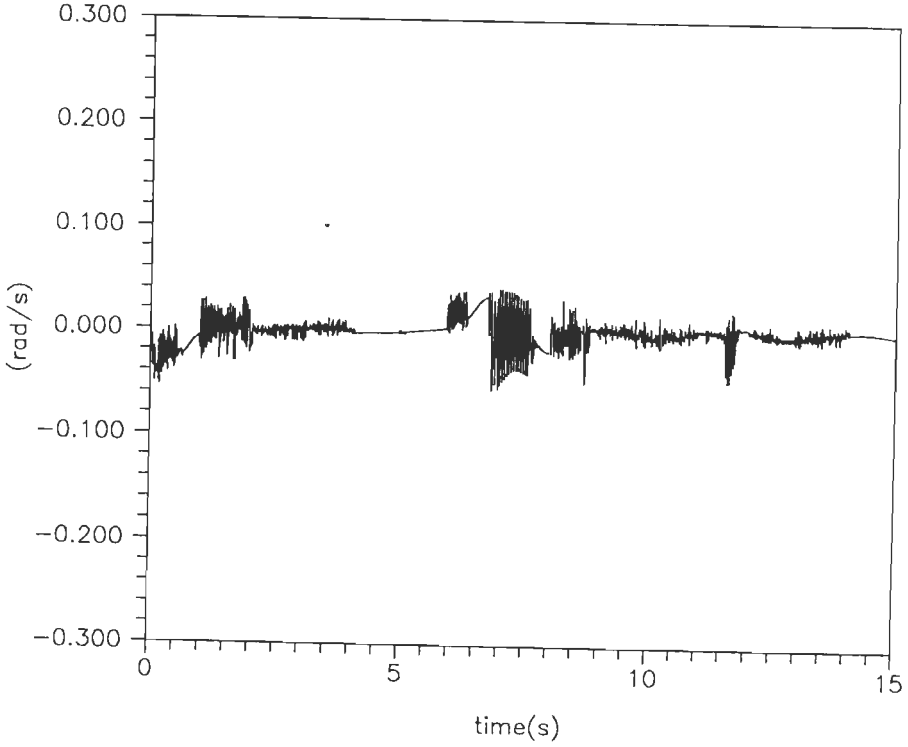

Fig.5.92 Velocity error for test signal 'J' (Proposed case, section 4.2.2), joint-2.

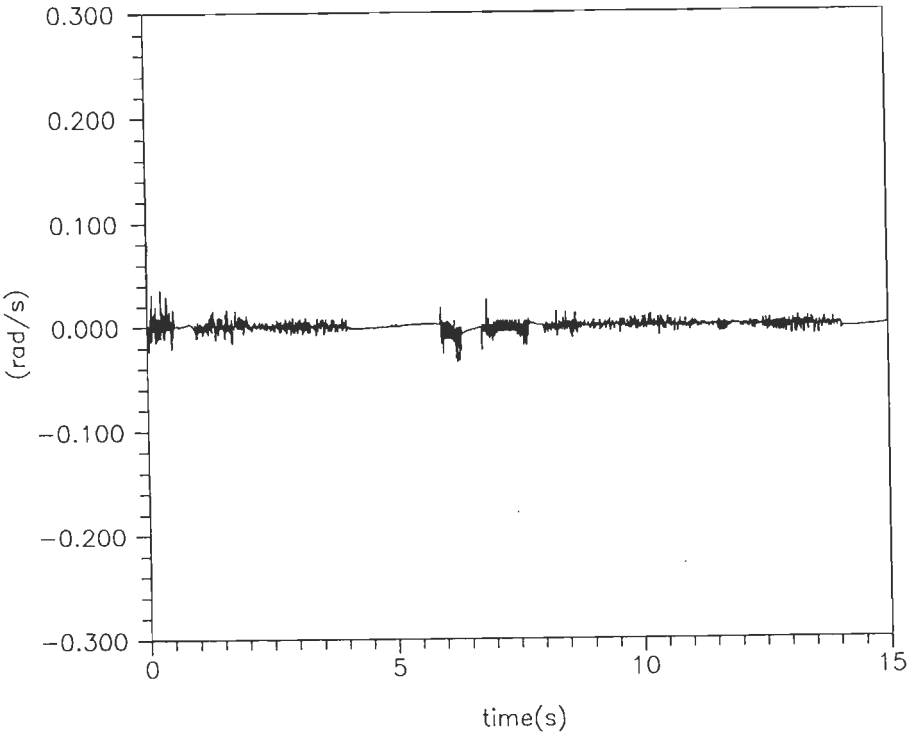

Fig.5.93 Velocity observation error for test signal 'l'(Proposed case, section 4.2.2), joint-1.

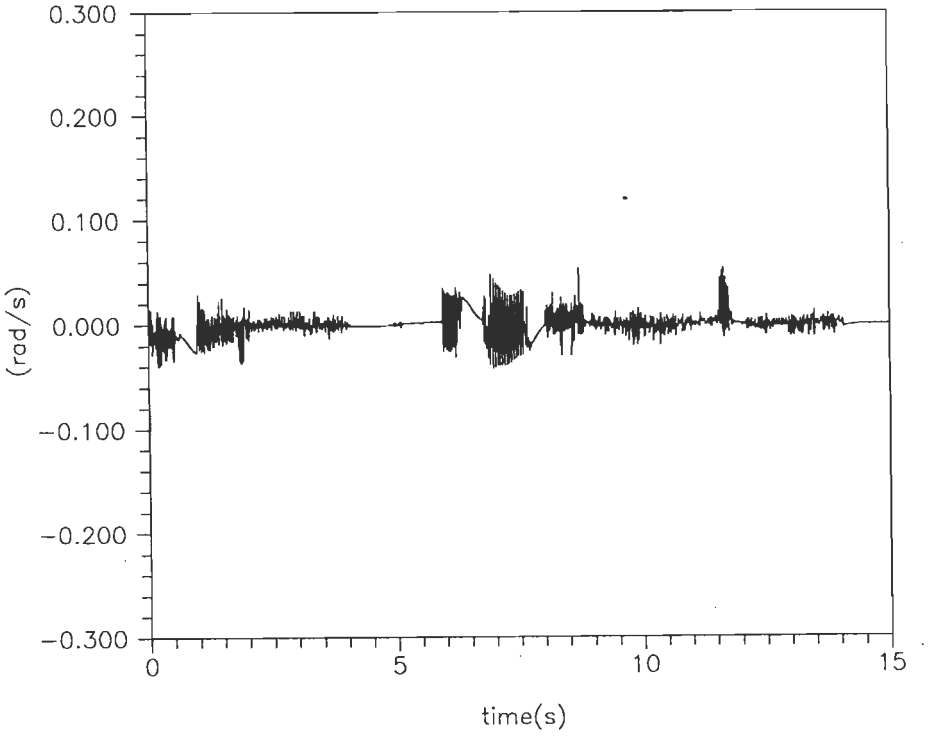

Fig.5.94 Velocity observation error for test signal 'j'(Proposed case, section 4.2.2), joint-2.

5.7 SIMULATION OF EXTENDED NONLINEAR SLIDING OBSERVER AIDED CONTROLLER STRUCTURE

The illustration of presented scheme of section 4.2.3 is carried out with a two-DOF robot system (5.1). The coefficients matrix of system equation is represented by (5.6). Desired trajectories (test signals 'I','J') are shown in Fig.5.73 and Fig.5.74 (see (5.10)). Various error graphs are compared with existing work [8] with following design values:

Λ_1 = diag [0.07,0.07] ; $\Gamma_1 = \Gamma_2$ = diag[500, 500]; Q = diag [35,25];

$\Gamma_{e1} = \Gamma_{e2}$ = diag[5,5]; K_1 = diag[280, 280]; K_2 = diag [5, 5]; σ = 23;

L_1 = diag [0.05,0.05]; $\xi_o = \xi_1 = \xi_2 = 0.05$;

In this case, it is assumed that coefficients of system dynamics are known. Various error response of robot are shown in Fig.5.95-5.110 for existing and proposed work both. The error response for existing case[8] and proposed case are placed in Table VII.

Table - VII

Maximum errors for Canudas case [8] and proposed case

Response	Canudas's Case[8]		Proposed Case	
	Joint -1	Joint -2	Joint -1	Joint -2
Tracking errors (%)	1.2	1.63	0.22	0.14
Observation error (Position) (%)	3.2	4.8	0.55	1.03
Velocity errors (rad/s)	0.0075	0.0252	0.0042	0.0047
Velocity observation errors (rad/s)	0.1675	0.730	0.0142	0.0125

The proposed case gives significant improvements with respect to various error response in comparison to [8].

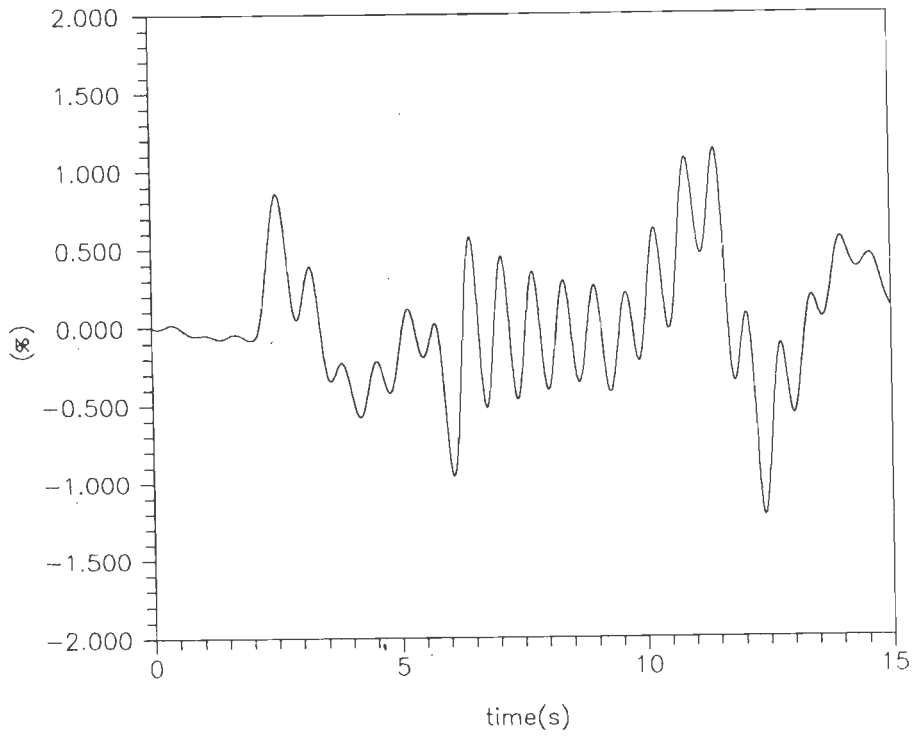

Fig.5.95 Tracking error as percent of max. input for test signal 'l' (Canudas case[8]), joint-1.

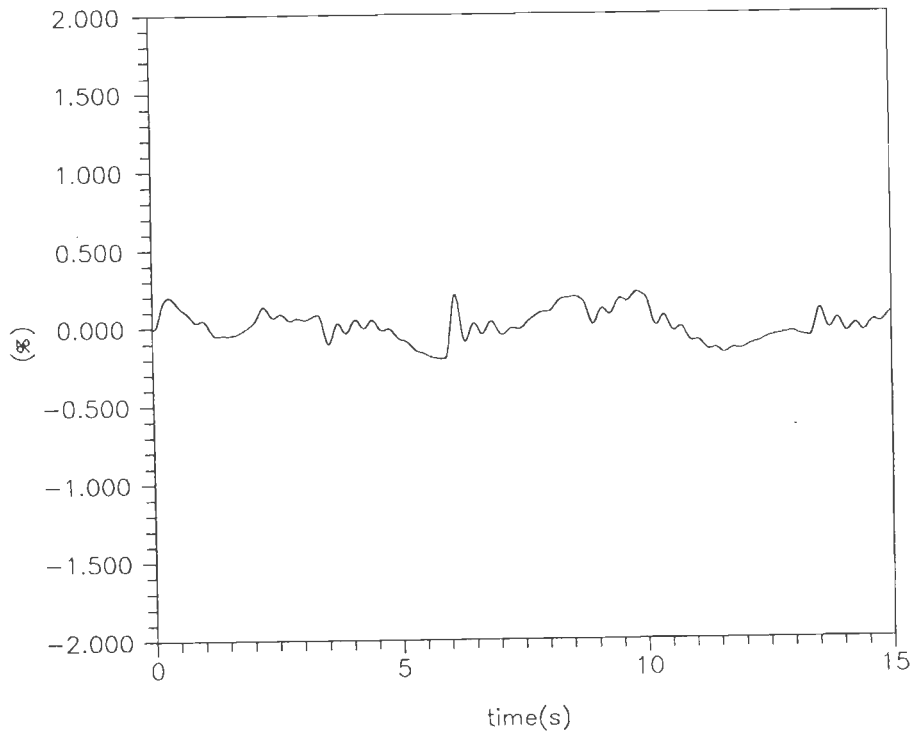

Fig.5.96 Tracking error as percent of max. input for test signal 'l' (Proposed case, section 4.2.3), joint-1.

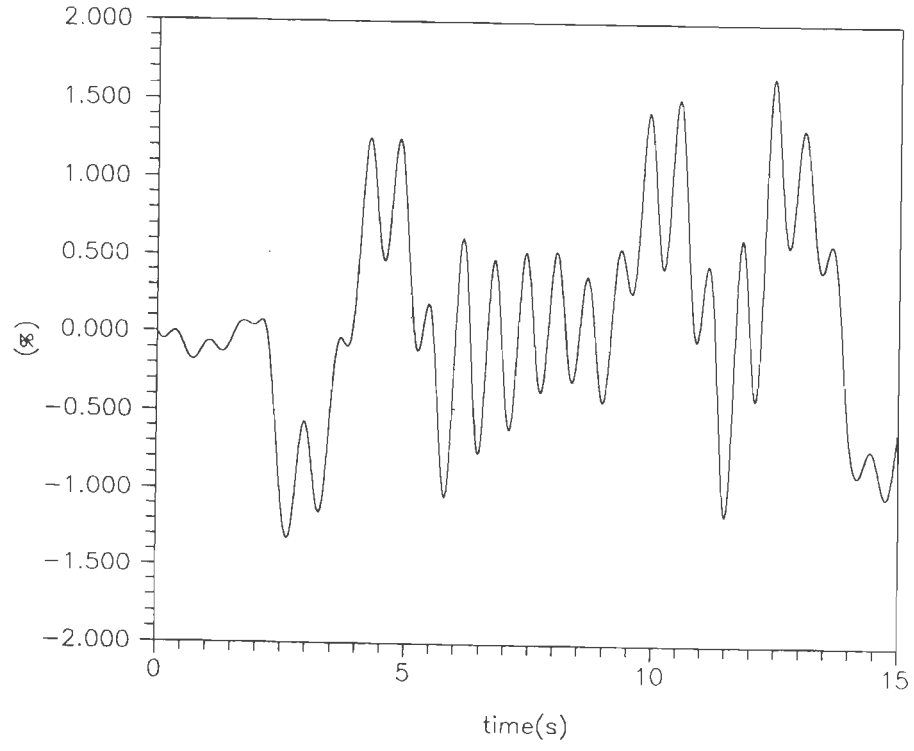

Fig.5.97 Tracking error as percent of max. input for test signal 'J' (Canudas case[8]), joint-2.

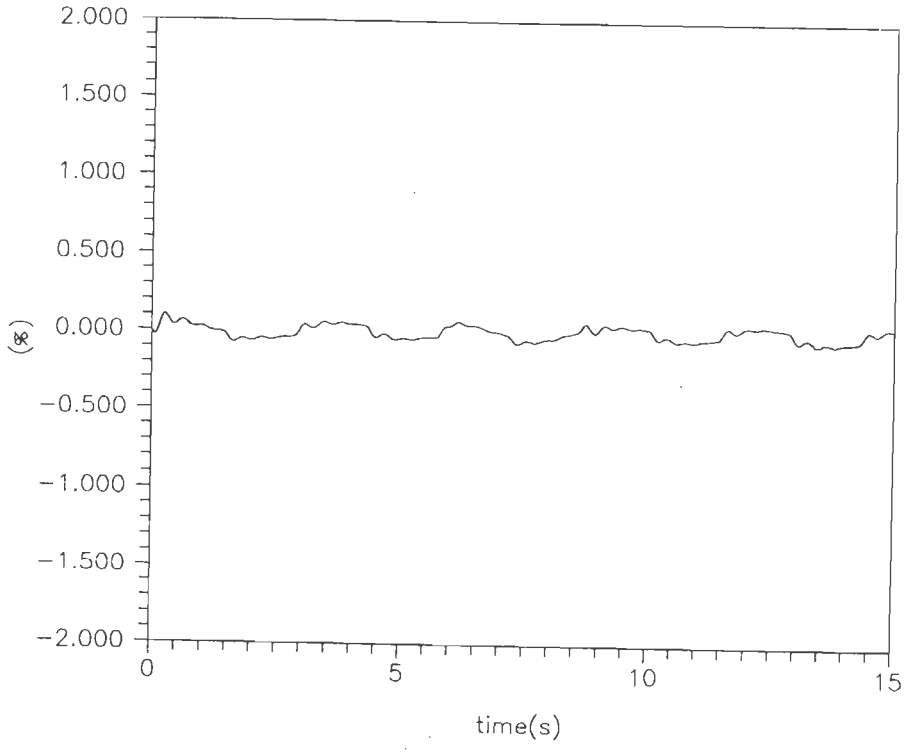

Fig.5.98 Tracking error as percent of max. input for test signal 'J' (Proposed case, section 4.2.3), joint-2.

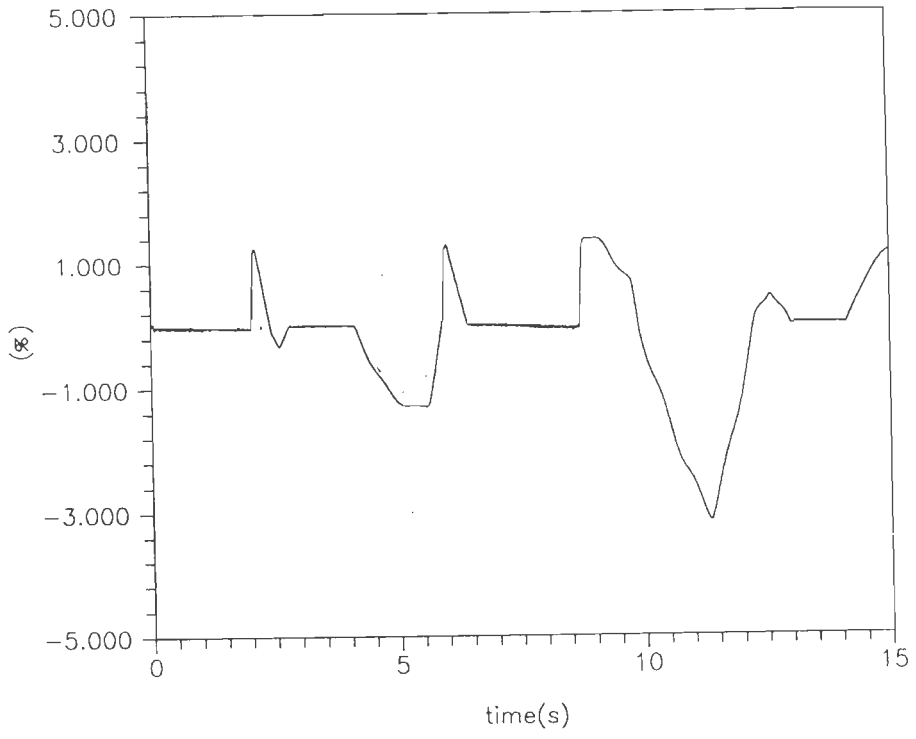

Fig.5.99 Observation error (position) as percent of max. input for test signal 'l'(Canudas case[8]),joint-1.

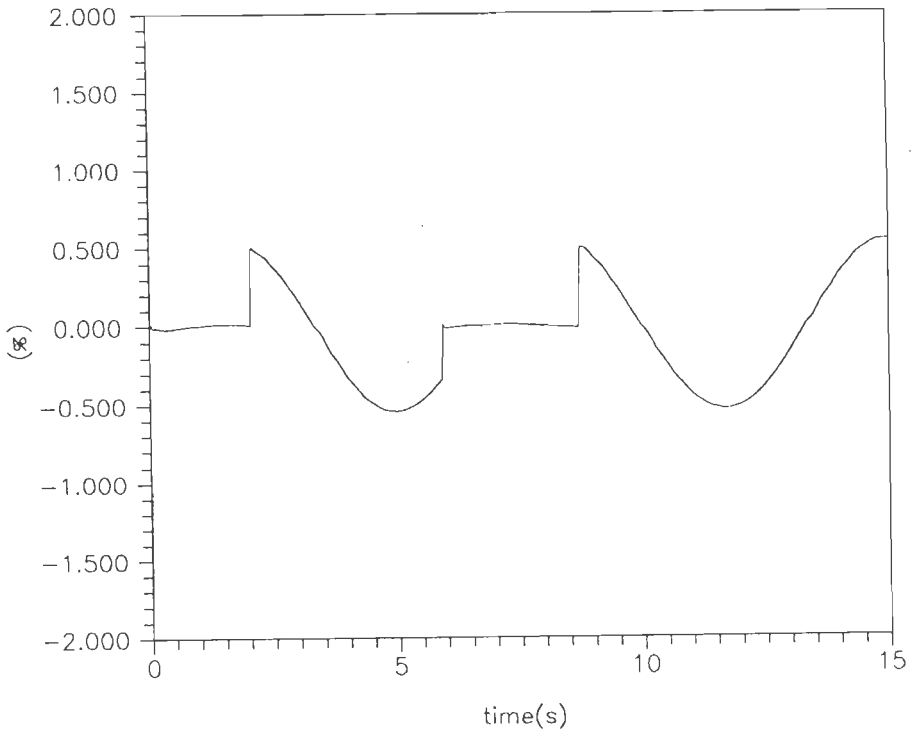

Fig.5.100 Observation error (position) as percent of max. input for test signal 'l'(Proposed case, section 4.2.3),joint-1.

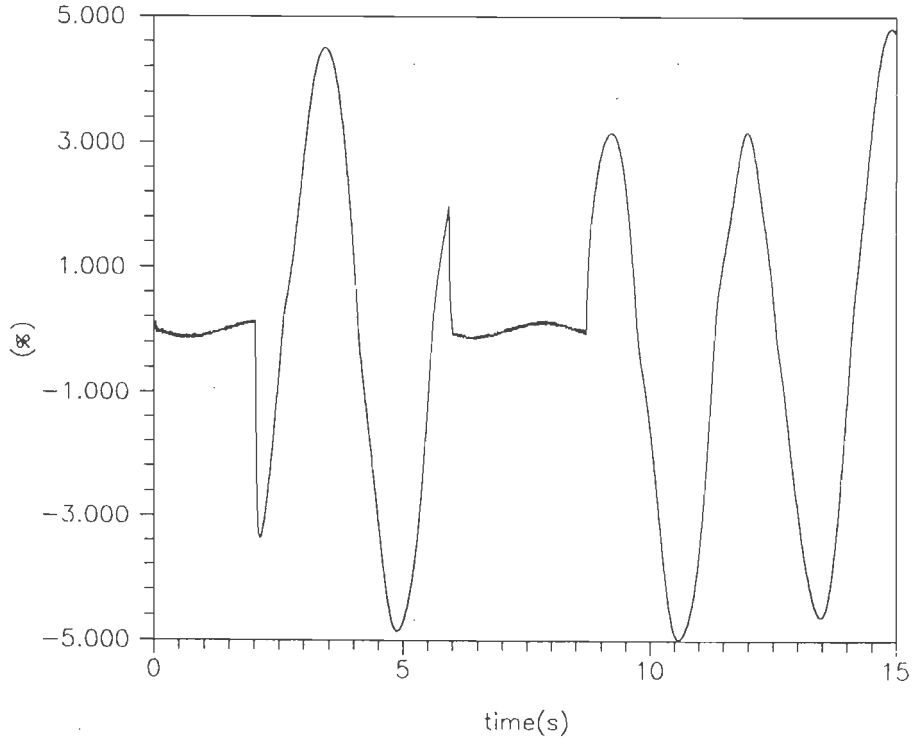

Fig.5.101 Observation error (position) as percent of max. input for test signal 'J'(Canudas case[8]),joint-2.

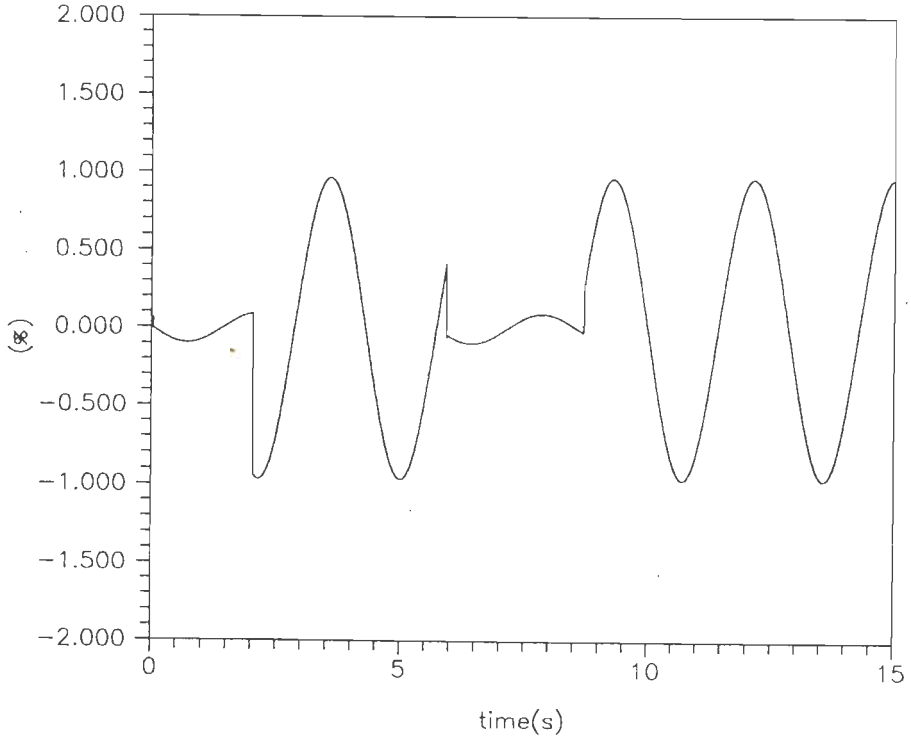

Fig.5.102 Observation error (position) as percent of max. input for test signal 'J'(Proposed case, section 4.2.3),joint-2.

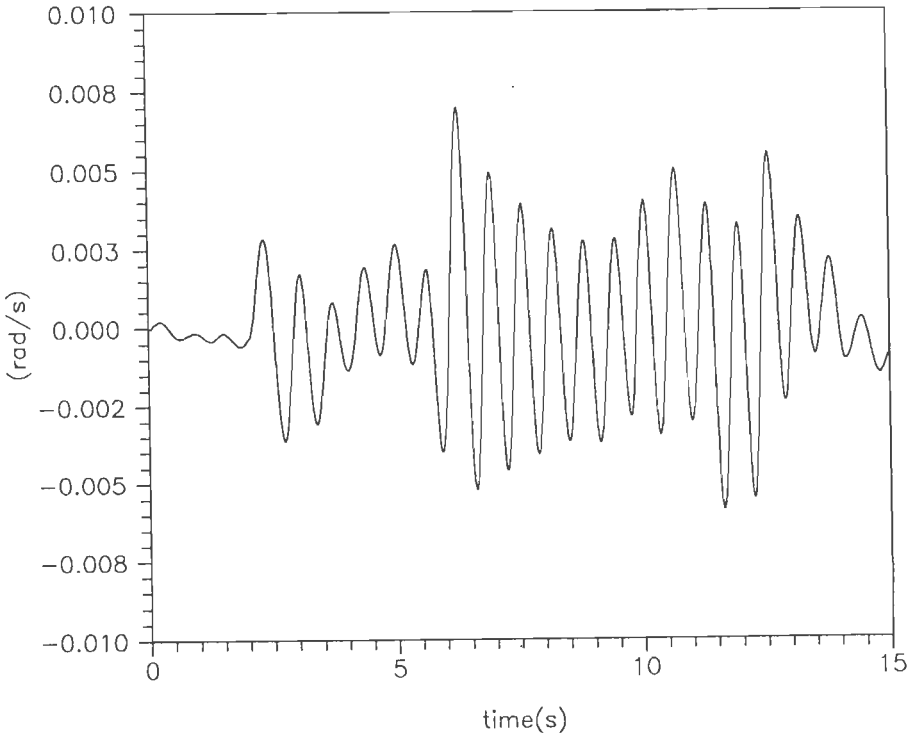

Fig.5.103 Velocity error for test signal 'l'(Canudas case[8]), joint-1.

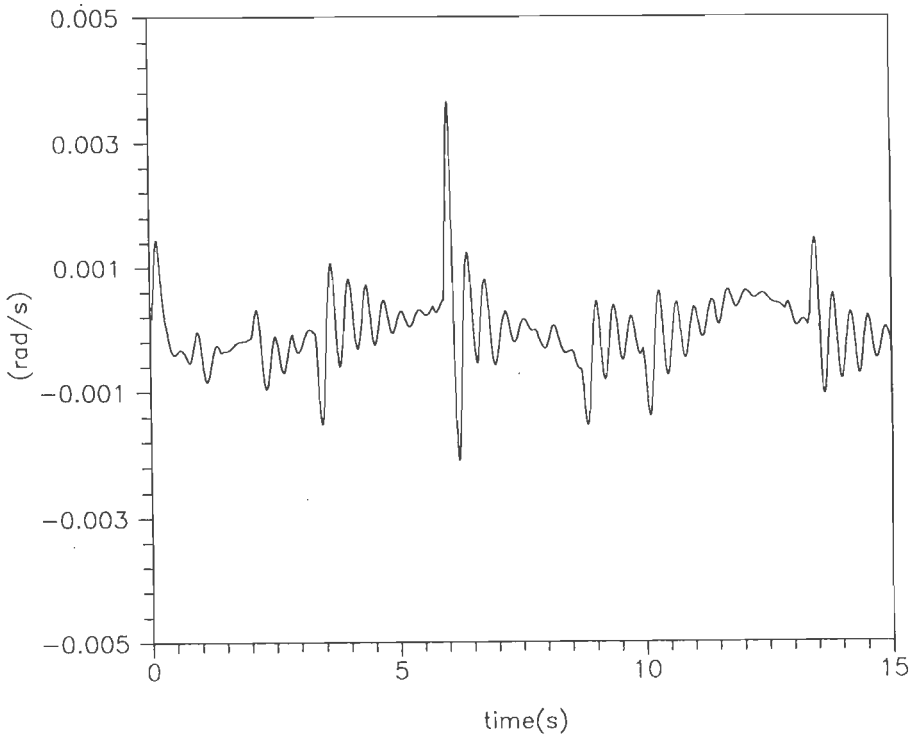

Fig.5.104 Velocity error for test signal 'l'(Proposed case, section 4.2.3), joint-1.

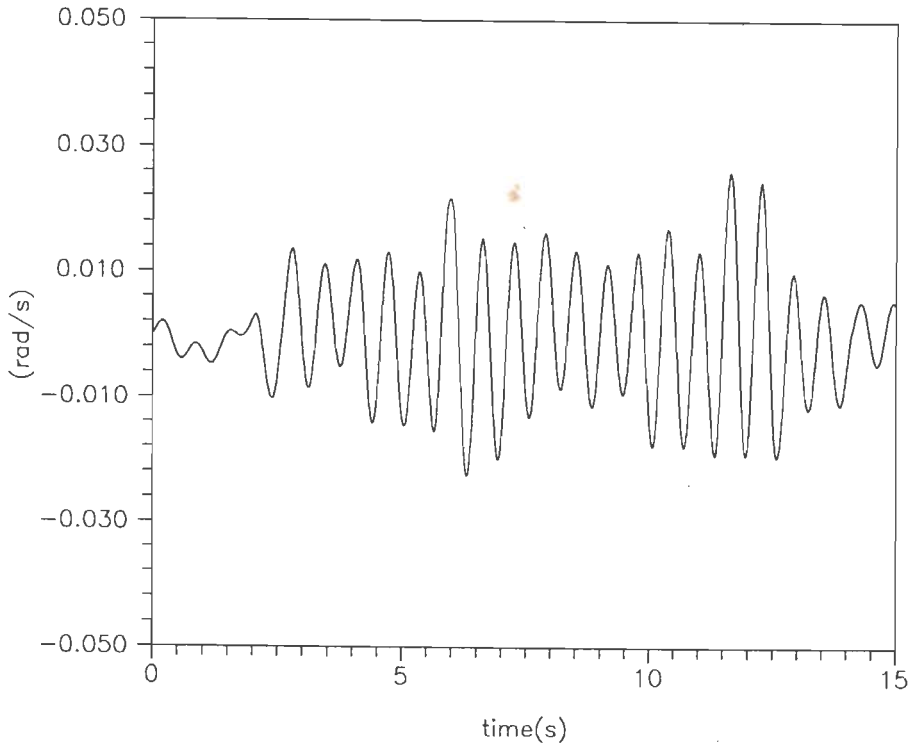

Fig.5.105 Velocity error for test signal 'J'(Canudas case[8]), joint-2.

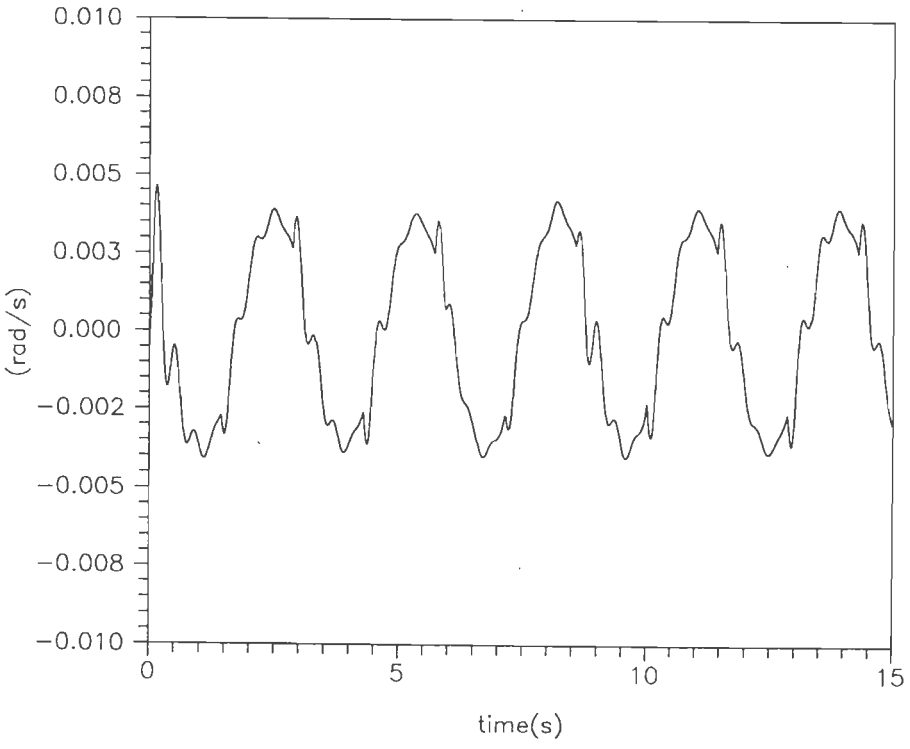

Fig.5.106 Velocity error for test signal 'J'(Proposed case, section 4.2.3), joint-2.

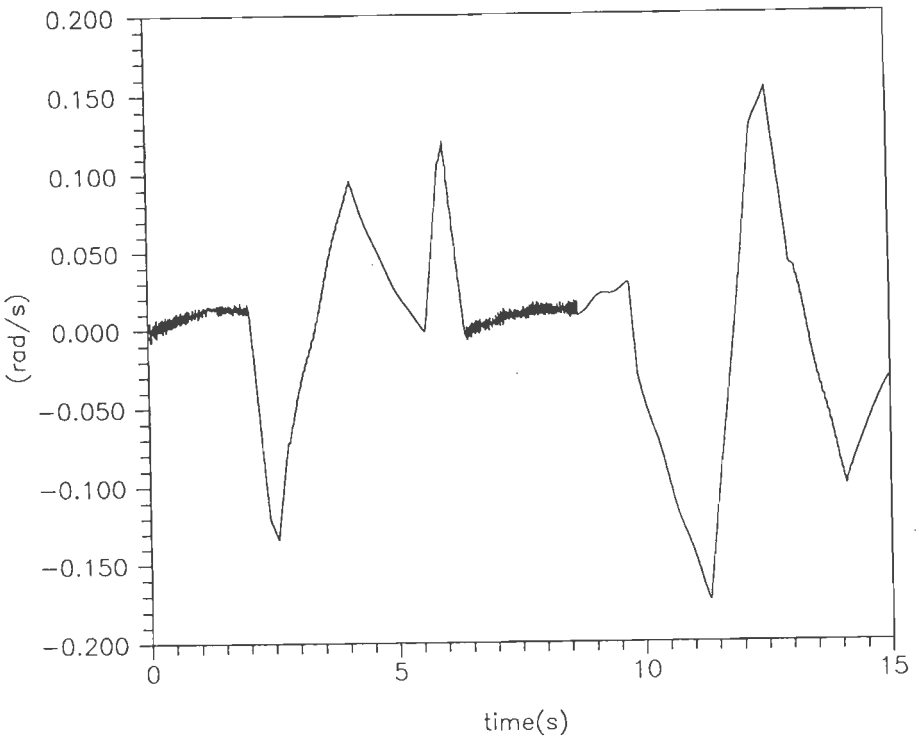

Fig.5.107 Velocity observation error for test signal 'I'(Canudas case[8]), joint-1.

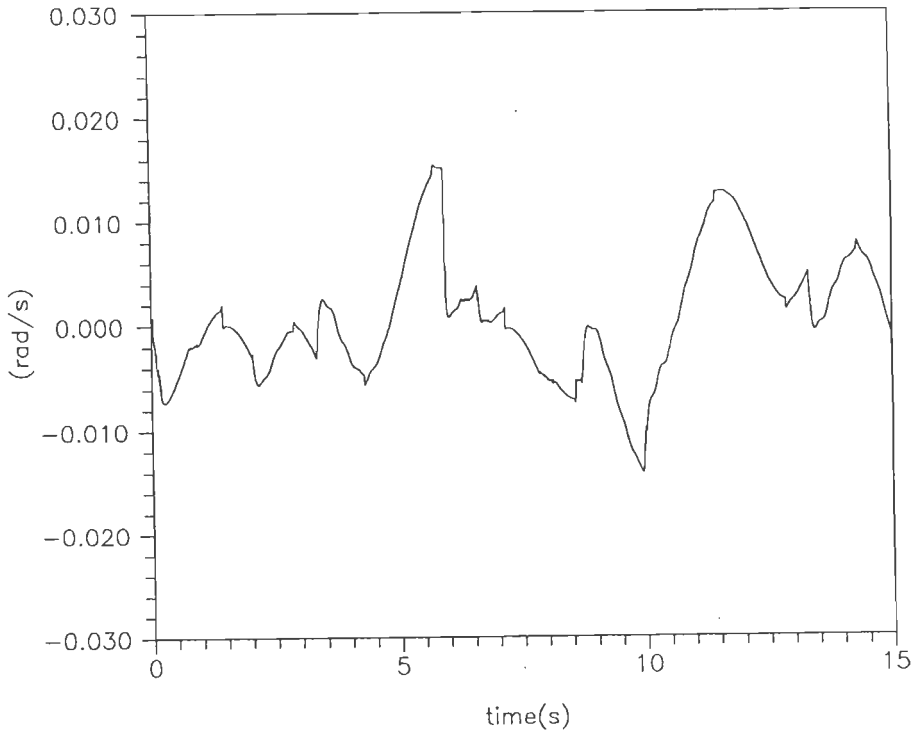

Fig.5.108 Velocity observation error for test signal 'I'(Proposed case, section 4.2.3), joint-1.

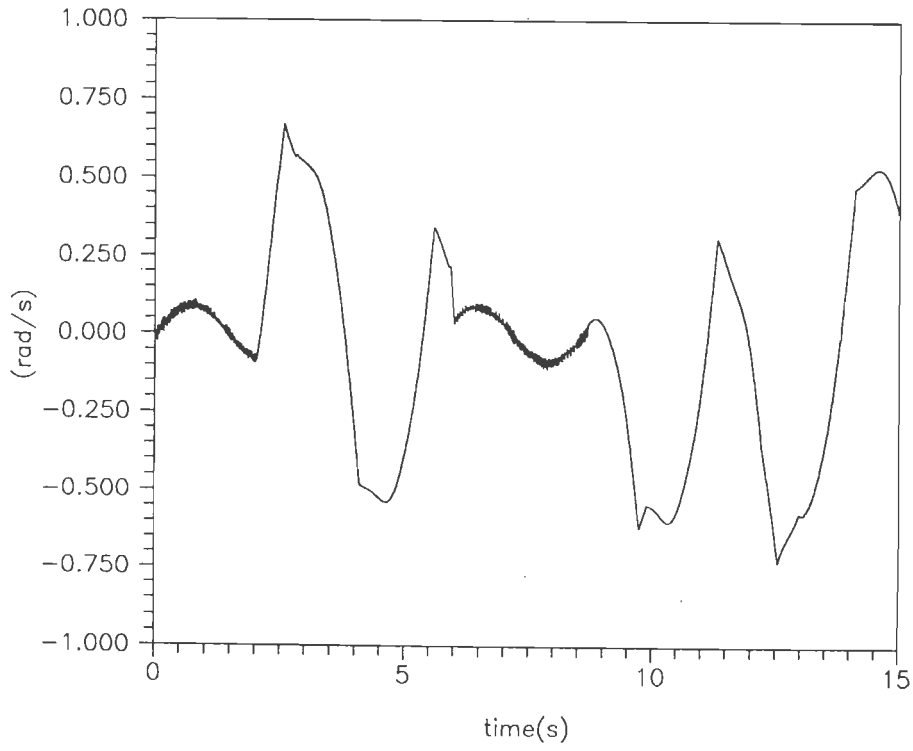

Fig.5.109 Velocity observation error for test signal 'J' (Canudas case[8]), joint-2.

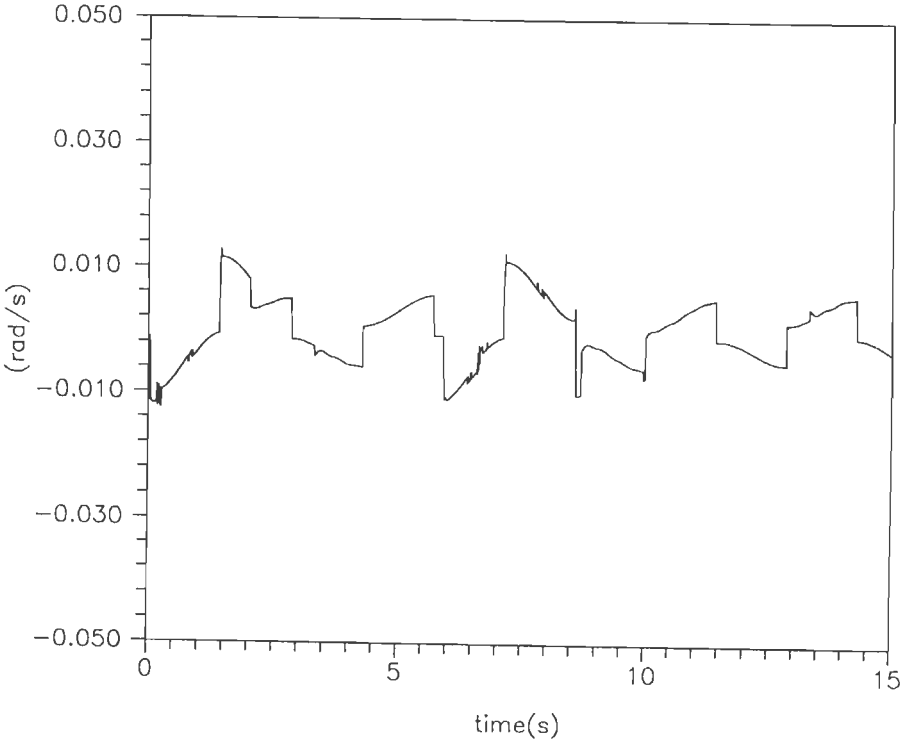

Fig.5.110 Velocity observation error for test signal 'J'(Proposed case, section 4.2.3), joint-2.

5.8 SIMULATION OF SIGN-SIGN BASED NONLINEAR SLIDING OBSERVER AIDED CONTROLLER

The controller which uses the disturbance vector, in contrast to structure used for simulation results in section 5.7, and observer structure is based on sign-sign function of tracking error and observation error respectively (section 4.2.4). These combined structure is illustrated with simple illustration of two-DOF robot system (Fig. 5.72) and its physical parameters are described by (5.6). In order to show the improvements in tracking performance, desired trajectories (test signal 'I','J') as shown in Fig. 5.73 and Fig.5.74 (see also (5.10)) are used for simulation purpose. It is assumed that the disturbance vector τ_d has the form of some fundamental component of cosine function. The following parameters are set as follows:

Λ_1 = diag [0.07,0.07] ; Γ_1 = diag[500, 500]; Γ_2 = diag[100, 100]; Q = diag [35,25]; $\Gamma_{e1} = \Gamma_{e2}$ = diag[5,5]; K_1 = diag[580, 580]; K_2 = diag [5, 5]; σ = 23; L_1 = diag [0.05, 0.05]; L_2 = diag[0.001, 0.001]; $\xi_o = \xi_1 = \xi_2$ = 0.05; τ_d = 0.05 (cos2t+cos3t)

Various errors graphs are shown in Fig.5.111-5.118 and also its maximum value are given in Table -VIII.

Table - VIII

Maximum errors for proposed case (sign-sign function based sliding observer)

Response	Proposed Case	
	Joint -1	Joint-2
Tracking errors (%)	0.12	0.026
Observation errors (Position) (%)	0.55	1.03
Velocity errors (rad/s)	0.0026	0.0042
Velocity observation errors (rad/s)	0.0122	0.0106

Clearly, Table-VIII indicates the better performance of the proposed scheme regarding various error response with compared to previous results.

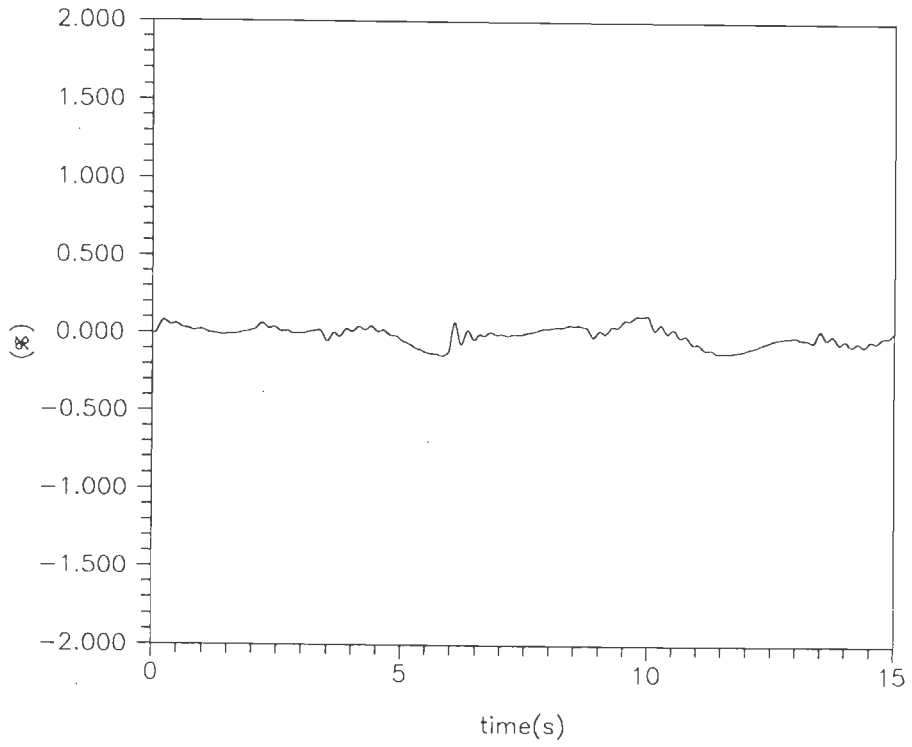

Fig.5.111 Tracking error as percent of max. input for test signal 'I' (Proposed case, section 4.2.4), joint-1.

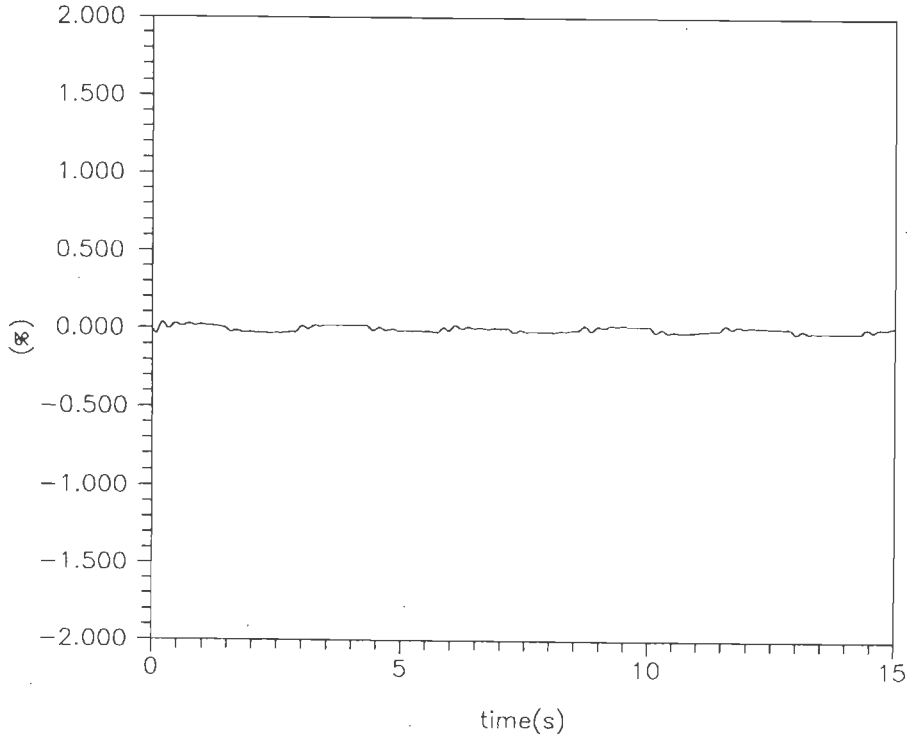

Fig.5.112 Tracking error as percent of max. input for test signal 'J' (Proposed case, section 4.2.4), joint-2.

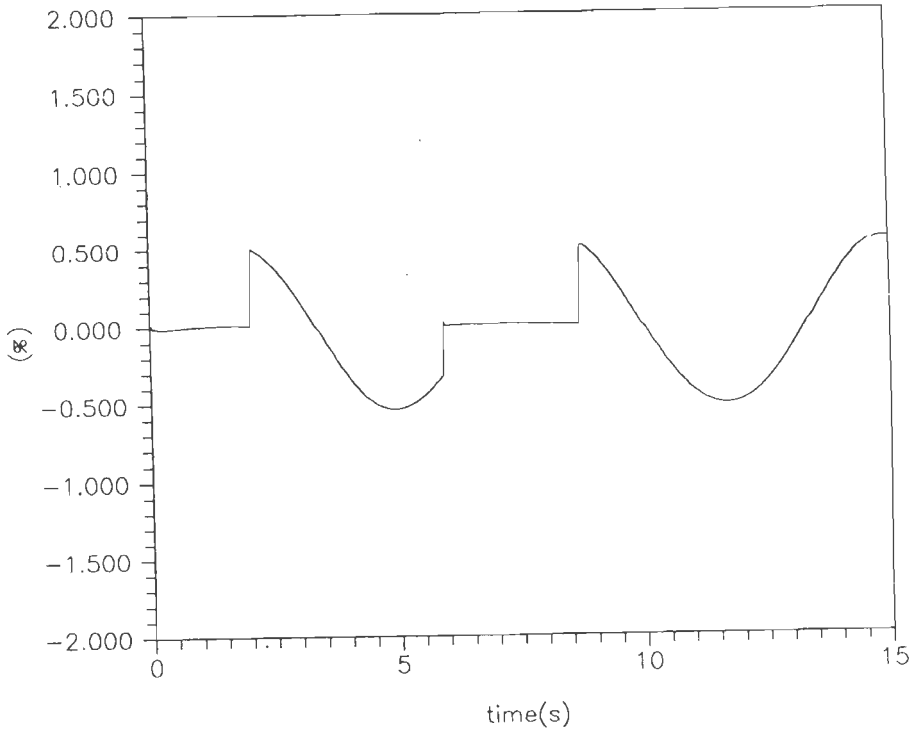

Fig.5.113 Observation error (position) as percent of max. input for test signal 'I'(Proposed case, section 4.2.4),joint-1.

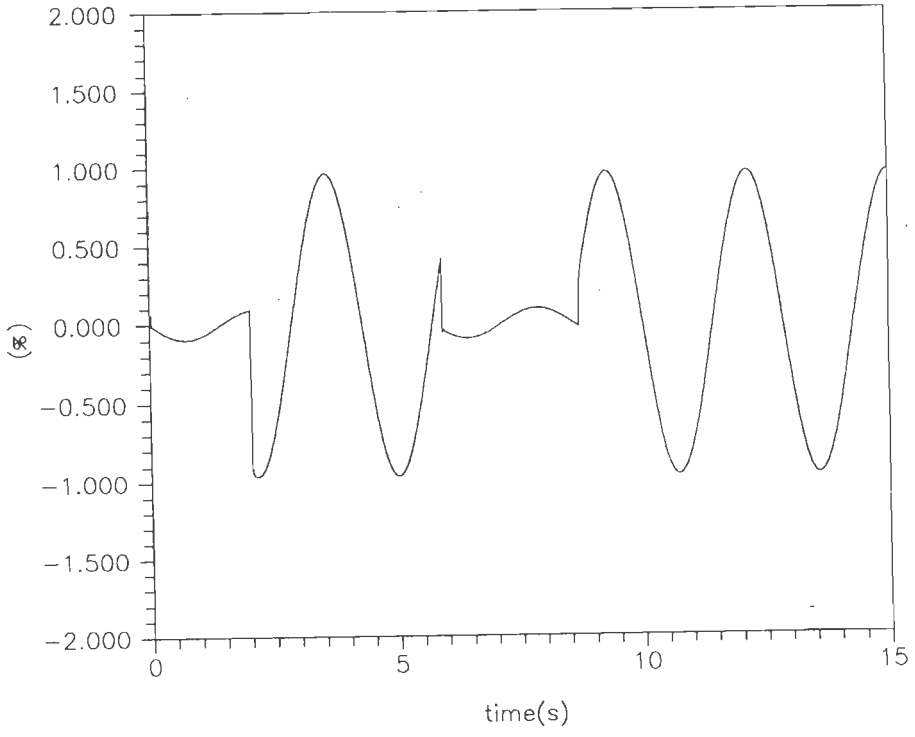

Fig.5.114 Observation error (position) as percent of max. input for test signal 'J'(Proposed case, section 4.2.4),joint-2.

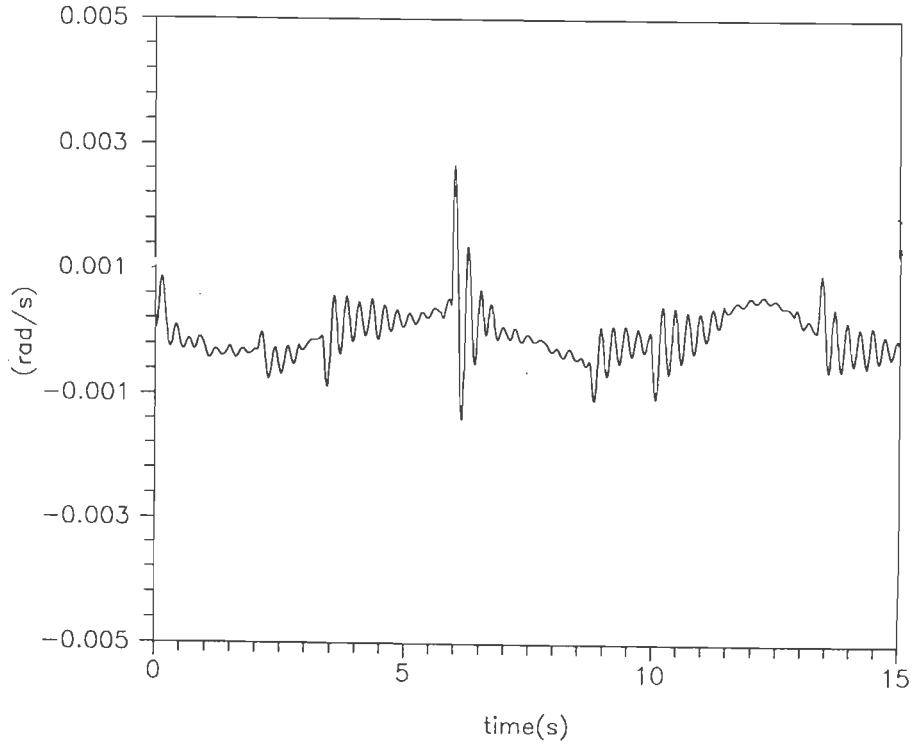

Fig.5.115 Velocity error for test signal 'I'(Proposed case, section 4.2.4), joint-1.

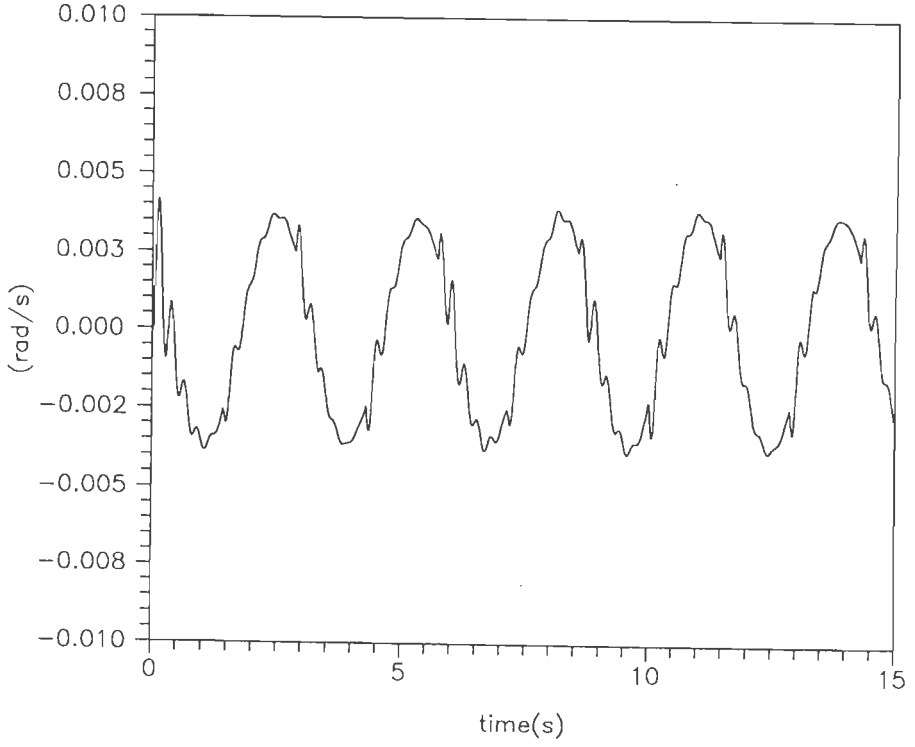

Fig.5.116 Velocity error for test signal 'J'(Proposed case, section 4.2.4), joint-2.

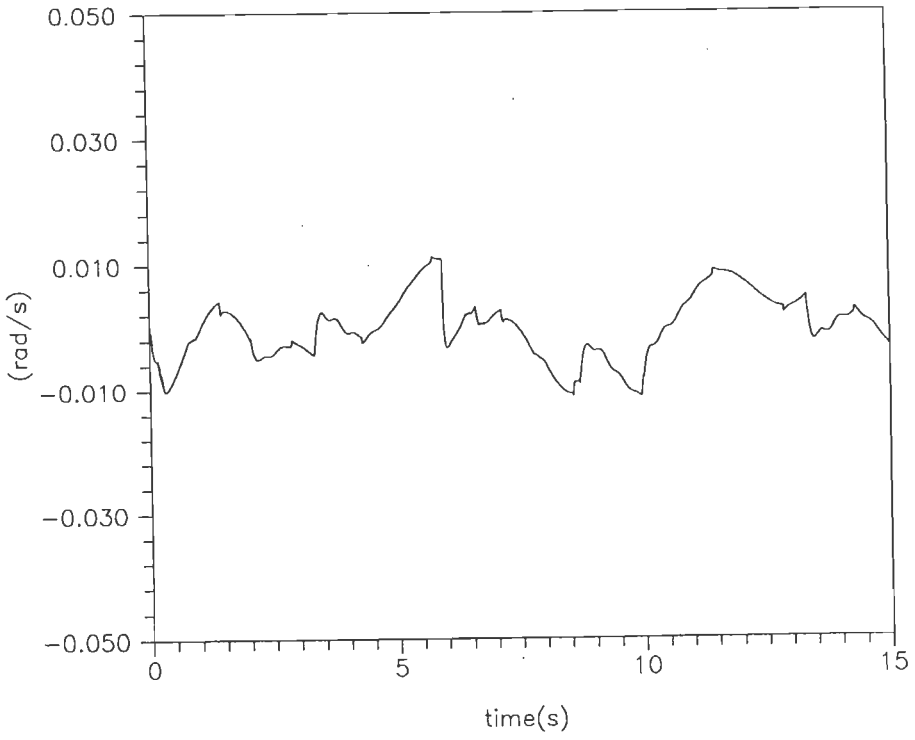

Fig.5.117 Velocity observation error for test signal 'l'(Proposed case, section 4.2.4), joint-1.

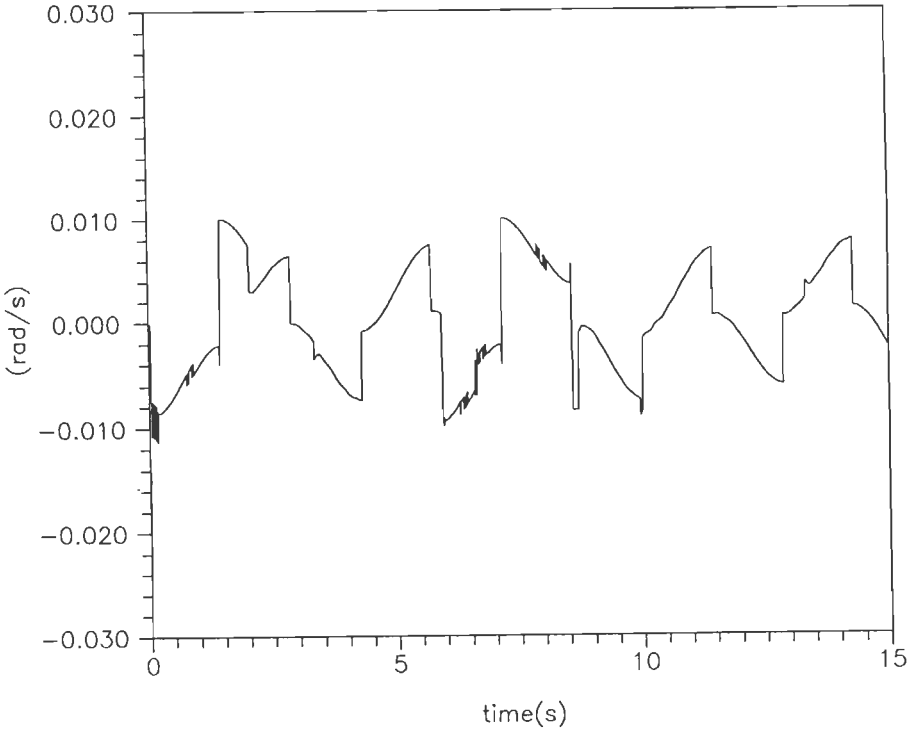

Fig.5.118 Velocity observation error for test signal 'j'(Proposed case, section 4.2.4), joint-2.

5.9 SIMULATION OF MODEL-BASED ADAPTIVE CONTROLLER STRUCTURE

In order to compare the tracking performance of sliding observer based controller structure with model-based adaptive controller structure, simulation results are also reported in Table -IX. They include the tracking error as percentage basis and velocity error in rad/s for the test signal 'I' an 'J' (Fig. 5.73-5.74, (5.10)). A simple two-DOF robot system (Fig. 5.72) with physical parameters as described in (5.6) is used for simulation of model-based adaptive controller structure.

Table-IX

Maximum errors for model-based adaptive controller

Cases	Tracking error (%)		Velocity error (rad/s)		Set value
	Joint -1	Joint -2	Joint-1	Joint-2	
Whitcomb case	5.1231	3.8230	0.0323	0.0852	$\varepsilon_o = 0.045$
Proposed controller Section 3.2.1	1.267	0.3221	0.0068	0.0168	$K_1 = diag[10,5]$ $K_2 = diag[5,1]$
Berghuis case	1.7921	1.5310	0.0452	0.0410	$\varepsilon_o = 0.045$
Proposed case-1 Section 3.2.2	0.3201	0.5001	0.0034	0.0082	$K_1 = diag[10,5]$ $K_2 = diag[5,1]$
Proposed case-2	0.1825	0.2598	0.0032	0.0073	$\sigma_n = 9000/$
Proposed case-3	0.4253	0.6528	0.0049	0.0123	
proposed bounded form (Section 3.2.3)	0.1320	0.2139	0.0092	0.0132	

The error graphs are shown in Fig.119-144. Applying the desired trajectories (test signal 'I', 'J') for these cases also, it is observed that the tracking performance of model-based controller structure is better than that of [10].

It is also observed that nonlinear sliding observer aided control structure is superior among proposed cases regarding their tracking performance because of using full dynamics model in observer structure and estimated velocity is fed back to controller structure.

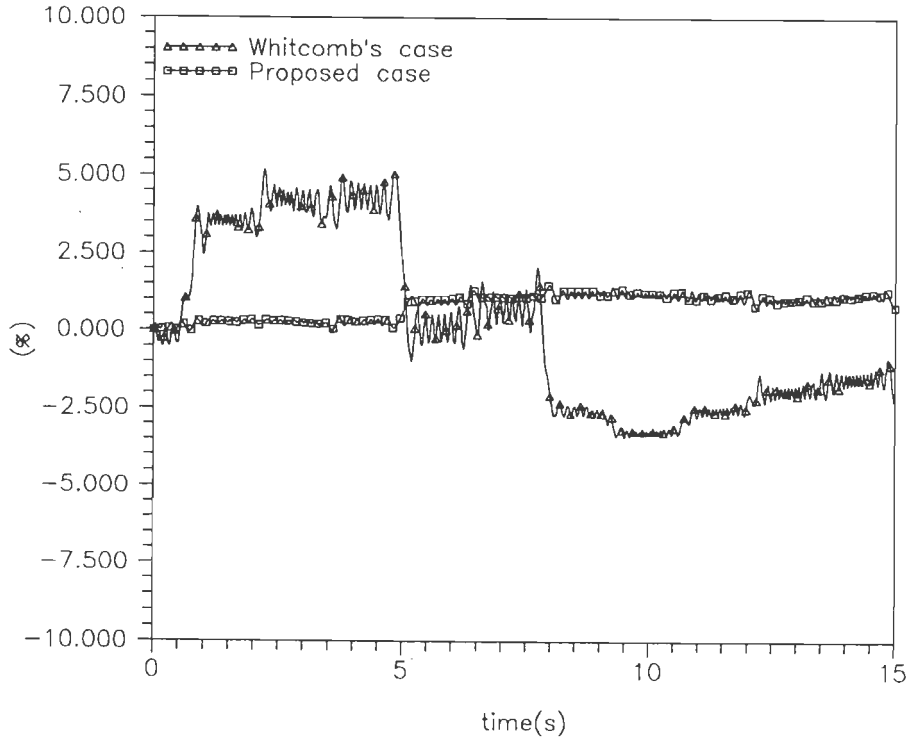

Fig.5.119 Tracking error as percent of max. input for test signal 'I',joint-1.

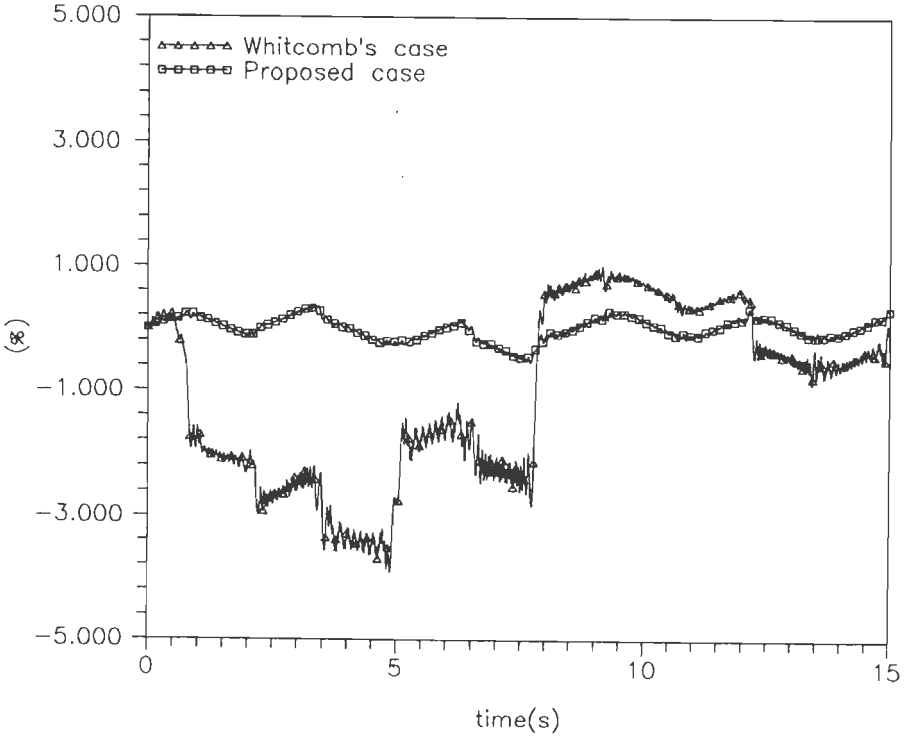

Fig.5.120 Tracking error as percent of max. input for test signal 'J',joint-2.

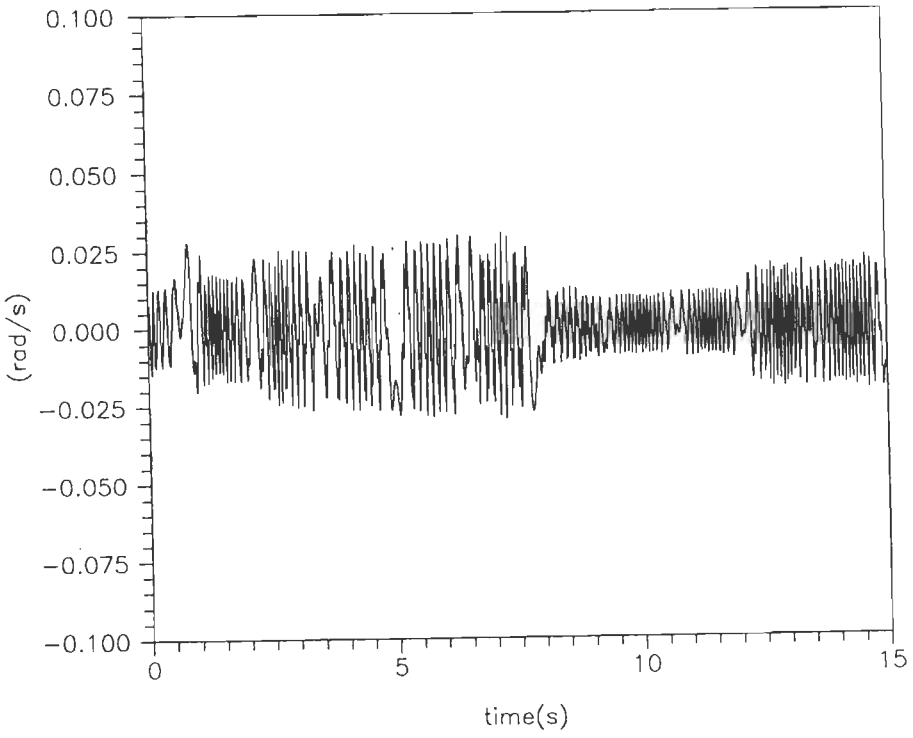

Fig.5.121 Velocity error for test signal'I' (Whitcomb's case), joint-1.

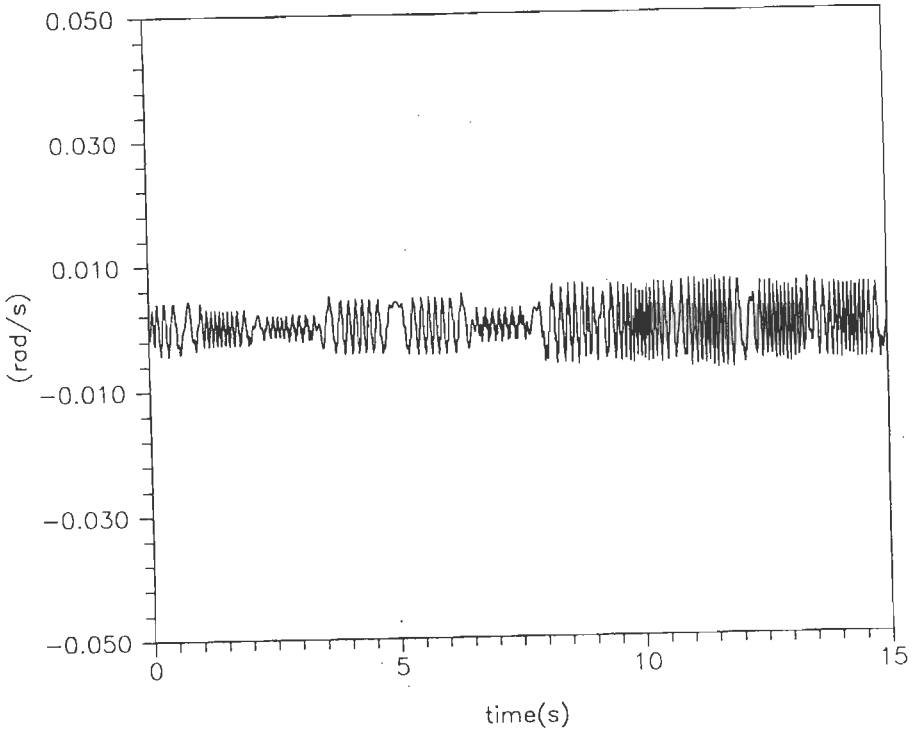

Fig. 5.122 Velocity error for test signal'I'(Proposed case),joint-1.

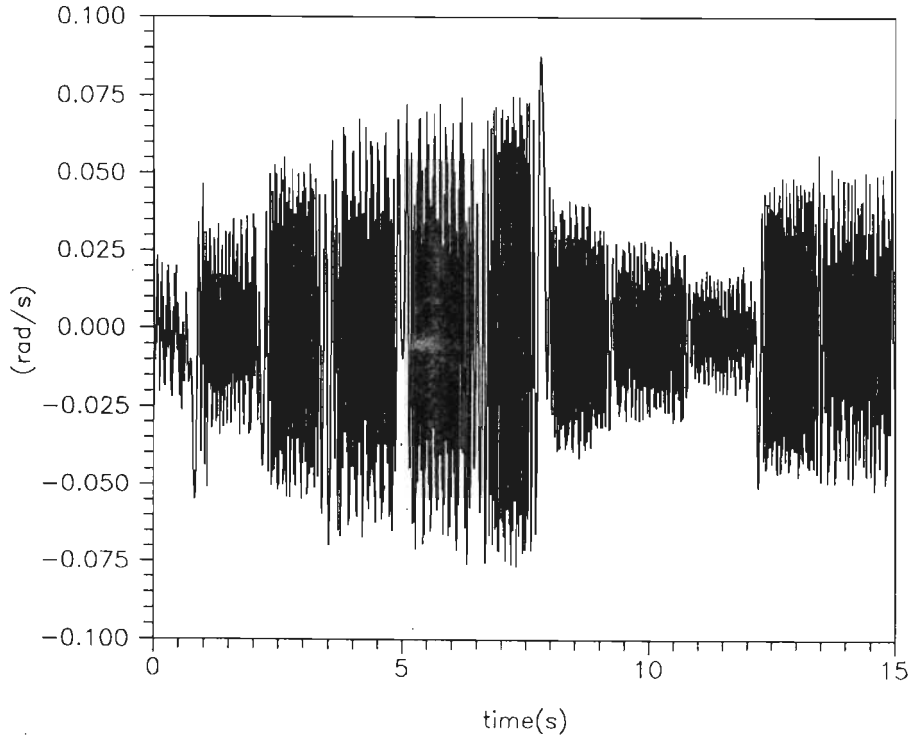

Fig.5.123 Velocity error for test signal 'J' (Whitcomb's case),joint-2.

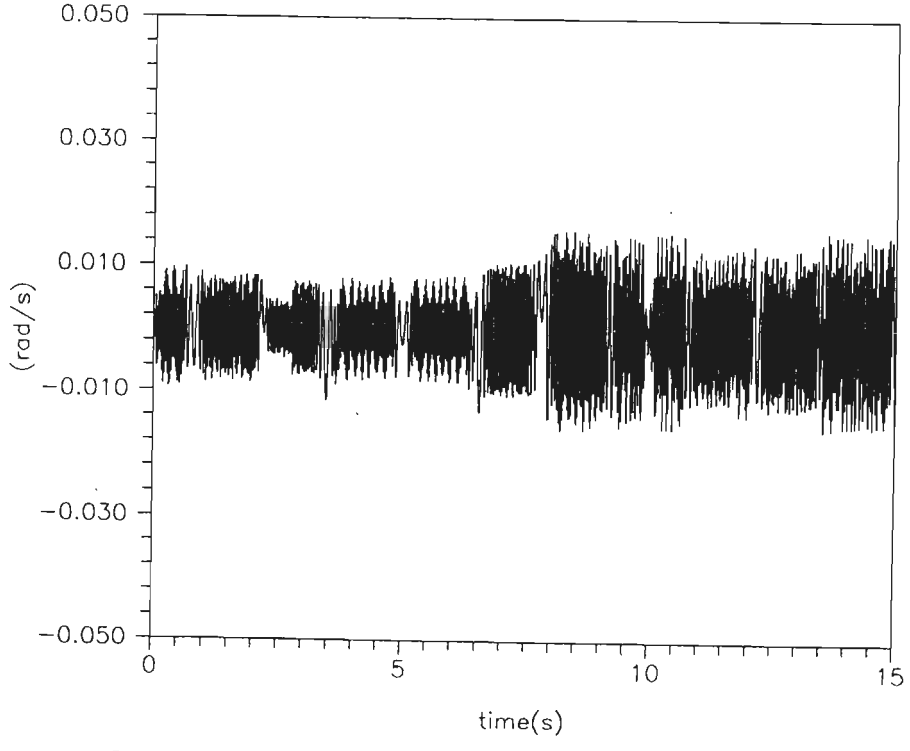

Fig.5.124 Velocity error for test signal 'J'(Proposed case), joint-2.

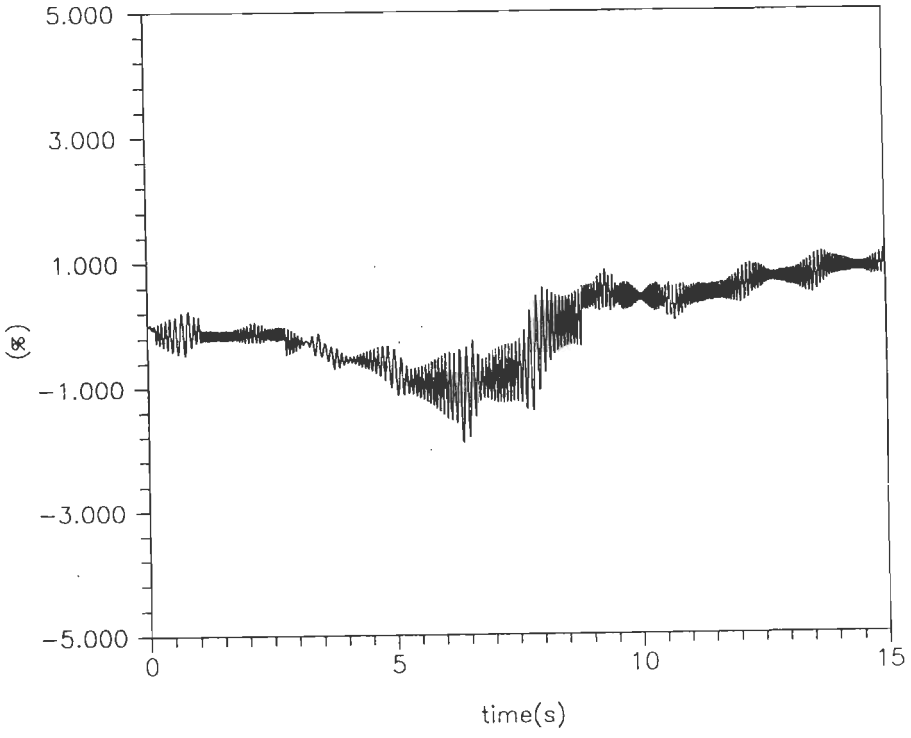

Fig.5.125 Tracking error as percent of max. input for test signal 'I'(Berghuis case), joint-1.

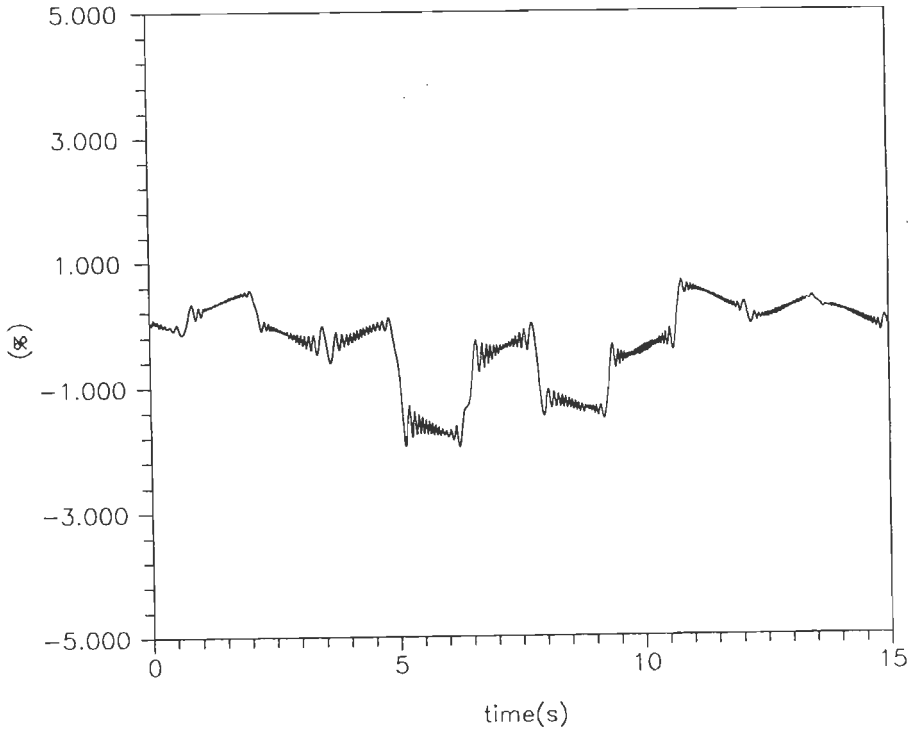

Fig.5.126 Tracking error as percent of max. input for test signal 'J'(Berghuis case), joint-2.

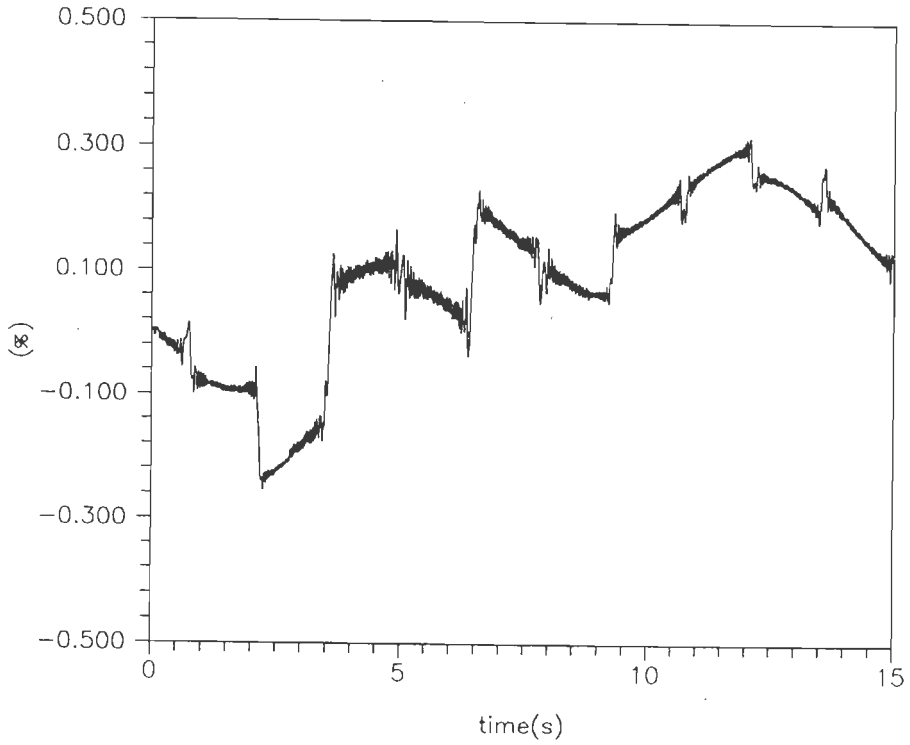

Fig.5.127 Tracking error as percent of max. input for test signal 'I'(Proposed case-1), joint-1.

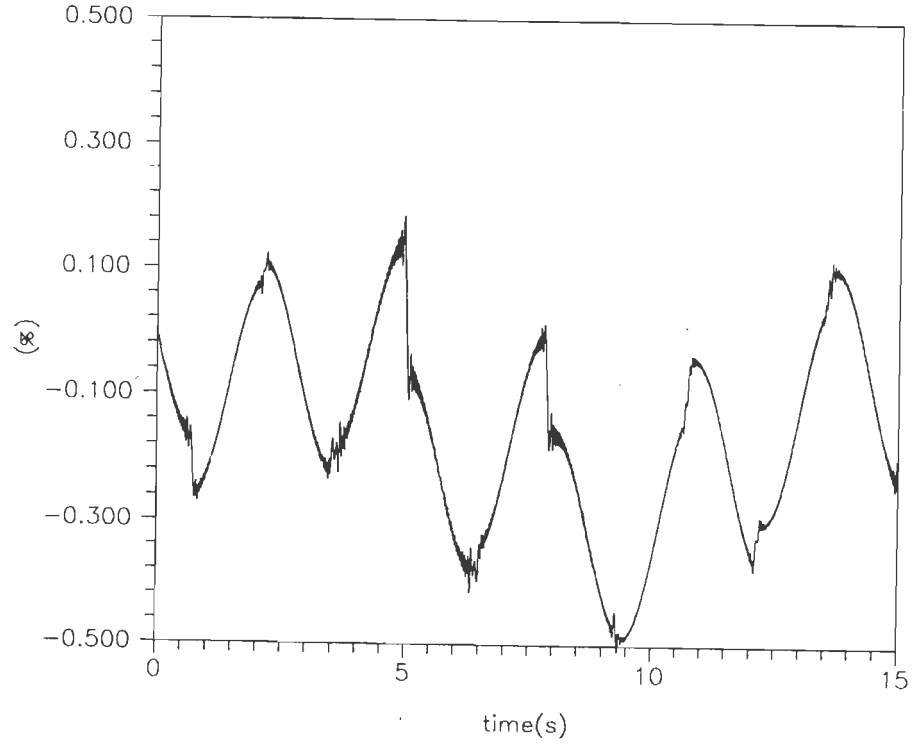

Fig.5.128 Tracking error as percent of max. input for test signal 'J'(Proposed case-1), joint-2.

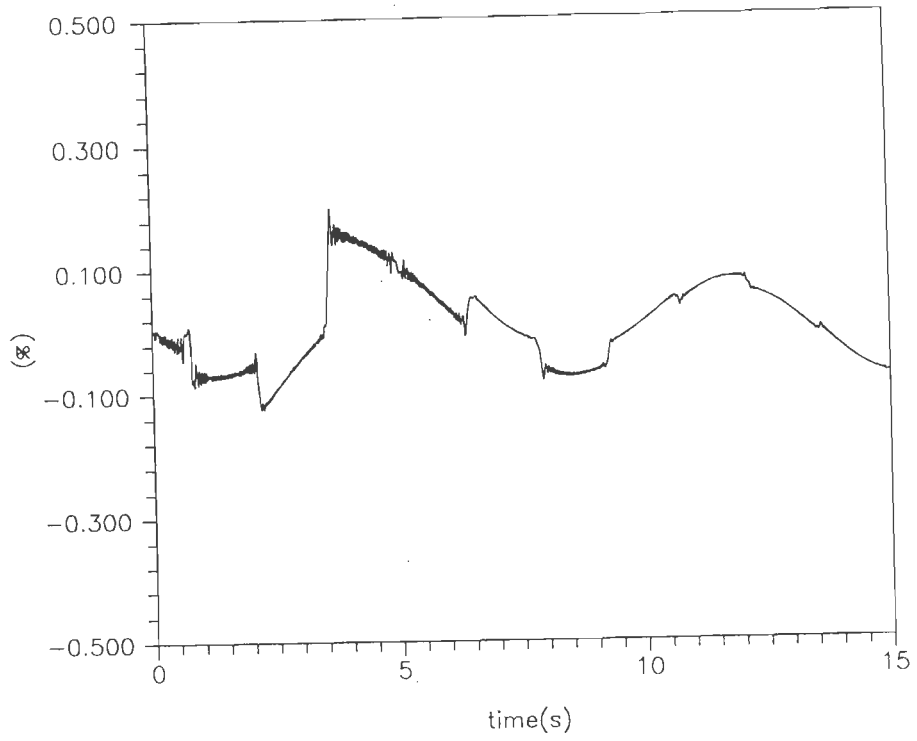

Fig.5.129 Tracking error as percent of max. input for test signal 'I'(Proposed case-2), joint-1.

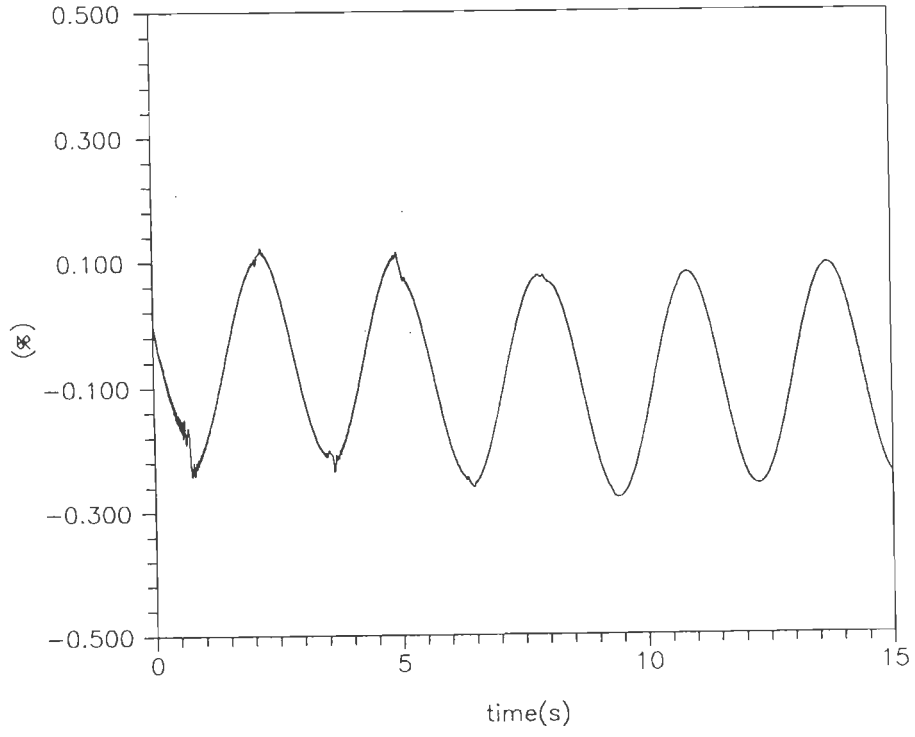

Fig.5.130 Tracking error as percent of max. input for test signal 'J'(Proposed case-2), joint-2.

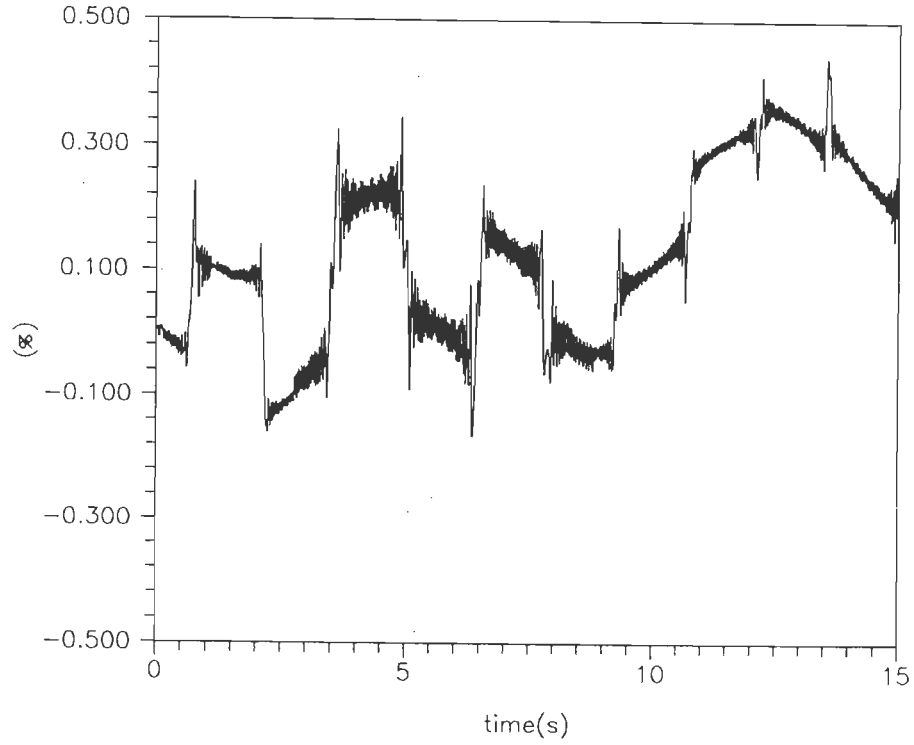

Fig.5.131 Tracking error as percent of max. input for test signal 'I'(Proposed case-3), joint-1.

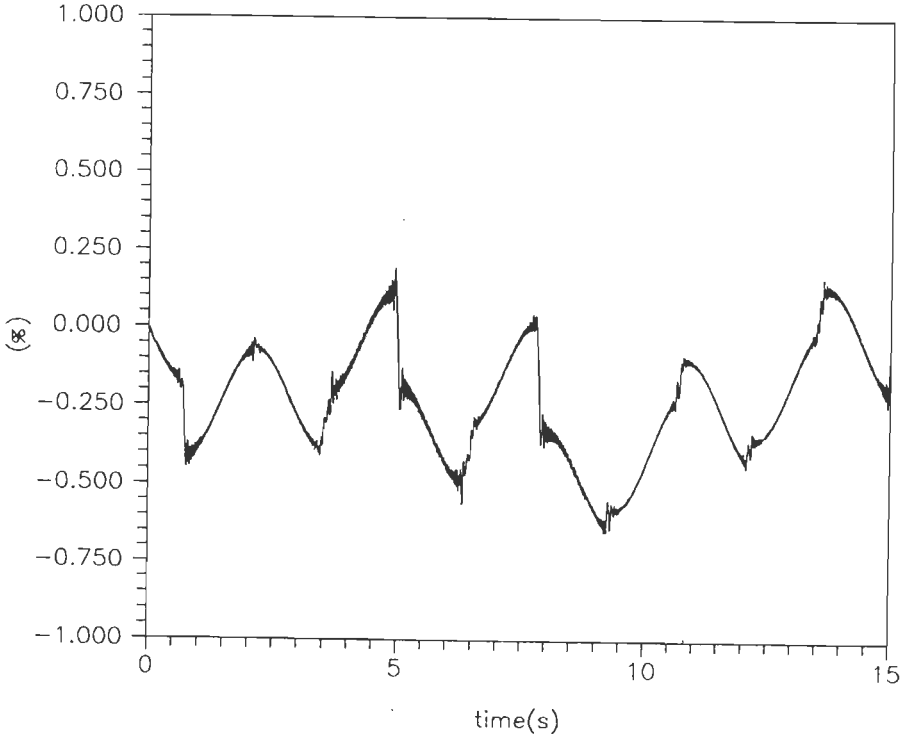

Fig.5.132 Tracking error as percent of max. input for test signal 'J'(Proposed case-3), joint-2.

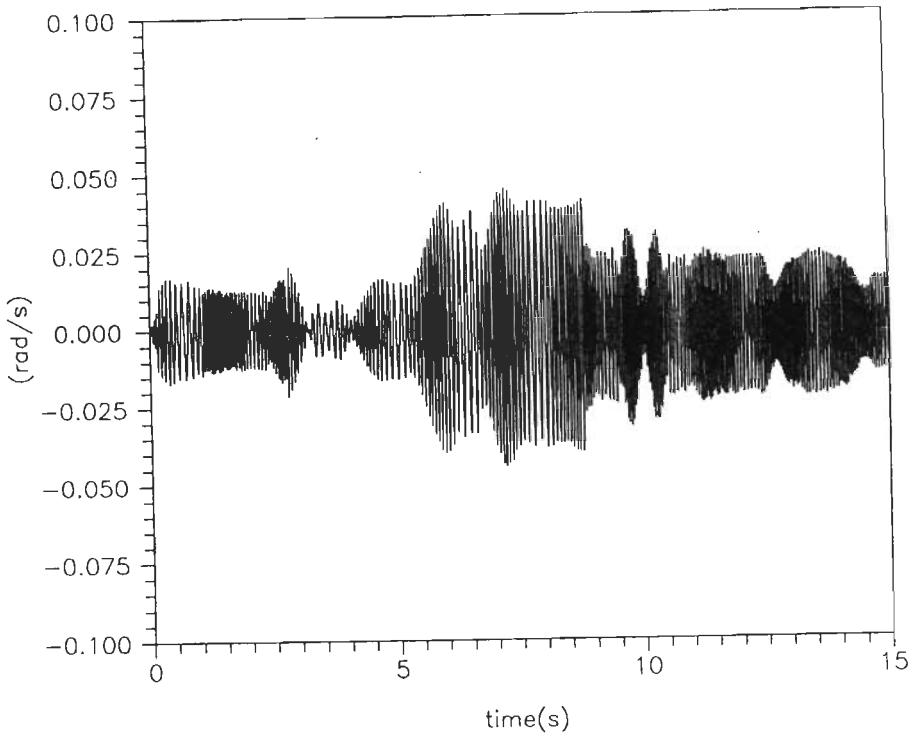

Fig.5.133 Velocity error for test signal 'I'(Berghuis case), joint-1.

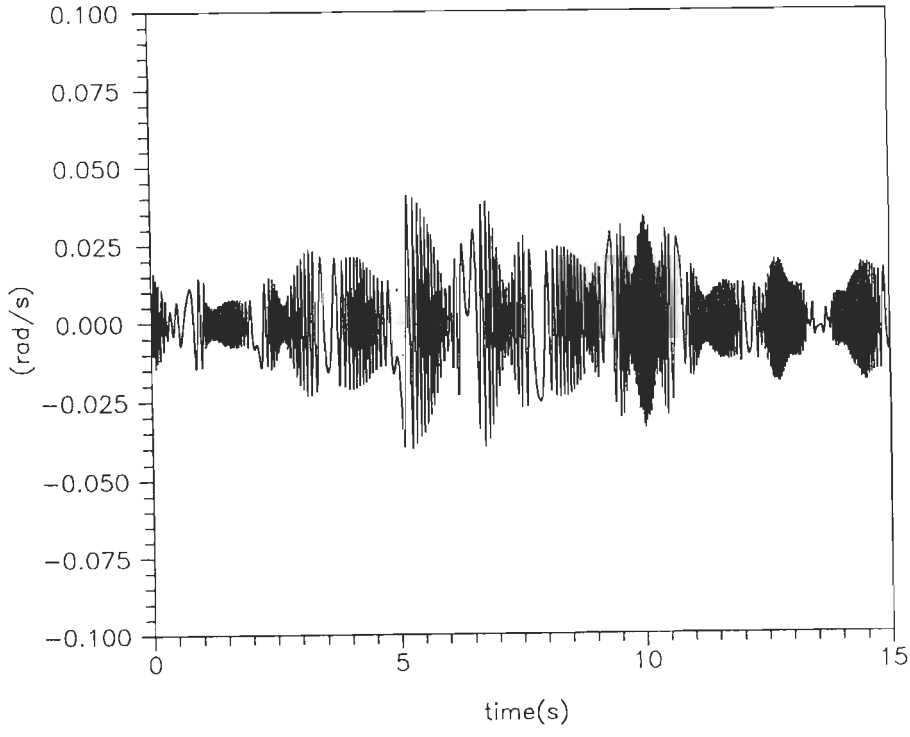

Fig.5.134 Velocity error for test signal 'J'(Berghuis case), joint-2.

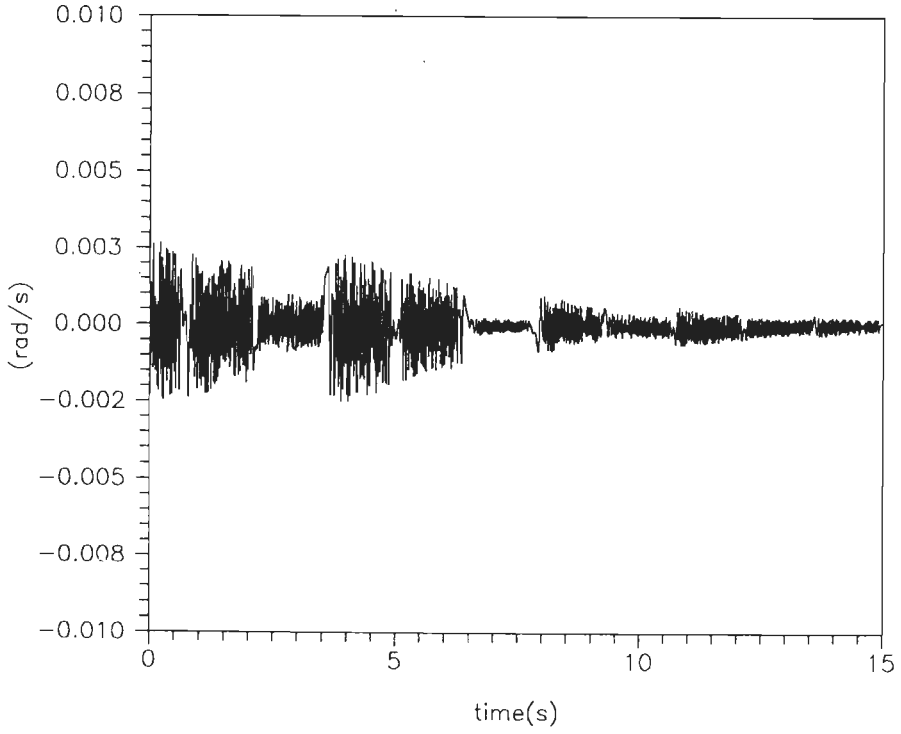

Fig.5.135 Velocity error for test signal 'I'(Proposed case-1), joint-1.

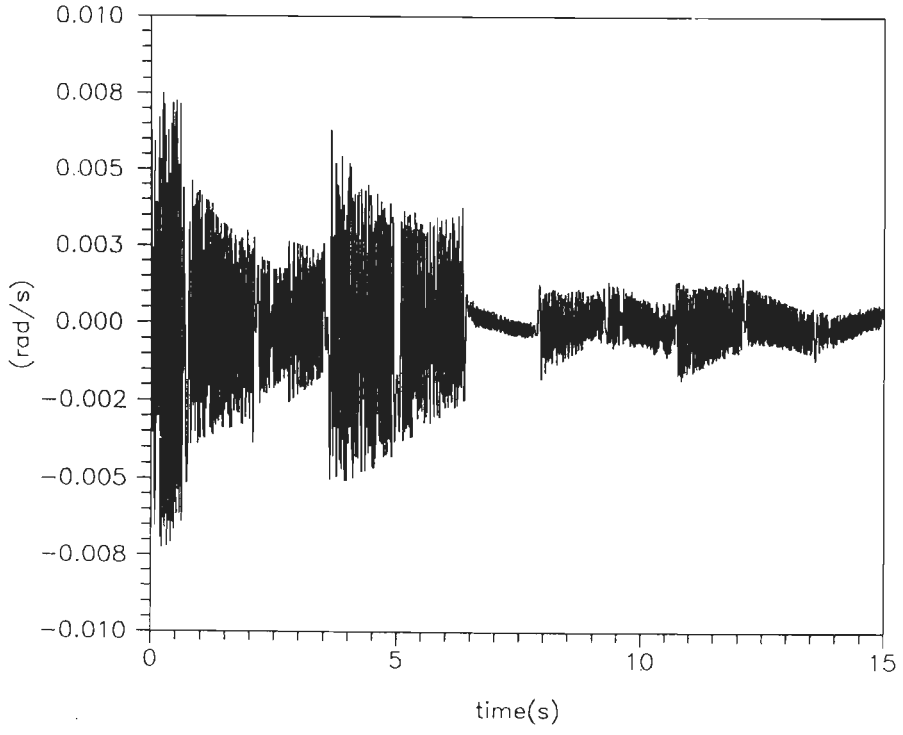

Fig.5.136 Velocity error for test signal 'J'(Proposed case-1), joint-2.

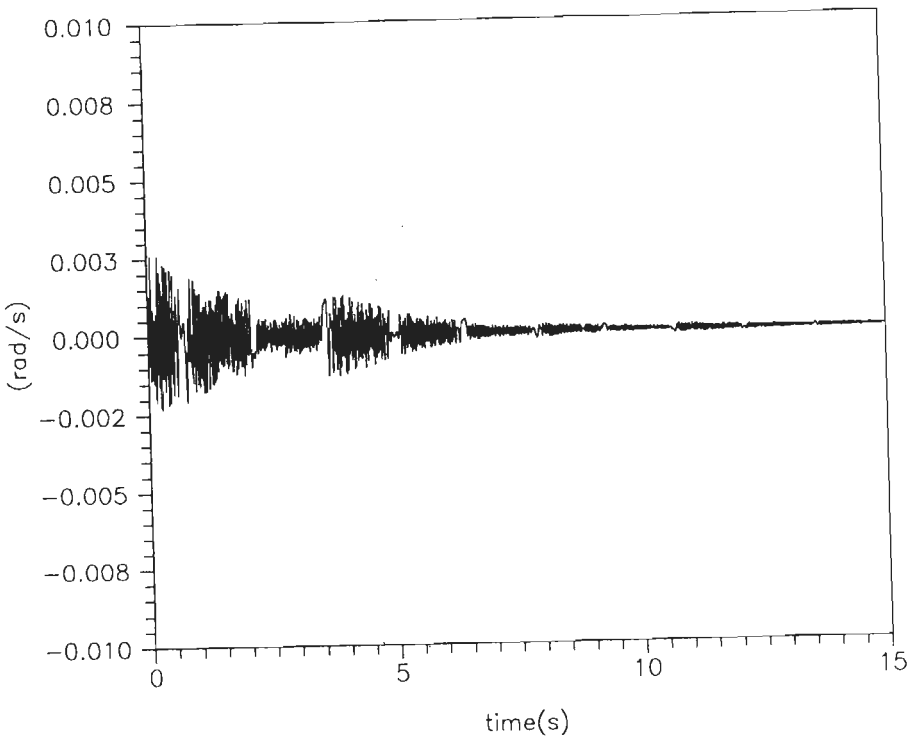

Fig.5.137 Velocity error for test signal 'I'(Proposed case-2), joint-1.

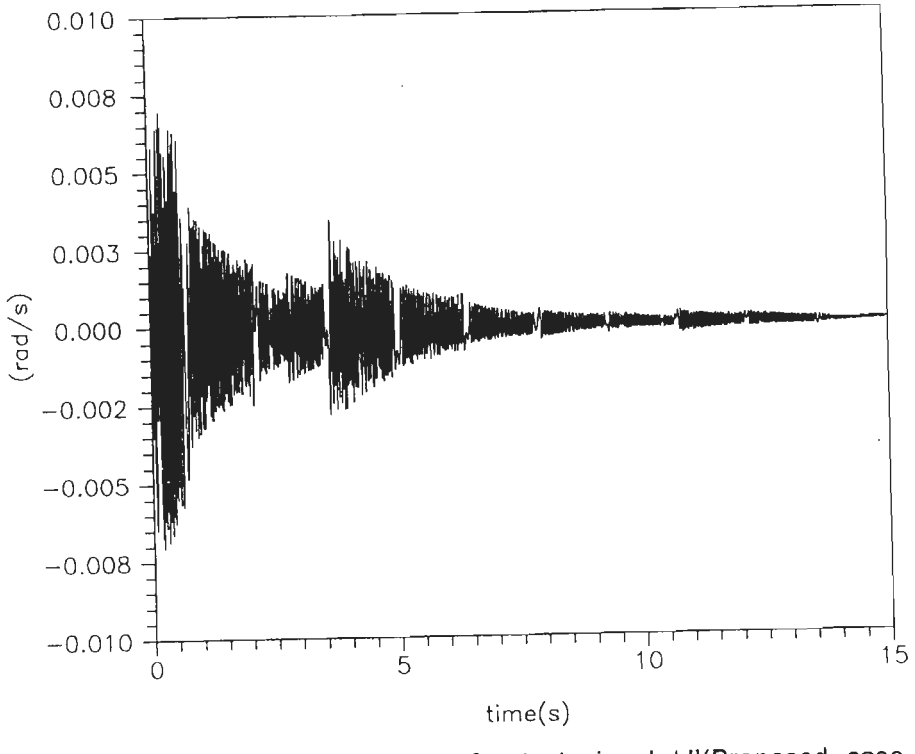

Fig.5.138 Velocity error for test signal 'J'(Proposed case-2), joint-2.

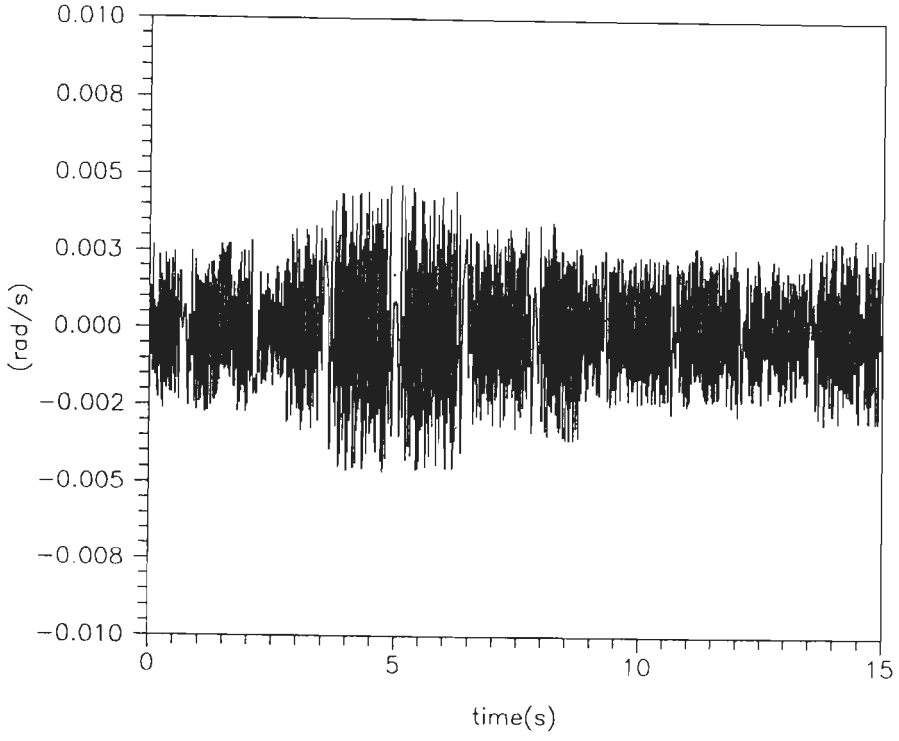

Fig.5.139 Velocity error for test signal 'I'(Proposed case-3), joint-1.

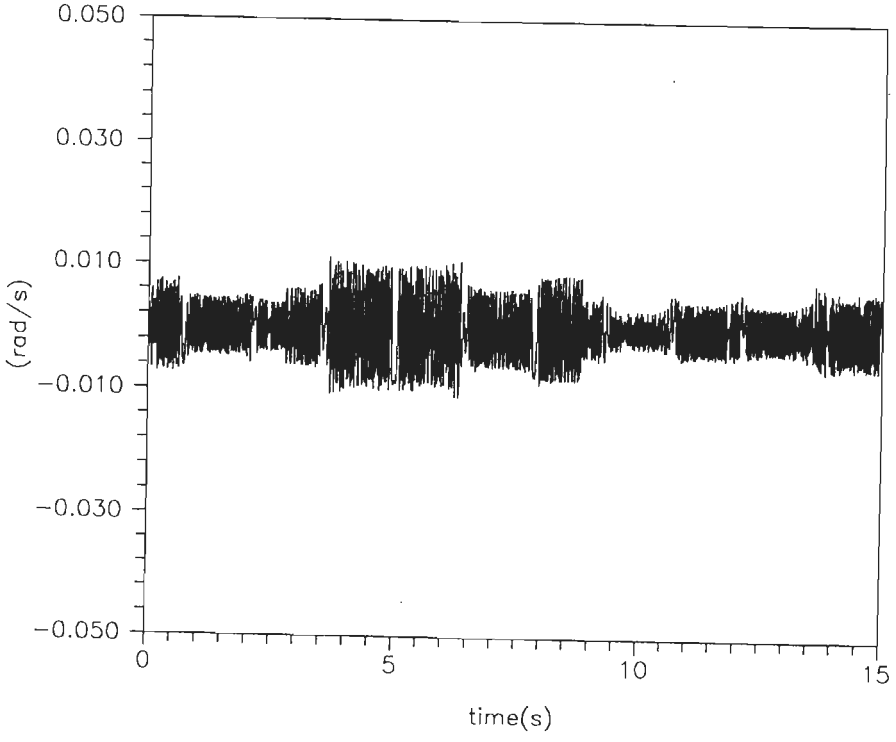

Fig.5.140 Velocity error for test signal 'J'(Proposed case-3), joint-2.

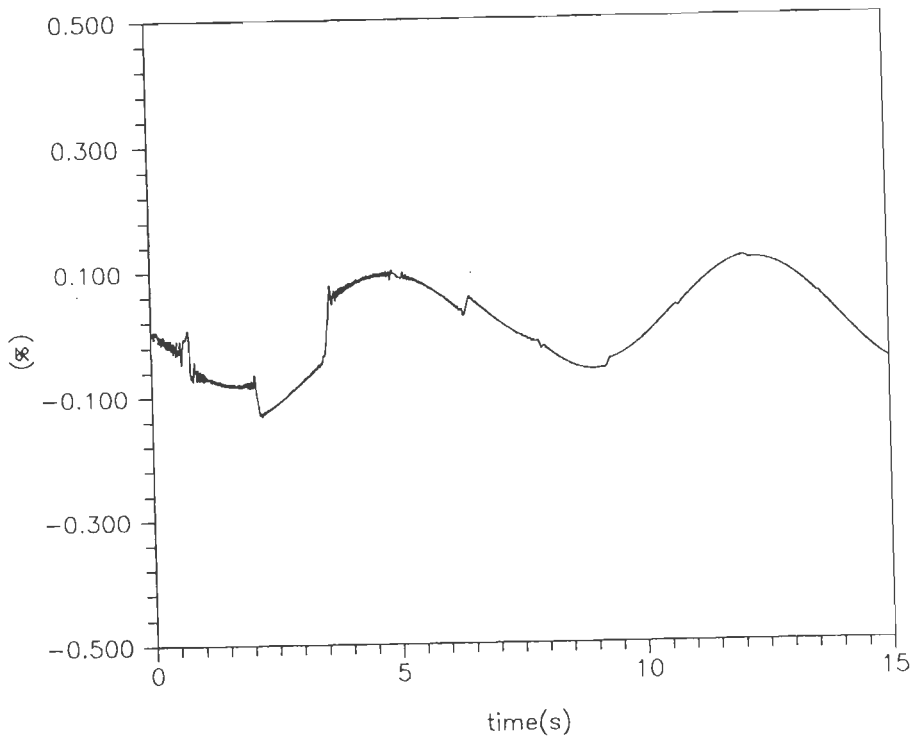

Fig.5.141 Tracking error as percent of max. input for test signal 'I'(Proposed bounded form), joint-1.

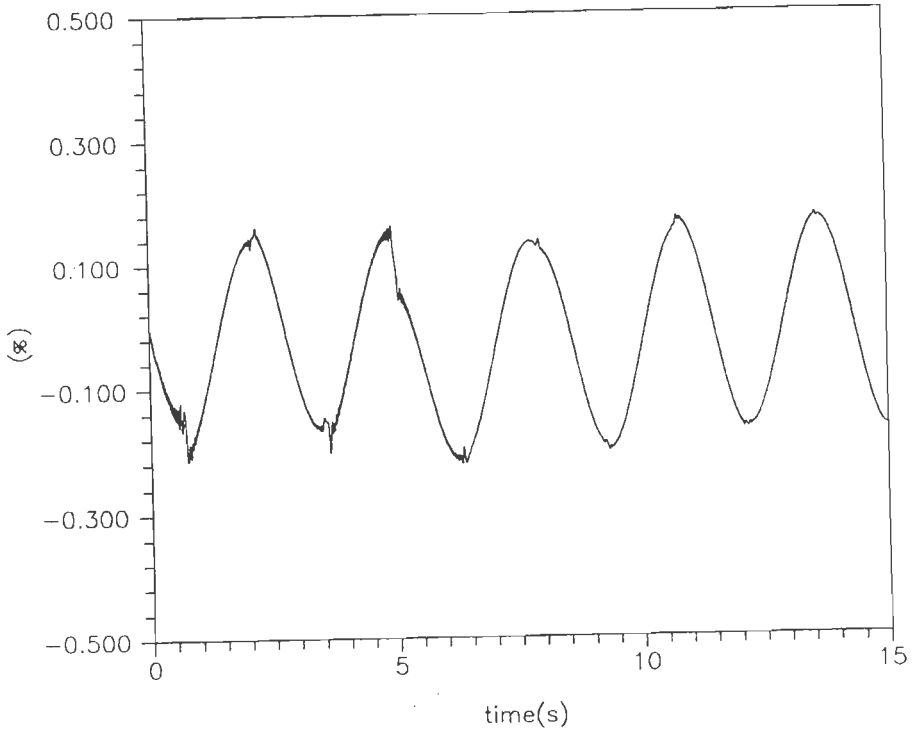

Fig.5.142 Tracking error as percent of max. input for test signal 'J'(Proposed bounded form), joint-2.

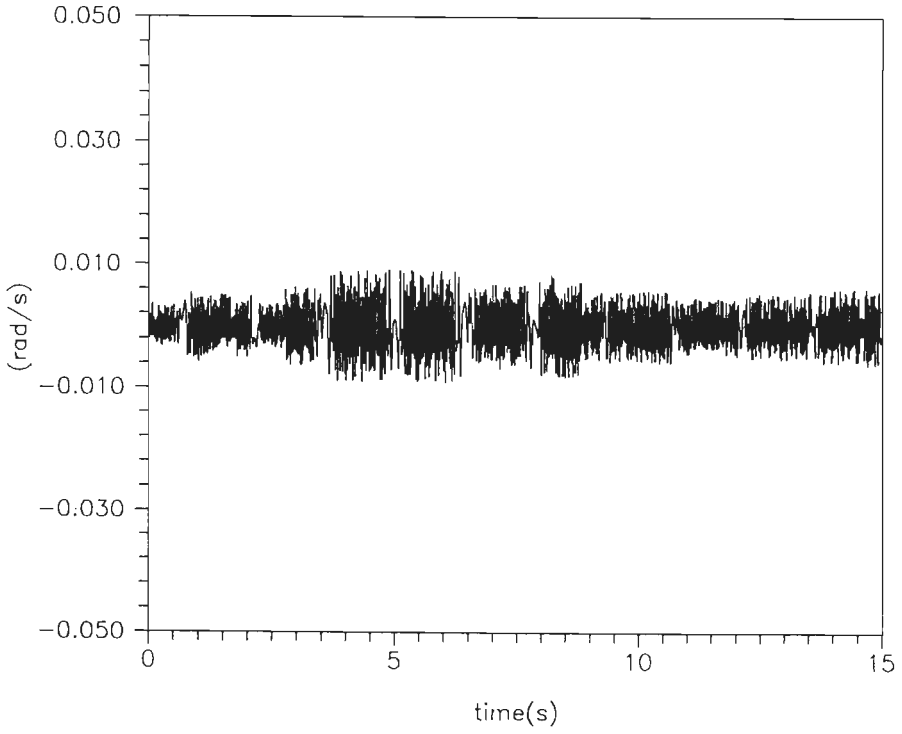

Fig.5.143 Velocity error for test signal 'I'(Proposed bounded form), joint-1.

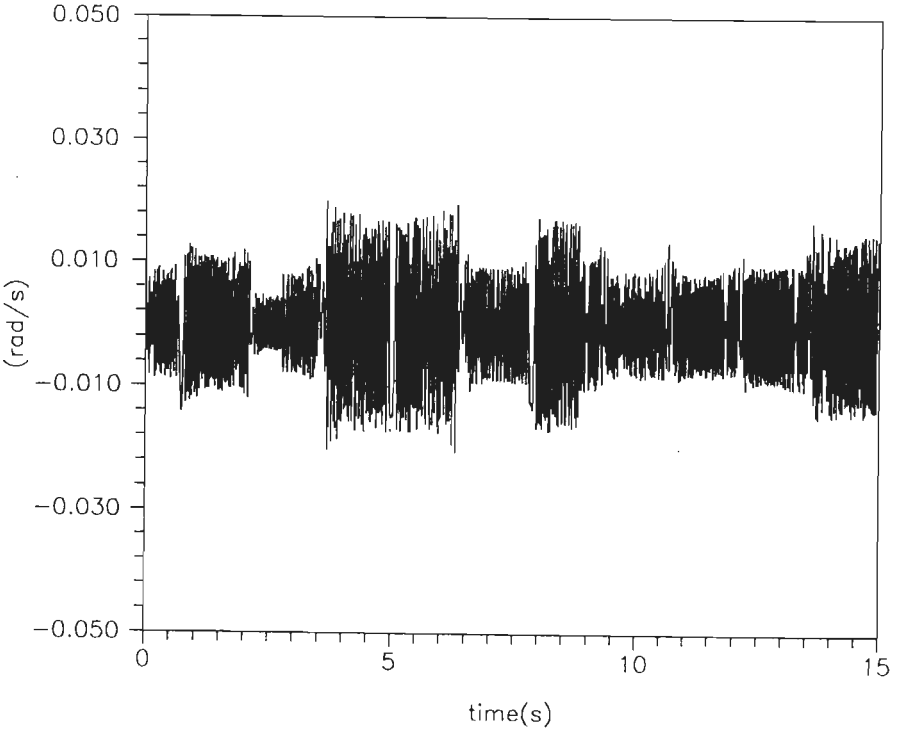

Fig.5.144 Velocity error for test signal 'J'(Proposed bounded form), joint-2.

Chapter - 6

CONCLUSIONS AND SUGGESTIONS FOR FUTURE WORK

6.1 CONCLUSIONS

In summary, the contributions of the proposed controller structures are to improve the tracking performance in comparison to available structures. The proposed control schemes are, first, model-based adaptive control and, second, sliding observer aided controller structure for trajectory tracking of robot manipulators. In order to reduce the controller-system mismatch, the acceleration term is included in existing controller structure [84] for relatively noise free situation. A new form of adaptation law results which in turn gives significant improvements in tracking performance. Apart from this, the nonlinear compensator based three variations of model-based adaptive controllers are proposed having different form of sliding surfaces. The purpose of using nonlinear feedback compensator term is to compensate the additional error which arises due to modification of adaptation signal. Simulation results show significant reduction in tracking error and velocity error in comparison to [7]. Among three cases, case-1 and case-2 have larger region of attraction in comparison to [7].

In distinct form, an adaptive controller structure is proposed wherein estimation is based on upper bound of the parameter rather than parameter itself. This is based on the inverse dynamics model of robot manipulators with a premise that if each parameter is known within some bounds the parameter adaptation can be prevented from going out of bounds and thus it makes the system more robust.

This proposed scheme gives drastic reduction in tracking error and velocity error in comparison to [7].

In order to look better tracking performance, the observers are employed to estimate the joint velocities because the actual velocities are often contaminated with high level of noise. The proposed controller-observer scheme with new uncertainty vector for adaptive case gives drastic reduction in tracking error and velocity error when compared with [10]. On the other hand, the nonlinear sliding observer based controller structures are found promising in view of the nonlinear nature of robot manipulators. Using this approach, two new nonlinear sliding observer aided controller structure are proposed for trajectory tracking of robot manipulators. Significant reduction in error response are observed through simulation. Larger region of attraction is noticed for the proposed scheme when compared with [8].

The results contained herein were obtained through an approach substantially different from that presented in [84],[7],[10],[8], respectively. On the contrary to [84], a new form of adaptive law is proposed. Its performance show good tracking. Including nonlinear compensator and different form of sliding surface, adaptive controller structures are constructed to enhance trajectory tracking performance in comparison to [7]. In order to account dynamic interaction between controller and observer, a new form of sliding observer based controller structures are proposed to ensure better tracking when compared with [10], [8], respectively. This thesis represents some improved results in model-based adaptive and also sliding observer aided controller structure for trajectory tracking of robot manipulators.

6.2 SUGGESTION FOR FUTURE WORK

The presented work in this thesis supports the foundation for further work in the development of control methods and applications of model-based adaptive and sliding observer based control to robot manipulators. The following studies are suggested for future research works.

(i) An important topic of future research would be an extension of this thesis to actual on-line implementation of the proposed control schemes.

(ii) The proposed control schemes should be utilized to control direct drive robots and with flexible links.

(iii) Model-based adaptive controller structure still require improvements to cope with parameter uncertainty and errors in model because of the errors still lie with it.

(iv) Inclusion of actuator dynamics and gear train friction in model-based adaptive controller structure should be one of the future approach for rigid and flexible robots.

(v) In controller-observer schemes, different type of observer scheme should be employed with controller for robot manipulators. It may be consider as one of the areas for future work.

(vi) Finally, schemes to decrease the sensitivity of disturbances due to parameter variation should be developed to improve the flexibility of the schemes.

References

REFERENCES

[1] Ambrosino, G., Celentano, G., and Garofalo, F., "Robust Model Tracking Control for a Class of Nonlinear Plants," IEEE Trans. Automat. Cont., vol. AC-30, no. 3, pp. 275-279, 1985.

[2] Arimoto, S., and Miyazaki, F., "Stability and Robustness of PID Feedback Control for Robot Manipulators of Sensory Capability," Robotics Research, First Int. Sympos., edited by M. Brady and R. Paul, M.I.T. Press, pp. 783-799, 1984.

[3] Asada, H., and Slotine, J.J.E., Robot Analysis and Control, John Wiley and Sons, 1986.

[4] Balestrino, A., Demaria, G., and Sciavicco, L., "An Adaptive Model Following Control for Robotic Manipulators," ASME J. Dynam. Syst., Meas. Contr., vol. 105, no. 3, pp. 143-151, 1983.

[5] Bayard, D.S., and Wen, J.T., "New Class of Control Laws for Robotic Manipulators: Part-2 Adaptive Case," Int. J. Cont., vol. 47, no. 5, pp. 1387-1406, 1988.

[6] Berghuis, H., and Nijmeijer, H., "A Passivity Approach to Controller - Observer Design for Robots," IEEE Trans. Robotics Automat., vol. 9, no. 6, pp. 740-754, 1993.

[7] Berghuis, H., Ortega, R., and Nijmeijer, H.,"A Robust Adaptive Robot Controller," IEEE Trans. Robotics Automat., vol. 9, no. 6, pp. 825-830, 1993.

[8] Canudas de Wit, C., Fixot, N., and Åström, K.J., "Trajectory Tracking in Robot Manipulators via Nonlinear Estimated State Feedback," IEEE Trans. Robotics Automat., vol. 8., no. 1, pp. 138-144, 1992.

[9] Canudas de Wit, C., and Fixot, N., "Robot Control Via Robust Estimated State Feedback," IEEE Trans. Automat. Cont., vol. 36, no. 12, pp. 1497-1501, 1991.

[10] Canudas de Wit, C., and Fixot, N., "Adaptive Control of Robot Manipulators via Velocity Estimated Feedback," IEEE Trans. Automat. Cont., vol. 37, no. 8, pp. 1234-1237, 1992.

[11] Chen, Y.H., "On the Deterministic performance of Uncertain Dynamical Systems," Int. J. Cont., vol. 43, no. 5, pp. 1557-1579, 1986.

[12] Chen, Y.H., "Robust Computed Torque Scheme for Mechanical Manipulators : Nonadaptive Versus Adaptive," ASME J. Dynam. Syst., Meas. Contr., vol. 113, no. 2, pp. 324-327, 1991.

[13] Choi, Y.K., Chung, M.J., and Bien, Z., "An Adaptive Control Scheme for Robot Manipulators," Int. J. Cont., vol. 44, no. 4, pp. 1185-1191, 1986.

[14] Colbaugh, R., Glass, K., and Pittman, P., "Adaptive Control for A Class of Hamiltonian Systems," Computers Elect. Engng., vol. 20, no. 1, pp. 21-38, 1994.

[15] Corless, M.J., and Leitmann, G., "Continuous State Feedback Guaranteeing Uniform Ultimate Boundedness for Uncertain Dynamic Systems," IEEE Trans. Automat. Cont., vol AC-26, no. 5, pp. 1139-1144, 1981.

[16] Craig, J.J., Adaptive Control of Mechanical Manipulators, Addison-Wesley Publishing Company, 1988.

[17] Craig, J.J., Hsu., P., and Sastry, S.S., "Adaptive Control of Mechanical Manipulators," Int. J. Robotics Res., vol. 6, no. 2, pp. 16-28, 1987.

[18] Davison, E.J., and Goldenberg, A., "Robust Control of a General Servomechanism Problem: The Servo Compensator," Automatica, vol. 11, pp. 461-471, 1975.

[19] Desilva, C.W., and Winssen, J.V., "Least Squares Adaptive Control for Trajectory Following Robots," ASME J. Dynam. Syst., Meas. Contr., vol. 109, no. 2, pp. 104-109, 1987.

[20] Dubowsky, S., and Desforges, D.T., "The Application of Model - Referenced Adaptive Control to Robotic Manipulators," ASME J. Dynam. Syst., Meas. Contr., vol. 101, no. 2, pp. 193-200, 1979.

[21] Elevitch, C.R., Sethares, W.A., Rey,G.J., and Johnson, Jr., C.R., "Quiver Diagrams and Signed Adaptive Filters," IEEE Trans. Acoust.,Speech, Signal Processing, vol. 37, no. 2, pp. 227-236, 1989.

[22] Eweda, E., "Convergence Analysis of an Adaptive Filter Equipped with the Sign-Sign Algorithm," IEEE Trans. Automat. Cont., vol. 40, no. 10, pp. 1807-1811, 1995.

[23] Feng, G., "A New Adaptive Control Algorithm for Robot Manipulators in Task Space," IEEE Trans. Robotics Automat., vol. 11, no. 3, pp. 457-462, 1995.

[24] Feng, G., and Palaniswami, M., "Adaptive Control of Robot Manipulators in Task Space," IEEE Trans. Automat. Cont., vol. 38, no. 1, pp. 100-104, 1993.

[25] Gilbert, E.G., and Ha, I.J., "An Approach to Nonlinear Feedback Control with Applications to Robotics," IEEE Trans. Syst., Man, Cybern., vol. SMC-14, no. 6, pp. 879-884, 1984.

[26] Goodwin, G.C., Hill, D.J., and Palaniswami, M., "A Perspective On Convergence of Adaptive Control Algorithms," Automatica, vol. 20, no. 5, pp. 519-531, 1984.

[27] Gourdeau, R., and Schwartz, H.M., "Adaptive Control of Robotic Manipulators: Experimental Results," in Proc. of IEEE Conf. Robotics Automat., pp. 8-15, 1991.

[28] Gu, K., and Tongue, B.H., "A New Strategy for Adaptive Motion Control of Robots," ASME J. Dynam. Syst., Meas. Contr., vol. 112, no. 3, pp. 410-416, 1990.

[29] Hsia, T.C., "Adaptive Control of Robotic Manipulators- A Review," in Proc. IEEE Int. Conf. Robotics Automat., vol. 1, pp. 183-189, 1986.

[30] Hsu, P., Bodson, M., Sastry, S., and Paden, B., "Adaptive Identification and Control for Manipulators Without Using Joint Accelerations," in Proc. IEEE Int. Conf. Robotics Automat., vol. 3, pp. 1210-1214, 1987.

[31] Ioannou, P.A., and Kokotovic, P.V., "Instability Analysis and Improvement of Robustness of Adaptive Control," Automatica, vol. 20, no. 5, pp. 583-594, 1984.

[32] Ioannou, P.A., and Tsakalis, K.S., "A Robust Direct Adaptive Controller," IEEE Trans. Automat. Cont., vol. AC-31, no. 11, pp. 1033-1043, 1986.

[33] Jankovic, M., "Observer Based Control for Elastic Joint Robots," IEEE Trans. Robotics Automat., vol. 11, no. 4, pp. 618-623, 1995.

[34] Kang, H., Vachtsevanos, G., and Lewis, F.L., "Lyapunov Redesign for Structural Convergence Improvement in Adaptive Control," IEEE Trans. Automat. Cont., vol. 35, no. 2, pp. 250-253, 1990.

[35] Kelly, R., Carelli, R., and Ortega, R., "Adaptive motion Control Design of Robot Manipulators : An Input -Output Approach," Int. J. Cont., vol. 50, no. 6, pp. 2563-2581, 1989.

[36] Khosla, P.K., and Kanade, T., "Experimental Evaluation of Nonlinear Feedback and Feedforward Control Schemes for Manipulators," Int. J. Robotics Res., vol. 7, no. 1, pp. 18-28, 1988.

[37] Koo, K. Mo., and Kim, J. H., "Robust Control of Robot Manipulators with parametric Uncertainty," IEEE Trans. Automat. Cont., vol. 39, no. 6, pp. 1230-1233, 1994.

[38] Kovio, A.J., and Guo, T.H., "Adaptive Linear Controller for Robotic Manipulators," IEEE Trans. Automat. Cont., vol. AC-28, no. 2, pp. 162-171, 1983.

[39] Kreutz, K., "On Manipulator Control by Exact Linearization," IEEE Trans. Automat. Cont., vol. 34, no. 7, pp. 763-767, 1989.

[40] Kuo, C.Y., and Wang, T.S.P., "Nonlinear Robust Industrial Robot Control," ASME J. Dynam. Syst., Meas. Contr. vol. 111, no. 1, pp. 24-30, 1989.

[41] Landau, I.D., "Evolution of Adaptive Control," ASME J. Dynam. Syst., Means. Contr., vol. 115, no. 2(B), pp. 381-391, 1993.

[42] Leahy, Jr., M.B., and Whalen, P.V., "Direct Adaptive Control for Industrial Manipulators," in Proc. IEEE Int. Conf. Robotics Automat., pp. 1666-1672, 1991.

[43] Lee, C.S.G., and Chung, M.J., "An Adaptive Control Strategy for Mechanical Manipulators," IEEE Trans. Automat. Cont., vol. AC-29, no. 9, pp. 837-844, 1984.

[44] Lee, C.S.G., and Lee, B.H., "Resolved Motion Adaptive Control for Mehanical Manipulators," ASME J. Dynam. Syst., Meas. Contr., vol. 106, no. 2, pp. 134-142, 1984.

[45] Lim, K.Y., and Eslami, M., "Adaptive Controller Designs for Robot Manipulator Systems Using Lyapunov Direct Method," IEEE Trans. Automat. Cont., vol. AC-30, no. 12, pp. 1229-1233, 1985.

[46] Lim, K.Y., and Eslami, M., "Robust Adaptive Controller Designs for Robot Manipulator Systems," IEEE J. Robotics Automat., vol. RA-3, no. 1, pp. 54-66, 1987.

[47] Luh, J.Y.S., Walker, M.W., and Paul, R.P.C., "Resolved-Acceleration Control of Mechanical Manipulators," IEEE Trans. Automat. Cont., vol. AC-25, no. 3, pp. 468-474, 1980.

[48] Mahmoud, M.S., "Robust Control of Robot Arms Including Motor Dynamics," Int. J. Cont., vol. 58, no. 4, pp. 853-873, 1993.

[49] Mahmoud, M.S., and Hajeer, H.Y., "A Globally Convergent Adaptive Controller for Robot Manipulators," IEEE Trans. Automat. Cont., vol. 39, no. 1, pp. 148-151, 1994.

[50] Middleton, R.H., "Adaptive Control for Robot Manipulators Using Discrete Time Identification," IEEE Trans. Automat. Cont., vol. 35, no. 5, pp. 633-637, 1990.

[51] Mills, J.K., and Goldenberg, A.A., "A New Robust Robot Controller," in Proc. IEEE Int. Conf. Robotics Automat., vol. 2, pp. 740-745, 1986.

[52] Miyasato, Y., and Oshima, Y., "Non-linear Adaptive Control for Robotic Manipulators with Continuous Control inputs," Int. J. Cont., vol. 49, no. 2, pp. 545-559, 1989.

[53] Narendra, K.S., and Annaswamy, A.M., Stable Adaptive Systems, Prentice Hall, 1989.

[54] Narendra, K.S., and Balakrishnan, J., "Improving Transient Response of Adaptive Control System Using Multiple Models and Switching," IEEE Trans. Automat. Cont., vol. 39, no. 6, pp. 1861-1866, 1994.

[55] Narendra, K.S., Lin, Y.H., and Valavani, L.S., "Stable Adaptive Controller Design, Part II : Proof of Stability," IEEE Trans. Automat. Cont., vol. AC-25, no. 3, pp. 440-448, 1980.

[56] Nicosia, S., and Tomei, P., "Model Reference Adaptive Control Algorithms for Industrial Robots," Automatica, vol. 20, no. 5, pp. 635-644, 1984.

[57] Nicosia, S., and Tomei, P., "Robot Control by Using only Joint Position Measurements," IEEE Trans. Automat. Cont., vol. 35, no. 9, pp. 1058-1061, 1990.

[58] Ortega, R., Loria, A., and Kelly, R., "A Semiglobally Stable Output Feedback PI^2D Regulator for Robot Manipulators," IEEE Trans. Automat. Cont., vol. 40, no. 8, pp. 1432-1436, 1995.

[59] Ortega, R., and Spong, M.W., "Adaptive Motion Control of Rigid Robots : A Tutorial," in Proc. 27th IEEE Conf. Decision Cont., pp. 1575-1584, 1988.

[60] Pandian, S.R., and Hanmandlu, M., "Adaptive Generalized Model-Based Control of Robot Manipulators," Int. J. Cont., vol. 58, no. 4, pp. 835-852, 1993.

[61] Qu, Z., and Dorsey, J., "Robust Tracking Control of Robots by a Linear Feedback Law," IEEE Trans. Automat. Cont., vol. 36, no. 9, pp. 1081-1084, 1991.

[62] Sadegh, N., and Gulgielmo, K., "Design and Implementation of Adaptive and Repetitive Controllers for Mechanical Manipulators," IEEE Trans. Robotics Automat., vol. 8, no. 3, pp. 395-400, 1992.

[63] Sadegh, N., and Horowitz, R., "Stability Analysis of an Adaptive Controller for Robotic Manipulators," in Proc. IEEE Int. Conf. Robotics Automat., vol. 3, pp. 1223-1229, 1987.

[64] Sadegh, N., and Horowitz, R.,"Stability and Robustness Analysis of a Class of Adaptive Controllers for Robotic Manipulators," Int. J. Robotics Res., vol. 9, no. 3, pp. 74-92, 1990.

[65] Schilling, R.J., Fundamentals of Robotics Analysis and Control, Prentice Hall, 1990.

[66] Sastry, S., and Bodson, M., Adaptive Control-Stability, Convergence, and Robustness, prentice Hall, 1989.

[67] Seraji, H., "An Approach to Multivariable Control of Manipulators, " ASME J. Dynam. Syst., Meas. Contr., vol. 109, no. 2, pp. 146-154, 1987.

[68] Seraji, H., "A New Approach to Adaptive Control of Manipulators," ASME J. Dynam. Syst., Meas. Contr., vol. 109, no. 3, pp. 193-202, 1987.

[69] Singh, S.N., "Adaptive Model Following Control of Nonlinear Robotic Systems," IEEE Trans. Automat. Cont., vol. AC-30, no. 11, pp. 1099-1100, 1985.

[70] Skowronski, J.M., "Nonlinear Model Tracking by Robot Manipulators," ASME J. Dynam. Syst., Meas. Contr., vol. 111, no. 3, pp. 437-443, 1989.

[71] Slotine, J.J.E., and Li, W., "Adaptive Strategies in Constrained Manipulation," in Proc. IEEE Int. Conf. Robotics Automat., vol. 2, pp. 595-601, 1987.

[72] Slotine , J.J.E., and Li, W., "Adaptive Manipulator Control : A Case Study," in Proc. IEEE Int. Conf. Robotics Automat., vol. 3, pp. 1392-1400, 1987.

[73] Slotine , J.J.E., and Li, W., "On the Adaptive Control of Robot Manipulators," Int. J. Robotics Res., vol. 6, no. 3, pp. 49-59, 1987.

[74] Spong, M.W., "On the Robust Control of Robot Manipulators," IEEE Trans. Automat. Cont., vol. 37, no. 11, pp. 1782-1786, 1992.

[75] Spong, M.W., and Ortega, R., "On Adaptive Inverse Dynamics Control of Rigid Robots," IEEE Trans. Automat. Cont., vol. 35, no. 1, pp. 92-95, 1990.

[76] Spong, M.W., Thorp, J.S., and Kleinwaks, J.M., "Robust Microprocessor Control of Robot manipulators," Automatica, vol. 23, no. 3, pp. 373-379, 1987.

[77] Spong, M.W., and Vidyasagar, M., "Robust Linear Compensator Design for Nonlinear Robotic Control," IEEE J. Robotics Automat., vol. RA-3, no. 4, pp. 345-351, 1987.

[78] Takegaki, M., and Arimoto, S., "An adaptive Trajectory Control of Manipulators," Int. J. Cont., vol. 34, no. 2, pp. 219-230, 1981.

[79] Takegaki, M., and Arimoto, S., "A New Feedback Method for Dynamic Control of Manipulators," ASME J. Dynam. Syst., Meas. Contr., vol. 103, no. 2, pp. 119-125, 1981.

[80] Tomei, P., "Adaptive PD Controller for Robot Manipulators," IEEE Trans. Robotics Automat., vol. 7, no. 4, pp. 565-570, 1991.

[81] Tourassis, V.D., "Principles and Design of Model-Based Robot Controllers," Int. J. Cont., vol. 47, no. 5, pp. 1267-1275, 1988.

[82] Voronov, A.A., and Rutkovsky, V.Yu., "State-of-the-art and Prospects of Adaptive Systems," Automatica, vol. 20, no. 5, pp. 547-557, 1984.

[83] Wen, J.T., and Bayard, D.S., "New Class of Control Laws for Robotic Manipulators: Part 1. Non-Adaptive Case," Int. J. Cont., vol. 47, no. 5, pp. 1361-1385, 1988.

[84] Whitcomb, L.L., Rizzi, A.A., and Koditschek, D.E., "Comparative Experiments with a New Adaptive Controller for Robot Arms," IEEE Trans. Robotics Automat., vol. 9, no. 1, pp. 59-70, 1993.

[85] Yuan, J., "Adaptive Control of Robotic Manipulators Including Motor Dynamics," IEEE Trans. Robotics Automat., vol. 11, no. 4, pp. 612-617, 1995.

[86] Zak, S. H., "On the Stabilization and Observation of Nonlinear/Uncertain Dynamic Systems," IEEE Trans. Automat. Cont. vol. 35, no. 5, pp. 604-607, 1990.

[87] Zhihong, M., and Palaniswami, M., "Robust Tracking Control for Rigid Robotic Manipulators," IEEE Trans. Automat. Cont., vol. 39, no. 1, pp. 154-159, 1994.

[88] Zhihong, M., and Palaniswami, M., "A Robust Tracking Control Scheme for Rigid Robotic Manipulators with Uncertain Dynamics," Computers Elect. Engng., vol. 21, no. 3, pp. 211-220, 1995.

Appendix

A1.1 STABILITY ANALYSIS OF PROPOSED ADAPTIVE CONTROLLER STRUCTURE USING ACCELERATION TERM

Consider the Lyapunov function candidate

$$V = \frac{1}{2} e_1^T K_1 e_1 + \frac{1}{2} e_2^T M(q)\, e_2 + \epsilon\, e_1^T M(q)\, e_2 + \frac{1}{2} \tilde{\theta}^T kg^{-1} \tilde{\theta} \qquad (a1.1)$$

$$= \frac{1}{2} e^T \begin{bmatrix} K_1 & \epsilon M \\ \epsilon M & M \end{bmatrix} e + \frac{1}{2} \tilde{\theta}^T kg^{-1} \tilde{\theta}$$

$$= \frac{1}{2} e^T P_n e + \frac{1}{2} \tilde{\theta}^T kg^{-1} \tilde{\theta} \qquad (a1.2)$$

The time derivative of the Lyapunov function along the trajectories (3.8) is

$$\dot{V} = e_2^T K_1 e_1 + e_2^T (\frac{1}{2} \dot{M} - P(q)C) e_2 + \epsilon\, e_1^T (\dot{M} - P(q)C) e_2 + \dot{\epsilon}\, e_1^T M\, e_2$$
$$+ \epsilon\, e_2^T M\, e_2 - e_2^T P(q)\, K_1 e_1 - e_2^T P(q)\, K_2 e_2 - \epsilon\, e_1^T P(q)\, K_1 e_1 - \epsilon\, e_1^T P(q)\, K_2 e_2$$
$$- e_2^T P(q)\, W\, \tilde{\theta} - \epsilon\, e_1^T P(q)\, W\, \tilde{\theta} + \tilde{\theta}^T kg^{-1} \dot{\tilde{\theta}} \qquad (a1.3)$$

where $P(q) = \hat{M}\, M'^{-1}$, $M' = [\hat{M}(q) + K_3 I]$, $\lambda_m(P) \le \|P(q)\| \le \lambda_M(P)$

Moreover, applying the properties of C(..) and skew symmetry properties, $\frac{1}{2}\dot{M} - C = 0$ [59], we have

$$|e_2^T (\frac{1}{2} \dot{M} - P(q)C)\, e_2| \le (1+\lambda_M(P))\, C_M \|e_2\|^3 + (1+\lambda_M(P))\, C_M\, \rho_1 \|e_2\|^2 \qquad (a1.4)$$

$$|\epsilon e_1^T (\dot{M} - P(q)C)\, e_2| \le 2\, \epsilon_o\, C_M \|e_2\|^2 + 2\, \epsilon\, C_M\, \rho_1 \|e_1\| \|e_2\| + \epsilon_o\, C_M\, \lambda_M(P) \|e_2\|^2$$
$$+ \epsilon\, C_M\, \rho_1\, \lambda_M(P) \|e_1\| \|e_2\| \qquad (a1.5)$$

$$|\dot{\epsilon}\, e_1^T M\, e_2| \le \epsilon\, \lambda_M(M) \|e_2\|^2 \qquad (a1.6)$$

where ρ_1 is defined in section 3.2.1.2. $\lambda_m(.)$ and $\lambda_M(.)$ denote minimum and maximum eigen values, respectively.

Substituting (a1.4), (a1.5) and (a1.6) in (a1.3), we find

$$\dot{V} \leq -\frac{1}{2}\left[\lambda_m(P).\lambda_m(K_2) - 2\alpha_1 - \epsilon_o\left((4+2\lambda_M(P))C_M + 4\lambda_M(M)\right)\right]\|e_2\|^2$$

$$-e^T\begin{bmatrix} \epsilon\,\lambda_m(P).\lambda_m(K_1) & -\frac{\epsilon}{2}[\lambda_M(P)+2]C_M\rho_1 + \frac{\epsilon}{2}\lambda_M(P).\lambda_M(K_2) + \frac{\epsilon}{2}[(\lambda_M(P)-1)\,\epsilon^{-1}\,\lambda_M(K_1)] \\ -\frac{\epsilon}{2}[\lambda_M(P)+2]C_M\rho_1 + \frac{\epsilon}{2}\lambda_M(P).\lambda_M(K_2) + \frac{\epsilon}{2}[(\lambda_M(P)-1)\,\epsilon^{-1}\,\lambda_M(K_1)] & \frac{1}{2}\lambda_m(P).\lambda_m(K_2) \end{bmatrix} e$$

$$+ \tilde{\theta}^T W^T P(q)^T (e_2 + \epsilon e_1) + \tilde{\theta}^T kg^{-1}\dot{\tilde{\theta}} \qquad \text{(a1.7)}$$

where $\alpha_1 = (\lambda_M(P) + 1)(\rho_1 + \|e_2\|)C_M$

$\dot{V}$ is negative definite if

$$\lambda_m(K_2) > \frac{2\alpha_1 + \epsilon_o\left((4+2\lambda_M(P))C_M + 4\lambda_M(M)\right)}{\lambda_m(P)} \qquad \text{(a1.8)}$$

with

$$\epsilon_o\left((4+2\lambda_M(P))C_M + 4\lambda_M(M)\right) > 2\alpha_1$$

$$\dot{\hat{\theta}} = kg\,W^T P(q)^T (e_2 + \epsilon e_1) \qquad \text{(a1.9)}$$

and

$$\epsilon_o < \min\left[\frac{\lambda_m(P)\,\lambda_m(K_2) - 2\alpha_1}{(4+2\lambda_M(P))C_M + 4\lambda_M(M)},\ \frac{2(\lambda_m(P))^2\lambda_m(K_1)\,\lambda_m(K_2)}{\{-[\lambda_M(P)+2]C_M\rho_1 + \lambda_M(P)\lambda_M(K_2) + [(\lambda_M(P)-1)\epsilon^{-1}\lambda_M(K_1)]\}^2}\right]$$

(a1.10)

In this case

$$\dot{V} \leq - \epsilon \lambda_m (Q_n) \|e\|^2 \qquad \text{(a1.11)}$$

where,

$$Q_n \stackrel{\Delta}{=} \begin{bmatrix} \lambda_m(P).\lambda_m(K_1) & -\frac{1}{2}[\lambda_M(P) + 2]C_M\rho_1 + \frac{1}{2}\lambda_M(P)\lambda_M(K_2) \\ & + \frac{1}{2}[(\lambda_M(P)-1)\epsilon_o^{-1}\lambda_M(K_1)] \\ -\frac{1}{2}[\lambda_M(P) + 2]C_M\rho_1 + \frac{1}{2}\lambda_M(P).\lambda_M(K_2) & \frac{1}{2\epsilon_o}\lambda_m(P).\lambda_m(K_2) \\ + \frac{1}{2}[(\lambda_M(P)-1)\epsilon_o^{-1}\lambda_M(K_1)] & \end{bmatrix}$$

(a1.12a)

Let $x^T = [e_1^T, e_2^T]$, $\|\dot{q}\| \leq k_c$

The matrix that appears in (a1.12a) is positive definite if

$$\|e_2\| < \left[\frac{2\lambda_m(P)(\lambda_m(K_1)\lambda_m(K_2))^{1/2} - \lambda_M(P)\lambda_M(K_2) - [(\lambda_m(P)-1)\epsilon_o^{-1}\lambda_M(K_1)]}{(\lambda_M(P)+2)\ C_M}\right] - k_c$$

(a1.12b)

which is true if

$$\|x\| < \left[\frac{2\lambda_m(P)(\lambda_m(K_1)\lambda_m(K_2))^{1/2} - \lambda_M(P)\lambda_M(K_2) - [(\lambda_m(P)-1)\epsilon_o^{-1}\lambda_M(K_1)]}{(\lambda_M(P)+2)\ C_M}\right] - k_c$$

(a1.12c)

Noting that the right hand side of (a1.12c) is positive by hypothesis (a1.8) and (a1.9).

Morever,

$$\frac{1}{2} L_m \|x\|^2 \leq V(x) \leq \frac{1}{2} L_M \|x\|^2 \qquad \text{(a1.12d)}$$

V(x) is a positive definite decrescent function. From (a1.12a), (a1.12c) and (a1.12d), one can get if

$$\|x(0)\| < \sqrt{\frac{L_m}{L_M}} \left\{ \left[\frac{2\lambda_m(P)(\lambda_m(K_1)\lambda_m(K_2))^{1/2} - \lambda_M(P)\lambda_M(K_2) - [(\lambda_m(P)-1)\epsilon_o^{-1}\lambda_M(K_1)]}{(\lambda_M(P)+2)\, C_M} \right] - k_c \right\} \qquad \text{(a1.12e)}$$

then,

$$V(x) \leq V(x(0)) \qquad \forall t \geq 0$$

$$\dot{V}(x) \leq -\beta_{1o} \|e\|^2 \qquad \forall t \geq 0$$

with β_{1o} a positive constant.

Remark A1 : The role of K_3 in P(q) causes the upper boundedness of P(q) by unity so lower bound on P(q) is always less than unity. In this situation $\hat{\theta}$ (or $\tilde{\theta}$) remain bounded for all $t \geq 0$ if e_1 and $\hat{\theta}$ are bounded at $t = 0$. It is necessary to show $e \rightarrow 0$ as $t \rightarrow \infty$ means $e_1 \rightarrow 0$, $e_2 \rightarrow 0$ as $t \rightarrow \infty$. It can be easily proved by applying Barbalat's lamma, that $\lim_{t \rightarrow 0} \dot{V} = 0$, which implies $\lim_{t \rightarrow \infty} e = 0$.

Remark A2 : For $\dot{V} \leq 0$, the necessary condition $\lambda_m(K_2)$ should satisfy the inequality (a1.8) with sufficient condition $\epsilon_o ((4 + 2\lambda_M(P))C_M + 4\lambda_M(M)) > 2\alpha_1$.

Remark A3 : The size of the region of attraction can be enlarged by increasing the gain constant K_2(see a1.8) and keeping the K_3 small.

A1.2 ANALYSIS OF THE CONVERGENCE RATE

Consider the closed-loop system (3.8). The rate of convergence of the error trajectories towards a ball $S(r_f)$, $r_f > r_m$; is exponential with a rate [48] 2β, $\beta(\epsilon_o, e_o, e_{2o}, r_f) = S1\text{-}T1(e_{2o}, r_f)$

Assume $\quad r_M > \|e\| > r_f > r_m \quad , \quad \Delta = \left[\frac{\lambda_M(P_n)}{\lambda_m(P_n)}\right]^{1/2}$ (a1.13)
$\quad\quad r_M > \|e_o\| > r_f$

By using $e^T P_n e \geq \lambda_m(P_n)\ \|e\|^2 \geq \lambda_m(P_n)^2\ r_f^2$, (a1.1) and (a1.7), the following expression is derived ((a1.8) and (a1.9) must be satisfied) (recalling [48]) as

$$\frac{-\dot{V}(e)}{V(e)} \geq 2\left[\epsilon\ \lambda_m((Q_n)P_n^{-1}) - \frac{\beta_2\ \Delta^3\ \|e_2\|^3 - \beta_1\ \Delta^2\ \|e_2\|^2}{\lambda_m(P_n)\|e\|^2}\right] \qquad (a1.14)$$

where,

$$\beta_1 = \frac{1}{2}\left[\lambda_m(P).\ \lambda_m(K_2) - \epsilon_o\ ((4+2\lambda_M(P))C_M + 4\lambda_M(M))\right] - (\lambda_M(P)+1)\rho_1 C_M \qquad (a1.15)$$

$$\beta_2 = (\lambda_M(P)+1)C_M \qquad (a1.16)$$

since $\dot{V}(e) \leq 0$, $V(e) \leq V(e_o)$ or equivalently

$$e^T P_n e \leq e_o^T\ P_n\ e_o \qquad (a1.17)$$

using (a1.13), $\quad \|e\| \leq \Delta\ \|e_o\|$ (a1.18)
$\quad\quad \|e_2\| \leq \Delta\ \|e_{2o}\|$

substituting in (a1.14),

$$\frac{-\dot{V}(e)}{V(e)} \geq 2\left[\epsilon\ \lambda_m((Q_n)P_n^{-1}) - \frac{\beta_2\ \Delta^3\ \|e_{2o}\|^3 - \beta_1\ \Delta^2\ \|e_{2o}\|^2}{r_f^2\ \lambda_m(P_n)}\right]$$

$$\geq 2\ [S1\text{-}T1(e_{2o}, r_f)] \qquad (a1.19)$$

The above inequality implies that

$$V(e) \leq Ve(o)e^{-2(S1-T1)(t-t_o)} \qquad \text{(a1.20)}$$

$$\text{i.e. } \|e\| \leq \Delta \|e_o\| e^{-2(S1-T1)(t-t_o)} \qquad \text{(a1.21)}$$

It states that the exponential convergence rate of trajectory e(t) towards a ball $S(r_f)$ is at least (S1-T1). It follows that the maximum time needed to settle in a ball $S(r_f)$; $r_f > r_m$, is given (S1-T1 > 0) by

$$T(\epsilon, e_o, e_{2o}, r_f) = \frac{1}{S1\text{-}T1(e_{2o}, r_f)} \ln \left| \frac{\Delta \|e_o\|}{r_f} \right| \qquad \text{(a1.22)}$$

The rate of convergence depends upon the proper choice of matrix Q_n.

A2.1 STABILITY ANALYSIS OF PROPOSED ADAPTIVE CONTROLLER STRUCTURE USING NONLINEAR COMPENSATOR

(i) For case - 1

Consider the Lyapunov function candidate

$$V = \frac{1}{2} S_1^T M(q) S_1 + \frac{1}{2} e^T K_2 e + \frac{1}{2} \tilde{\theta}^T kg^{-1} \tilde{\theta} \qquad (a2.1)$$

Taking the time derivative of (a2.1) along the error trajectories (3.28) and applying skew symmetry properties i.e. $\frac{1}{2}\dot{M} - C = 0$, we find

$$\dot{V} = S_1^T M(q) (\ddot{e} + \lambda_o \dot{e}) + e^T K_2 \dot{e} + \frac{1}{2} S_1^T \dot{M}(q) (\dot{e} + \lambda_o e) + \tilde{\theta}^T kg^{-1} \dot{\tilde{\theta}} \qquad (a2.2)$$

$$= -\lambda C_M \|S_1\|^2 + \lambda \lambda_o C_M \|S_1\| \|e\| - \lambda e_1 C_M \|S\| + C_M \|e\| \|S_1\|^2 - \lambda_m(K_2) \|S_1\|^2 + \lambda_M(K_2) \|S_1\| \|e\| - \lambda_o \lambda_m(K_2) \|e\|^2 - \sigma_{n1} \|e\|^2 \|S_1\|^2 + S_1^T W(q, \dot{q} - \lambda e, \dot{r} - \lambda_o e, \ddot{r} - \lambda_o \dot{e}) \tilde{\theta} + \tilde{\theta}^T kg^{-1} \dot{\tilde{\theta}} \qquad (a2.3)$$

$$= -[\lambda C_M + \lambda_m(K_2)] \|S_1\|^2 + [\lambda \lambda_o C_M + \lambda_M(K_2)] \|S_1\| \|e\| - \lambda \rho_1 C_M \|S\| + \lambda C_M \|e\| \|S_1\|^2 - \sigma_{n1} \|e\|^2 \|S_1\|^2 - \lambda_o \lambda_m(K_2) \|e\|^2 + S_1^T W(q, \dot{q} - \lambda e, \dot{r} - \lambda_o e, \ddot{r} - \lambda_o \dot{e}) \tilde{\theta} + \tilde{\theta}^T kg^{-1} \dot{\tilde{\theta}} \qquad (a2.4)$$

$$\dot{V} \leq -\lambda_o \begin{bmatrix} \|S_1\| \\ \|e\| \end{bmatrix}^T \lambda_m(Q_1) \begin{bmatrix} \|S_1\| \\ \|e\| \end{bmatrix} - \lambda_{o1} C_M \|S_1\| [\rho_1 - \|S_1\| \|e\|] - \sigma_{n1} \|e\|^2 \|S_1\|^2 + S_1^T W(q, \dot{q} - \lambda e, \dot{r} - \lambda_o e, \ddot{r} - \lambda_o \dot{e}) \tilde{\theta} + \tilde{\theta}^T kg^{-1} \dot{\tilde{\theta}} \qquad (a2.5)$$

where,

$$\lambda_m(Q_1) = \begin{bmatrix} \dfrac{\lambda_{o1} C_M + \lambda_m(K_2)}{\lambda_o} & -\dfrac{1}{2}\left[\lambda_o C_M + \dfrac{\lambda_M(K_2)}{\lambda_o}\right] \\ -\dfrac{1}{2}\left[\lambda_o C_M + \dfrac{\lambda_M(K_2)}{\lambda_o}\right] & \lambda_m(K_2) \end{bmatrix}$$

For satisifying $\dot{V} \leq 0$, the following conditions are implies

$$\rho_1 \geq \|e\| \, \|S_1\| \tag{a2.6}$$

$$\lambda_M(K_2) \leq \left(2\sqrt{(\lambda_o C_M + \lambda_m(K_2))\, \lambda_m(K_2)\lambda_o}\right) - \lambda_{o1}\, \lambda_o C_M \tag{a2.7}$$

$$0 < \lambda_{o1} < \frac{\sigma_{n1}}{C_M} \tag{a2.8}$$

$$\dot{\hat{\theta}} = - kg\, W^T(q, \dot{q} - \lambda e, \dot{r} - \lambda_o e, \ddot{r} - \lambda_o \dot{e})\, (\dot{e} + \lambda_o e) \tag{a2.9}$$

In this case

$$\dot{V} \leq -\lambda_o \begin{bmatrix} \|S_1\| \\ \|e\| \end{bmatrix}^T \lambda_m(Q_1) \begin{bmatrix} \|S_1\| \\ \|e\| \end{bmatrix} \tag{a2.10}$$

$\dot{V}$ is nonpositive.

The region of attraction is given by defining $x^T = [e, \dot{e}]^T$:

V(x) is a positive definite decrescent function. Besides,

$$\frac{1}{2} L_m \|x\|^2 \leq V(x) \leq \frac{1}{2} L_M \|x\|^2$$

From, (a2.5), one can find

$$\|x\| < \sqrt{\frac{L_m}{L_M}} \left[\frac{-\lambda_o C_M - (\lambda_o^2 C_M^2 - 4\, \sigma_{n1} p)^{1/2}}{2\sigma_{n1}}\right] \tag{a2.10a}$$

where,

$$p = \frac{1}{4}\frac{\left[\lambda_o C_M + \frac{\lambda_M(K_2)}{\lambda_o}\right]^2}{\lambda_m(K_2)} - \left(\frac{\lambda_{o1} C_M + \lambda_m(K_2)}{\lambda_o}\right)$$

Decreasing σ_{n1} one can enlarge the region of attraction. The right side of the equation is positive by hypothesis (a2.7). From (a2.10) and (1a2.10a), one can get

$$\dot{V}(x) \leq - \beta^{\equiv} \begin{bmatrix} \|S_1\| \\ \|e\| \end{bmatrix}^2 \qquad \text{(a2.10b)}$$

with $\beta^{\equiv}$ a positive constant.

(iii) For Case - 2

Consider the Lyapunov function candidate

$$V = \frac{1}{2} S_2^T M(q) S_2 + \frac{1}{2} e^T K_1 e + \frac{1}{2} \tilde{\theta}^T kg^{-1} \tilde{\theta} \qquad \text{(a2.11)}$$

Taking the time derivative of (a2.11) along the error trajectories (3.30), we find

$$\dot{V} = S_2^T M(q)\dot{S}_2 + e^T K_1 \dot{e} + \frac{1}{2} S_2^T \dot{M}(q) S_2 + \tilde{\theta}^T kg^{-1} \dot{\tilde{\theta}} \qquad \text{(a2.12)}$$

Substituting $\dot{S}_2$, apply properties of C(...) and skew symmetry properties, we find

$$\dot{V} = - S_2^T \lambda \lambda_o C(q,\dot{q})e + S_2^T \lambda\lambda_o C(q,e)\dot{e} - S_2^T \lambda_o K_1 e - S_2^T \lambda_o K_2 \dot{e} - S_2^T \lambda_o \sigma_{n2} \|e\|^2 S_2$$
$$- S_2^T \lambda_o^2 M(q)\dot{e} - S_2^T \lambda_o W(q,\dot{q} - \lambda e, \dot{r}, \dot{r}^{\cdot} - \lambda_o \dot{e})\tilde{\theta} + \lambda S_2^T M(q)\dot{e} + \dot{\lambda} S_2^T M(q)e$$
$$+ \dot{e}^T K_1 e + \frac{1}{2} S_2^T \lambda \dot{M}(q)e + \tilde{\theta}^T kg^{-1} \dot{\tilde{\theta}} \qquad \text{(a2.13)}$$

Moreover, we have

$$\dot{\lambda}\, S_2^T M(q)e \le \lambda_o M_M(\|S_2\|^2 + \|S_2\|\,\|\lambda e\|) \tag{a2.14}$$

$$\lambda\lambda_o S_2^T C(q,\dot{e})e \le \lambda_o C_M (\|S_2\|^2 + \|S_2\|\,\|\lambda e\|) \tag{a2.15}$$

$$\frac{1}{2} S_2^T\lambda \dot{M}(q)e - S_2^T \lambda\, \lambda_o C(q,\dot{q})e \le (1-\lambda_o)[\lambda_o^{-1} C_M(\|S_2\| + \|\lambda e\|)(\|S_2\| \|\lambda e\|) + C_M \rho_1 \|S_2\|\,\|\lambda e\|)] \tag{a2.16}$$

Substituting (a2.14), (a2.15), (a2.16) into (a2.13), with some manipulation, we find

$$\dot{V} \le - \begin{bmatrix} \|S_2\| \\ \|\lambda e\| \end{bmatrix}^T \lambda_m(Q_2) \begin{bmatrix} \|S_2\| \\ \|\lambda e\| \end{bmatrix} - \frac{2}{\lambda_o^2} \lambda_m(K_1)\|S_2\|\,\|\lambda e\|^2 - \frac{\sigma_{n2}}{\lambda_o^3} \|S_2\|^2\,\|\lambda e\|^2 + S_2^T \lambda_o W(q,\dot{q} - \lambda e, \dot{r}, \ddot{r} - \lambda_o \dot{e})\tilde{\theta} + \tilde{\theta}^T kg^{-1} \dot{\tilde{\theta}} \tag{a2.17}$$

where,

$$\lambda_m(Q_2) = \begin{bmatrix} \lambda_m(K_2) + ((\lambda_o-1)/\lambda_o)C_M + \lambda_o C_M & -\frac{1}{2}[\lambda_M(K_2) + (\lambda_o-1)(\rho_1 + \lambda_o)C_M] \\ -\frac{1}{2}[\lambda_M(K_2) + (\lambda_o-1)(\rho_1 + \lambda_o)C_M] & \frac{\lambda_o-1}{\lambda_o} C_M \end{bmatrix}$$

For satisifying $\dot{V} \le 0$, the following conditions are implies

$$\lambda_m(K_1) \ge \frac{\sigma_{n2}}{2\lambda_o} \|S_2\| \tag{a2.18}$$

$$\sigma_{n2} > 0 \tag{a2.19}$$

$$\lambda_o < 1 \tag{a2.20}$$

$$\lambda_m(K_2) > \frac{\{[\frac{1}{2}(-\lambda_M(K_2) + (1-\lambda_o)C_M\rho_1 - \lambda_o C_M)]^2 - ((\lambda_o-1)/\lambda_o)C_M) - \lambda_o C_M\}\lambda_o C_M}{\lambda_o - 1} \quad \text{(a2.21)}$$

$$\dot{\hat{\theta}} = -\lambda_o\, kg\, W^T(q,\dot{q}-\lambda e,\dot{r},\ddot{r}-\lambda_o\dot{e})\,(\lambda_o\dot{e}+\lambda e) \quad \text{(a2.22)}$$

In the present case

$$\dot{V} \leq -\begin{bmatrix}\|S_2\| \\ \|\lambda e\|\end{bmatrix}^T \lambda_m(Q_2)\begin{bmatrix}\|S_2\| \\ \|\lambda e\|\end{bmatrix} \quad \text{(a2.23)}$$

$\dot{V}$ is nonpositive.

The region of attraction is determined by defining $x^T=[e,\dot{e}]^T$: it is found from (a2.17)

$$\|x\| < \sqrt{\frac{L_m}{L_M}}\left\{\left[\frac{-2(((\lambda_m(K_2)((\lambda_o-1)/\lambda_o)C_M+\lambda_o C_M)^{1/2})\frac{\lambda_o-1}{\lambda_o} - \frac{1}{2}\lambda_M(K_2))}{(\lambda_o-1)\,C_M}\right] - \frac{1}{2}(\lambda_o-1)\lambda_o C_M - k_c\right\} \quad \text{(a2.23a)}$$

where $\|\dot{q}\| \leq k_c$. By virtue of hypothesis (a2.18),(a2.21), $\dot{V}$ is nonpositive. From (a2.23) and (a2.23a), one can derive

$$\dot{V}(x) \leq -\beta'' \begin{bmatrix}\|S_2\| \\ \|\lambda e\|\end{bmatrix}^2$$

where β'' is a positive constant.

(iii) For Case - 3

Consider the Lyapunov function candidate

$$V = \frac{1}{2} S_3^T M(q) S_3 + \frac{1}{2} e^T K_1 e + \frac{1}{2} \tilde{\theta}^T kg^{-1} \tilde{\theta} \qquad (a2.24)$$

Taking the time derivative of (a2.24) along the error trajectories (3.31), we get

$$\dot{V} = S_3^T M(q) \dot{S}_3 + e^T K_1 \dot{e} + \frac{1}{2} S_3^T \dot{M}(q) S_3 + \tilde{\theta}^T kg^{-1} \dot{\tilde{\theta}} \qquad (a2.25)$$

$$= S_3^T M(q) \ddot{e} + \lambda S_3^T M(q) \dot{e} + \dot{\lambda} S_3^T M(q) e + e^T K_1 \dot{e}$$

$$+ \frac{1}{2} S_3^T \dot{M}(q) S_3 + \tilde{\theta}^T kg^{-1} \dot{\tilde{\theta}} \qquad (a2.26)$$

$$\dot{V} = - S_3^T [C(q,\dot{q})\dot{e} + \lambda C(q,e)\dot{r} + K_1 e + K_2 \dot{e} + \sigma_{n3} \|e\|^2 S_3$$

$$- W(q,\dot{q} - \lambda e, \dot{r}, \ddot{r})\tilde{\theta}] + \lambda S_3^T M(q)\dot{e} + \dot{\lambda} S_3^T M(q) e$$

$$+ \dot{e}^T K_1 e + \frac{1}{2} S_3^T \dot{M}(q)(\dot{e} + \lambda e) + \tilde{\theta}^T kg^{-1} \dot{\tilde{\theta}} \qquad (a2.27)$$

Moreover, we have

$$\dot{\lambda} S_3^T M(q) e \leq \lambda_o M_M (\|S_3\|^2 + \|S_3\| \|\lambda e\|) \qquad (a2.28)$$

$$\lambda S_3^T C(q,\dot{e}) e \leq \lambda_o C_M (\|S_3\|^2 + \|S_3\| \|\lambda e\|) \qquad (a2.29)$$

Substituting (a2.28), (a2.29) in (a2.27), using physical properties and skew symmetric properties, we find

$$\dot{V} \leq - \begin{bmatrix} \|S_3\| \\ \|\lambda e\| \end{bmatrix}^T \lambda_m(Q_3) \begin{bmatrix} \|S_3\| \\ \|\lambda e\| \end{bmatrix} - \sigma_{n3} \|e\|^2 \|S_3\|^2$$

$$+ S_3^T W(q,\dot{q} - \lambda e, \dot{r}, \ddot{r})\tilde{\theta} + \tilde{\theta}^T kg^{-1} \dot{\tilde{\theta}} \qquad (a2.30)$$

where,

$$\lambda_m(Q_3) = \begin{bmatrix} \lambda_m(K_2) - \lambda_o C_M - 2\lambda_o M_M & -\frac{1}{2}[\lambda_M(K_2) + (\rho_1 + \lambda_o)C_M] \\ -\frac{1}{2}[\lambda_M(K_2) + (\rho_1 + \lambda_o)C_M] & \lambda_o^{-1}\lambda_m(K_1) \end{bmatrix}$$

For satisifying $\dot{V} \leq 0$, the following conditions are implies:

$$\sigma_{n3} > 0 \tag{a2.31}$$

$$\lambda_m(K_1) > \frac{\frac{1}{4}[(-\lambda_M(K_2) - \lambda_o C_M)]^2}{\lambda_o^{-1}[\lambda_M(K_2) - \lambda_o C_M - 2\lambda_o M_M]} \tag{a2.32}$$

$$\dot{\hat{\theta}} = -\, kg\, W^T(q,\dot{q} - \lambda e, \dot{r}, \ddot{r})\,(\dot{e} + \lambda e) \tag{a2.33}$$

In this situation

$$\dot{V} \leq -\begin{bmatrix} \|S_3\| \\ \|\lambda e\| \end{bmatrix}^T \lambda_m(Q_3) \begin{bmatrix} \|S_3\| \\ \|\lambda e\| \end{bmatrix} - \sigma_{n3}\, \|e\|^2\, \|S_3\|^2 \tag{a2.34}$$

$\dot{V}$ is nonincreasing function.

Similarly, it can derived from (a2.34) the region of attraction as

$$\|x\| < \sqrt{\frac{L_m}{L_M}} \left[\frac{\frac{1}{2}[\lambda_M(K_2) + (\rho_1 + \lambda_o)C_M]}{(\lambda_o^{-1}\lambda_m(K_1))^{1/2}} - [\lambda_m(K_2) - \lambda_o C_M - 2\lambda_o M_M]^{1/2} \right] \Big/ \sqrt{\sigma_{n3}} \tag{a2.34a}$$

The upper bound on K_2 if increaed or keeping σ_{n3} low value, the region of attraction can be enlarged. Noting that the right hand side of (a2.34a) is positive by hypothesis (a2.32). One can find easily

$$\dot{V}(x) \leq -\beta' \begin{bmatrix} \|S_3\| \\ \|\lambda e\| \end{bmatrix}^2 \qquad \forall t \geq 0$$

with β' a positive constant.

LEMMA A1

For the additional error, introduced by the replacement of q and $\dot{q}$ to r and $\dot{r}$ in $W(q,\dot{q},\ddot{q})$ to form $W(q,\dot{q} - \lambda e,\ldots)$, the resulting error is bounded by S_i and e, i = 1,2,3.

PROOF :

$$\text{Let } [W(q,\dot{q},\ddot{q}) - W(q,\dot{q} - \lambda e,\ldots)]\ \theta = \Delta W(S_i,e) \qquad \text{(a2.35)}$$

where,

$$S_1 = e + \lambda_o e, \quad S_2 = \lambda_o \dot{e} + \lambda e, \quad S_3 = \dot{e} + \lambda e$$

From Equation (3.28), one can formulate the additional error as

$$M(q)\dot{S}_1 + C(q,\dot{q})\ (S_1 + \lambda e) - \lambda C\ (q,e)\ S_1 = \Delta W(S_1,e) \qquad \text{(a2.36)}$$

Let,

$$P_1 = M(q)\dot{S}_1 \qquad \text{(a2.37)}$$

Applying the MVT (Mean Value Theorem) to M(q) [64], we get

$$P_1 = \left[\sum_{i=1}^{i=n} \frac{\partial M}{\partial q_1} (r + e)\ de_1 \right] \dot{S}_1 \qquad \text{(a2.38)}$$

Taking the Norm, we obtain

$$S^T P_1 \leq bm1(\dot{S}_1)\ \|S_1\|\ \|e\| \qquad \text{(a2.39)}$$

where,

$$0 \le bm1(\dot{S}_1) \le_q^{sup} \left[\sum_{i=1}^{i=n} \left| \frac{\partial M}{\partial q_1} \dot{S}_1 \right|^2 \right] \qquad (a2.40)$$

Similarly,

$$P_2 = C(q,\dot{q}) (S_1 + \lambda e) - \lambda C(q,e) S_1 \qquad (a2.41)$$

Applying the MVT, we find

$$P_2 = \left[\int_0^1 \frac{\partial C}{\partial q} (r+e, \dot{r} + \dot{e})\, dei \right] (S_1 + \lambda e) + \lambda C(q,e) S_1 \qquad (a2.42)$$

Taking the norm, one can write

$$S^T P_2 \le bc1(\dot{r},\dot{e}) \|S_1\|^2 \|e\| + \lambda bc2(\dot{r},\dot{e}) \|S_1\| \|e\|^2 + \lambda bc3[\|S_1\| \|e\|^2 + \|S_1\|^2 \|e\|] \qquad (a2.43)$$

Where,

$$0 \le bc1(\dot{r},\dot{e}) \le_q^{sup} \left[\sum_{i=1}^{i=n} \sum_{j=1}^{j=n} \left| (\dot{r} + S_1 - \lambda_o e)^T \frac{\partial C^i}{\partial q_1} (\dot{r} + S_1 - \lambda_o e) \right|^2 \right]^{1/2}$$

$$0 \le bc2(\dot{r},\dot{e}) \le_q^{sup} \left[\sum_{i=1}^{i=n} \left| C^i (r + S_1 - \lambda_o e) \right|^2 \right]^{1/2}$$

$$0 \le bc3 \le_q^{sup} \left[\sum_{i=1}^{i=n} \left| C^i \right|^2 \right]^{1/2}$$

Adding the terms, we find

$$S_1^T \Delta W(S_1,e) \leq bm1(\dot{S}_1)\|S_1\|\|e\| + bc1(\dot{r},\dot{e})\|S_1\|^2\|e\| + \lambda bc2(\dot{r},\dot{e})\|S_1\|\|e\|^2 + \lambda bc3[\|S_1\|^2\|e\| + \|S_1\|\,\|e\|^2] \quad \text{(a2.44)}$$

Let,

$$b1 \leq bm1(\dot{S}_1)$$

$$b2 \leq (bc1(\dot{r},\dot{e}) + \lambda bc3)$$

$$b3 \leq (bc2(\dot{r},\dot{e}) + bc3)$$

Substituting in (a2.44), we find

$$S_1^T \Delta W(S_1,e) \leq b1\|S_1\|\|e\| + b2\|S_1\|^2\|e\| + \lambda b3\|S_1\|\|e\|^2 + \lambda bc3[\|S_1\|^2\|e\| + \|S_1\|\,\|e\|^2] \quad \text{(a2.45)}$$

after some manipulation, we obtained as

$$S_1^T \Delta W(S_1,e) \leq (b1 + \frac{b2}{4})\|S_1\|^2 + (\frac{b1}{4} + \lambda\frac{b3}{4})\|e\|^2 + b2\|S_1\|^2\|e\|^2 + \lambda b3 - b1(\|S_1\| + \frac{1}{2}\|e\|^2) - b2\|S_1\|^2[\frac{1}{2} - \|e\|^2] - \lambda b3\|e\|^2[\frac{1}{2} - \|S_1\|^2 \quad \text{(a2.46)}$$

Applying,

$$\|e\| < \frac{1}{2}\,,\ \|S_1\| < \frac{1}{2}$$

and for simplicity, we choose $b1 \approx b2 \approx b3 \approx \sigma_n$

$$S_1^T \Delta W(S_1,e) \leq \sigma_n [\,\|S_1\|^2 + \frac{\|e\|^2}{4} + \lambda_o\|S_1\|^2\|e\|^2] \quad \text{(a2.47)}$$

By approximation, one can write

$$S_1^T \Delta W(S_1,e) \leq \lambda_o \sigma_n \|S_1\|^2\|e\|^2 \leq S_1^T \sigma_{n1}\|e\|^2 S_1 \quad \text{(a2.48)}$$

hence,

$$\Delta W(S_1,e) \leq \sigma_{n1} \|e\|^2 S_1 \qquad \text{(a2.49)}$$

Similarly, one can derived for case-2, as

$$S_2^T \Delta W(S_2,e) \leq [bc1(\dot{r},\dot{e}) + \lambda bc12(\dot{r},\dot{e})]\, \lambda_o^{-1}[\|S_2\|^2 - \lambda \|S_2\| \|e\|] + \lambda_o^{-1}\, \lambda bc13\, \|S_2\|^2 \|e\|$$
$$-\lambda_o^{-1}\lambda^2 bc14\, \|S_2\|\, \|e\|^2 \leq S_2^T\, \sigma_{n2}\, \|e\|^2\, S_2 \qquad \text{(a2.50)}$$

and for case -3, as

$$S_3^T \Delta W(S_3,e) \leq [bm11(\ddot{e})\|S_3\|\|e\|] + bc22(\dot{r},\dot{e})[\|S_3\|^2\|e\| + 2\lambda\|S_3\|\|e\|^2]$$
$$+ bc23\, \|S_3\|^2\|e\| + \lambda bc23\|S_3\|\, \|e\|^2 \leq S_3^T\, \sigma_{n3}\, \|e\|^2\, S_3 \qquad \text{(a2.51)}$$

Equation (a2.49) , (a2.50) and (a2.51) show the additional error bounded by respective S_i and e, i = 1,2,3 (see [64] for details information).

A3.1 STABILITY ANALYSIS OF BOUNDED FORM OF ADAPTIVE CONTROLLER STRUCTURE

Consider the Lyapunov function candidate

$$V = \frac{1}{2} S^T M(q) S + \frac{1}{2} e^T K_1 e + \frac{1}{2} \tilde{\theta}^T kg^{-1} \tilde{\theta} \qquad (a3.1)$$

Taking the time derivative of (a3.1) along the error trajectories (3.41), we get

$$\dot{V} = S^T M(q)\dot{S} + e^T K_1 \dot{e} + \frac{1}{2} S^T \dot{M}(q) S + \tilde{\theta}^T kg^{-1} \dot{\tilde{\theta}} \qquad (a3.2)$$

Substituting $\dot{S} = \ddot{e} + \dot{\lambda} e + \lambda \dot{e}$ in (a3.2), we get

$$\dot{V} = S^T M(q)\ddot{e} + \lambda S^T M(q)\dot{e} + \dot{\lambda} S^T M(q) e + e^T K_1 \dot{e} + \frac{1}{2} S^T \dot{M}(q) S + \tilde{\theta}^T kg^{-1} \dot{\tilde{\theta}} \qquad (a3.3)$$

Applying properties of C(...) and skew symmetric properties i.e. $\frac{1}{2}\dot{M}$-C = 0, we find

$$\dot{V} = -\lambda S^T C(q,\dot{e})e + \lambda S^T C(q,\dot{r})e - S^T K_1 \|e\| - S^T K_2 \|\dot{e}\| - S^T \sigma_n \|e\|^2 S + S^T W(\|\dot{q} - \lambda e\|, \dot{r}, \ddot{r})\tilde{\theta} + \lambda S^T M(q)\dot{e} + \dot{\lambda} S^T M(q) e + \dot{e}^T K_1 e + \tilde{\theta}^T kg^{-1} \dot{\tilde{\theta}} \qquad (a3.4)$$

Moreover, we have

$$\dot{\lambda} S^T M(q) e \le \lambda_o M_M (\|S\|^2 + \|S\| \|\lambda e\|) \qquad (a3.5)$$

$$\lambda S^T C(q,\dot{e}) e \le \lambda_o C_M (\|S\|^2 + \|S\| \|\lambda e\|) \qquad (a3.6)$$

Substituting (a3.5) and (a3.6) into (a3.4), we find

$$\begin{aligned}\dot{V} \le & - \lambda_m(K_2)\, \|S\|^2 + \lambda\, M_M\, \|S\|^2 + \lambda_o\, M_M\, \|S\|^2 + \lambda_o\, C_M\, \|S\|^2 \\ & + \lambda_M(K_2)\, \|S\|\, \|\lambda e\| - \lambda\, M_M\, \|S\|\, \|\lambda e\| + \lambda_o\, M_M\, \|S\|\, \|\lambda e\| \\ & + \lambda_o C_M\, \|S\|\, \|\lambda e\| + \rho_1\, C_M\, \|S\|\, \|\lambda e\| - \lambda^{-1}\, \lambda_m(K_1)\, \|\lambda e\|^2 \\ & - \sigma_n \|e\|^2\, \|S\|^2 + S^T\, W(\|\dot{q} - \lambda e\|, \dot{r}, \ddot{r})\tilde{\theta} + \tilde{\theta}^T\, kg^{-1}\, \dot{\tilde{\theta}} \end{aligned} \qquad \text{(a3.7)}$$

$\|\hat{\theta}\|$ is adjusted for $\dot{V} \le 0$ as

$$\begin{aligned} \dot{\tilde{\theta}} &= - kg\, W^T(q, \dot{q} - \lambda e, \dot{r}, \ddot{r})\, (\dot{e} + \lambda e) \\ \|\hat{\theta}\| &= \tilde{\theta} + \theta^*(q) \end{aligned} \qquad \text{(a3.8)}$$

hence,

$$\dot{V} \le - \begin{bmatrix} \|S\| \\ \|\lambda e\| \end{bmatrix}^T \lambda_m(Q) \begin{bmatrix} \|S\| \\ \|\lambda e\| \end{bmatrix} - \sigma_n\, \|e\|^2\, \|S\|^2 \qquad \text{(a3.9)}$$

where,

$$\lambda_m(Q) = \begin{bmatrix} \lambda_m(K_2) - \lambda_o C_M - 2\, \lambda_o M_M & - \frac{1}{2}\, [\lambda_M(K_2) + (\rho_1 + \lambda_o) C_M] \\ - \frac{1}{2}\, [\lambda_M(K_2) + (\rho_1 + \lambda_o) C_M] & \lambda_o^{-1}\, \lambda_m(K_1) \end{bmatrix}$$

$\dot{V}$ is nonincreasing function. From sqaure integrability and uniform continuity of 'e' conclude that it converge to zero. The region of attraction is given by (a2.34a).

A4.1 APPLICATION OF THE FILIPPOV'S SOLUTION CONCEPT

This concept shows that the dynamics on the switching surface is an average of dynamics on each side of the discontinuity surface.

Let $\Lambda_1 = \lambda_1 I$, with $\lambda_1 > 0$. The region (see (4.26)) $\tilde{x}_1 = 0$, i.e. $\|\tilde{x}_2\| \leq \lambda_1$, described as sliding band or sliding patch [10].

The dynamic behavior in the sliding patch of observation error (4.26) is given as:

$$\dot{\tilde{x}}_2 = \ddot{r} - W(x_1, \dot{q}_r, \hat{\theta})S - \Lambda_2 \Lambda_1^{-1} \tilde{x}_2 + \eta + v(\Lambda_1^{-1} \tilde{x}_2) \qquad \text{(a4.1)}$$

The new form of variables are considered as :

$$\text{sgn}(\tilde{x}_1) = \Lambda_1^{-1} \tilde{x}_2 \qquad \text{(a4.2)}$$

$$\ddot{q}_r = \ddot{q}_r' + \Lambda \Lambda_1 \text{sgn}(\tilde{x}_1) \qquad \text{(a4.3)}$$

A4.2 STABILITY ANALYSIS OF SLIDING OBSERVER BASED ADAPTIVE CONTROLLER WITH NEW UNCERTAINTY VECTOR

In this section, the stability proof of the scheme in the sliding patch and also the closed-loop analysis for augmented error system are investigated.

A4.2.1 Stability in Sliding Patch

Consider the following the Lyapunov function candidate

$$V = \frac{1}{2} S^T M S + \frac{1}{2} \tilde{x}_2^T \tilde{x}_2 + \frac{1}{2} \tilde{\theta}^T \Gamma \tilde{\theta} \qquad \text{(a4.4)}$$

Taking the time derivative of the Lyapunov function along (4.24) and (4.26), we find

$$\dot{V} = S^T M \dot{S} + \frac{1}{2} S^T \dot{M} S + \tilde{x}_2^T \dot{\tilde{x}}_2 + \tilde{\theta}^T \Gamma \dot{\tilde{\theta}}$$

$$= S^T [Y\tilde{\theta} - K_2 S - CS + W \tilde{x}_2] + \frac{1}{2} S^T \dot{M} S$$

$$+ \tilde{x}_2^T [\dot{r}^{\cdot} - \Lambda_2 \Lambda_1^{-1} \tilde{x}_2 + W^T S + \eta + v] + \tilde{\theta}^T \Gamma \dot{\tilde{\theta}} \qquad \text{(a4.5)}$$

According to definition of C(...) and applying skew symmetry properties i.e. $(1/2(\dot{M}))-C = 0$, we find

$$\dot{V} = S^T K_2 S - \tilde{x}_2^T \Lambda_2 \Lambda_1^{-1} \tilde{x}_2 + \tilde{\theta}^T [Y^T S + \Gamma \dot{\tilde{\theta}}] + \tilde{x}_2^T [\eta + v + \dot{r}^{\cdot}] \qquad \text{(a4.6)}$$

For $\dot{V} \leq 0$, one can derive

$$\dot{\hat{\theta}} = \Gamma^{-1} Y^T (x_1, x_2, \dot{q}_r, \dot{q}_r^{\cdot}) S \qquad \text{(a4.7)}$$

$$v = \begin{cases} -(\phi(\dot{r},\tau) + \|\dot{r}^{\cdot}\|) . \tilde{x}_2 / \|\tilde{x}_2\| & \text{if } \|\tilde{x}_2\| \neq 0 \\ 0 & \text{if } \|\tilde{x}_2\| = 0 \end{cases} \qquad \text{(a4.8)}$$

Using (a4.2) and (a4.3), one can write

$$\dot{\hat{\theta}} = -\Gamma^{-1} Y(x_1, \hat{x}_2 - \Lambda_1 \mathrm{sgn}(\tilde{x}_1), \dot{q}_r, \dot{q}_r^{\cdot} + \Lambda\Lambda_1 \mathrm{sgn}(\tilde{x}_1))(S' - \Lambda_1 \mathrm{sgn}(\tilde{x}_1)) \qquad \text{(a4.9)}$$

and

$$v = v(\dot{r}, \tau, \tilde{x}_2, \dot{r}^{\cdot})$$

$$= \begin{cases} -[\phi(\dot{r},\tau) + \|\dot{r}^{\cdot}\|] \Lambda_1 \mathrm{sgn}(\tilde{x}_1)/\lambda_1 & \text{if } \|\Lambda_1 \mathrm{sgn}(\tilde{x}_1)\| \neq 0 \\ 0 & \text{if } \|\Lambda_1 \mathrm{sgn}(\tilde{x}_1)\| = 0 \end{cases} \qquad \text{(a4.10)}$$

with above definitions

$$\dot{V} \leq -\lambda_m(K_2)\|S\|^2 - \lambda_m(\Lambda_2 \Lambda_1^{-1})\|\tilde{x}_2\|^2, \quad \text{if } \tilde{x}_2 \neq 0 \tag{a4.11}$$

$$\dot{V} \leq -\lambda_m(K_2)\|S\|^2, \quad \text{if } \tilde{x}_2 = 0 \tag{a4.12}$$

The region in the sliding patch is characterized as closed set so that trajectories should lie within it.

Defining,

$$\lambda_{max}[L] = \max[\lambda_{sup}M, \lambda_{sup}(K_2), \lambda_{sup}(\Gamma)]$$

$$\lambda_{min}[L] = \min[\lambda_{inf}M, \lambda_{inf}(K_2), \lambda_{inf}(\Gamma)]$$

Since $\dot{V} \leq 0$, $V(t) \leq V(0)$, for all $t \geq 0$

$$\lambda_{min}(L)\|e_s\|^2 \leq V \leq V(0) \leq \lambda_{max}\|e_s(0)\|^2$$

where,

$$e_s^T = [S^T \; \tilde{x}_2 \; \tilde{\theta}^T] \tag{a4.13}$$

hence,

$$\|e_s(0)\|^2 \leq \frac{\lambda_{min}(L)}{\lambda_{max}(L)} \cdot \lambda_1 \tag{a4.14}$$

If, $\lambda_{min}(L) \approx \lambda_{max}(L)$, then

$$\|e_s(0)\|^2 \leq \lambda_1 \tag{a4.15}$$

so that $e_s(t)$ lie in sliding patch.

A4.2.2 Stability of Closed-loop System

The closed-loop stability is investigated based on the reduced order manifold dynamics and tracking error dynamics. From (4.24), the tracking error dynamics equation can be expressed in state-space representation as:

$$\begin{aligned}\dot{e}_1 &= e_2 \\ \dot{e}_2 &= -M(x_1)^{-1}\,[(C(x_1,x_2) + K_2 + M(x_1)\Lambda)\,e_2 \\ &\quad + (C(x_1,x_2) + K_2)\,\Lambda e_1 - Y\,\tilde{\theta} - W\,\tilde{x}_2]\end{aligned} \qquad \text{(a4.16)}$$

The augmented error is defined as

$$Z = \begin{bmatrix} e_1 \\ e_2 \\ \tilde{x}_2 \end{bmatrix} \qquad \text{(a4.17)}$$

The closed-loop analysis is based on the augmented error Z.

Now, consider the Lyapunov function candidate

$$V = \frac{1}{2} S^T M S + \frac{1}{2} e_1^T K_2 e_1 + \frac{1}{2} \tilde{x}_2^T \tilde{x}_2 + \frac{1}{2} \tilde{\theta}^T \Gamma \tilde{\theta} \qquad \text{(a4.18)}$$

Taking the time derivative along (4.26) and (a4.16) and using the skew symmetry properties, we find

$$\dot{V} \le -\Lambda \begin{bmatrix} e_1 \\ e_2 \\ \tilde{x}_2 \end{bmatrix}^T \lambda_m(Q) \begin{bmatrix} e_1 \\ e_2 \\ \tilde{x}_2 \end{bmatrix} \qquad \text{(a4.19)}$$

$$\dot{V} \le -\Lambda\, \lambda_m(Q)\, \|Z\|^2 \qquad \text{(a4.20)}$$

where,

$$\lambda_m(Q) = \begin{bmatrix} \Lambda\,\lambda_m(K_2) & \lambda_M(K_2) & 0 \\ & +\frac{1}{2\Lambda}\,\lambda_M(K_2) & \\ \lambda_M(K_2) & \lambda_m(K_2)/\Lambda & 0 \\ +\frac{1}{2\Lambda}\,\lambda_M(K_2) & & \\ 0 & 0 & \lambda_m(\Lambda_2\Lambda_1^{-1})/\Lambda \end{bmatrix} \qquad \text{(a4.21)}$$

If (a4.9) and (a4.10) are satisfied, the convergence of augmented error depends upon the choice of matrix Q i.e., setting of K_2, choice of Λ,Λ_1 and Λ_2. Thus for $\dot{V} \leq 0$, the following inequality should be satisfied

$$\lambda_m(K_2) > \lambda_M(K_2)\,(\,1 + \frac{1}{2\Lambda}\,) \qquad \text{(a4.22)}$$

The matrix that appears in (a4.21) is positive definite. Let $x^T = [e,\dot{e}]^T$; Morever,

$$\frac{1}{2}\,L_m \|x\|^2 \leq V(x) \leq \frac{1}{2}\,L_M\,\|x\|^2$$

From (a4.18), it is clear that V(x) is a positive definite decrescent function. Since $\dot{V}$ is nonpositive by hypothesis (a4.22). Hence, the region of attraction is the entire state-space, that is, defined by L_m and L_M.

A5.1 STABILITY ANALYSIS OF TRACKING ERROR BASED SLIDING OBSERVER AIDED ADAPTIVE CONTROLLER

Applying the Filippov's solution concept (reduced order manifold dynamics, see section A4.1) to observation error dynamics (4.45), the dynamic behaviour of (4.45) chanage as,

$$\dot{\tilde{x}}_2 = \ddot{r} - W(x_1, \dot{q}_r, \hat{\theta})S - \Gamma_e e_1 - \Lambda_2 \Lambda_1^{-1} \tilde{x}_2 + \eta + v(\Lambda_1^{-1} \tilde{x}_2) \qquad \text{(a5.1)}$$

where,

$$\Lambda_1^{-1} \tilde{x}_2 = \text{sgn}(\tilde{x}_1) \quad \text{(a5.2)}$$

$$\ddot{q}_r = \ddot{q}_r' + \Lambda \Lambda_1 \text{sgn}(\tilde{x}_1) \qquad \text{(a5.3)}$$

In order to investigate the stability in the sliding patch, consider the Lyapunov function (a4.4) as,

$$V = \frac{1}{2} S^T M S + \frac{1}{2} \tilde{x}_2^T \tilde{x}_2 + \frac{1}{2} \tilde{\theta}^T \Gamma \tilde{\theta} \qquad \text{(a5.4)}$$

Following the similar procedure in Appendix-IV and taking the time derivative of the Lyapunov function, we find

$$\begin{aligned} \dot{V} &= S^T M \dot{S} + \frac{1}{2} S^T \dot{M} S + \tilde{x}_2^T \dot{\tilde{x}}_2 + \tilde{\theta}^T \Gamma \dot{\tilde{\theta}} \\ &= S^T [Y\tilde{\theta} - K_2 S - CS + W \tilde{x}_2] + \frac{1}{2} S^T \dot{M} S \\ &\quad + \tilde{x}_2^T [\ddot{r} - \Gamma_e e_1 - \Lambda_2 \Lambda_1^{-1} \tilde{x}_2 + W^T S + \eta + v] + \tilde{\theta}^T \Gamma \dot{\tilde{\theta}} \end{aligned} \qquad \text{(a5.5)}$$

Applying the properties of C(...) and skew symmetric properties i.e. $(1/2(\dot{M}))-C = 0$, we find

$$\dot{V} = S^T K_2 S - \tilde{x}_2^T \Lambda_2 \Lambda_1^{-1} \tilde{x}_2 + \tilde{\theta}^T [Y^T S + \Gamma \dot{\tilde{\theta}}] + \tilde{x}_2^T [\eta + v + \ddot{r} - \Gamma_e e_1] \qquad (a5.6)$$

For $\dot{V} \leq 0$, one can get

$$\dot{\hat{\theta}} = - \Gamma^{-1} Y^T (x_1, x_2, \dot{q}_r, \ddot{q}_r) S \qquad (a5.7)$$

$$v = \begin{cases} -(\phi(\dot{r},\tau) + \|\ddot{r}\|).\tilde{x}_2/\|\tilde{x}_2\| & \text{if } \|\tilde{x}_2\| \neq 0 \\ 0 & \text{if } \|\tilde{x}_2\| = 0 \end{cases} \qquad (a5.8)$$

Using (a5.2) and (a5.3), the form of (a5.7) and (a5.8) are modified as follows:

$$\dot{\hat{\theta}} = - \Gamma^{-1} Y(x_1, \hat{x}_2 - \Lambda_1 \text{sgn}(\tilde{x}_1), \dot{q}_r, \ddot{q}_r + \Lambda\Lambda_1 \text{sgn}(\tilde{x}_1)) (S' - \Lambda_1 \text{sgn}(\tilde{x}_1) \qquad (a5.9)$$

and

$$v = v(\dot{r}, \tau, \tilde{x}_2, \ddot{r})$$

$$= \begin{cases} -[\phi(\dot{r},\tau) + \|\ddot{r}\|] \Lambda_1 \text{sgn}(\tilde{x}_1)/\lambda_1 & \text{if } \|\Lambda_1 \text{sgn}(\tilde{x}_1)\| \neq 0 \\ 0 & \text{if } \|\Lambda_1 \text{sgn}(\tilde{x}_1)\| = 0 \end{cases} \qquad (a5.10)$$

with above definitions

$$\dot{V} \leq -\lambda_m(K_2)\|S\|^2 - \lambda_m(\Lambda_2 \Lambda_1^{-1}) \|\tilde{x}_2\|^2 - \lambda_M(\Gamma_e)\|e\| \qquad \text{if } \tilde{x}_2 \neq 0 \qquad (a5.11a)$$

$$\dot{V} \leq - \lambda_m(K_2)\|S\|^2 \qquad \text{if } \tilde{x}_2 = 0 \qquad (a5.11b)$$

Using the same arguments in Appendix-IV, from (a4.11)- (a4.15), it follows that $e_{s1}(t)$ lie in the sliding patch; $e_{s1}(t) = [S^T, \tilde{x}_2^T, \tilde{\theta}^T, e^T]$

The closed-loop stability is investigated based on the reduced order

manifold dynamics and tracking error dynamics. From (4.24), the tracking error dynamics equation can be expressed in state-space representation as

$$\begin{aligned}\dot{e}_1 &= e_2 \\ \dot{e}_2 &= -M(x_1)^{-1}\,[(C(x_1,x_2) + K_2 + M(x_1)\Lambda)\,e_2 \\ &\quad + (C(x_1,x_2) + K_2)\,\Lambda e_1 - Y\,\tilde{\theta} - W\,\tilde{x}_2]\end{aligned} \qquad \text{(a5.12)}$$

Stability proof for the augmented error system is investigated by following the same procedure as described from (a4.18)-(a4.20). The augmented error is defined as $Z^T = [e_1, e_2, \tilde{x}_2]^T$.

Now, consider the Lyapunov function candidate

$$V = \frac{1}{2}S^T M S + \frac{1}{2} e_1^T K_2 e_1 + \frac{1}{2}\tilde{x}_2^T \tilde{x}_2 + \frac{1}{2}\tilde{\theta}^T \Gamma \tilde{\theta} \qquad \text{(a5.13)}$$

Taking the time derivative along (4.44) and (a4.45), and using the skew symmetry properties, we find

$$\dot{V} \le -\Lambda\,\lambda_m(Q_s)\,\|Z\|^2 \qquad \text{(a5.14)}$$

where,

$$\lambda_m(Q_s) = \begin{bmatrix} \Lambda\,\lambda_m(K_2) & \lambda_M(K_2) & \frac{1}{2}\lambda_M(\Gamma_e) \\ & + \frac{1}{2\Lambda}\lambda_M(K_2) & \\ \lambda_M(K_2) & \lambda_m(K_2)/\Lambda & 0 \\ + \frac{1}{2\Lambda}\lambda_M(K_2) & & \\ \frac{1}{2}\lambda_M(\Gamma_e) & 0 & \lambda_m(\Lambda_2\Lambda_1^{-1})/\Lambda \end{bmatrix} \qquad \text{(a5.15)}$$

If the following condition is satisfied :

$$\lambda_M(K_2) < \frac{\left[\frac{1}{4}\frac{[\lambda_M(\Gamma_e)]^2\,\lambda_m(K_2)}{\lambda_m(\Lambda_2\Lambda_1^{-1})} - [\lambda_m(K_2)]^2\right]^{1/2}}{\left[1+\frac{1}{2\Lambda}\right]} \qquad \text{(a5.16)}$$

$\dot{V}$ is nonincreasing function. If (a5.9) and (a5.10) are satisfied, the convergence of augemented error depends upon the choice of matrix Q_s i.e., setting of K_2, choice of Λ,Λ_1 and Λ_2.

The matrix that appears in (a5.15) is positive definite by hypothesis (4.49). Let $x^T = [e,\dot{e}]^T$:
Moreover,

$$\frac{1}{2} L_m \|x\|^2 \le V(x) \le \frac{1}{2} L_M \|x\|^2$$

From (a5.13), it is found that V(x) is a positive decrescent function. Since $\dot{V}$ is non positive by (a5.16). Hence, the region of attraction is the entire state-space defined by L_m and L_M.

A6.1 PHYSICAL PROPERTIES

The following model properties are inherent to robot dynamics and are usefull for designing the controller-observer structure [8].

$$\text{(i)} \quad M(x_1) = M(x_1)^T > \longrightarrow M(x_1)^{-1} \text{ exists} \tag{a6.1}$$

$$\text{(ii)} \quad \sigma_o > \|M(x_1)\| > 0 \text{ and } \sigma'_o \|M(x_1)^{-1}\| > 0 \tag{a6.2}$$

$$\text{(iii)} \quad g(x_1) \leq \sigma_1 \tag{a6.3}$$

$$\text{(iv)} \quad \|C(x_1,x_2)\| \leq \sigma_2 \|x_2\|^2 \tag{a6.4}$$

$$\text{(v)} \quad \pi_o(x_1,\chi) = \frac{\partial}{\partial x_2} \{C(x_1,x_2)x_2\}_{x_2=\chi} \tag{a6.5}$$

$$\text{(vi)} \quad \pi_1(x_1,\chi) = \frac{\partial}{\partial x_2} \{C(x_1,x_2)\ \chi\}_{x_2=\chi} \tag{a6.6}$$

A6.2 STABILITY ANALYSIS OF EXTENDED NONLINEAR SLIDING OBSERVER AIDED CONTROLLER STRUCTURE

Consider the Lyapunov function candidate with $e^T = [e_1\ e_2]^T$

$$V(e,\tilde{x}_2) = \frac{1}{2}e_1^T K_1 e_1 + \frac{1}{2}e_2^T M(x_1)e_2 + \frac{1}{2}\tilde{x}_2^T M(x_1)\tilde{x}_2 + e_1^T M(x_1)e_2 \tag{a6.7}$$

Taking the time derivative of the Lyapunov function along the error trajectories (4.59) and (4.60), we find

$$\dot{V}(e,\tilde{x}_2) = e_1^T K_1 e_2 + e_2^T M(x_1)\dot{e}_2 + \frac{1}{2}e_2^T \dot{M}(x_1)e_2 + \tilde{x}_2^T M(x_1)\dot{\tilde{x}}_2 + \frac{1}{2}\tilde{x}_2^T \dot{M}(x_1)\tilde{x}_2 + e_2^T M(x_1)e_2 + e_1^T M(x_1)\dot{e}_2 + e_1^T \dot{M}(x_1)e_2 \tag{a6.8}$$

Applying the properties of skew symmetry i.e. $\frac{1}{2}\dot{M} - C = 0$, we find

$$\dot{V}(e,\tilde{x}_2) = e_1^T K_1 e_2 - e_2^T M(x_1) K_2 \tilde{x}_2 - 2 e_2^T M(x_1) K_2 e_2 - e_2^T M(x_1) K_1 e_1 + e_2^T M(x_1) e_2$$
$$- e_1^T M(x_1) K_2 \tilde{x}_2 - e_1^T M(x_1) K_1 e_1 + \tilde{x}_2^T M(x_1) \ddot{r} - \tilde{x}_2^T (1+\sigma^2) \tilde{x}_2 - \tilde{x}_2^T M(x_1) \Gamma_{e2} e_1^2$$
$$- \tilde{x}_2^T C(x_1,\tilde{x}_2)(\tilde{x}_2 - \Gamma_{e1} e_1^2) - \tilde{x}_2^T Q(\tilde{x}_2 - \Gamma_{e1} e_1^2) + \tilde{x}_2^T C(x_1,e_2) \Gamma_{e1} e_1^2 + \tilde{x}_2^T C(x_1,\dot{r}) \Gamma_{e1} e_1^2$$
$$+ 5 \tilde{x}_2^T C(x_1,\dot{r}) e_2 + 2 e_1^T C(x_1,\dot{r}) e_2 + e_2^T C(x_1,\dot{r}) e_2 + 2 e_1^T C(x_1,\dot{r}) \tilde{x}_2 + e_1^T C(x_1,e_2) e_2$$
$$+ \tilde{x}_2^T C(x_1,e_2) e_2 - \tilde{x}_2^T M(x_1) L_1 \mathrm{sgn}(\tilde{x}_2) \xi \qquad \text{(a6.9)}$$

Assume the following bounds

$$\lambda_m(M) \le \|M(x_1)\| \le \lambda_M(M)$$
$$\lambda_m(K_1) \le \|K_1\| \le \lambda_M(K_1)$$
$$\lambda_m(K_2) \le \|K_2\| \le \lambda_M(K_2)$$
$$\lambda_m(\Gamma_{e1}) \le \|\Gamma_{e1}\| \le \lambda_M(\Gamma_{e1})$$
$$\lambda_m(\Gamma_{e2}) \le \|\Gamma_{e2}\| \le \lambda_M(\Gamma_{e2}) \qquad \text{(a6.10)}$$

and

$$c_o = \|C(x_1,\dot{r})\| \le C_M \|\dot{r}\|$$
$$c_1 = \|C(x_1,e_2)\| \le C_M \|e_2\|$$
$$c_2 = \|C(x_1,\tilde{x}_2)\| \le C_M \|\tilde{x}_2\|$$
$$q_o = \lambda_{min}\{Q\} \qquad \text{(a6.11)}$$

Applying (a6.10) and (a6.11) in (a6.9), we find

$$\dot{V}(e,\tilde{x}_2) \le -e_o^T \begin{bmatrix} \lambda_m(M)\,\lambda_m(K_1) & \frac{1}{2}[\lambda_M(M)-1]\,\lambda_M(K_1) - c_o - \frac{1}{2}c_1 & \frac{1}{2}\lambda_M(M)\lambda_M(K_2) - c_o - c_3\|e_1\| \\ \frac{1}{2}[\lambda_M(M)-1]\,\lambda_M(K_1) - c_o - \frac{1}{2}c_1 & 2\lambda_m(M)[\lambda_m(K_2)-1] - c_o - \frac{5}{2}c_o - \frac{1}{2}c_1 & \frac{1}{2}\lambda_M(M)\,\lambda_M(K_2) \\ \frac{1}{2}\lambda_M(M)\,\lambda_M(K_2) - c_o - c_3\|e_1\| & \frac{1}{2}\lambda_M(M)\,\lambda_M(K_2) - \frac{5}{2}c_o - \frac{1}{2}c_1 & c_2 + q_o + (1+\sigma^2) \end{bmatrix} e_o$$
$$+ \tilde{x}_2^T M(x_1) [\ddot{r} - L_1 \mathrm{sgn}(\tilde{x}_2) \xi] \qquad \text{(a6.12)}$$

where,

$$c_3 = \frac{1}{2}\lambda_M(M)\,\lambda_M(\Gamma_{e2}) - \frac{1}{2}\lambda_M(\Gamma_{e2}) - \frac{1}{2}q_o\,\lambda_M(\Gamma_{e2}) - (c_1 + c_o)\,\lambda_M(\Gamma_{e1})$$

$\dot{V}(e, \tilde{x}_2)$ is negative definite if

$$\mathrm{sgn}(\tilde{x}_2) = \frac{L_1^{-1}\,\ddot{r}}{\xi} \Rightarrow \|L_1\,\xi\| \geq \|\ddot{r}\| \qquad \text{(a6.13)}$$

In the present case

$$\dot{V}(e, \tilde{x}_2) \leq -\lambda_{inf}\{M(e_1)\}\,\|e_o\|^2 \qquad \text{(a6.14)}$$

where $M(e_1)$ is a function of tracking error e_1, and V as

$$V(e, \tilde{x}_2) < \frac{1}{2}p_{max}\,\|e_o\|^2 + \lambda_M(M)\,\|e_1\|\,\|e_2\|$$

where, $p_{max} = \max[\lambda_M(K_1)\,\lambda_M(M)]$

Using these two upper bounds, we get

$$\frac{\dot{V}(e_o)}{V(e_o)} \leq -\frac{\lambda_{inf}\{M(e_1)\}\,\|e_o\|^2}{\frac{1}{2}p_{max}\,\|e_o\|^2 + \lambda_M(M)\,\|e_1\|\,\|e_2\|} \leq -\frac{\lambda_{inf}\{M(e_1)\}\,\|e_o\|^2}{P_{max}} \qquad \text{(a6.15)}$$

where , $P_{max} = P_{max}(p_{max}, \|e_o\|, \|e_1\|, \|e_2\|)$

Integrating (a6.15) both sides, we find

$$V(e_o) \leq V(e_o(0))\,e^{-1/P_{max}\int_o^t \lambda_{inf}\{M(e_1(\tau))\}\|e_o\|^2\,d\tau}$$

$$\leq V(e_o(0))\,e^{-\zeta_1(t)} \qquad \text{(a6.16)}$$

from which one can get

$$\|e_o\|^2 \leq \Delta\,\|e_o(0)\|^2\,e^{-\zeta_1(t)} \qquad \text{(a6.17)}$$

where $\Delta = \dfrac{\max\{\lambda_M(K_1), \lambda_M(M), \lambda_M(K_2)\}}{\min\{\lambda_m(K_1), \lambda_m(M), \lambda_m(K_2)\}}$ (a6.18)

For exponential stability , the following condition must be satisfied:

$$\zeta_1 > 0 \tag{a6.19}$$

$$\lambda_{inf}\{M(e_1)\} > 0 \text{ for all } t \geq 0 \tag{a6.20}$$

if $\lambda_m(M)\ \lambda_m(K_1) > 0$ and

$$\lambda_m(K_1) > \frac{\left\{c_o + \frac{1}{2}c_1 - \frac{1}{2}(\lambda_M(M)-1)\ \lambda_M(K_1)\right\}^2}{\lambda_m(M)\left\{2\lambda_m(M)\ (\lambda_m(K_2)-1)-c_o\right\}} \tag{a6.21}$$

hence,

$$\lambda_{inf}\{M(e_1)\} > 0 \tag{a6.22}$$

Applying these inequality eq.(a6.14) is nonpositive and indicate that the augmented error e_o tends to zero asymptotically means $e_1 \rightarrow 0$, $e_2 \rightarrow 0$ and $\tilde{x}_2 \rightarrow 0$ as t approach ∞.

The matrix that appears in (a6.12) is positive definite if

$$e_1 < \frac{1}{c_3}\left\{\left\{\left\{\left(\frac{1}{2}[\lambda_M(M)-1](\lambda_M(K_1) - c_o - \frac{1}{2}c_1)\right) + [(\lambda_m(M)\lambda_m(K_1))\right.\right.\right.$$

$$(2\lambda_m(M)[\lambda_m(K_2)-1] - c_o)]^{1/2}\ (c_2+q_o+(1+\sigma^2))^{1/2} - (\lambda_m(M)\lambda_m(K_1))^{1/2}.$$

$$\left.\left.\left.\left(\frac{1}{2}\lambda_M(M)\lambda_M(K_2) - \frac{5}{2}c_o - \frac{1}{2}c_1\right)\right\} / (2\lambda_m(M)[\lambda_m(K_2)-1]-c_o)^{1/2}\right\} - \frac{1}{2}\lambda_M(M)\lambda_M(K_2) - c_o\right\} \tag{a6.23}$$

which is true if

$$\|x\| < \frac{1}{c_3}\left\{\left\{\left\{\left(\frac{1}{2}[\lambda_M(M)-1](\lambda_M(K_1) - c_o - \frac{1}{2}c_1)\right) + [(\lambda_m(M)\lambda_m(K_1))\right.\right.\right.$$

$$(2\lambda_m(M)[\lambda_m(K_2)-1] - c_o)]^{1/2} (c_2 + q_o + (1+\sigma^2))^{1/2} - (\lambda_m(M)\lambda_m(K_1))^{1/2}$$

$$(\tfrac{1}{2}\lambda_M(M)\lambda_M(K_2) - \tfrac{5}{2}c_o - \tfrac{1}{2}c_1)\Big\} / (2\lambda_m(M)[\lambda_m(K_2)-1]-c_o)^{1/2}\Big\} - \tfrac{1}{2}\lambda_M(M)\lambda_M(K_2) - c_o\Big\}$$

(a6.24)

where $x^T = [e,\dot{e}]^T$. By virute of hypotehsis (a6.13) and (a6.21), the right hand side of (a6.23) is positive. $\dot{V}(x)$ is nonpositive. Besides,

$$\tfrac{1}{2} L_m \|x\|^2 \le V(x) \le \tfrac{1}{2} L_M \|x\|^2 \qquad \text{(a6.25)}$$

From (a6.12), (a6.23) and (a6.25), we obtained if

$$\|x(o)\| < \frac{1}{c_3}\sqrt{\frac{L_m}{L_M}}\Big\{\Big\{\Big\{(\tfrac{1}{2}[\lambda_M(M)-1](\lambda_M(K_1) - c_o - \tfrac{1}{2}c_1)) + [(\lambda_m(M)\lambda_m(K_1))$$

$$(2\lambda_m(M)[\lambda_m(K_2)-1] - c_o)]^{1/2} (c_2 + q_o + (1+\sigma^2))^{1/2} - (\lambda_m(M)\lambda_m(K_1))^{1/2}$$

$$(\tfrac{1}{2}\lambda_M(M)\lambda_M(K_2) - \tfrac{5}{2}c_o - \tfrac{1}{2}c_1)\Big\} / (2\lambda_m(M)[\lambda_m(K_2)-1]-c_o)^{1/2}\Big\} - \tfrac{1}{2}\lambda_M(M)\lambda_M(K_2) - c_o\Big\}$$

(a6.26)

then, $V(x) \le V(x(0)) \qquad \forall t \ge 0$

$\dot{V}(x) \le -\beta_{12}\|e_o\|^2$ with β_{12} a positive constant.

A7.1 STABILITY ANALYSIS OF SIGN-SIGN BASED NONLINEAR SLIDING OBSERVER AIDED CONTROLLER STRUCTURE

To establish closed-loop system as exponentially asymptotically stable, consider the following Lyapunov function candidate with $e^T = [e_1 \; e_2]^T$

$$V(e, \tilde{x}_2) = \frac{1}{2} e_1^T K_1 e_1 + \frac{1}{2} e_2^T M(x_1) e_2 + \frac{1}{2} \tilde{x}_2^T M(x_1) \tilde{x}_2 + e_1^T M(x_1) e_2 \quad (a7.1)$$

Taking the time derivative of (a7.1) along 4.75 and 4.76 and applying skew symmetry properties i.e. $\frac{1}{2}\dot{M} - C = 0$, we find.

$$\dot{V}(e, \tilde{x}_2) \leq - e_o^T \begin{bmatrix} K_A & K_B & K_C \\ K_B & K_D & K_E \\ K_C & K_E & K_F \end{bmatrix} e_o$$

$$+ \tilde{x}_2^T M(x_1) [\ddot{r} - L_1 \, sgn(\tilde{x}_2) \, \xi - L_2 \, sgn(\tilde{x}_2) \, sgn(e_1)] - \|\tau_d\| \, \|e_2\| \quad (a7.2)$$

where $K_A = \lambda_m(M) \, \lambda_m(K_1)$, $K_B = \frac{1}{2} [\lambda_M(M) - 1] \, \lambda_M(K_1) - c_o - \frac{1}{2} c_1$,

$K_C = \frac{1}{2} \lambda_M(M) \, \lambda_M(K_2) - c_o - c_3 \|e_1\|$, $K_D = 2 \, \lambda_m(M) \, [\lambda_m(K_2) - 1] - c_o$,

$K_E = \frac{1}{2} \lambda_M(M) \, \lambda_M(K_2) - \frac{5}{2} c_o - \frac{1}{2} c_1$, $K_F = c_2 + q_o + (1 + \sigma^2)$,

$\lambda_m(M) \leq \|M(x_1)\| \leq \lambda_M(M)$, $\lambda_m(K_1) \leq \|K_1\| \leq \lambda_M(K_1)$, $\lambda_m(K_2) \leq \|K_2\| \leq \lambda_M(K_2)$,

$\lambda_m(\Gamma_{e1}) \leq \|\Gamma_{e1}\| \leq \lambda_M(\Gamma_{e1})$, $\lambda_m(\Gamma_{e2}) \leq \|\Gamma_{e2}\| \leq \lambda_M(\Gamma_{e2})$, $c_o = \|C(x_1, \dot{r})\| \leq C_M \|\dot{r}\|$,

$c_1 = \|C(x_1, e_2)\| \leq C_M \|e_2\|$, $c_2 = \|C(x_1, \tilde{x}_2)\| \leq C_M \|\tilde{x}_2\|$, $q_o = \lambda_{min}\{Q\}$,

and $c_3 = \frac{1}{2} \lambda_M(M) \, \lambda_M(\Gamma_{e2}) - \frac{1}{2} \lambda_M(\Gamma_{e2}) - \frac{1}{2} q_o \, \lambda_M(\Gamma_{e2}) - (c_1 + c_o) \, \lambda_M(\Gamma_{e1})$

$\dot{V}(e, \tilde{x}_2)$ is negative definite if

$$\| L_1 \xi + L_2 \| \geq \| \ddot{r} \| \qquad \text{(a7.3)}$$

$$\| \tau_d \| > 0$$

In the present case

$$\dot{V}(e, \tilde{x}_2) \leq - \lambda_{inf} \{ M(e_1) \} \| e_o \|^2 - \| \tau_d \| \| e_2 \| \qquad \text{(a7.4)}$$

where $M(e_1)$ is a function of tracking error e_1. Using the upper bounds of V and $\dot{V}$ to form $\dot{V}/V$, one can get $\| e_o \|^2 \leq \Delta \| e_o(0) \|^2 e^{-\zeta_1(t)}$, where

$$\zeta_1 = \frac{1}{P_{max}} \int_0^t \lambda_{inf}\{M(e_1(\tau_1))\} \| e_o \|^2 \, d\tau_1, \quad P_{max} = P_{max}(\lambda_M(K_1), \lambda_M(M), \| e_o \|, \| e_1 \|, \| e_2 \|) \qquad \text{(a7.5)}$$

$$\Delta = \frac{\max\{ \lambda_M(K_1), \lambda_M(M), \lambda_M(K_2)\}}{\min\{ \lambda_m(K_1), \lambda_m(M), \lambda_m(K_2)\}} \qquad \text{(a7.6)}$$

For exponential stability , the following inequality must be satisfied:

$\zeta_1 > 0$; $\lambda_{inf} \{M(e_1)\} > 0$ for all $t \geq 0$;

if $\lambda_m(M) \lambda_m(K_1) > 0$ and

$$\lambda_m(K_1) > \frac{\left\{ c_o + \frac{1}{2} c_1 - \frac{1}{2} (\lambda_M(M)-1) \lambda_M(K_1) \right\}^2}{\lambda_m(M)\left\{ 2 \lambda_m(M) (\lambda_m(K_2)-1) - c_o \right\}} \qquad \text{(a7.7)}$$

hence, $\lambda_{inf} \{M(e_1)\} > 0$

Applying these inequalities eq.(9) is nonpositive and indicates that augmented error e_o tends to zero asymptotically means $e_1 \rightarrow 0, e_2 \rightarrow 0$ and $\tilde{x}_2 \rightarrow 0$ as t approach ∞. The region of attraction is given by (a6.24, Appendix-VI).